Inelastic X-Ray Scattering of Synchrotron Radiation

Principles & Applications

Esen Ercan Alp

Advanced Photon Source,

Argonne National Laboratory, Argonne, Illinois 60439

alp@anl.gov

Cheiron School, Sept 14, 2007, Spring-8, Japan

Advanced Photon Source, APS

Argonne National Laboratory, Illinois USA

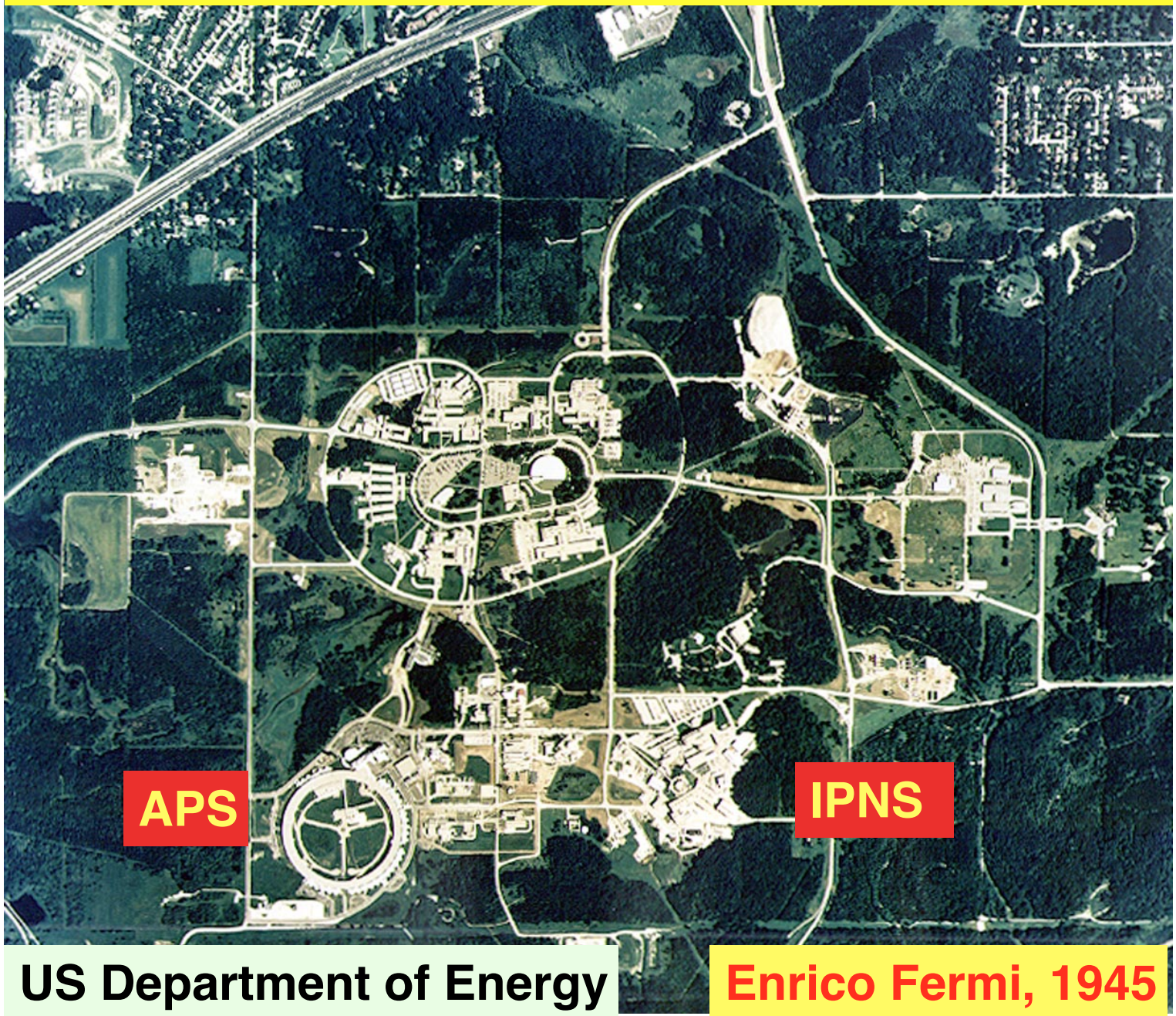

US Department of Energy

Enrico Fermi, 1945

Plan

- X-Ray Scattering
  - Characteristics of x-rays & synchrotron radiation
  - X-Ray scattering & spectroscopy
- Inelastic X-Ray Scattering & Spectroscopy
  - Momentum Resolved High Energy Resolution IXS
  - X-Ray Raman Scattering
  - X-Ray Emission Spectroscopy
  - Inelastic Nuclear Resonant X-Ray Scattering
  - High resolution and Magnetic Compton Scattering

IXS NRIXS Compton XRS RIXS MCS

NIS XES IUVS ....

Plan

- Part 1: Principles of x-ray scattering
- Part 2: High Resolution IXS
- Part 3: Nuclear Resonant IXS
- Part 4:
  - X-Ray Raman Scattering
  - X-Ray Emission Spectroscopy
  - Resonant IXS
  - Compton Scattering
    - High Resolution Compton Scattering
    - Magnetic Compton Scattering

Part 1

X-Ray Scattering: Principles

"The Academy awarded the Nobel Prize in Physics to Wilhelm Conrad Röntgen, Professor in the University of Munich, for the discovery with which his name is linked for all time: the discovery of the so-called Röntgen rays or, as he himself called them, X-rays. These are, as we know, a new form of energy and have received the name 'rays' on account of their property of propagating themselves in straight lines as light does. The actual constitution of this radiation of energy is still unknown. Several of its characteristic properties have, however, been discovered first by Röntgen himself and then by other physicists who have directed their researches into this field. And there is no doubt that much success will be gained in physical science when this strange energy form is sufficiently investigated and its wide field thoroughly explored."

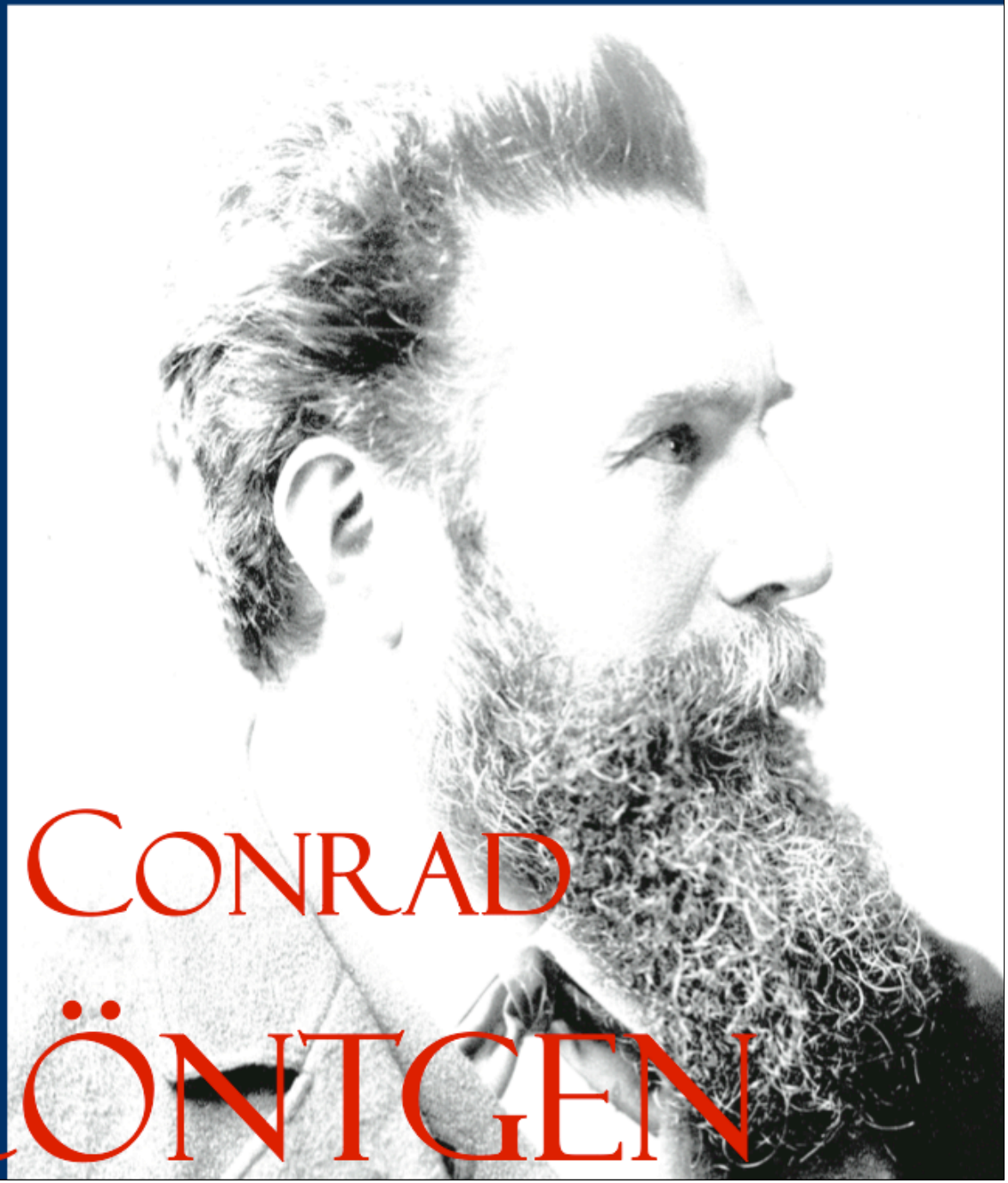

Wilhelm Conrad Röntgen

X-Ray World: 1895-2007

1) Electromagnetic spectrum : IR-VUV-Soft-Hard-Gamma
2) Röntgen's discovery
3) **X-ray sources:** x-ray tube, rotation anode, synchrotron radiation, dedicated storage ring with insertion devices, free electron laser, energy recovery LINAC, …
4) X-ray scattering, spectroscopy, imaging, and therapy
5) Barla, Einstein, Bragg's, von Laue, Debye, Compton, Watson & Crick, Mössbauer, … over a dozen Nobel prizes
   Last one: R. KORNBERG, Chemistry 2006

Nobel Prize in Chemistry, 2006, R. Kornberg, Stanford University

Molecular basis of eukaryotic transcription

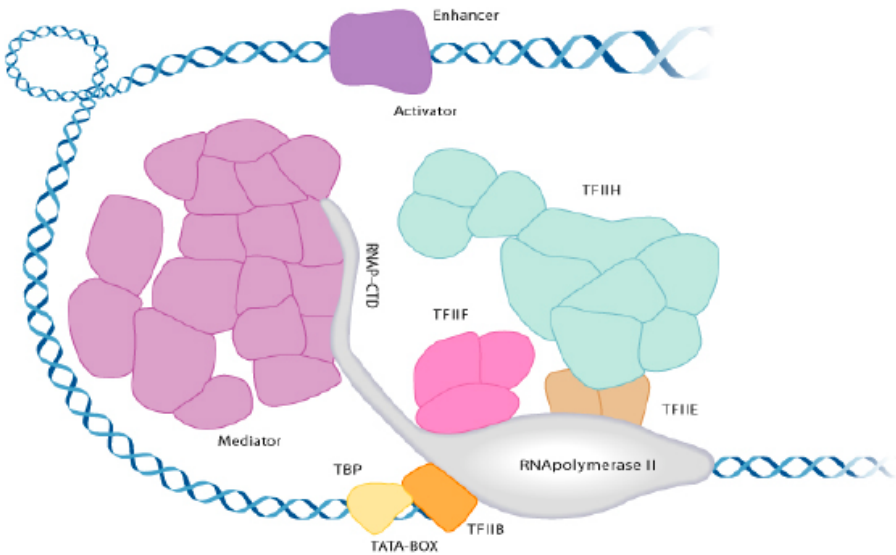

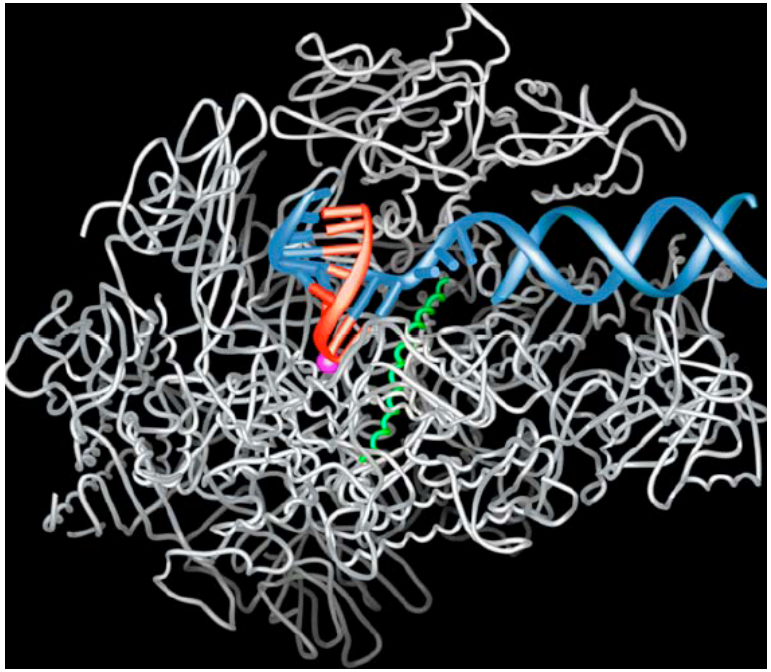

"Transcription is the process in a cell in which the genetic information stored in DNA is activated by the synthesis of complementary mRNA by enzymes called RNA polymerases. Eventually, the mRNA is translated by ribosomes into functional cell proteins. *Kornberg has made breakthrough progress in the molecular understanding of transcription and its regulation in eukaryotic cells. His combination of advanced biochemical techniques with* **structural determinations** *has enabled the atomic level reconstruction of RNA polymerase*".

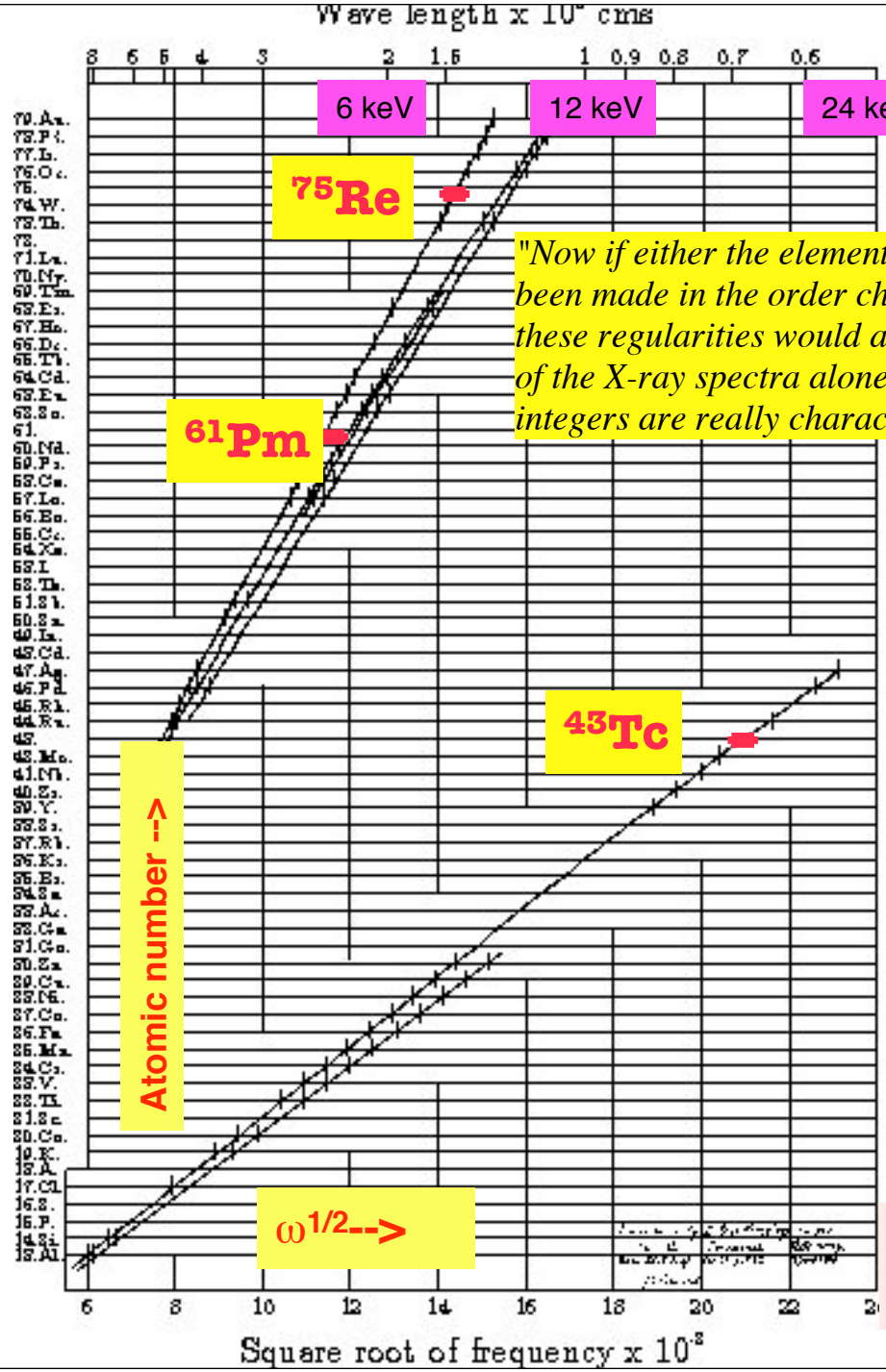

H.G. J. Moseley (1914)

"Now if either the elements were not characterized by these integers, or any mistake had been made in the order chosen or in the number of places left for unknown elements, these regularities would at once disappear. We can therefore conclude from the evidence of the X-ray spectra alone, without using any theory of atomic structure, that these integers are really characteristic of the elements."

Like Mendeelev's prediction of presence of Ga and Ge, Moseley, by plotting x-ray spectral energies against an integer number, predicted the presence of Tc, Pm,Hf, Os, and Re.

Another mystery was the presence of 2 lines for K-edges, and 4 lines for L-edges. This mystery could only be solved after the discovery of spin by Dirac.

Such a linear relationship does not exist In nuclear transitions

"curve drawn by H. G. J. Moseley in 1914 in the Electrical Laboratory.

(see Phil. Mag. Vol. 27. P703 April 1914) J S Townsend)."

Energy tunability, what does it mean ?

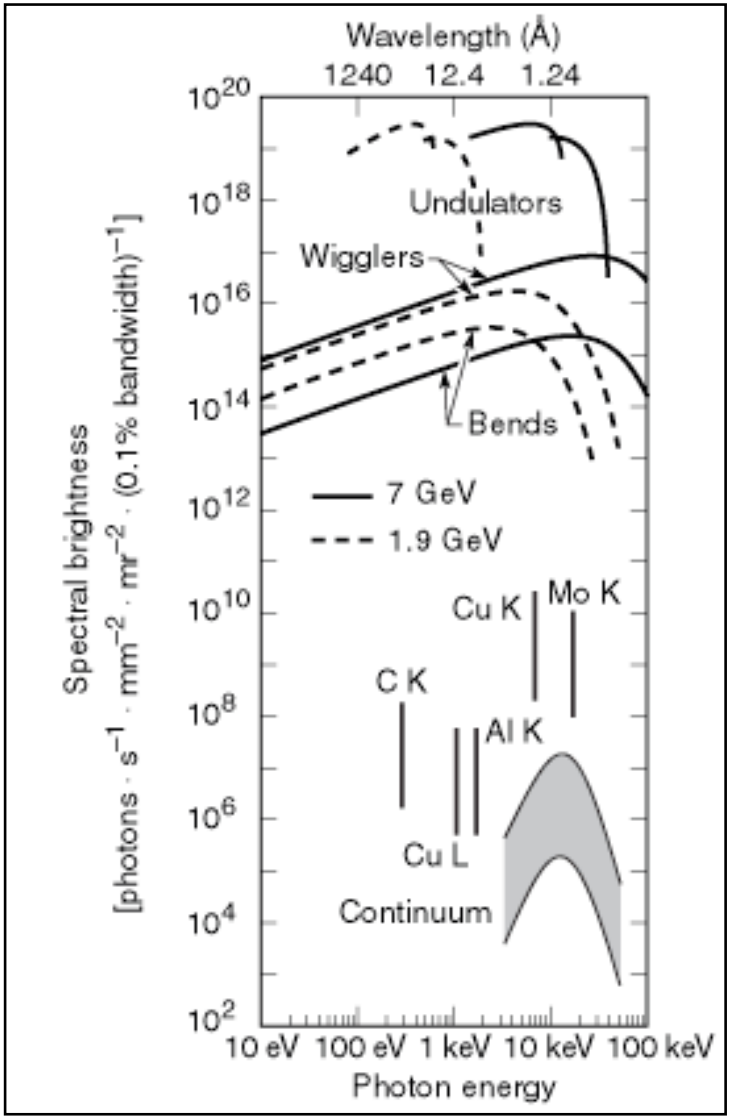

Table 1-1. Electron binding energies, in electron volts, for the elements in their natural forms.

Element	K 1s	L_1 2s	L_2 $2p_{1/2}$	L_3 $2p_{3/2}$	M_1 3s	M_2 $3p_{1/2}$	M_3 $3p_{3/2}$	M_4 $3d_{3/2}$	M_5 $3d_{5/2}$	N_1 4s	N_2 $4p_{1/2}$
1 H	13.6										
2 He	24.6*										
3 Li	54.7*										
4 Be	111.5*										
5 B	188*										
6 C	284.2*										
7 N	409.9*	37.3*									
8 O	543.1*	41.6*									
9 F	696.7*										
10 Ne	870.2*	48.5*	21.7*	21.6*							
11 Na	1070.8†	63.5†	30.65	30.81							
12 Mg	1303.0†	88.7	49.78	49.50							
13 Al	1559.6	117.8	72.95	72.55							
14 Si	1839	149.7*b	99.82	99.42							
15 P	2145.5	189*	136*	135*							
16 S	2472	230.9	163.6*	162.5*							
17 Cl	2822.4	270*	202*	200*							
18 Ar	3205.9*	326.3*	250.6†	248.4*	29.3*	15.9*	15.7*				
19 K	3608.4*	378.6*	297.3*	294.6*	34.8*	18.3*	18.3*				
20 Ca	4038.5*	438.4†	349.7†	346.2†	44.3 †	25.4†	25.4†				
21 Sc	4492	498.0*	403.6*	398.7*	51.1*	28.3*	28.3*				
22 Ti	4966	560.9†	460.2†	453.8†	58.7†	32.6†	32.6†				

Why synchrotron radiation for Mossbauer Spectroscopy ?

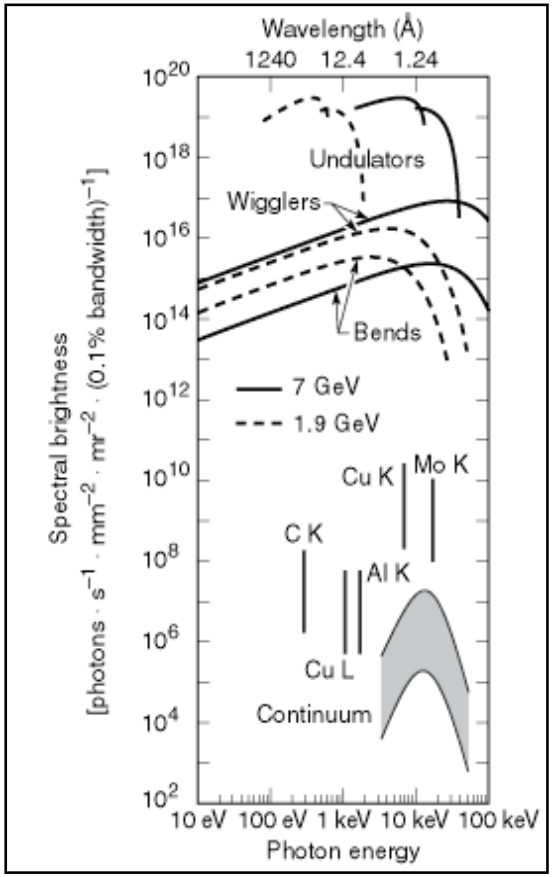

1. Bright and tunable over 100 keV with meV resolution
2. Collimated: good for monochromatization and focussing
3. Polarized; linear or circular with left or right handedness
4. Pulsed: suitable for time domain discrimination

Recoilless emission and absorption of γ- rays.

The distinction between x and γ is historical and relates to the origin of radiation:

electronic transitions :	x-rays
nuclear transitions :	γ-rays

They overlap in energy

^{181}Ta Mossbauer line:	6.238 keV γ-rays
U $_{K\alpha 1}$ - emission line:	98.439 keV x-rays

Energy tunability, what does it mean ?

Table 1-1. Electron binding energies (continued).

Element	K 1s	L_1 2s	L_2 $2p_{1/2}$	L_3 $2p_{3/2}$	M_1 3s	M_2 $3p_{1/2}$	M_3 $3p_{3/2}$	M_4 $3d_{3/2}$	M_5 $3d_{5/2}$	N_1 4s	N_2 $4p_{1/2}$	N_3 $4p_{3/2}$
71 Lu	63314	10870	10349	9244	2491	2264	2024	1639	1589	506.8*	412.4*	359.2*
72 Hf	65351	11271	10739	9561	2601	2365	2108	1716	1662	538*	438.2†	380.7†
73 Ta	67416	11682	11136	9881	2708	2469	2194	1793	1735	563.4†	463.4†	400.9†
74 W	69525	12100	11544	10207	2820	2575	2281	1872	1809	594.1†	490.4†	423.6†
75 Re	71676	12527	11959	10535	2932	2682	2367	1949	1883	625.4†	518.7†	446.8†
76 Os	73871	12968	12385	10871	3049	2792	2457	2031	1960	658.2†	549.1†	470.7†
77 Ir	76111	13419	12824	11215	3174	2909	2551	2116	2040	691.1†	577.8†	495.8†
78 Pt	78395	13880	13273	11564	3296	3027	2645	2202	2122	725.4†	609.1†	519.4†
79 Au	80725	14353	13734	11919	3425	3148	2743	2291	2206	762.1†	642.7†	546.3†
80 Hg	83102	14839	14209	12284	3562	3279	2847	2385	2295	802.2†	680.2†	576.6†
81 Tl	85530	15347	14698	12658	3704	3416	2957	2485	2389	846.2†	720.5†	609.5†
82 Pb	88005	15861	15200	13035	3851	3554	3066	2586	2484	891.8†	761.9†	643.5†
83 Bi	90524	16388	15711	13419	3999	3696	3177	2688	2580	939†	805.2†	678.8†
84 Po	93105	16939	16244	13814	4149	3854	3302	2798	2683	995*	851*	705*
85 At	95730	17493	16785	14214	4317	4008	3426	2909	2787	1042*	886*	740*
86 Rn	98404	18049	17337	14619	4482	4159	3538	3022	2892	1097*	929*	768*
87 Fr	101137	18639	17907	15031	4652	4327	3663	3136	3000	1153*	980*	810*
88 Ra	103922	19237	18484	15444	4822	4490	3792	3248	3105	1208*	1058	879*
89 Ac	106755	19840	19083	15871	5002	4656	3909	3370	3219	1269*	1080*	890*
90 Th	109651	20472	19693	16300	5182	4830	4046	3491	3332	1330*	1168*	966.4†
91 Pa	112601	21105	20314	16733	5367	5001	4174	3611	3442	1387*	1224*	1007*
92 U	115606	21757	20948	17166	5548	5182	4303	3728	3552	1439*b	1271*b	1043†

X-Ray Scattering

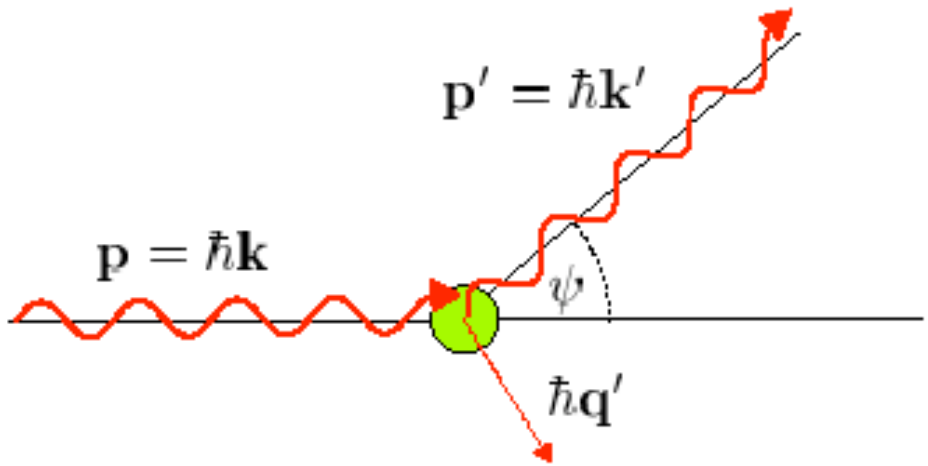

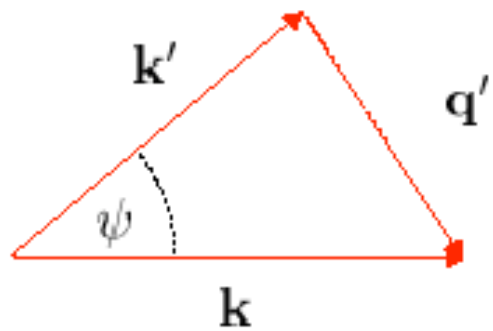

X-Ray Scattering

Elastic	Rayleigh or Thompson scattering, $E_i=E_f$
Inelastic	Compton scattering from free electrons, or scattering from collective excitations like phonons, $E_i \neq E_f$
Coherent	Path unknown: cross-correlation: e.g. diffraction
Incoherent	Path known; self-correlation: momentum integrated
Resonant	Near electronic or nuclear bound states: anomalous
Non-resonant	Away from resonances,
Grazing incidence total reflection	Micro-to-milliradians (1 degree= 17.5 mrad)
Small angle	Degrees
Wide angle	Tens of degrees
Surface diffraction	In-plane, crystal truncation rods, liquid structure
Polarization sensitive	Scattering from spin
X-ray interferometry	Bonse-Hart, Michelson-Morley, Fabry-Perot, …
X-ray standing wave	Surface structure and spectroscopy, Langmuir-Blodgett films
Time resoved	Minute-second-msec-μsec-nsec-psec-fsec From diffusion, to transport, to atomic bond formation

X-Ray Spectroscopy

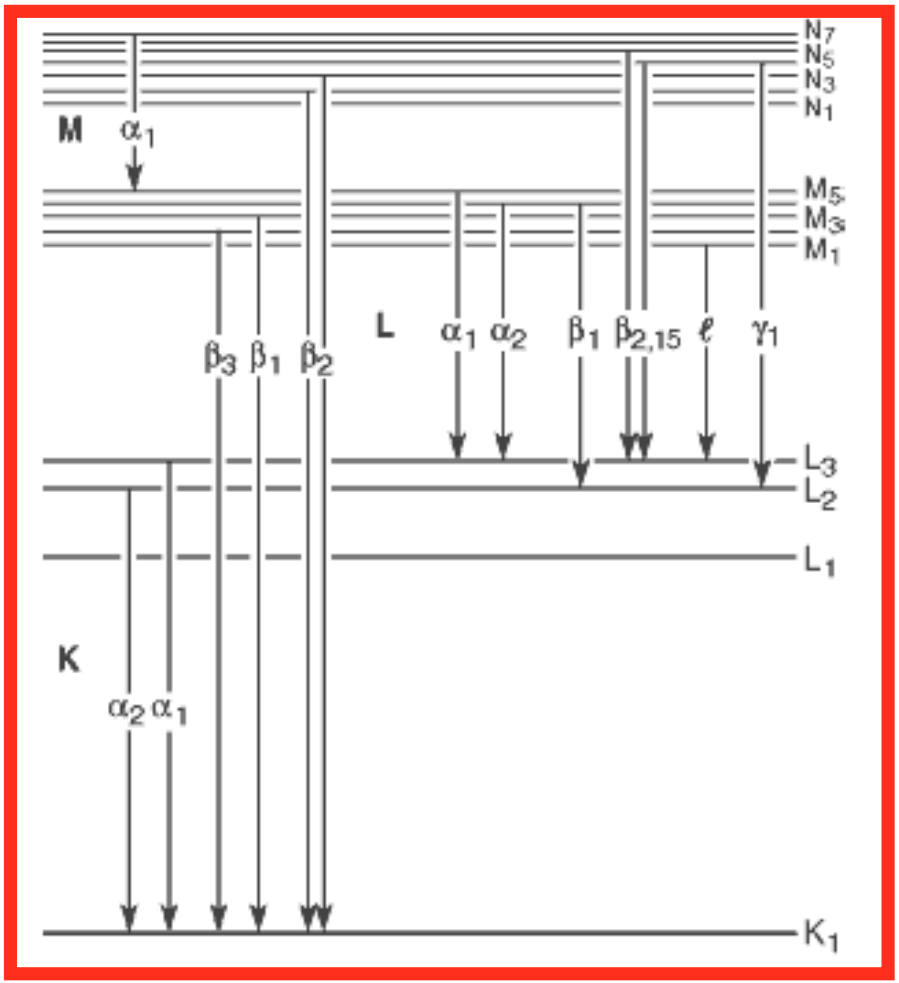

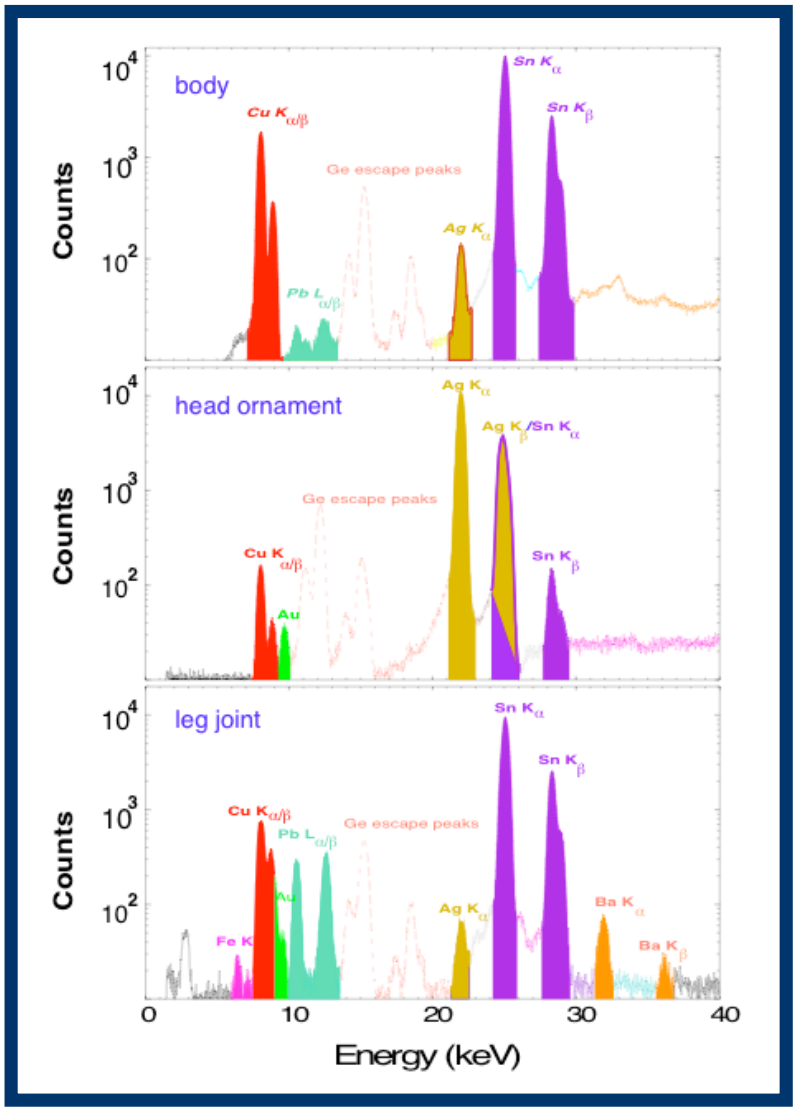

X-Ray Spectroscopy

X-ray absorption spectroscopy	**EXAFS**; atomic arrangements, bond distance, coordination no., symmtery, **XANES**: valence, **Magnetic circular dichroism**: spin-orbit magnetic moments
X-ray emission spectroscopy	Core-level atomic spectroscopy, valence
X-ray fluorescence spectroscopy	Quantitative analysis of elemental distribution
Inelastic x-ray scattering	Compton scattering for Fermi surface construction, phonon dispersion relations, phonon density of states, core-level spectroscopy, nuclear resonant scattering, x-ray Raman spectroscopy
X-Ray speckle spectroscopy	Slow dynamics from microscopic grains, correlation spectrosocpy in liquids,
X-Ray photoelectron spectroscopy	Valence level electron spectroscopy
Far and near Infra-red, VUV spectroscopy	Vibrational spectroscopy

Elements of Modern X-Ray Physics

Jens Als-Nielsen & Des McMorrow

J. Wiley, 2001

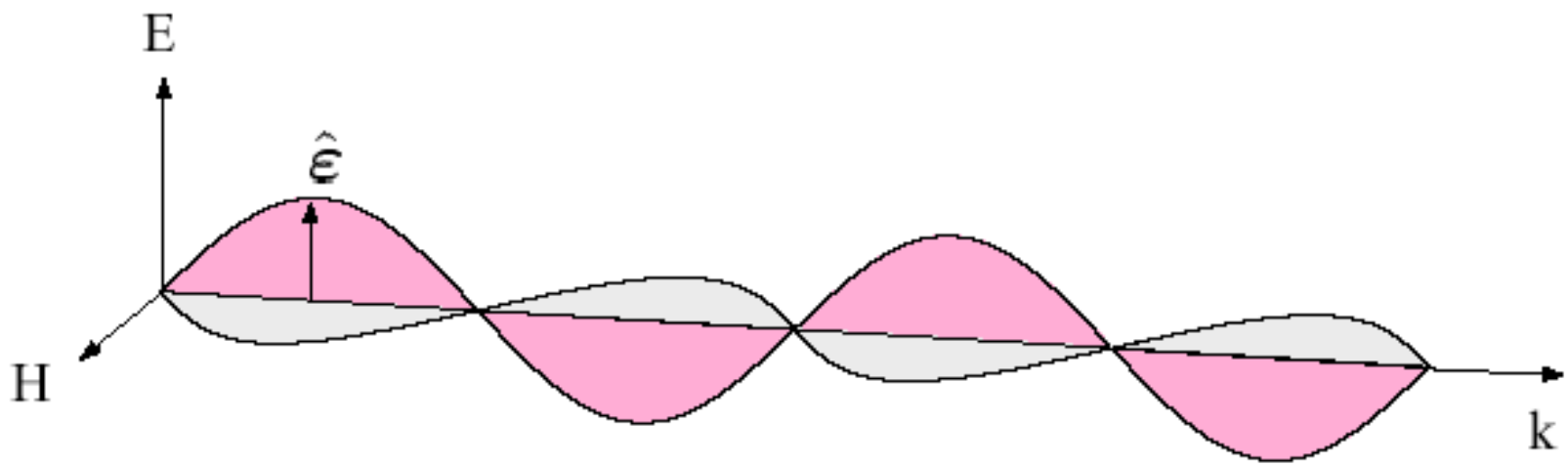

X-rays are transverse electromagnetic waves where electric and magnetic fields are perpendicular to the direction of propagation (Barla, 1904).

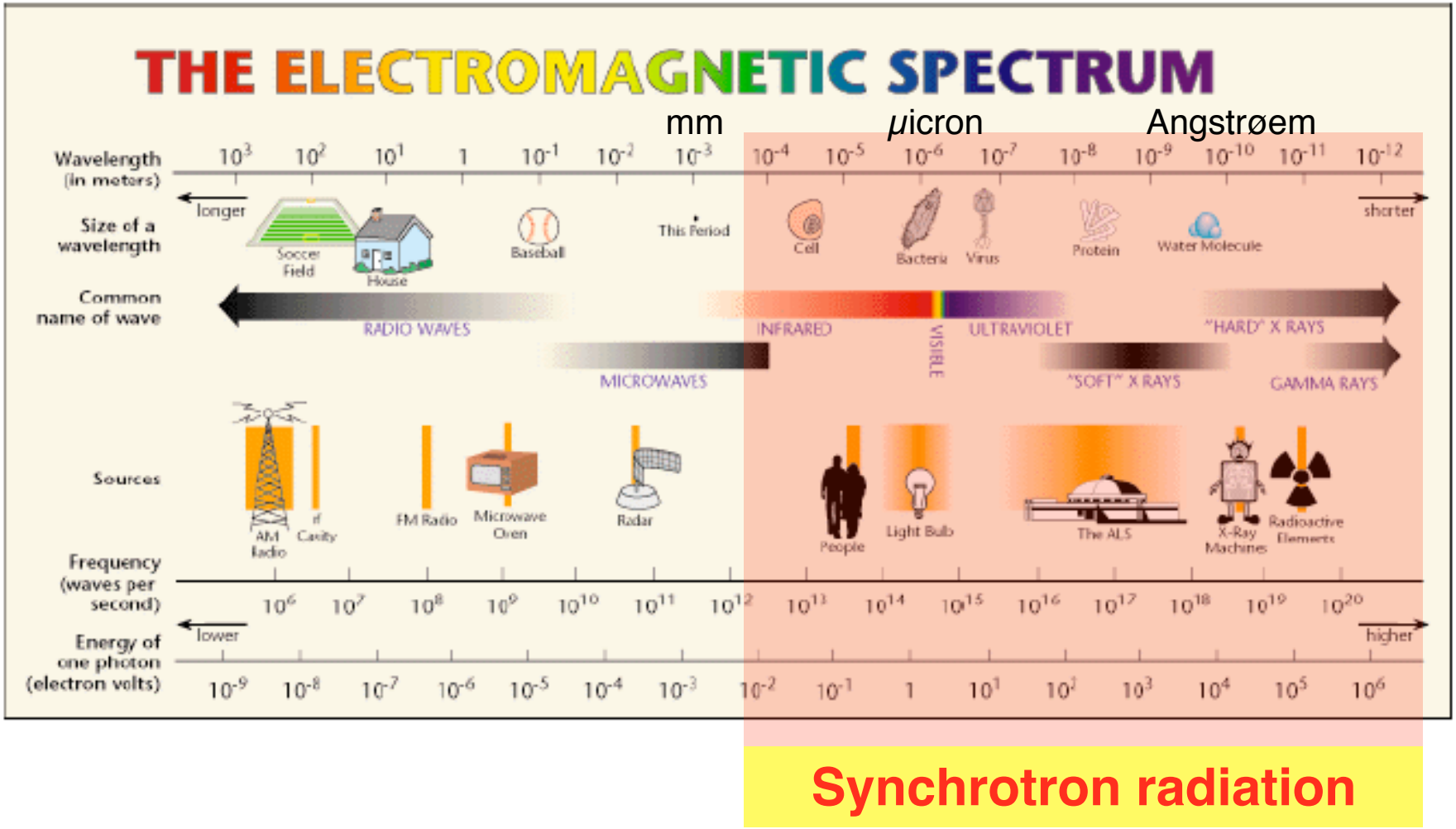

Synchrotron radiation

Electromagnetic waves

Spatial variation

k= wave number

λ=wavelength

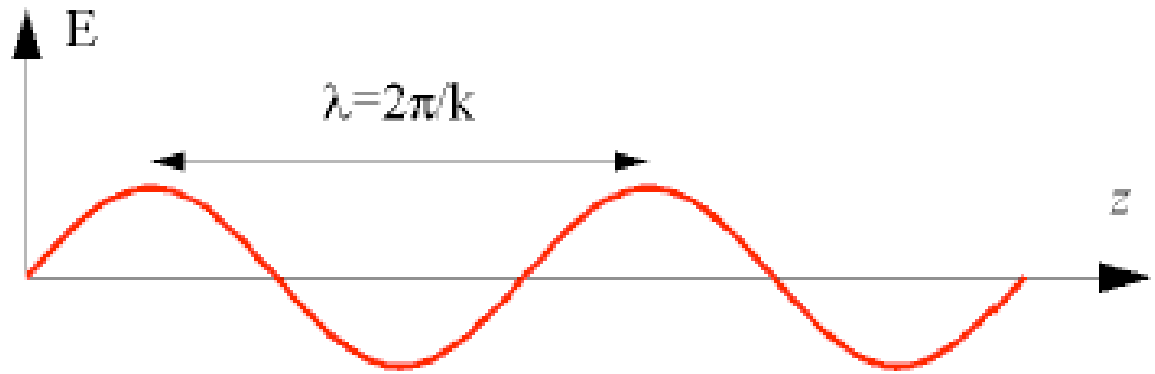

Temporal variation

ω = angular frequency

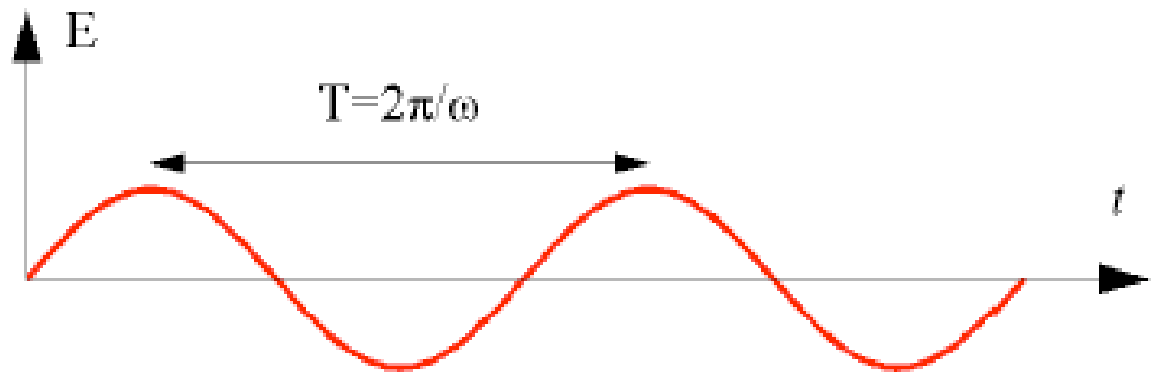

Top view showing high and low field amplitudes

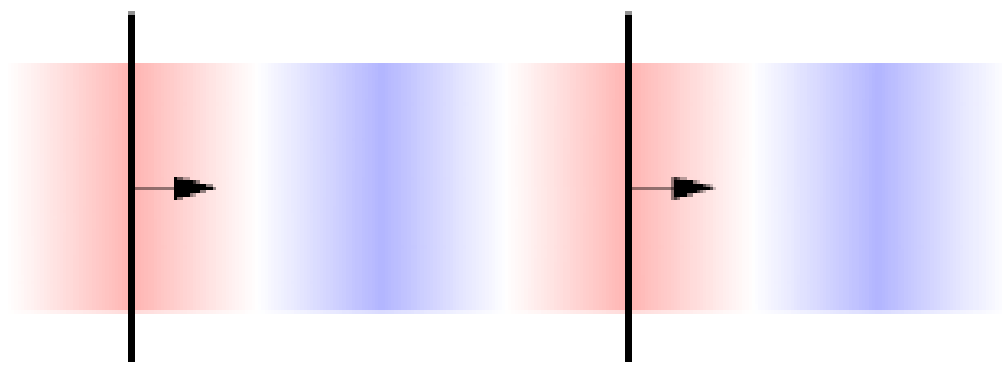

Classical description of scattering of radiation by a charged particle

In-plane

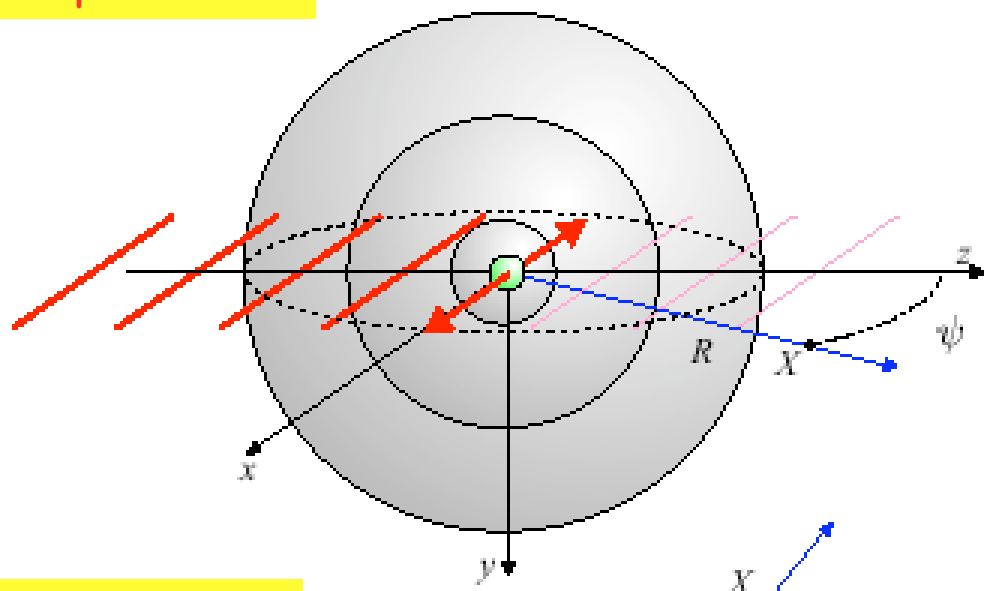

Out-of-plane

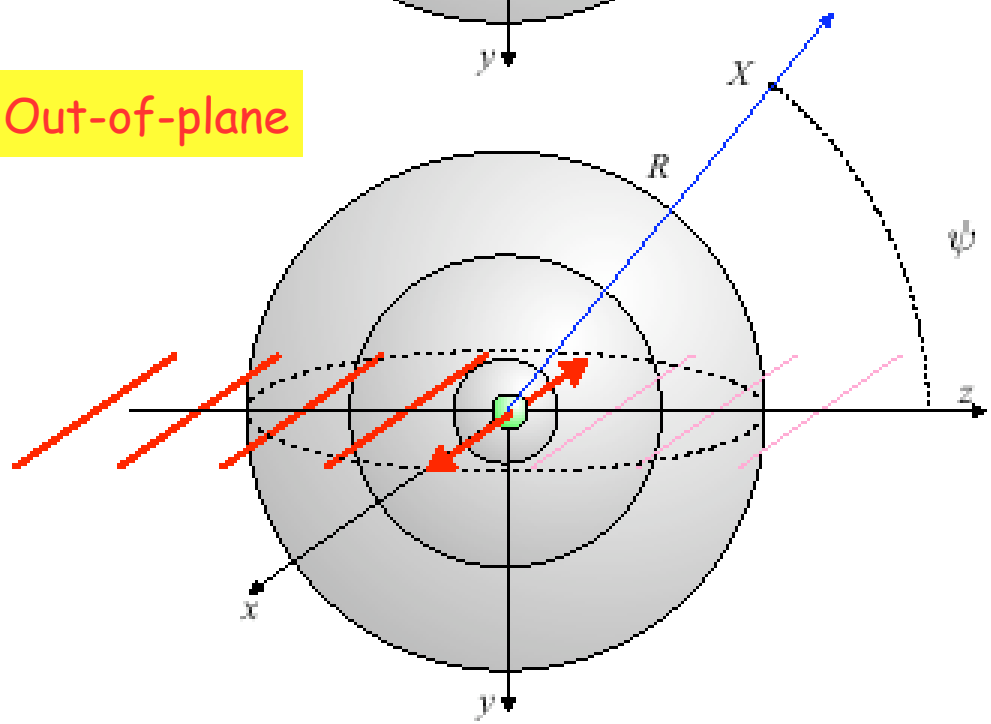

The incident plane wave incident upon an electron sets the electron in oscillation. The oscillating electron then radiates, experiencing a phase shift of π.

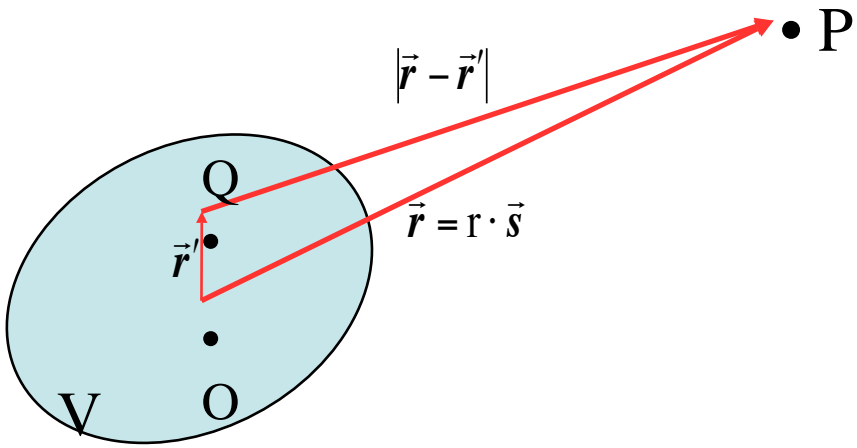

Principles of Optics

Born & Wolf

Cambridge University Press

7th edition (1999)

Scattering from one electron can be classically viewed as radiation emitted from a dipole.

The radiated field at a distance R as a function of time is given by:

$$E_{rad}(R,t) = \frac{-e}{4\pi\varepsilon_0 c^2 R} a_X(t'), \quad t' = t - R/c$$

Classical electron radius

Acceleration = force/mass

Acceleration seen by the observer at $\psi = \pi/2$ is zero:

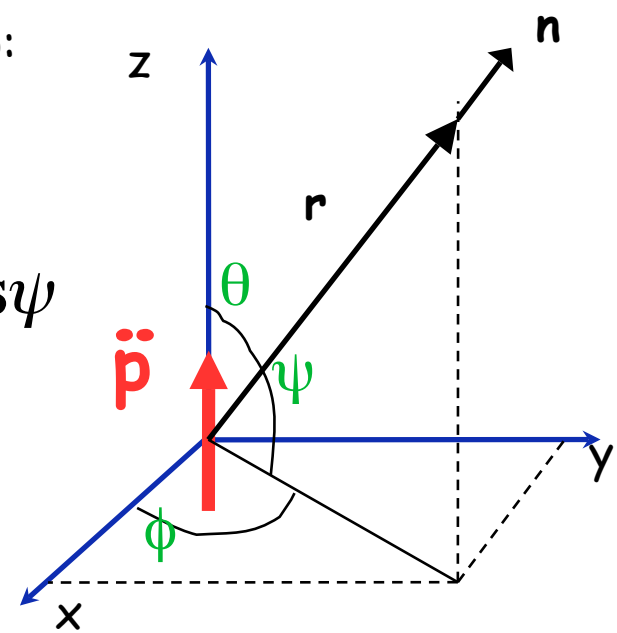

$$a_X(t') = \frac{-e}{m} E_{x0} e^{-i\omega t'} \cos\psi = \frac{-e}{m} E_{in} e^{-i\omega R/c} \cos\psi$$

$$E_{rad}(R,t) = -\frac{-e}{4\pi\varepsilon_0 c^2 R} \frac{-e}{m} E_{in} e^{-i\omega R/c} \cos\psi$$

$$\frac{E_{rad}(R,t)}{E_{in}} = -\frac{-e}{4\pi\varepsilon_0 c^2 R} \frac{-e}{m} \frac{e^{ikR}}{R} \cos\psi$$

$$r_0 = \frac{e^2}{4\pi\varepsilon_0 m c^2} = 2.82 \cdot 10^{-13} m$$

Classical electron radius

Thomson scattering length

Differential Scattering cross-section

$$\frac{I_{scattered}}{I_{incident}} = \left(\frac{d\sigma}{d\Omega}\right) = \frac{|E_{rad}|^2 R^2 \Delta\Omega}{|E_{inc}|^2 A_0} = r_0^2 \cos^2\psi$$

when all angles are included

$$\left(\frac{d\sigma}{d\Omega}\right) = \left(\frac{8\pi}{3}\right) r_0^2 = 0.655 \text{ barn, } 1 \text{ barn} = 10^{-24} \text{ cm}^2$$

The interesting aspect of this result is that the classical scattering Cross-section from an electron is INDEPENDENT of energy

Scattering cross-section (cont'd)

$$\left(\frac{d\sigma}{d\Omega}\right) = r_0^2 P$$

$$P = \begin{cases} 1 & \text{synchrotron radiation, vertical scattering plane} \\ \cos^2\varphi & \text{synchrotron radiation, horizontal scattering plane} \\ \frac{1}{2}\left(1+\cos^2\varphi\right) & \text{unpolarized source like x-ray tube} \end{cases}$$

Momentum and energy transfer in a scattering process

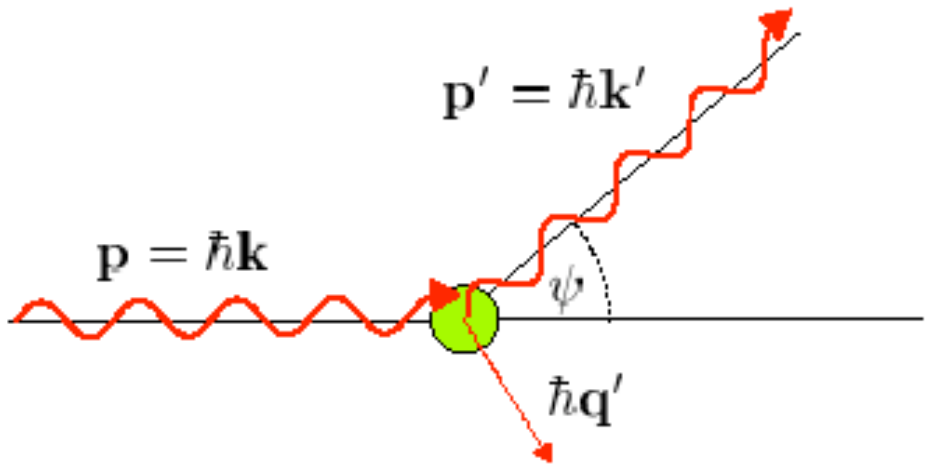

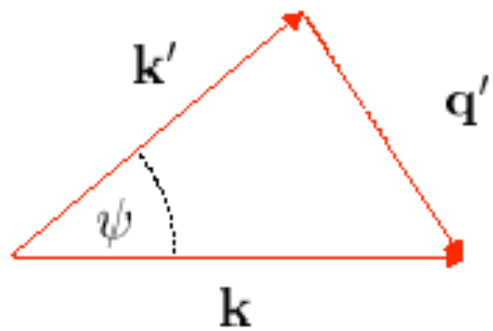

Scattering of electromagnetic waves from charged particles

Born Approximation

Consider a monochromatic electromagnetic field scattering from a isotropic, static medium with :

$$\nabla^2 E(r,\omega) + k^2 n^2(r,\omega) E(r,\omega) = 0$$

This equation has already some simplifications like dielectric constant has a slow variation with position, $\varepsilon(r,\omega) = n^2(r,\omega)$

where n is the index-of-refraction, or refraction index of the medium.

Born & Wolf, **Principles of Optics**, 7th edition, pp 695-700 (1999)

If we take a single Cartesian component of ***E (r,*ω*)*** as ***U (r,*ω*),***
we can write the following scalar equation ***:***

$$\nabla^2 U(\boldsymbol{r},\omega) + k^2 n^2(\boldsymbol{r},\omega) U(\boldsymbol{r},\omega) = 0$$

$$\nabla^2 U(\boldsymbol{r},\omega) + k^2 U(\boldsymbol{r},\omega) = -4\pi F(\boldsymbol{r},\omega) U(\boldsymbol{r},\omega)$$

$$F(\boldsymbol{r},\omega) = \frac{1}{4\pi}\left[n^2(\boldsymbol{r},\omega) - 1\right]$$ **: scattering potential**

If the field $U(\boldsymbol{r},\omega)$ is considered to be sum of incident and scattered fields

$$U(\boldsymbol{r},\omega) = U^i(\boldsymbol{r},\omega) + U^s(\boldsymbol{r},\omega)$$

One can approximate the incident field to be a plane wave,
which propogate according to Helmholtz equation:

$$(\nabla^2 + k^2) U^i(\boldsymbol{r},\omega) = 0$$

and the scattered field

$$(\nabla^2 + k^2) U^s(\boldsymbol{r},\omega) = -4\pi F(\boldsymbol{r},\omega) U(\boldsymbol{r},\omega)$$

An inhomogeneous differential equation can be solved using Green's function approach:

$$\left(\nabla^2 + \mathrm{k}^2\right) G(\vec{r} - \vec{r}', \omega) = -4\pi\delta\left(\vec{r} - \vec{r}'\right)$$

and choose $G(\vec{r} - \vec{r}', \omega) = \dfrac{e^{i\mathrm{k}|\mathbf{r}-\mathbf{r}'|}}{|\vec{r} - \vec{\mathrm{r}}'|}$

When the field propagates in a specific direction in real space,

$\vec{s}_0$**,the time independent part of** $U^i(r,w) = e^{\mathrm{ik}\,\vec{s}_0 \cdot \vec{r}}$**, and**

$$U(r,\omega) = e^{\mathrm{ik}\,\vec{s}_0 \cdot \vec{r}} + \int_V F(r',\omega)\, U(r',\omega) \frac{e^{i\mathrm{k}|\mathbf{r}-\mathbf{r}'|}}{|\vec{r} - \vec{\mathrm{r}}'|} \mathrm{d}^3\mathrm{r}'$$

This is an integral equation for the total field **U(r,**ω**)** within the scattering volume V. If the solution inside the volume V (i.e inside the scatterer, for which we have no idea, that's the reason we are doing the experiment) is known, then the solution for the exterior can be obtained.

First order Born approximation

For weakly scattering media, it is possible to obtain solution to the integral equation by a perturbation approach, provided that the scattering medium is weakly interacting with the probe of x-rays.

The first order Born approximation states that amplitude of the scattered wave far away from the scatterer depends entirely on one and only one Fourier component of the scattering potential, namely the one that corresponds to the transferred momentum $K=k(s-s_0)$.

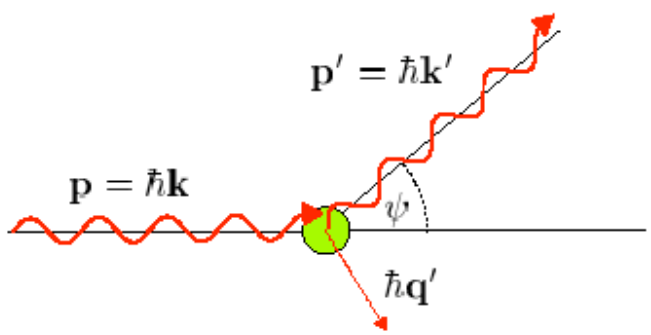

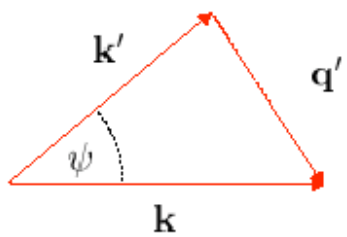

$K=k-k'$

Conservation of momentum has a correspondence between classical and quantum mechanical treatment:

$$\boldsymbol{p} = \hbar \boldsymbol{k}$$

$$\Delta \boldsymbol{p} = \boldsymbol{p} - \boldsymbol{p}' = \hbar \boldsymbol{k}'$$

If a plane wave is incident on the scatterer in the direction of s, the Fourier component of the scattering potential can be determined.

And if one has the ability to vary the amount of momentum transfer at will, then, the scattering potential can be reconstructed.

This is the essence of x-ray scattering experiments.

Scattering geometry and physics

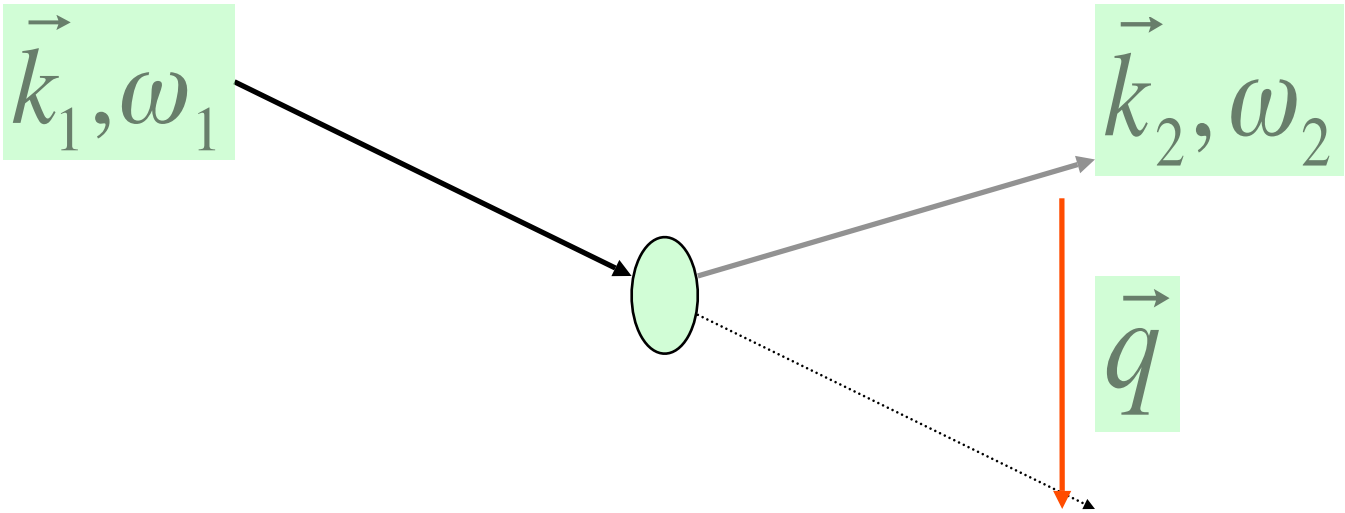

$\omega = \omega_1 - \omega_2$ energy transferred

$\vec{\mathbf{q}} = \vec{k}_1 - \vec{k}_2$ momentum transferred

Inelastic x-ray scattering geometry and physics

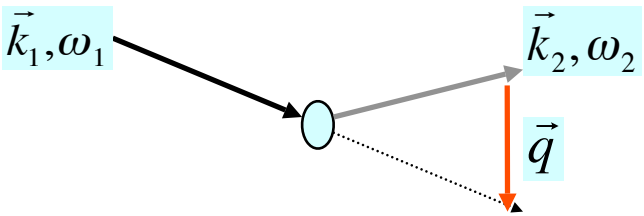

$\omega = \omega_1 - \omega_2$ energy transferred

$\mathbf{q} = \mathbf{k}_1 - \mathbf{k}_2$ momentum transferred

The goal of the experiments is to measure the scattering cross-section

$$\frac{d^2\sigma}{d\Omega d\omega}(\mathbf{q}, \hbar\omega)$$

$$\frac{d^2\sigma}{d\Omega d\omega}(q, \hbar\omega) \approx \left(\frac{d\sigma}{d\Omega}\right)_{Thompson} S(\mathbf{q}, \omega) + \text{ resonant terms}$$

$$S(\mathbf{q}, \omega) = \frac{1}{2\pi} \int dt e^{-i\omega t} \left\langle i \left| \sum_{jj'} e^{-i\mathbf{q}r_{j'}(t)} e^{i\mathbf{q}r_j(0)} \right| f \right\rangle$$

is the Fourier transform of the correlation of the phase of the scattering amplitude at different times

What is really measured ?

The goal of the experiments is to measure the scattering cross - section

$$\frac{d^2\sigma}{d\Omega\, d\omega}(\vec{\mathbf{q}}, \hbar\omega)$$

Double differential
Scattering cross-section

$$\frac{d^2\sigma}{d\Omega\, d\omega}(\vec{q}, \hbar\omega) \approx \left(\frac{d\sigma}{d\Omega}\right)_{Thompson} S(\vec{\mathbf{q}}, \omega) + \text{ resonant terms}$$

$$S(\vec{\mathbf{q}}, \omega) = \frac{1}{2\pi}\int dt e^{-i\omega t}\left\langle i \left| \sum_{jj} e^{-i\vec{\mathbf{q}} r_j(t)} e^{i\vec{\mathbf{q}} r_j(0)} \right| f \right\rangle$$

is the Fourier transform of the correlation of the phase of the scattering amplitude at different times

Scattering geometry and physics

The physical origin of the correlations depends on how $1/\vec{\mathbf{q}}$ compares with l_c, the characteristic length, of the system related to the spatial inhomogeneity.

when $\vec{\mathbf{q}} \cdot l_c << 1 \quad \Rightarrow$ COLLECTIVE BEHAVIOUR

when $\vec{\mathbf{q}} \cdot l_c >> 1 \quad \Rightarrow$ SINGLE PARTICLE BEHAVIOUR

when $\dfrac{1}{\vec{\mathbf{q}}} \approx d$ and $\omega \approx$ phonon frequency $\Rightarrow$ Collective ion excitation

when $\dfrac{1}{\vec{\mathbf{q}}} \approx r_c$ and $\omega \approx$ plasma frequency $\Rightarrow$ Valence electron excitation

What is being measured ?

$$\frac{d^2\sigma}{d\Omega\, \mathrm{d}\omega} = \underbrace{r_0^2 \frac{\omega_f}{\omega_i} \left|\mathbf{e}_i \cdot \mathbf{e}_f\right| N \sum_{i,f}}_{\text{Thomson cross section}} \underbrace{\left|\left\langle i \left| \sum e^{i\mathbf{Q}\mathbf{r}_\mathbf{j}} \right| f \right\rangle\right|^2 \delta(E_f - E_i - \mathbf{h}\omega)}_{\text{Dynamical structure factor S(Q,w)}}$$

$$S(\mathbf{Q},\omega) = \frac{1}{2\pi} \int dt\, e^{-i\omega t} \underbrace{\left\langle \phi_i \left| \sum_{ll'} f_l(\mathbf{Q}) e^{-i\mathbf{Q}\cdot\mathbf{r}_l(t)} f_{l'}(\mathbf{Q}) e^{i\mathbf{Q}\cdot\mathbf{r}_{l'}(0)} \right| \phi_i \right\rangle}_{\text{Density-density correlations}}$$

IXS: Inelastic X-Ray Scattering

IXS is a measurement technique based on knowledge of exact energy and momentum transfer realized during a scattering experiment, revealing dynamic information about the scattering system.

Since x-ray energies may extend from a few eV to a few hundred keV, and since it is possible to measure energy loss or gain with a resolution from nano-eV to keV, the type of dynamic phenomena observed in an IXS experiment extends from nuclear hyperfine interactions to collective excitations of atoms such as phonons, to electronic excitations like plasmons or magnons, and eventually core-valence electron boundary to reconstruct the Fermi surface or determine orbital occupancies.

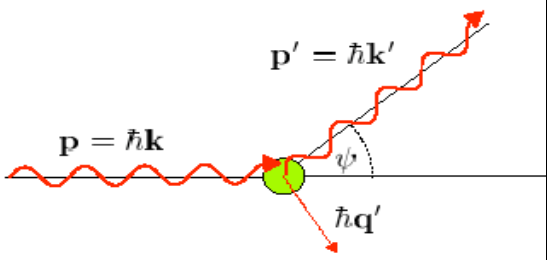

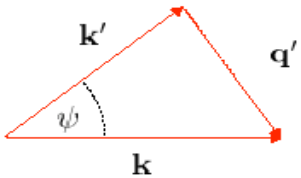

Parallel to the development of experimental energy and momentum resolution capabilities, the IXS methods have multiplied during the last century.

Starting with P. Debye, A. Compton and J. DuMond, and directly benefitting from the development of pure silicon and germanium, as well as synchrotron radiation and sophisticated detectors and analyzers, there are now many different IXS methods, often with overlapping and confusing names.

$\omega = \omega_1 - \omega_2$ energy transferred

$\vec{\mathbf{q}} = \vec{k}_1 - \vec{k}_2$ momentum transferred

IXS NRIXS Compton XRS RIXS MCS

NIS XES IUVS ....

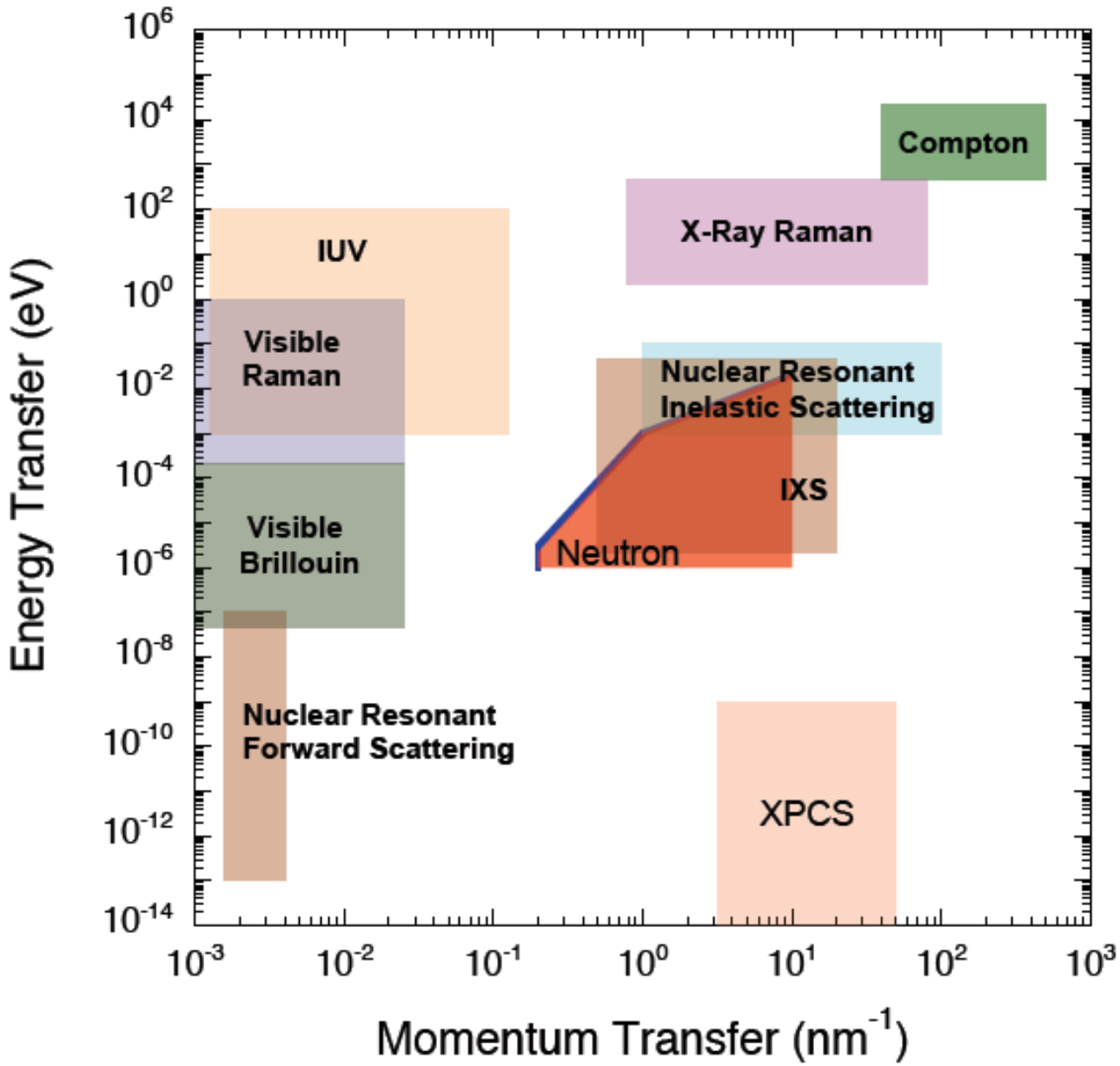
Energy Transfer (eV)
Momentum Transfer (nm^{-1})
10^{6}
10^{4}
10^{2}
10^{0}
10^{-2}
10^{-4}
10^{-6}
10^{-8}
10^{-10}
10^{-12}
10^{-14}
10^{-3}
10^{-2}
10^{-1}
10^{0}
10^{1}
10^{2}
10^{3}
Compton
X-Ray Raman
IUV
Visible Raman
Nuclear Resonant Inelastic Scattering
IXS
Neutron
Visible Brillouin
Nuclear Resonant Forward Scattering
XPCS

A SHORT SUMMARY OF CURRENT INELASTIC X-RAY SCATTERING TECHNIQUES

Technique	Source of interaction	Typical resolution	Deetection method	Location at the APS
Momentum-resolved, high energy resolution IXS: HERIX	Collective excitations of atoms, ions, molecules, PHONONS	1-3 meV	Back-scattering, curved and diced crystal analyzer	3-ID
Momentum-resolved, medium energy resolution resonant IXS: MERIX	Valence electrons near Fermi level	100-500 meV	Near-back-scattering, curved and diced crystal analyzer	9-ID, 12-ID, 33-ID
Momentum-integrated, nuclear resonant IXS: NRIXS	Collective excitations monitored through a nuclear resonance	0.5-2 meV	Nano-second time resolved detectors monitoring nuclear level decay	3-ID, 16-ID
High resolution Compton scattering: CS	Core and valence electrons	1 eV	Triple Laue crystal analyzer, PSD detector	
Magnetic Compton scattering: MCS	Spin polarized electrons	100 eV	Solid state detector	11-ID
X-ray Raman spectroscopy: XRS	Core electron excitations of low-Z elements	1 eV	Back-scattering curved flat analyzers	13-ID, 16-ID
X-ray emission spectroscopy: XES	X-ray fluorescence by incident photons: photon-in/photon-out	0.5 eV	Back-scattering curved flat analyzers	10-ID
Soft-X-ray IXS : PEEM	x-ray induced photoemission: photon-in/electron-out	5 meV	Electron spectrometer	4-ID

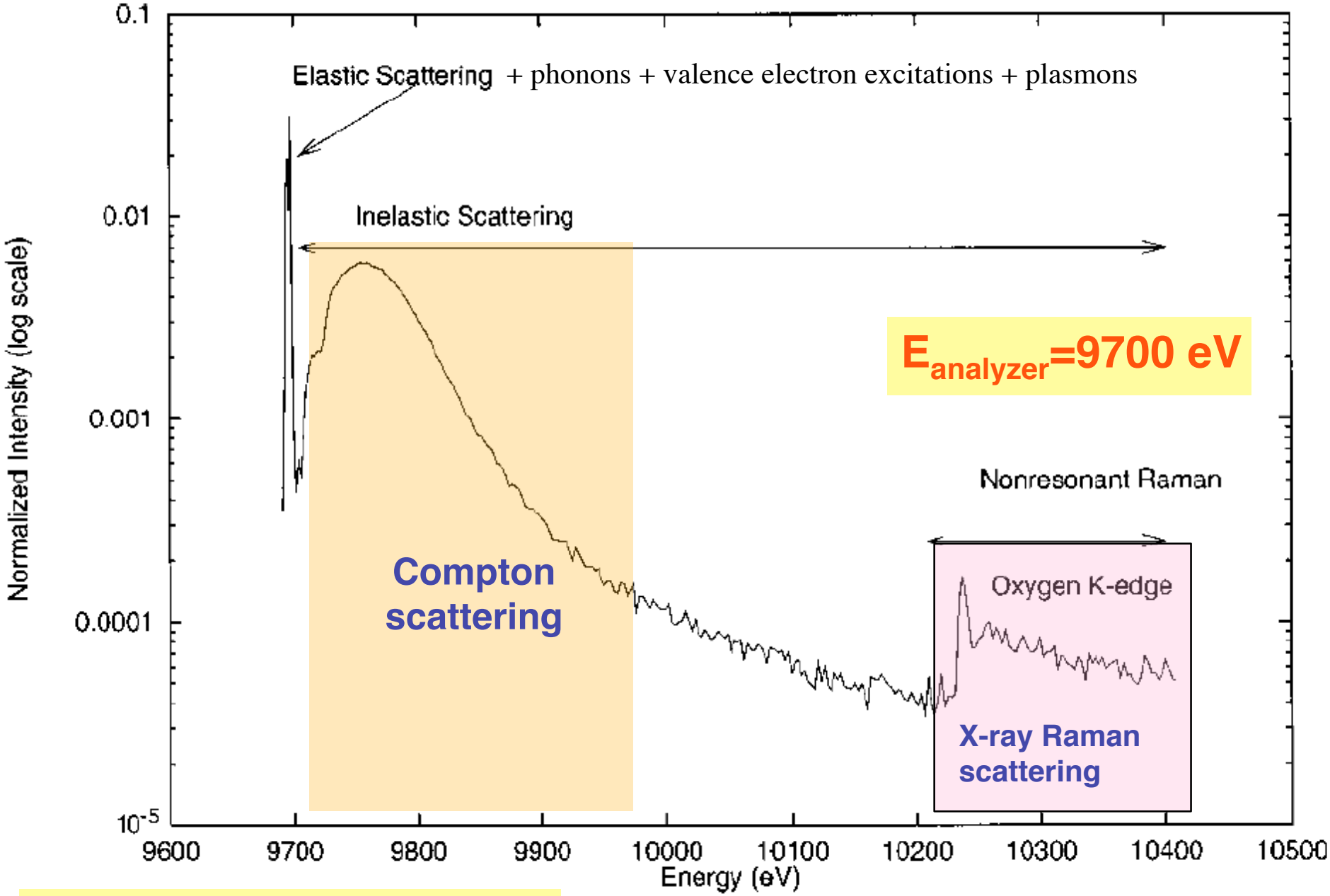

(D.T. Bowron et al, Phys. Rev. B 62 R9223)

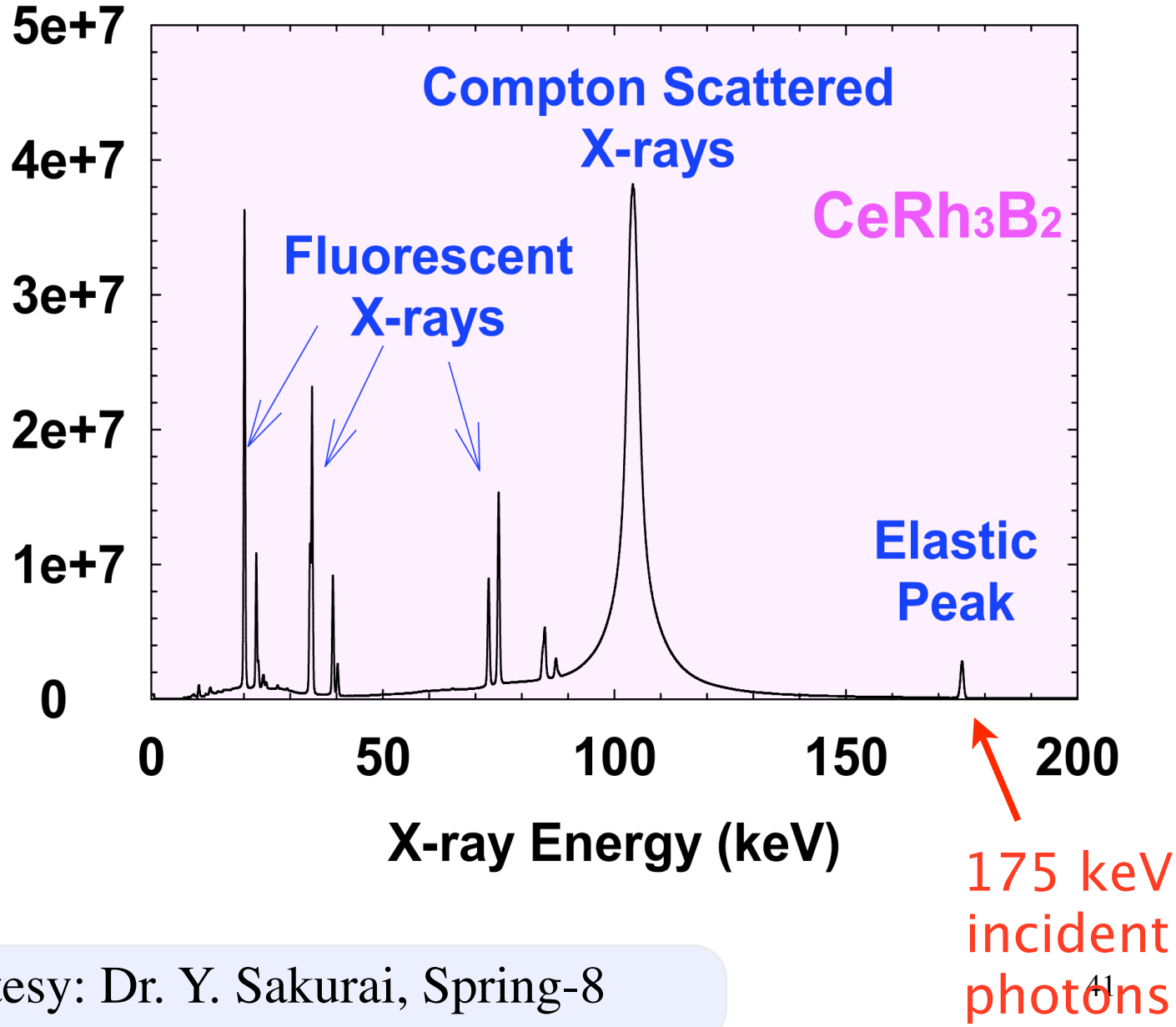

Courtesy: Dr. Y. Sakurai, Spring-8

Part 2

HERIX: High Energy Resolution Inelastic X-Ray scattering with meV and momentum resolution

What is it ?

- **High Resolution Inelastic X-Ray Scattering (IXS)**
  - Scattering from spatially localized or dispersed collective atomic or ionic excitations like PHONONS.
  - **Energy range: 15-30 keV,**
  - **Incident beam: monochromatic to 1 meV level, tunable over several eV,**
  - **Scattered beam: Incoherent, polychromatic over several hundred meV**
  - **Analyzer: Bent, diced or Si, crystal analyzer, temperature stabilized to 10 mK**
  - **Energy Resolution : ~ 1-2 meV**
  - **Momentum transfer: Relevant to distinguish localized versus spatially dispersed excitations, sound velocity, phonon dispersion curves**
- **Main Features:**
  - **Allows determination of phonon dispersion relations without any kinematic limitation that is suffered by neutrons, works for most elements, liquids and solid alike, suitable for extreme conditions**

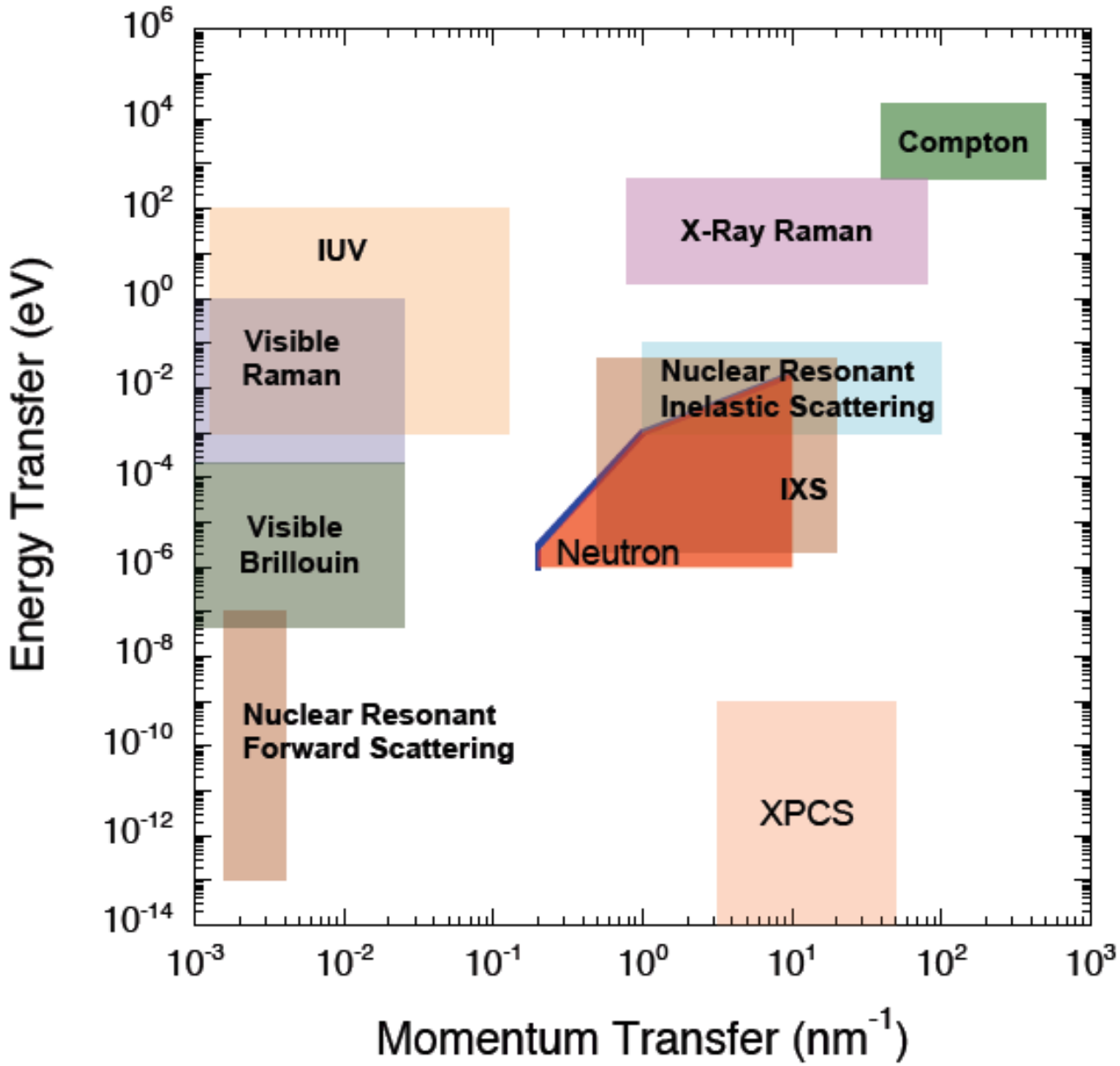
Compton
X-Ray Raman
IUV
Visible
Raman
Nuclear Resonant
Inelastic Scattering
IXS
Visible
Brillouin
Neutron
Nuclear Resonant
Forward Scattering
XPCS
Energy Transfer (eV)
Momentum Transfer (nm^{-1})
10^{6}
10^{4}
10^{2}
10^{0}
10^{-2}
10^{-4}
10^{-6}
10^{-8}
10^{-10}
10^{-12}
10^{-14}
10^{-3}
10^{-2}
10^{-1}
10^{0}
10^{1}
10^{2}
10^{3}

A SHORT SUMMARY OF CURRENT INELASTIC X-RAY SCATTERING TECHNIQUES

Technique	Source of interaction	Typical resolution	Deetection method	Location at the APS
Momentum-resolved, high energy resolution IXS: HERIX	Collective excitations of atoms, ions, molecules, PHONONS	1-3 meV	Back-scattering, curved and diced crystal analyzer	3-ID
Momentum-resolved, medium energy resolution resonant IXS: MERIX	Valence electrons near Fermi level	100-500 meV	Near-back-scattering, curved and diced crystal analyzer	9-ID, 12-ID, 33-ID
Momentum-integrated, nuclear resonant IXS: NRIXS	Collective excitations monitored through a nuclear resonance	0.5-2 meV	Nano-second time resolved detectors monitoring nuclear level decay	3-ID, 16-ID
High resolution Compton scattering: CS	Core and valence electrons	1 eV	Triple Laue crystal analyzer, PSD detector	
Magnetic Compton scattering: MCS	Spin polarized electrons	100 eV	Solid state detector	11-ID
X-ray Raman spectroscopy: XRS	Core electron excitations of low-Z elements	1 eV	Back-scattering curved flat analyzers	13-ID, 16-ID
X-ray emission spectroscopy: XES	X-ray fluorescence by incident photons: photon-in/photon-out	0.5 eV	Back-scattering curved flat analyzers	10-ID
Soft-X-ray IXS : PEEM	x-ray induced photoemission: photon-in/electron-out	5 meV	Electron spectrometer	4-ID

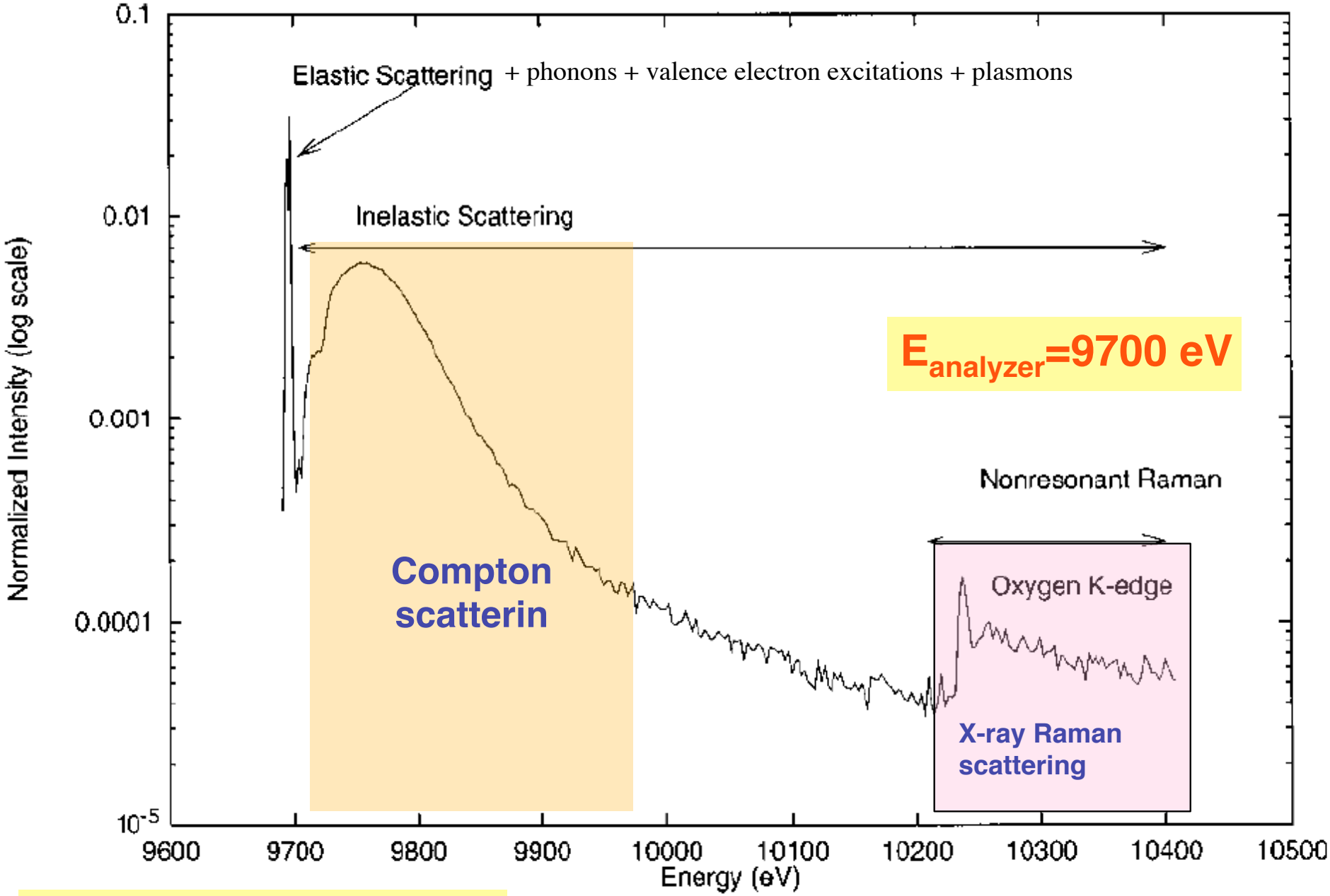

(D.T. Bowron et al, Phys. Rev. B 62 R9223)

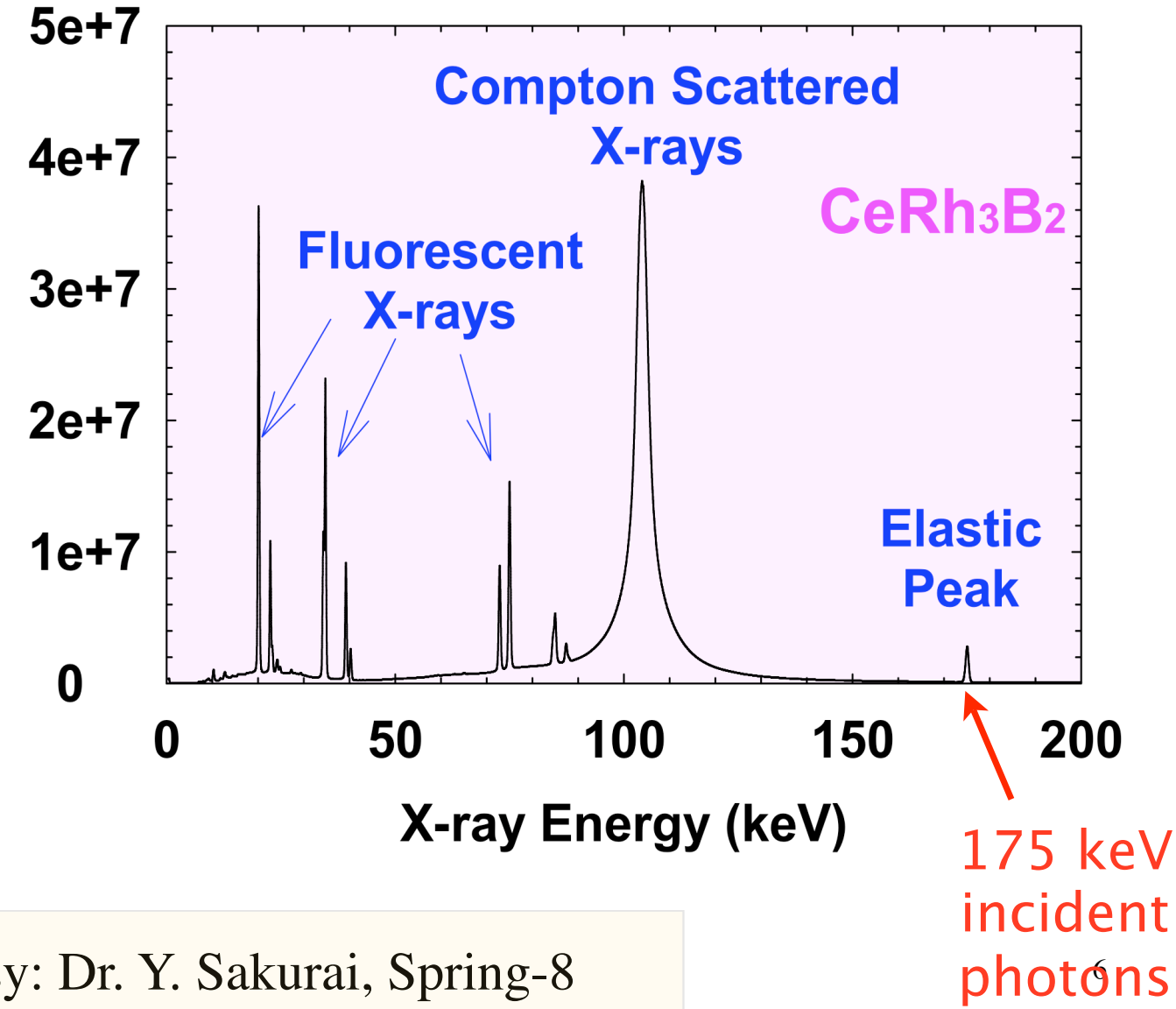

Courtesy: Dr. Y. Sakurai, Spring-8

Why X-Rays ?

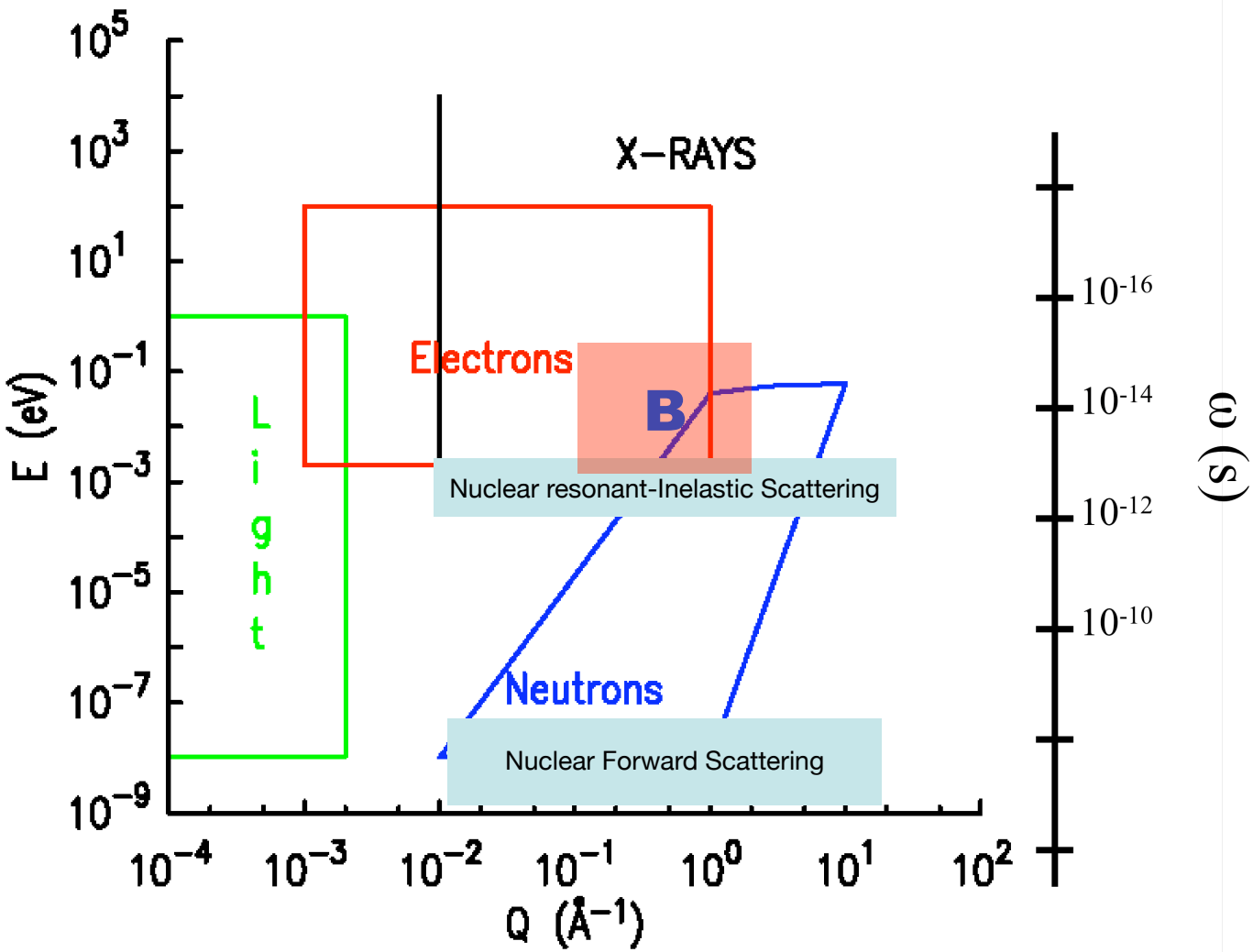
X-RAYS
Electrons
B
Light
Nuclear resonant-Inelastic Scattering
Neutrons
Nuclear Forward Scattering
E (eV)
Q (Å⁻¹)
ω (s)

Why x-rays instead of neutrons or visible light ?

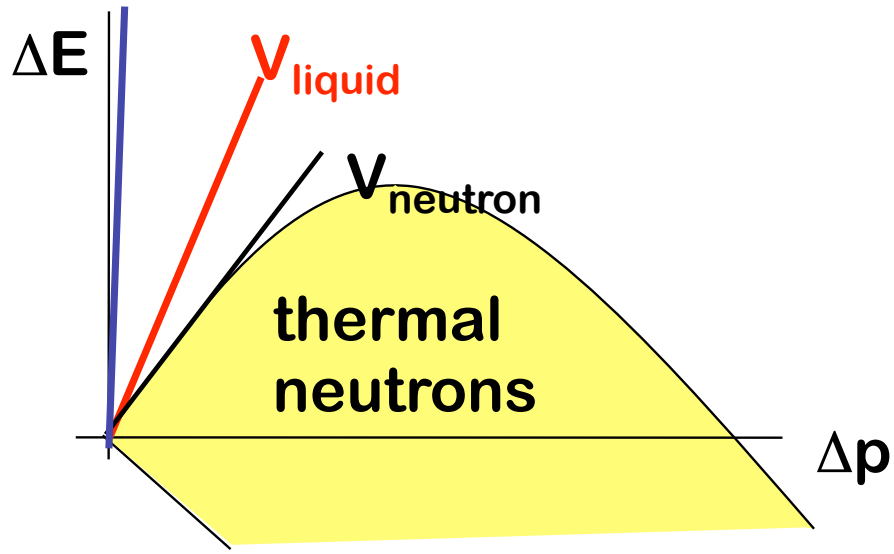

Limited momentum transfer capability of neutrons at low energies favor x-rays to study collective excitations with large dispersion, like sound modes.

When the sound velocity exceeds that of neutrons in the liquid, x-rays become unique. The low-momentum/high-energy transfer region is only accessible by x-rays.

High Melting Point Substances

Lindemann criterion: $mv_{sound}^2 \propto T_{melt}$

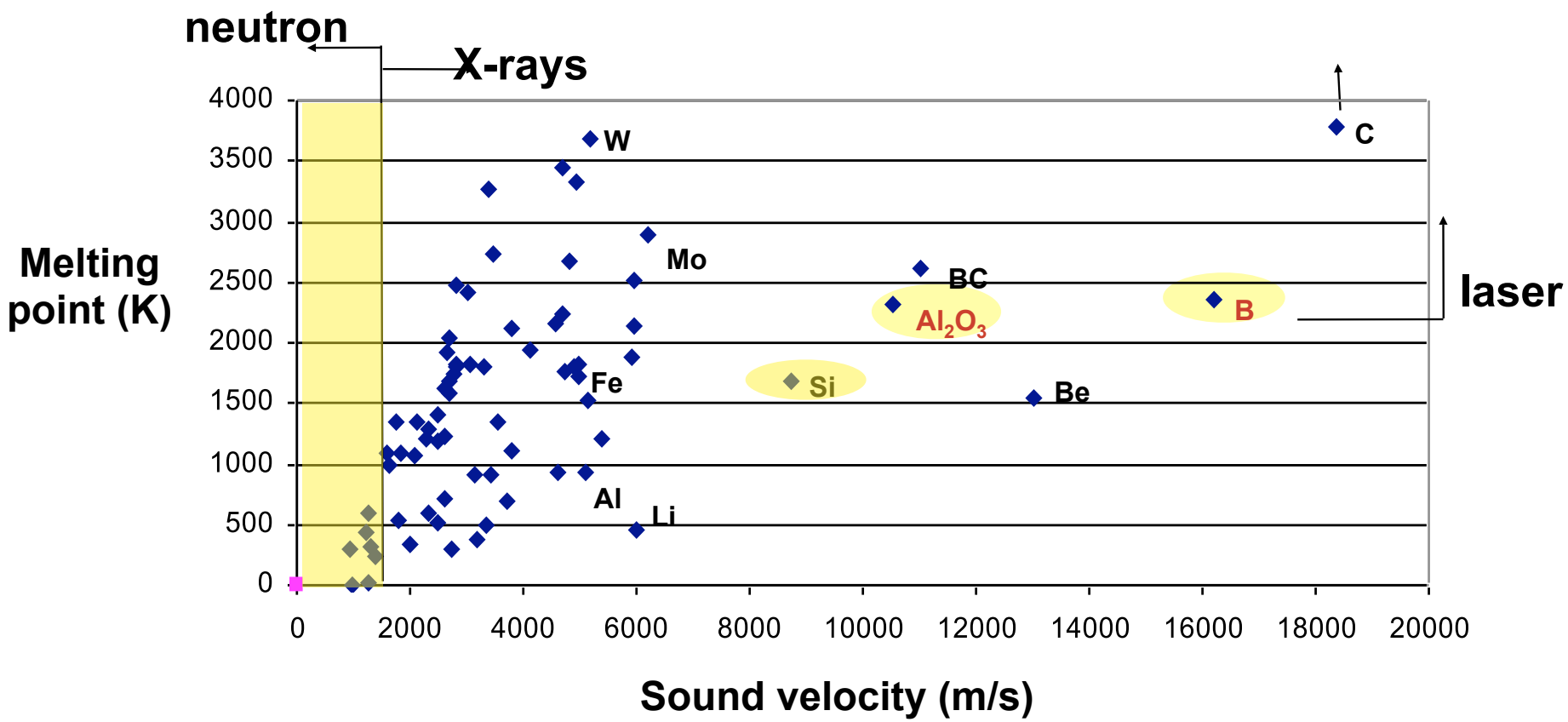

Why synchrotron radiation for Spectroscopy ?

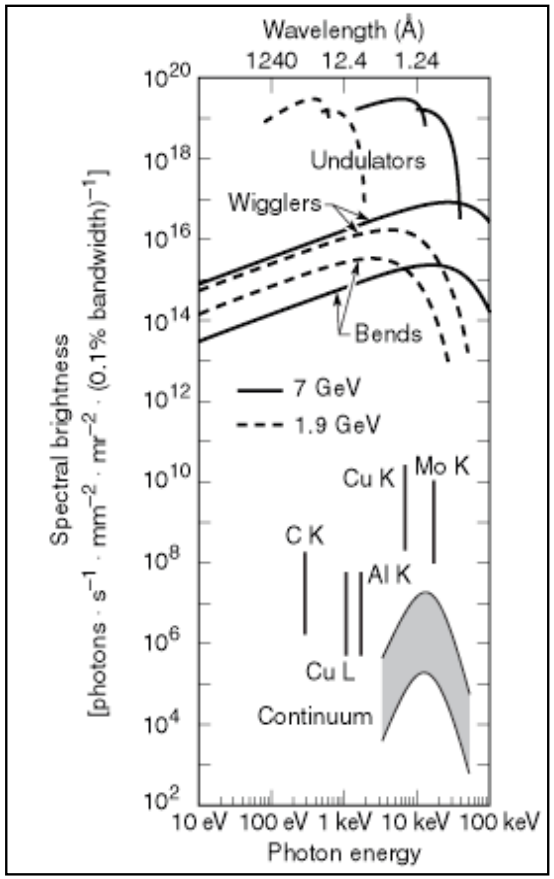

1. Bright and tunable over 100 keV with meV resolution
2. Collimated: good for monochromatization and focussing
3. Polarized; linear or circular with left or right handedness
4. Pulsed: suitable for time domain discrimination
5. Coherent: suitable for speckle and lensless imaging

The distinction between x and γ is historical and relates to the origin of radiation:

electronic transitions : x-rays
nuclear transitions : γ-rays

They overlap in energy

^{181}Ta Mössbauer line: 6.238 keV γ-rays
U $_{K\alpha 1}$ - emission line: 98.439 keV x-rays

Kinematics of Scattering : x-rays

$$\mathbf{Q} = \mathbf{k_i} - \mathbf{k_f}$$

$$\Delta E = E_f - E_i$$

$$Q^2 = k_i^2 + k_f^2 - 2k_i k_f \cos\theta$$

$$(Q/k_i)^2 = 1 + (1 - \Delta E/E_i)^2 - 2(1 - \Delta E/E_i)\cos\theta$$

$$E = hck$$

$$\Delta E << E_i$$

$$(Q/k_i) = 2\sin(\theta/2)$$

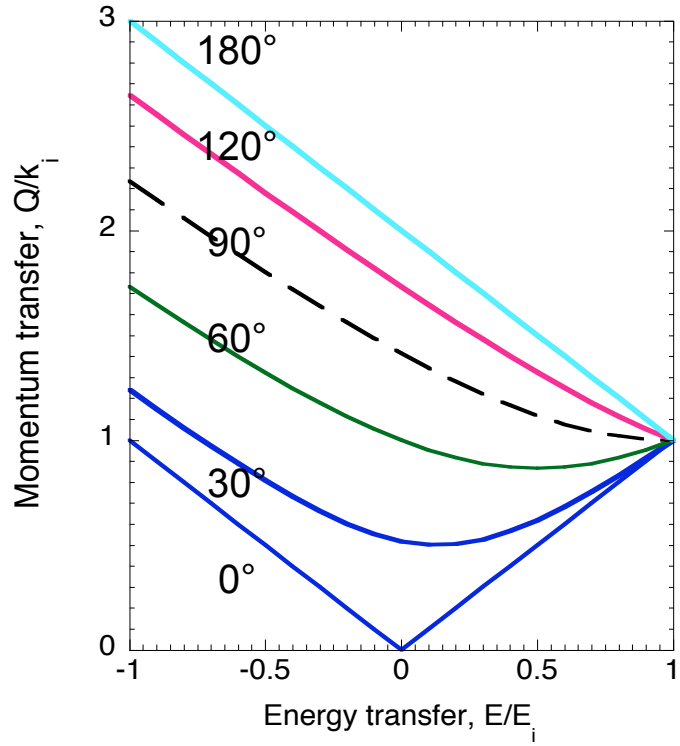

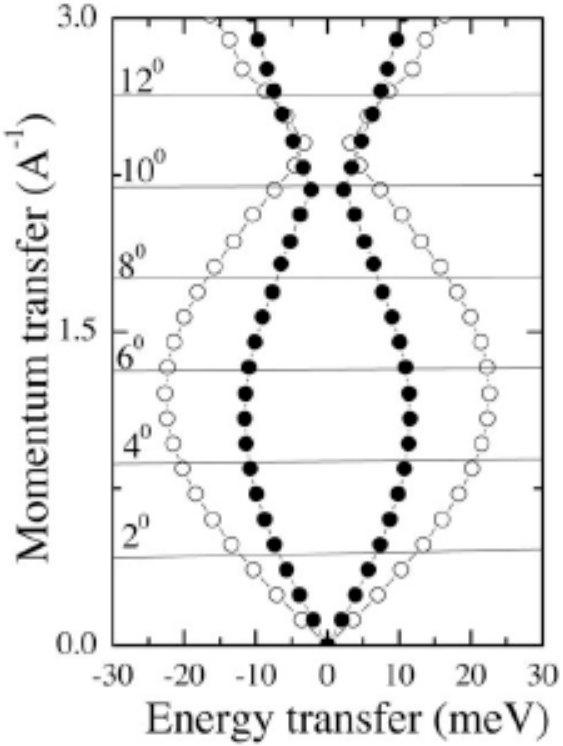

T. Scopingo, et al, Rev.Mod.Phys., 77 (2005) 881

Kinematics of Scattering : Neutrons

$$E(k) = \hbar^2 k^2 / 2m$$

$$\left(Q/k_i\right)^2 = 1 + (1 - \Delta E/E_i) - 2\sqrt{(1 - \Delta E/E_i)}\cos\theta$$

$\Delta E << E_i$ no longer true

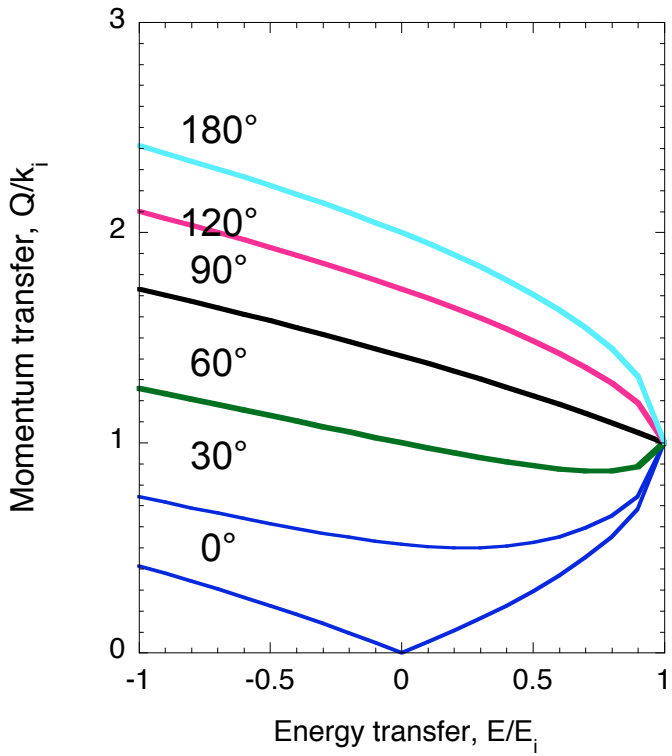

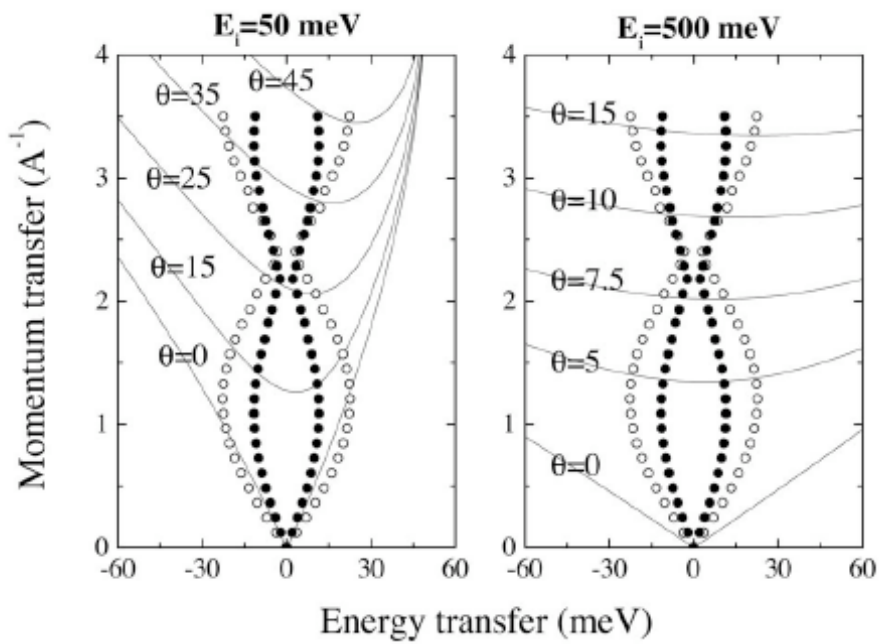

T. Scopingo, et al, Rev.Mod.Phys., 77 (2005) 881

Kinematics of Scattering : X-Rays versus Visible Light

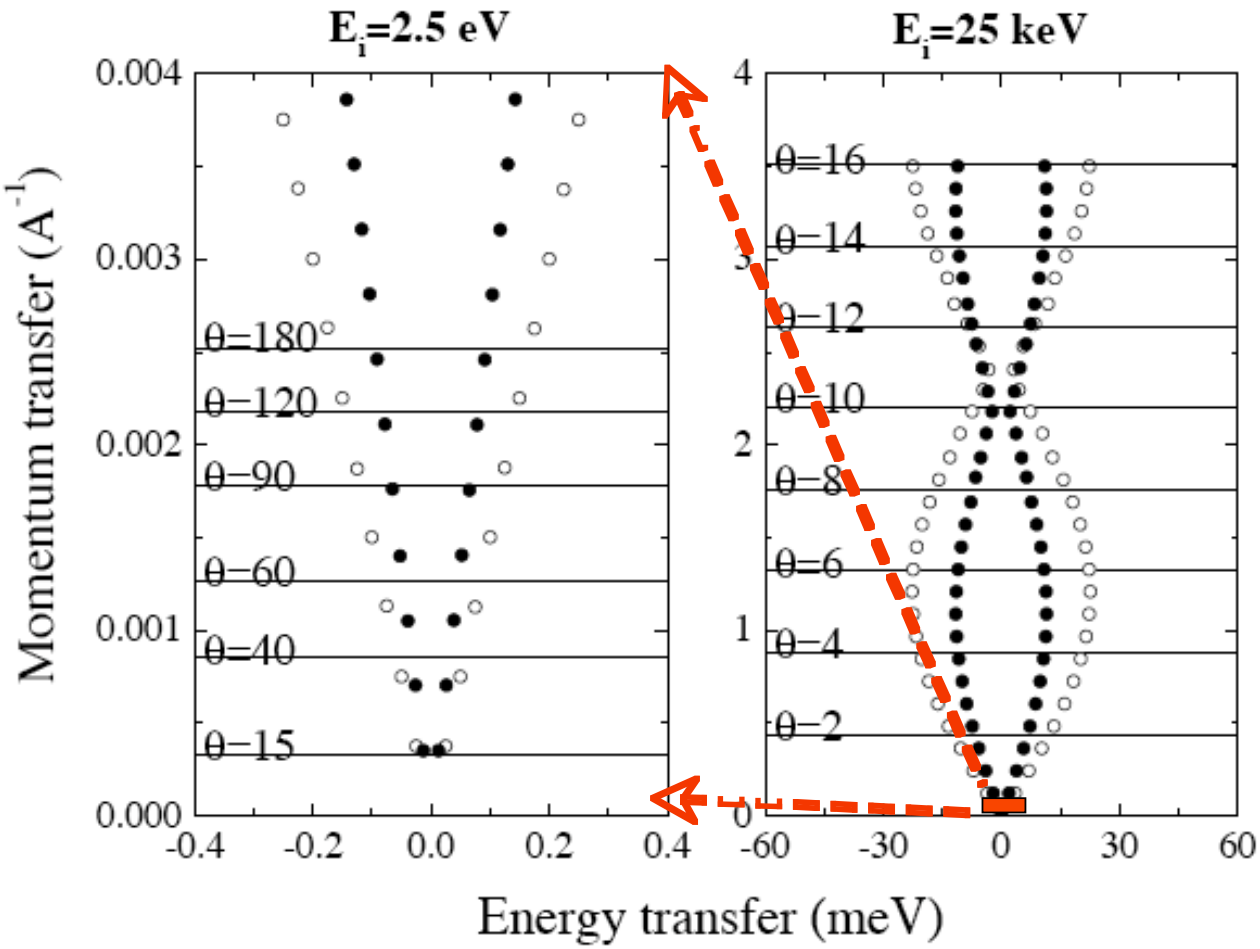

T. Scopingo, et al, Rev.Mod.Phys., 77 (2005) 881

$$E = \frac{2\hbar}{\pi} V_L Q_{\max} \sin\left(\frac{\pi}{2}\frac{Q}{Q_{\max}}\right)$$

$$E(meV) = 4.192 \cdot 10^{-4} \cdot V_L(\text{m/sec}) Q_{\max}(\text{nm}^{-1}) \cdot \sin\left(\frac{\pi}{2}\frac{Q}{Q_{\max}}\right)$$

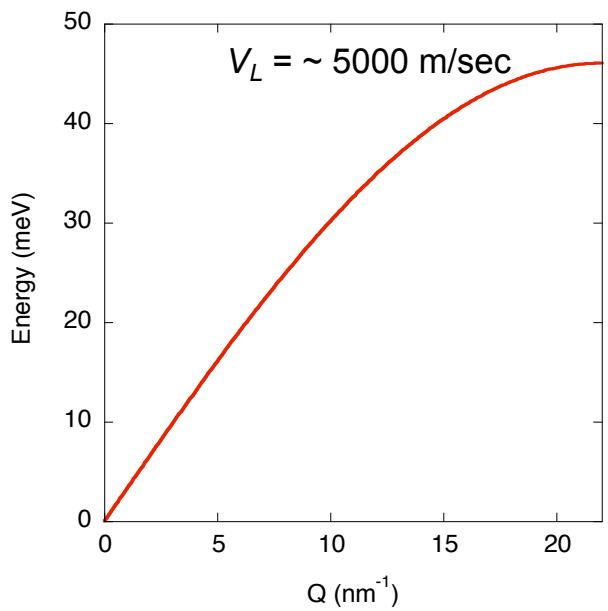

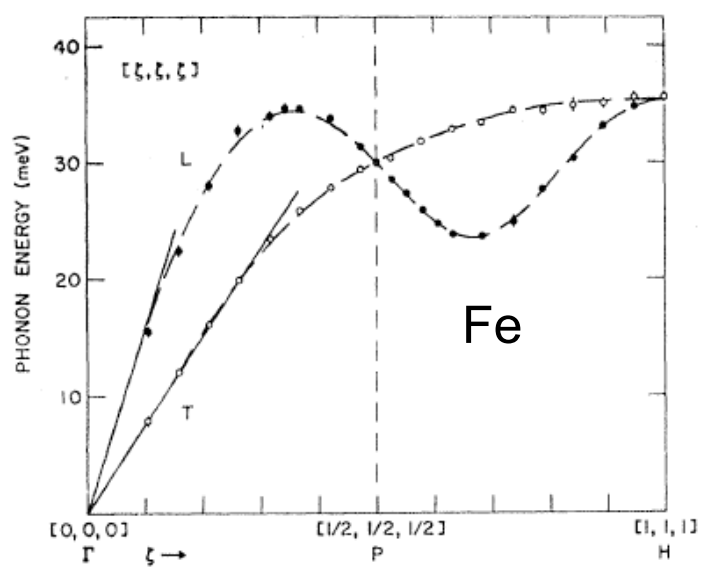

IXS Layout

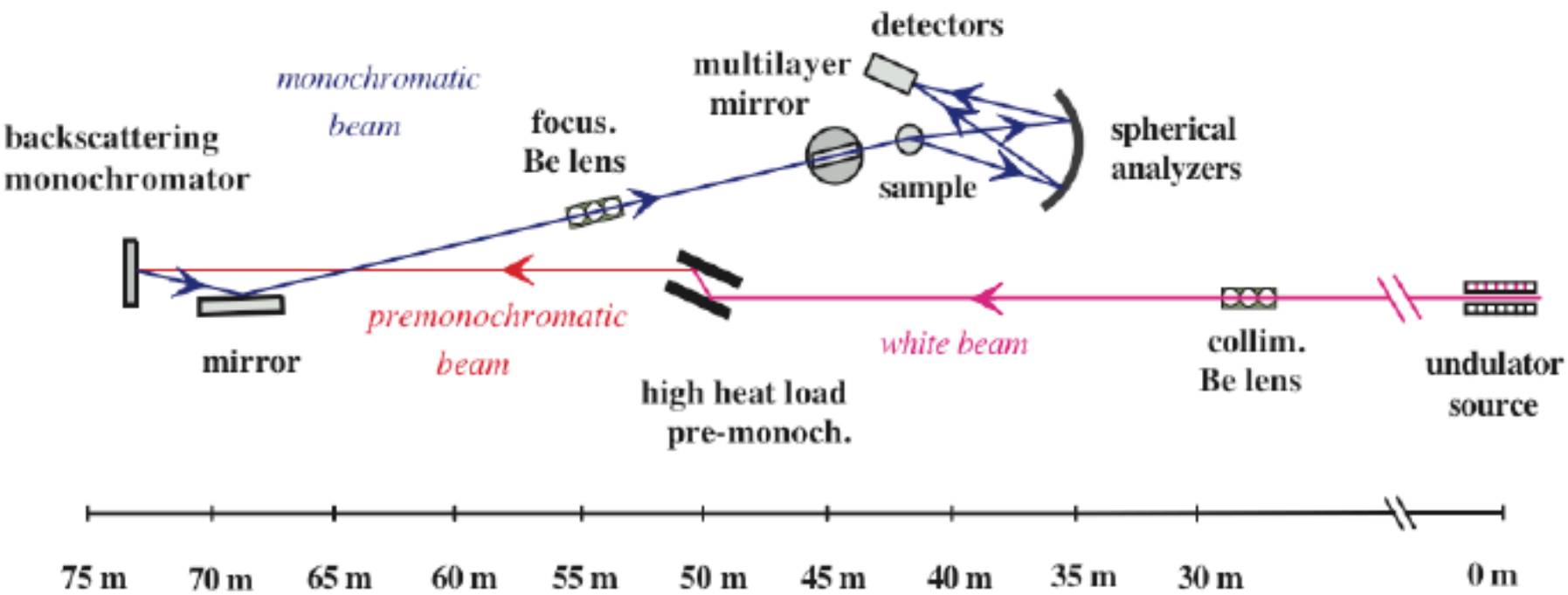
detectors
multilayer mirror
monochromatic beam
backscattering monochromator
focus. Be lens
spherical analyzers
sample
premonochromatic beam
mirror
white beam
collim. Be lens
undulator source
high heat load pre-monoch.
75 m
70 m
65 m
60 m
55 m
50 m
45 m
40 m
35 m
30 m
0 m

BL35XU hutch layout

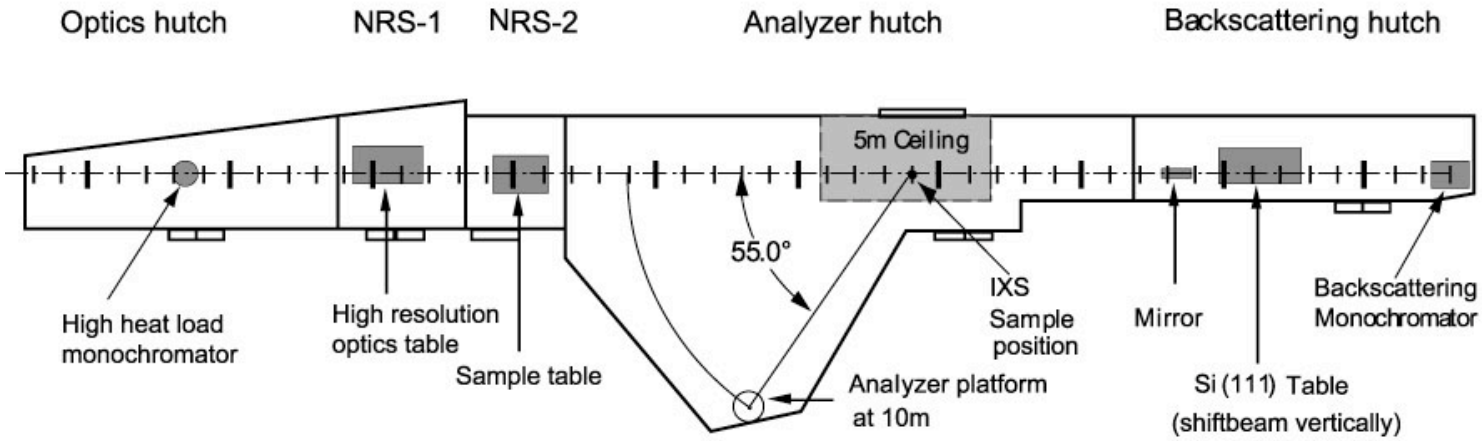

Beam path for inelastic X-ray scattering

(Vertical scattering plane)

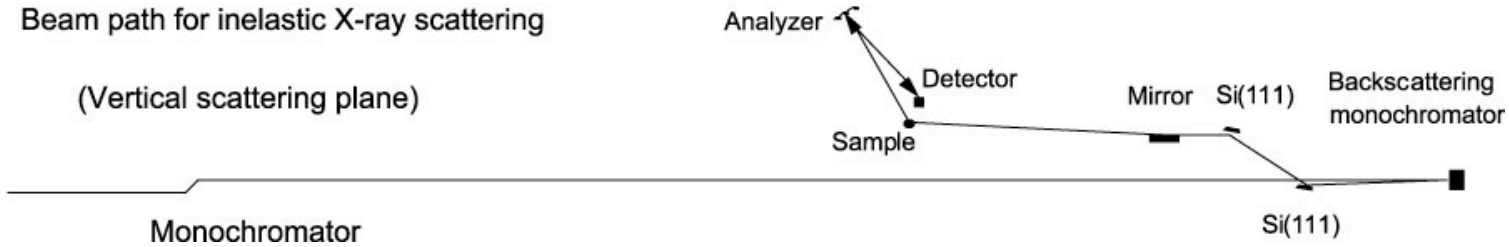

Set-up at 3-ID-C, APS

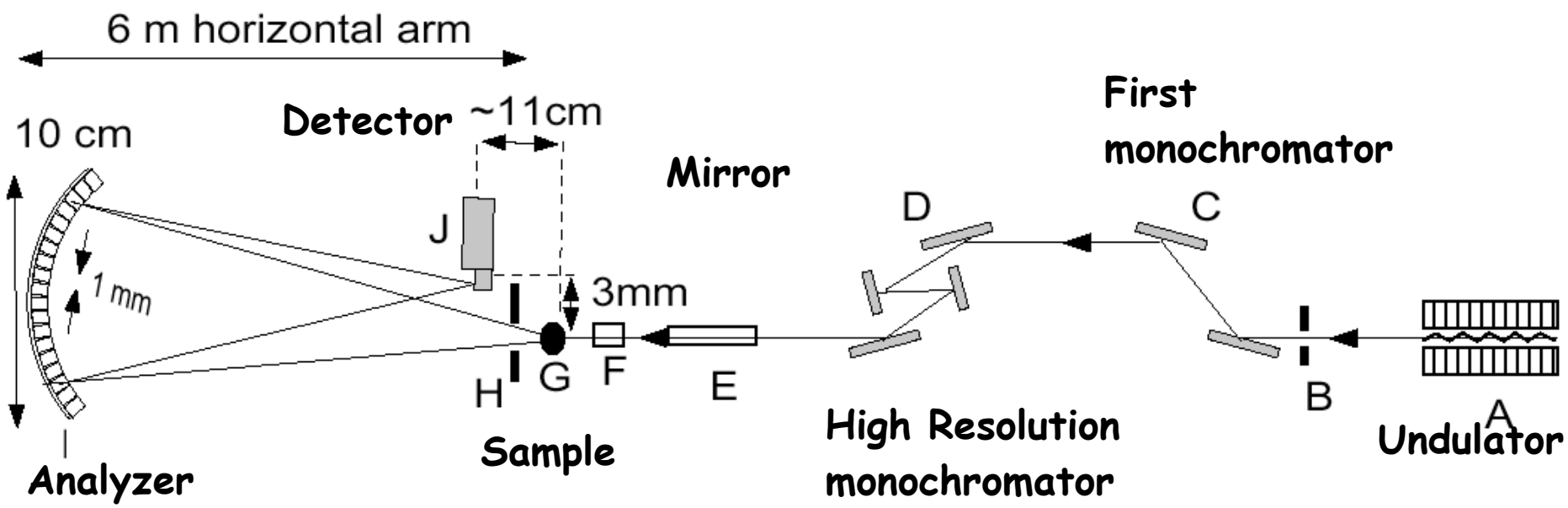

Inelastic X-Ray Scattering: two approaches

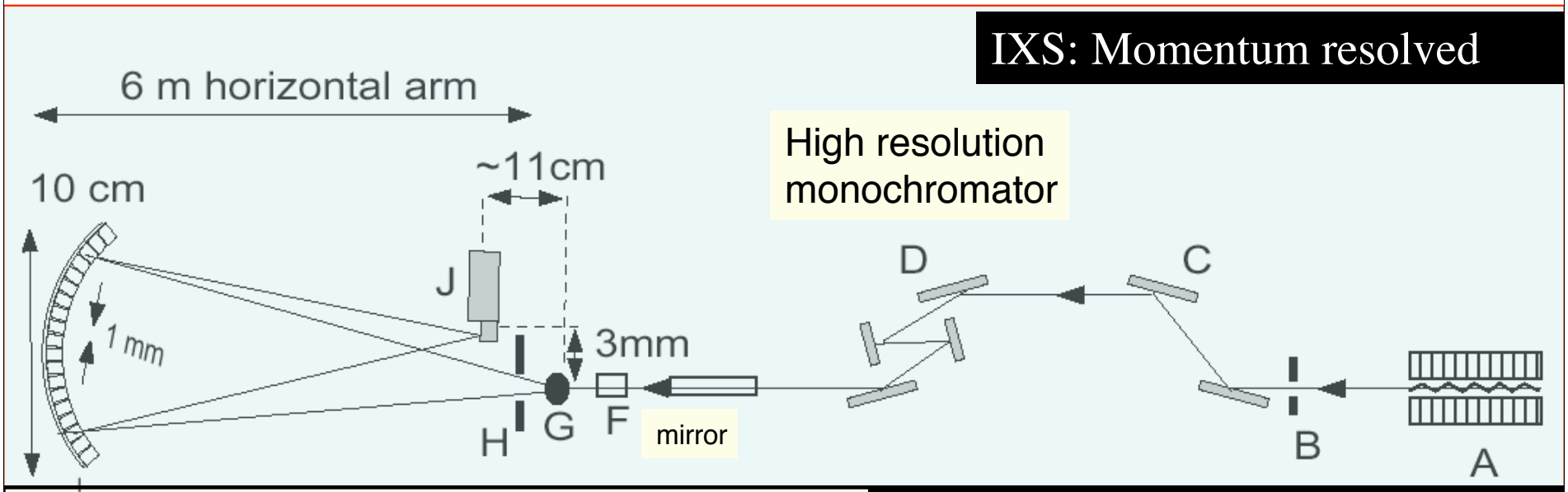

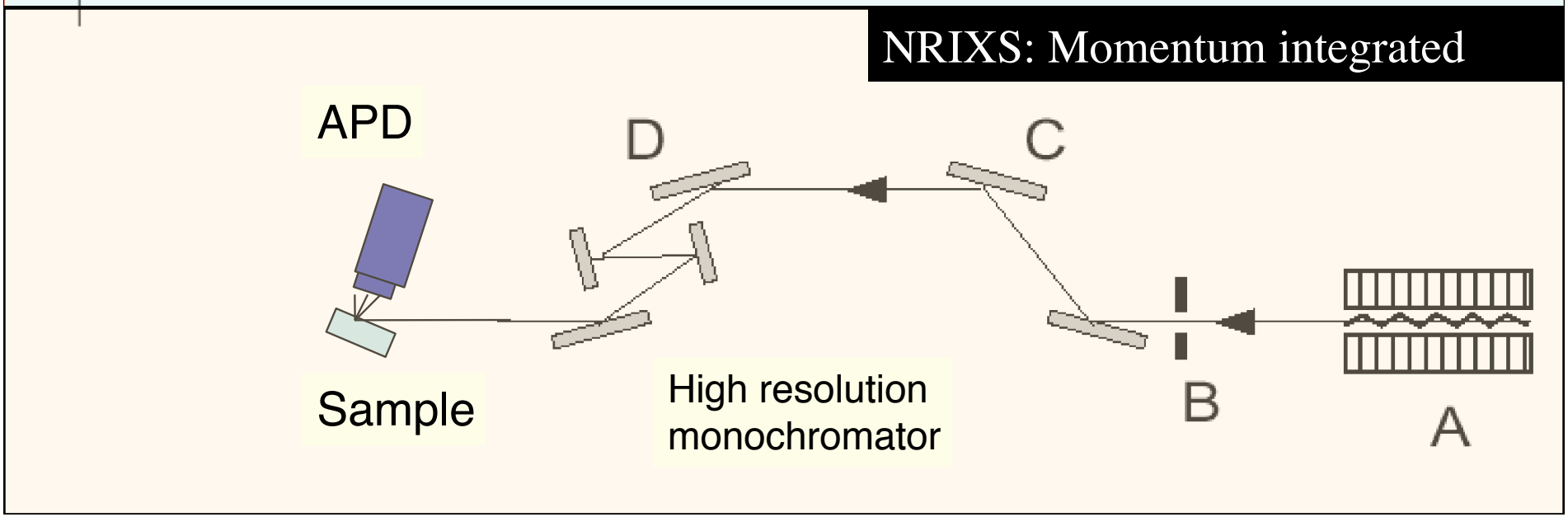

Inelastic X-Ray Scattering in the Synchrotron Era

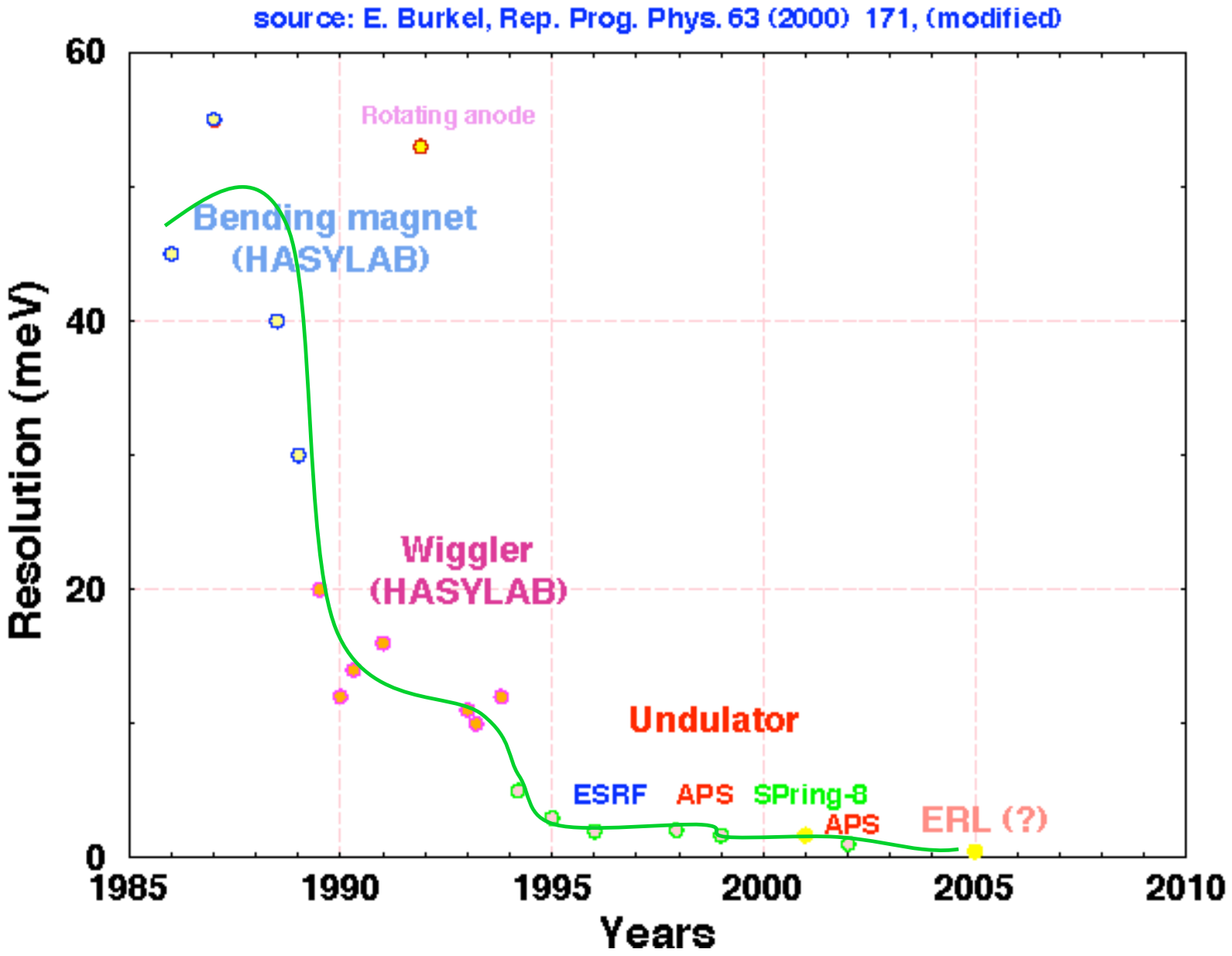

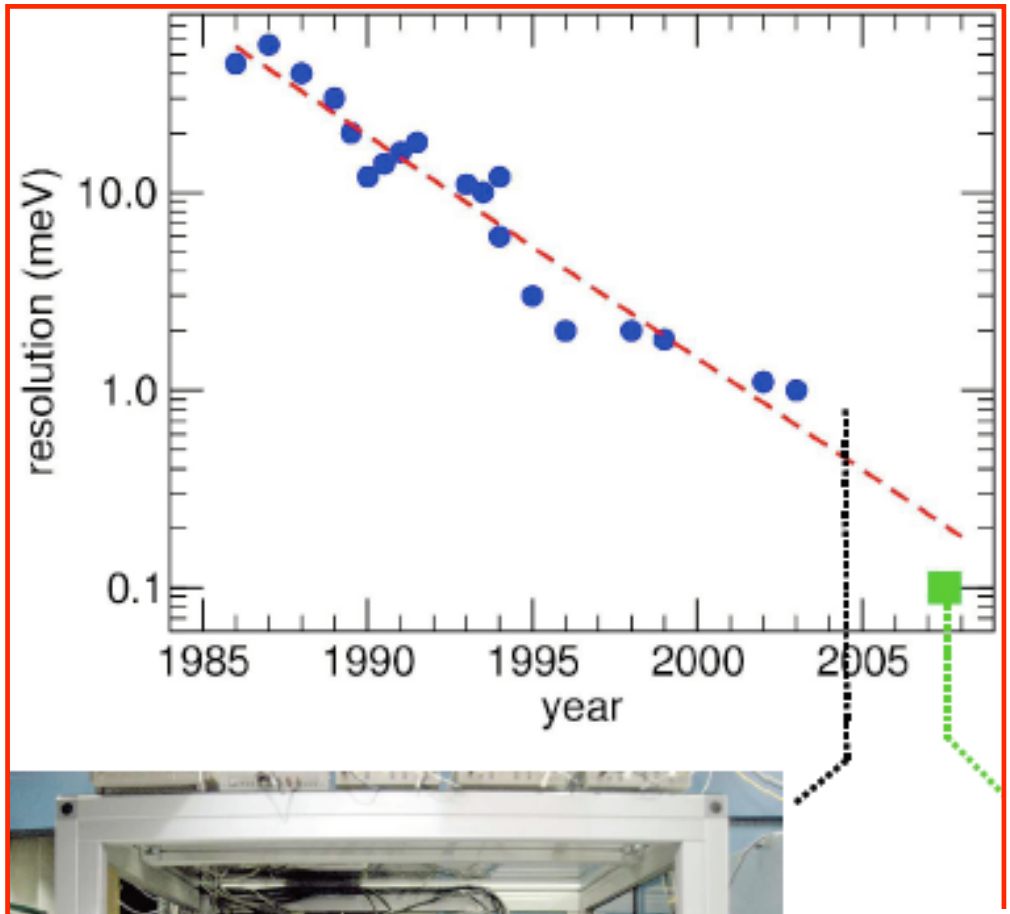

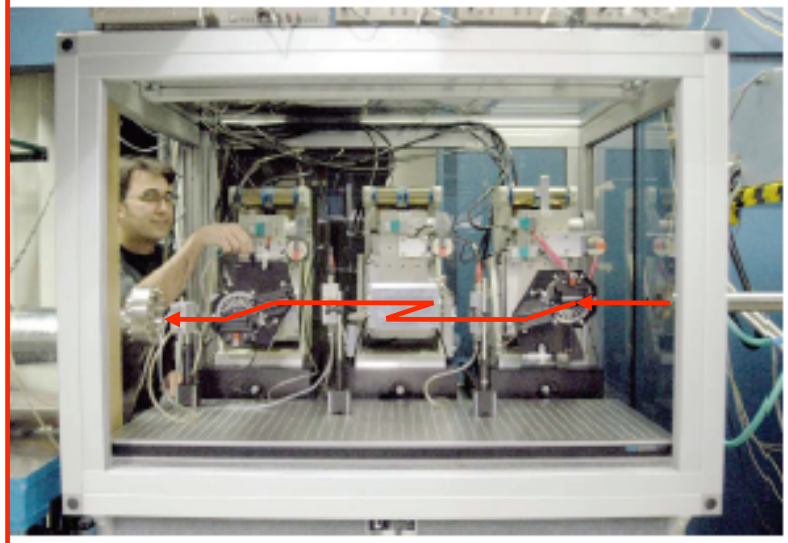

Where is the limit on silicon Based monochromatization techniques ?

We believe one can achieve 0.1 meV at 15 keV.

However, higher energy limits above 30 keV needs to be further developed.

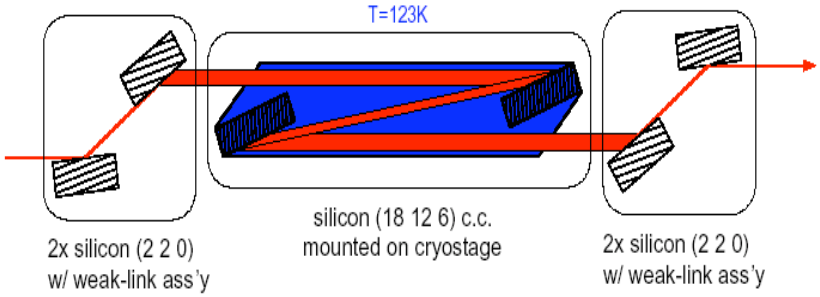

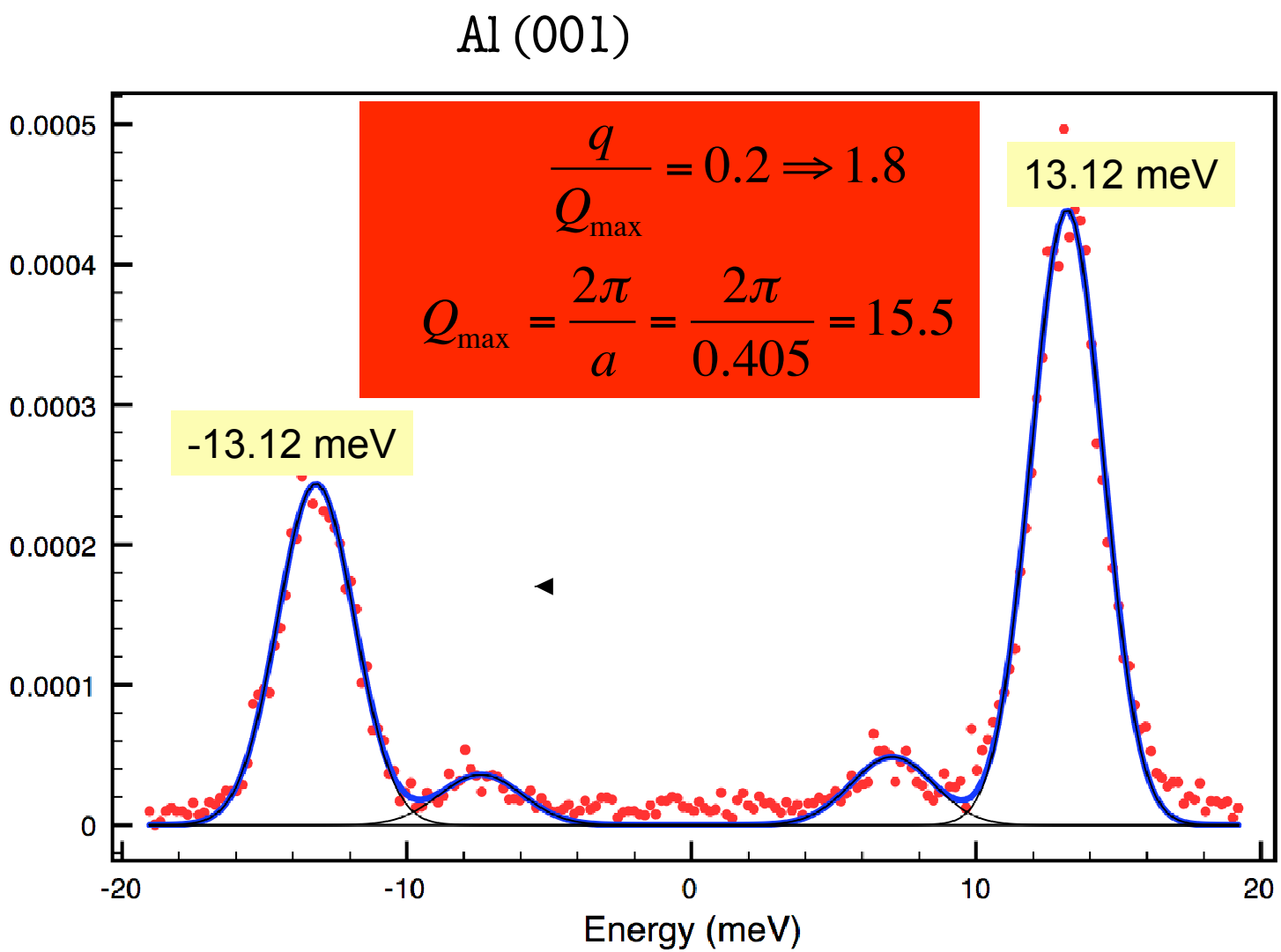
Al (001)
$\frac{q}{Q_{max}} = 0.2 \Rightarrow 1.8$
$Q_{max} = \frac{2\pi}{a} = \frac{2\pi}{0.405} = 15.5$
13.12 meV
-13.12 meV
0.0005
0.0004
0.0003
0.0002
0.0001
0
-20
-10
0
10
20
Energy (meV)

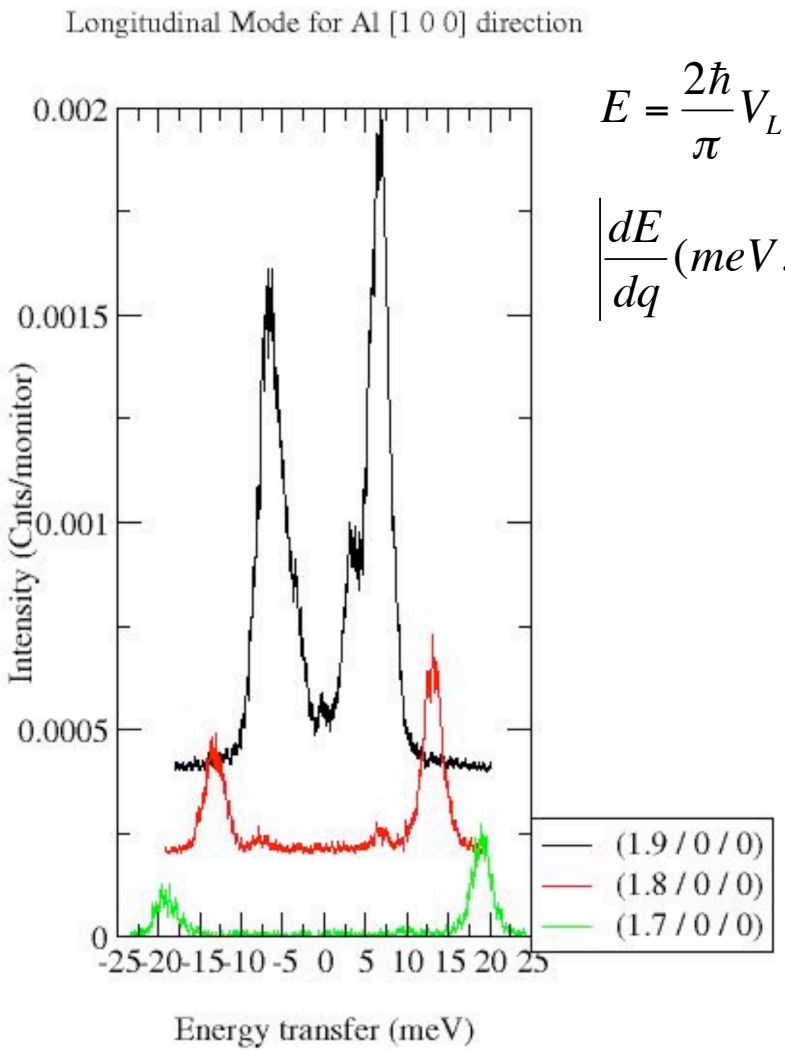

$$E = \frac{2\hbar}{\pi} V_L Q_{\max} \sin\left(\frac{\pi}{2}\frac{q}{Q_{\max}}\right)$$

$$\left|\frac{dE}{dq}(meV.nm)\right|_{q\sim 0} = \hbar \cdot V_L(\text{m/sec}) = 6.59 \cdot 10^{-4} \cdot V_L(\text{m/sec})$$

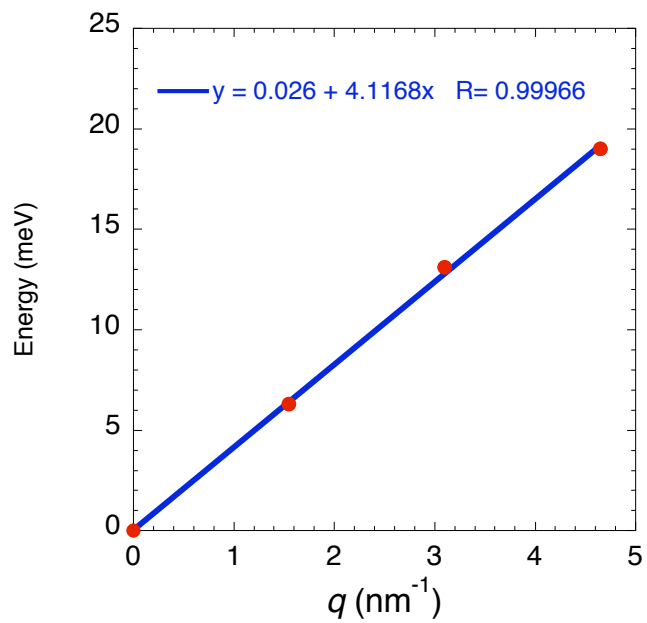

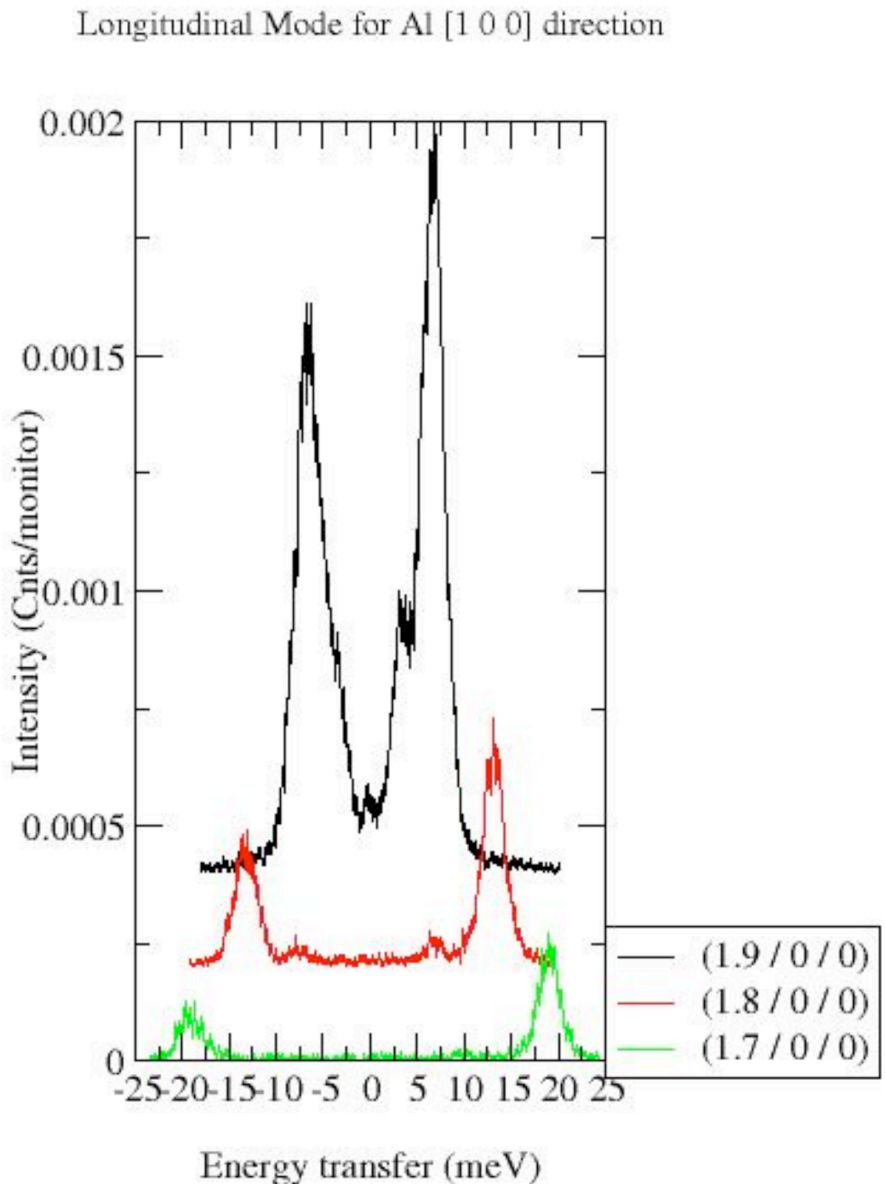
Longitudinal Mode for Al [1 0 0] direction
Intensity (Cnts/monitor)
0.002
0.0015
0.001
0.0005
0
-25 -20 -15 -10 -5 0 5 10 15 20 25
Energy transfer (meV)
(1.9 / 0 / 0)
(1.8 / 0 / 0)
(1.7 / 0 / 0)

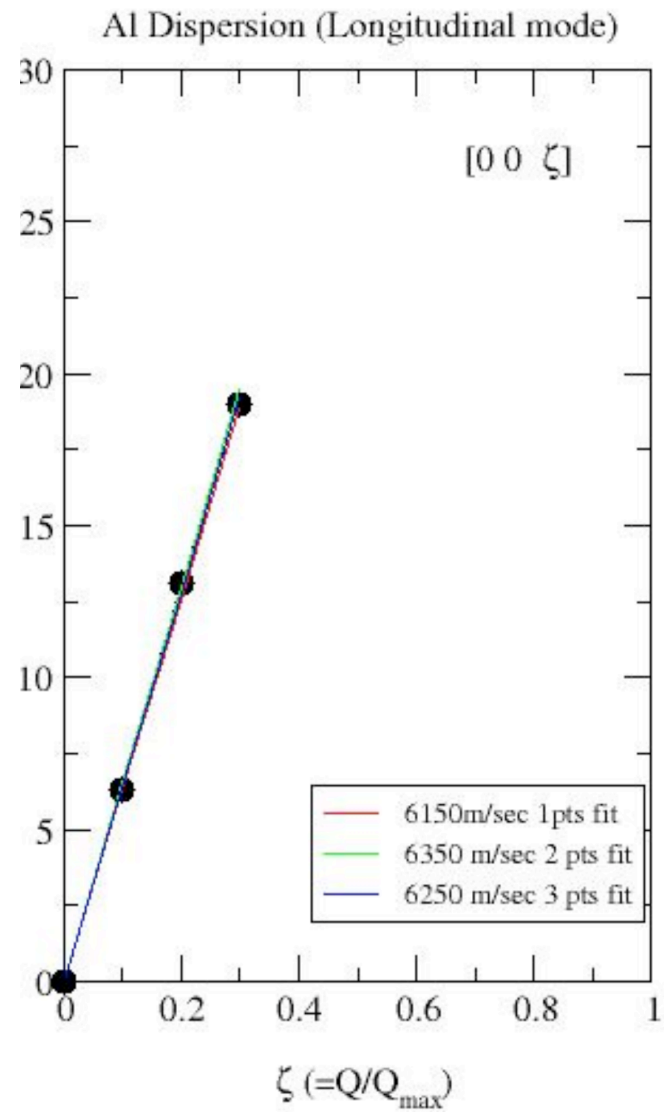
Al Dispersion (Longitudinal mode)
[0 0 ζ]
30
25
20
15
10
5
0
0 0.2 0.4 0.6 0.8 1
ζ (=Q/Q_max)
6150m/sec 1pts fit
6350 m/sec 2 pts fit
6250 m/sec 3 pts fit

$$\frac{3}{V_D^3} = \frac{1}{V_L^3} + \frac{2}{V_T^3}$$

$$V_{LA,[100]} = \sqrt{\frac{C_{11}}{\rho}}$$

$$V_{LA,[001]} = \sqrt{\frac{C_{33}}{\rho}}$$

$$V_{LA,[110]} = \sqrt{\frac{C44}{\rho}}$$

$$V_T^2 = \frac{3}{4}\left(V_L^2 - \frac{K}{\rho}\right)$$

$$V_L^2 = \frac{1}{\rho}\left(K + \frac{4}{3}G\right)$$

$$V_T^2 = \frac{G}{\rho}$$

V_D : Debye, aggregate sound velocity
V_P : Compressional, longitudinal, primary sound velocity
V_S :, Shear, transverse, secondary sound velocity

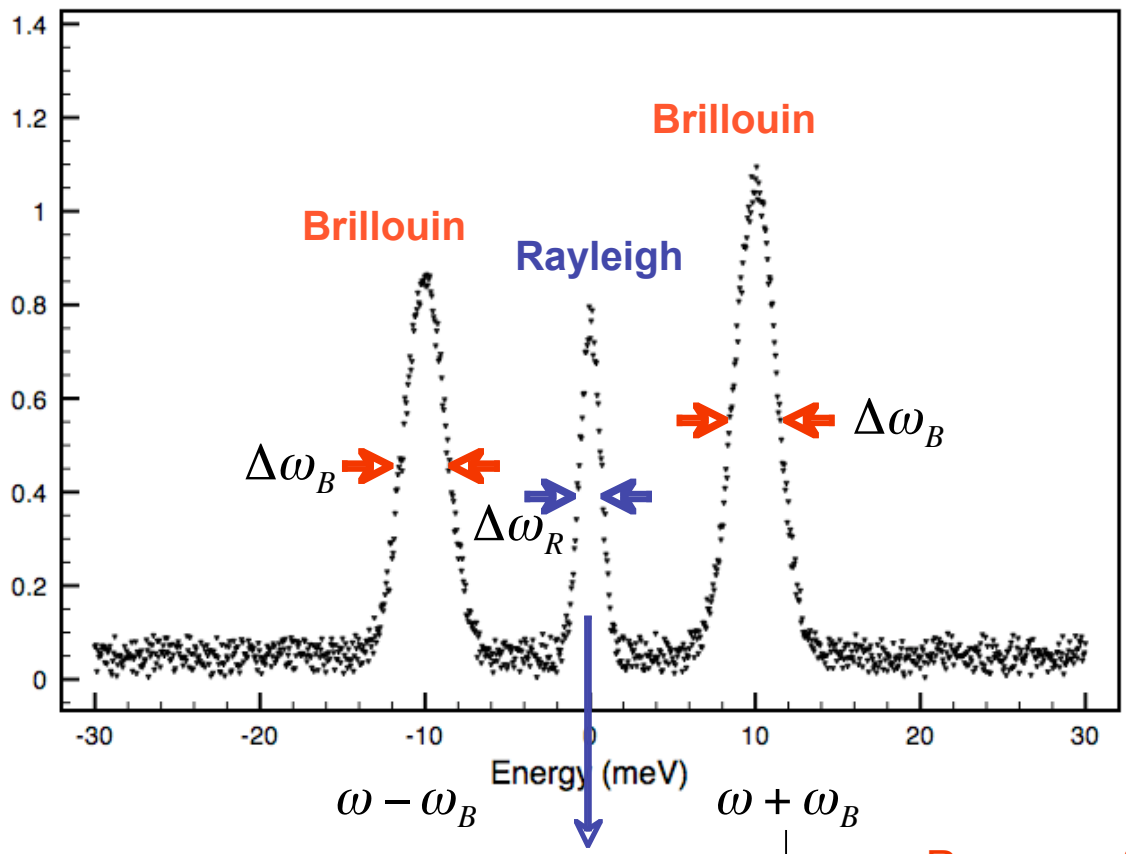

Entropy fluctuations, $\Delta\omega_R \sim \alpha q^2$

Concentration fluctuations $\Delta\omega_R \sim D q^2$

Pressure fluctuations

$$\omega_B(q) = V \cdot q$$

$$\Delta\omega_B \sim V q^2$$

Choice of energy

Si Reflection at 90 °	Energy (keV)	Resolution (meV)	Reflectivity (%)
18 6 0	21.657	1.23	78
11 11 11	21.747	0.83	70
13 11 9	21.985	0.81	69
15 11 7	22.685	0.70	68
20 4 0	23.280	0.87	76
12 12 12	23.724	0.80	75
14 14 8	24.374	0.69	74
22 2 0	25.215	0.576	71
13 13 13	25.701	0.37	60

Silicon as back-scattering analyzer

Limitations above 25 keV

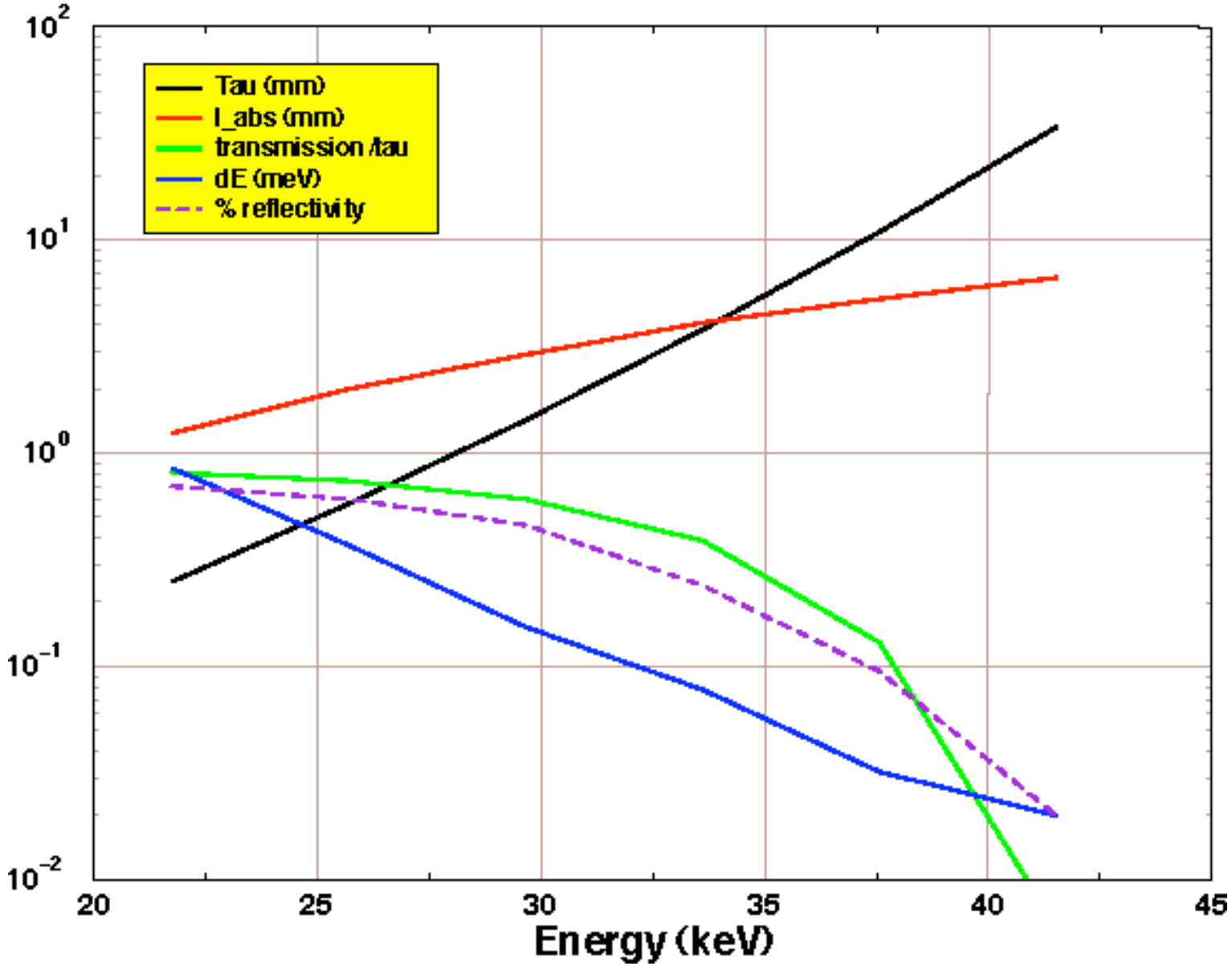

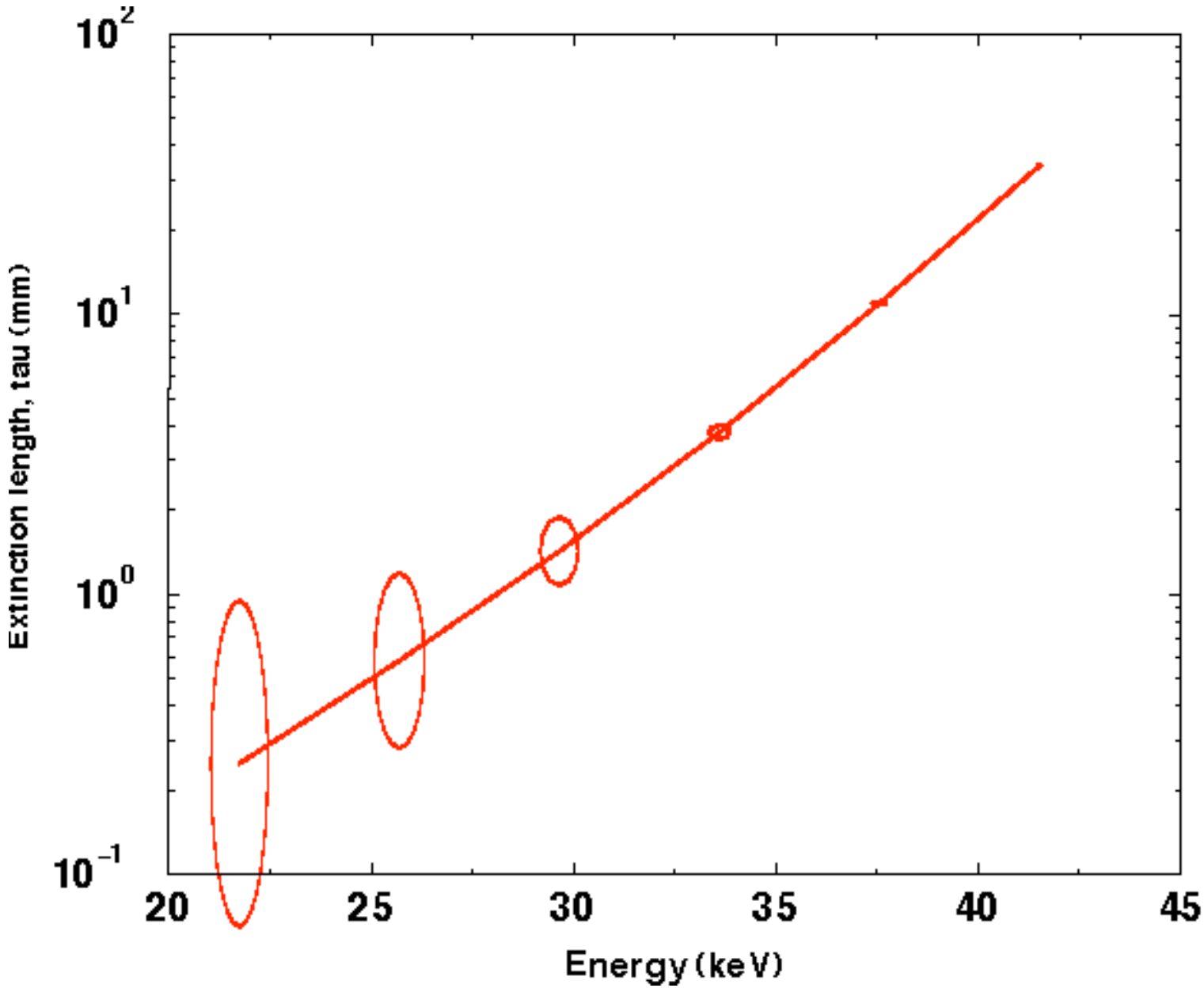
Extinction length, tau (mm)
10^{2}
10^{1}
10^{0}
10^{-1}
20
25
30
35
40
45
Energy (keV)

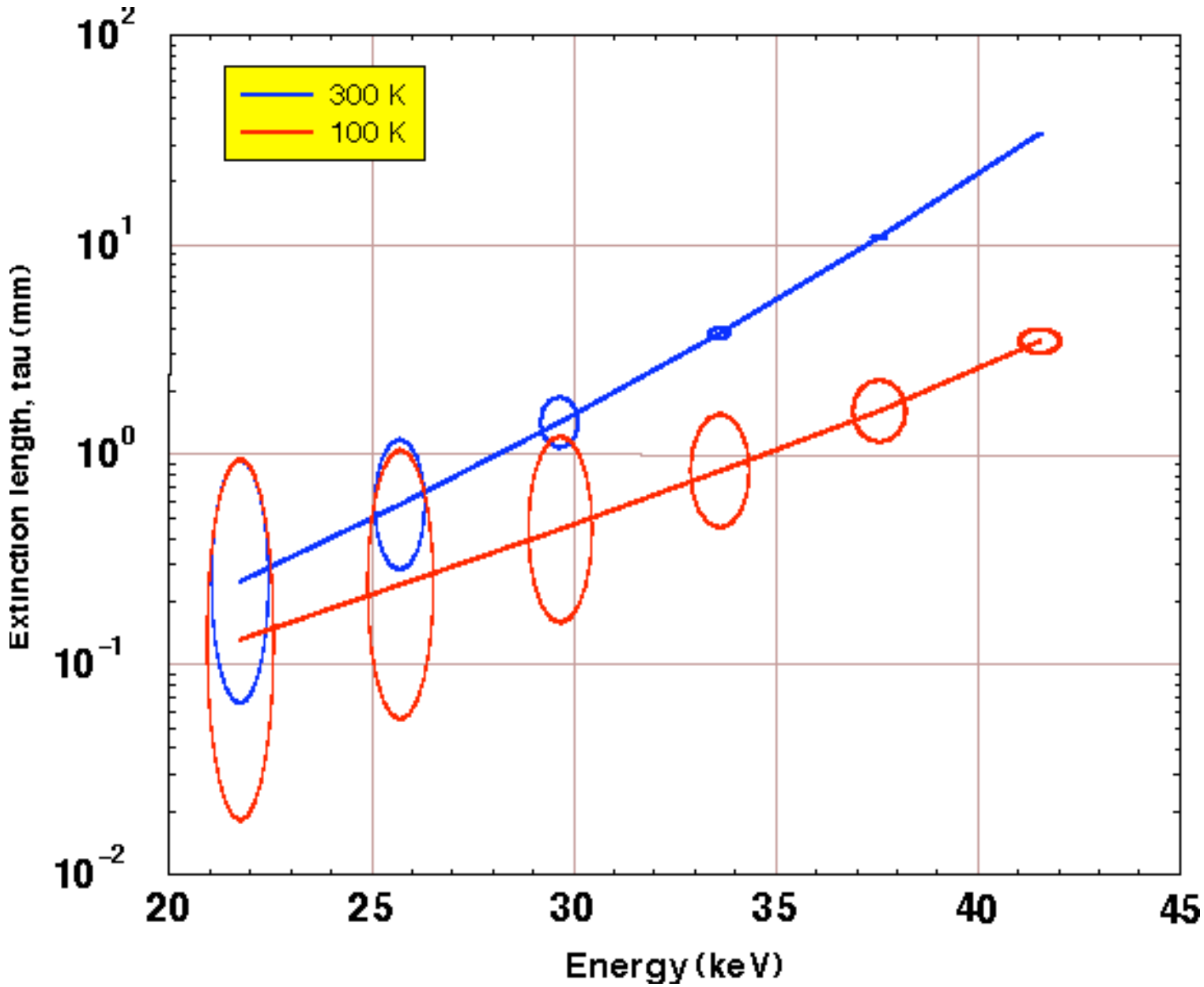
300 K
100 K
Extinction length, tau (mm)
Energy (keV)
10^{2}
10^{1}
10^{0}
10^{-1}
10^{-2}
20
25
30
35
40
45

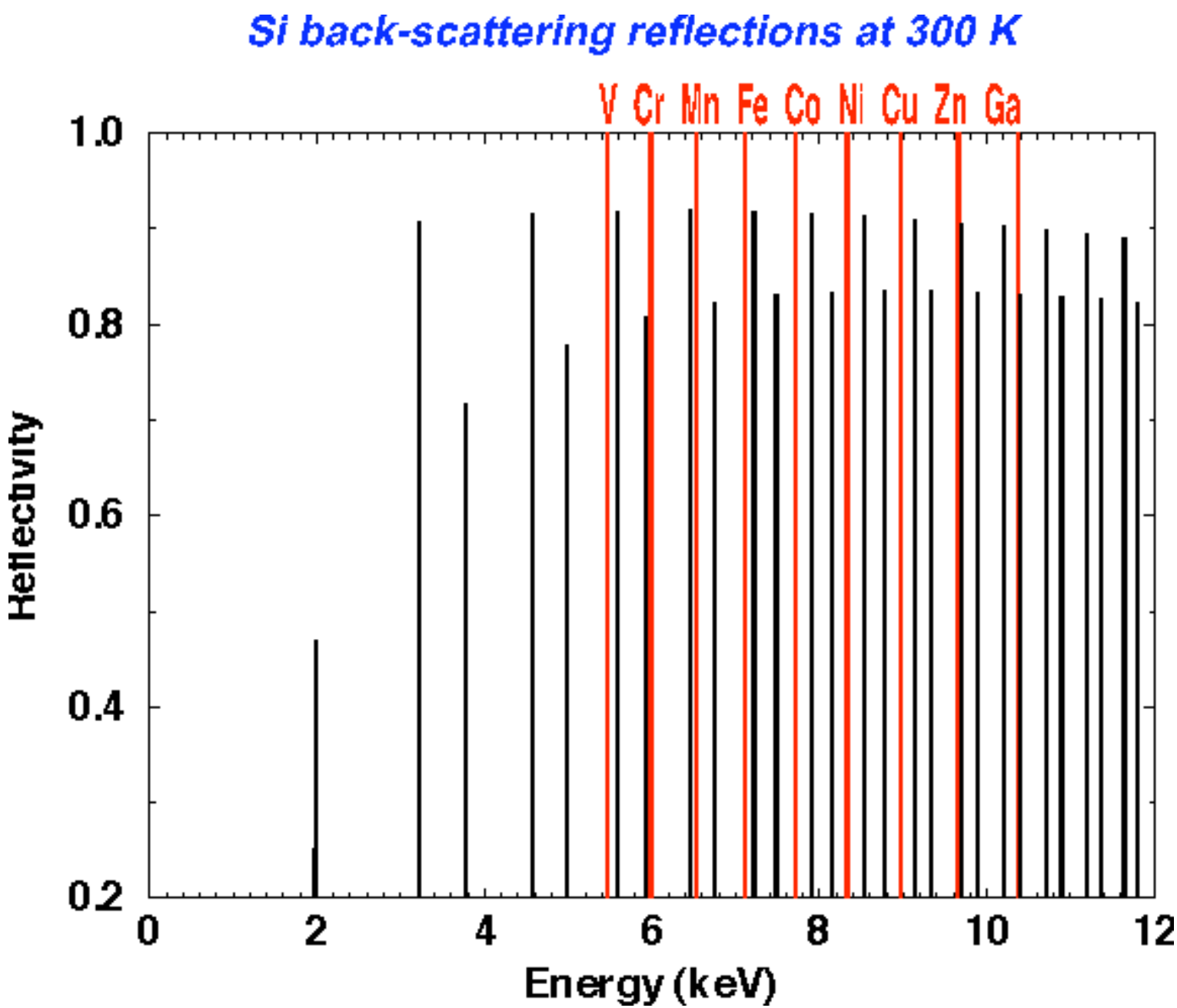
Si back-scattering reflections at 300 K
V Cr Mn Fe Co Ni Cu Zn Ga
1.0
0.8
0.6
0.4
0.2
Reflectivity
0
2
4
6
8
10
12
Energy (keV)

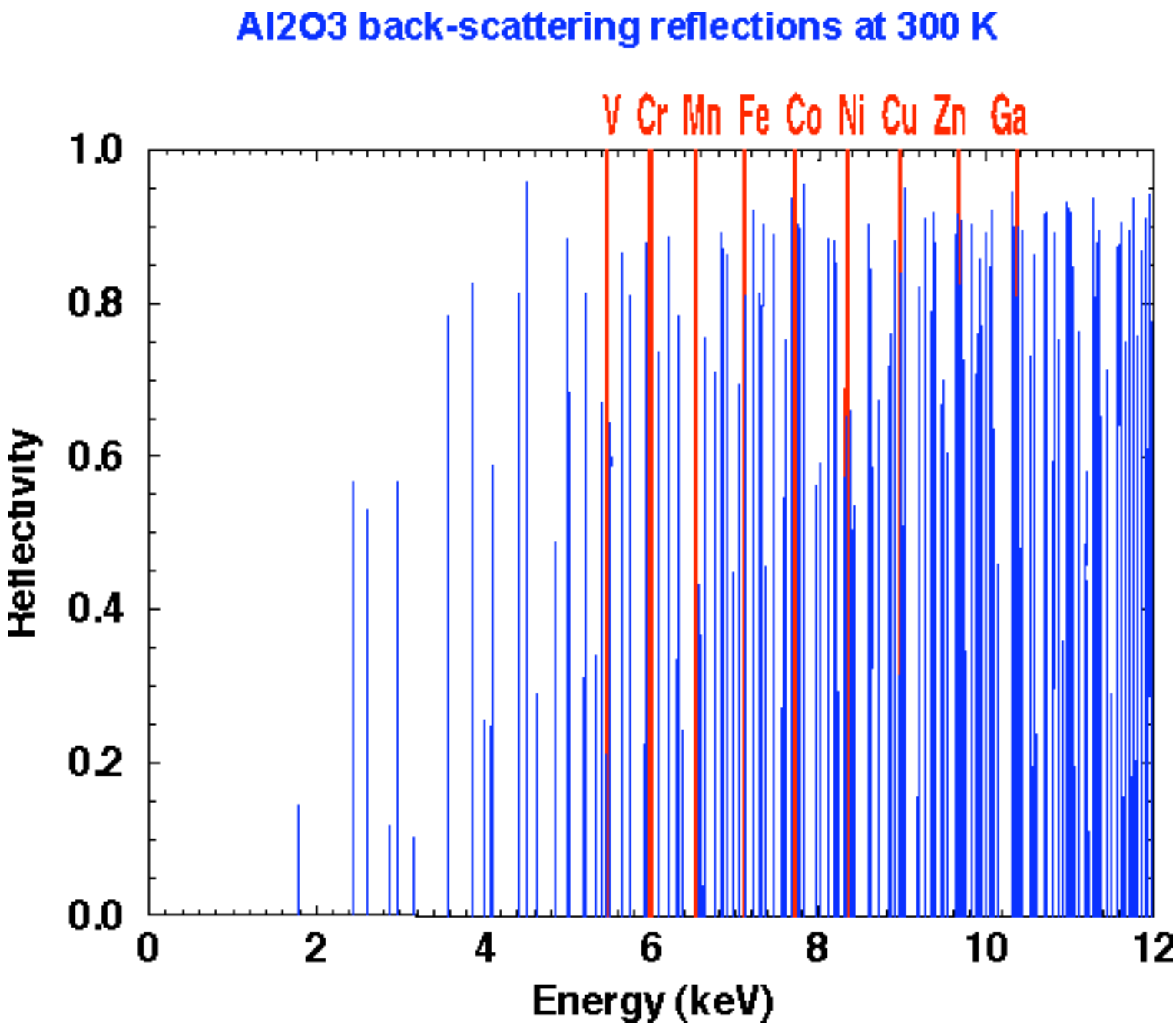
Al2O3 back-scattering reflections at 300 K
V
Cr
Mn
Fe
Co
Ni
Cu
Zn
Ga
Reflectivity
1.0
0.8
0.6
0.4
0.2
0.0
0
2
4
6
8
10
12
Energy (keV)

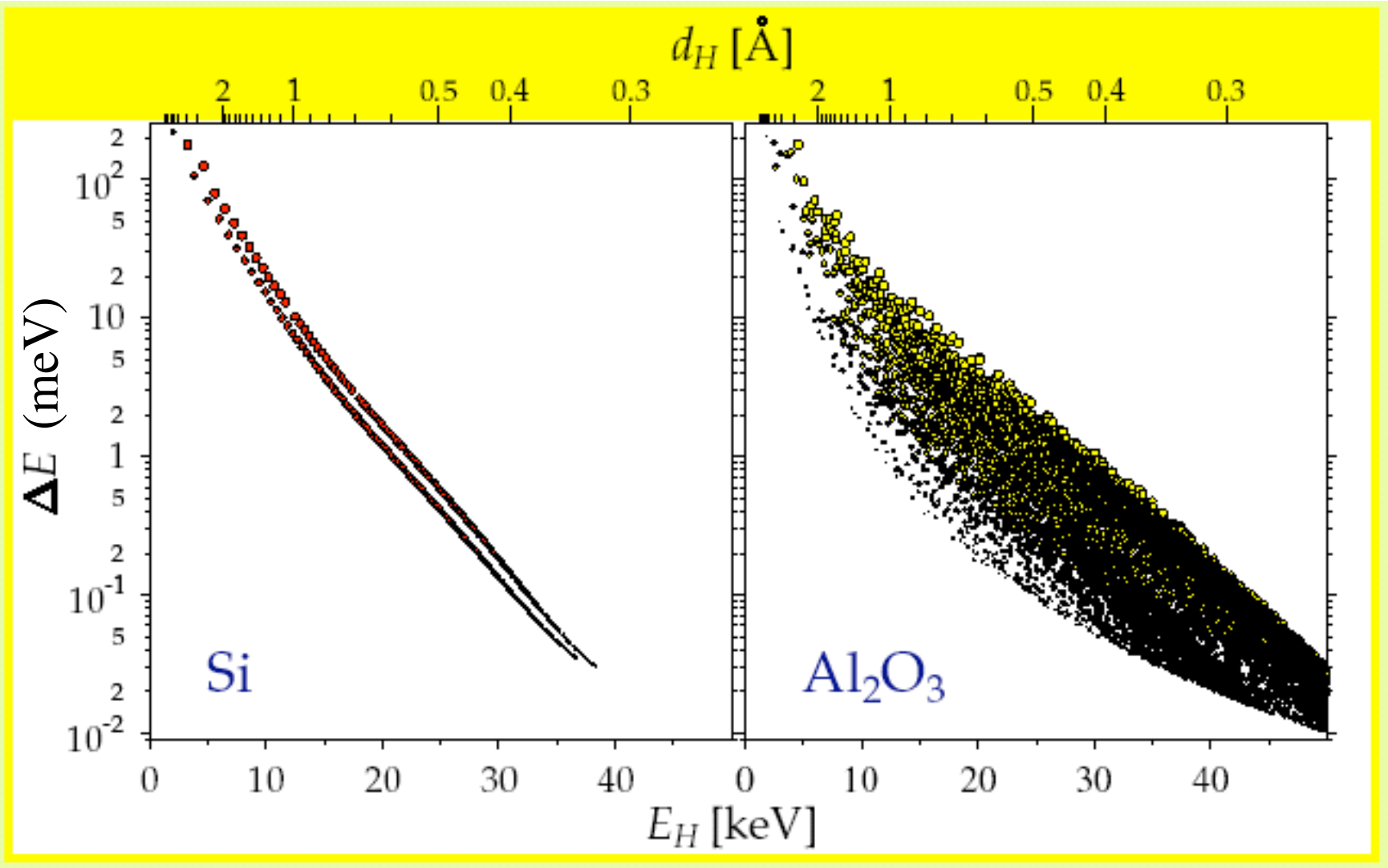

Courtesy: Y. Shvydko

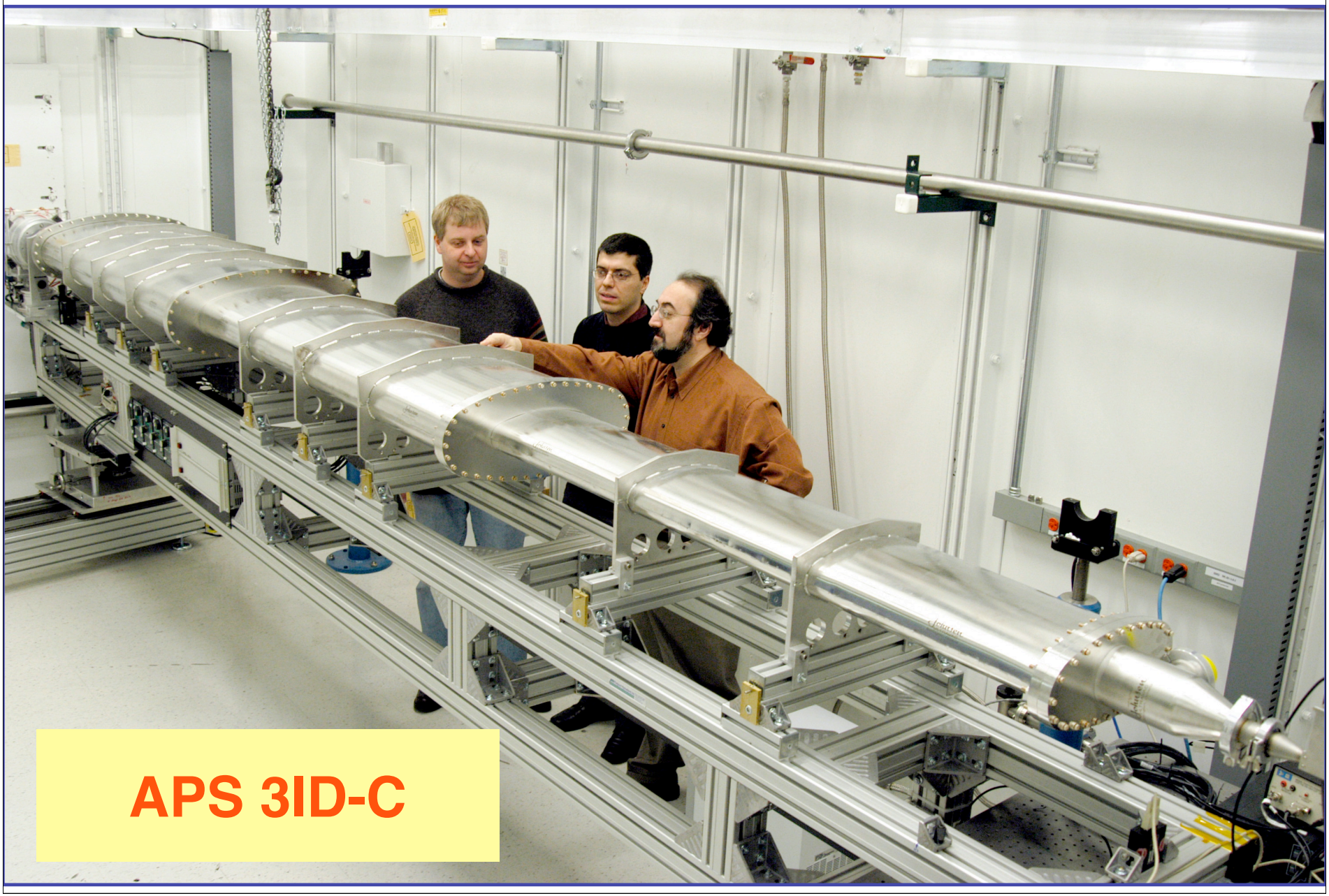
APS 3ID-C

30-ID-C: HERIX Spectrometer

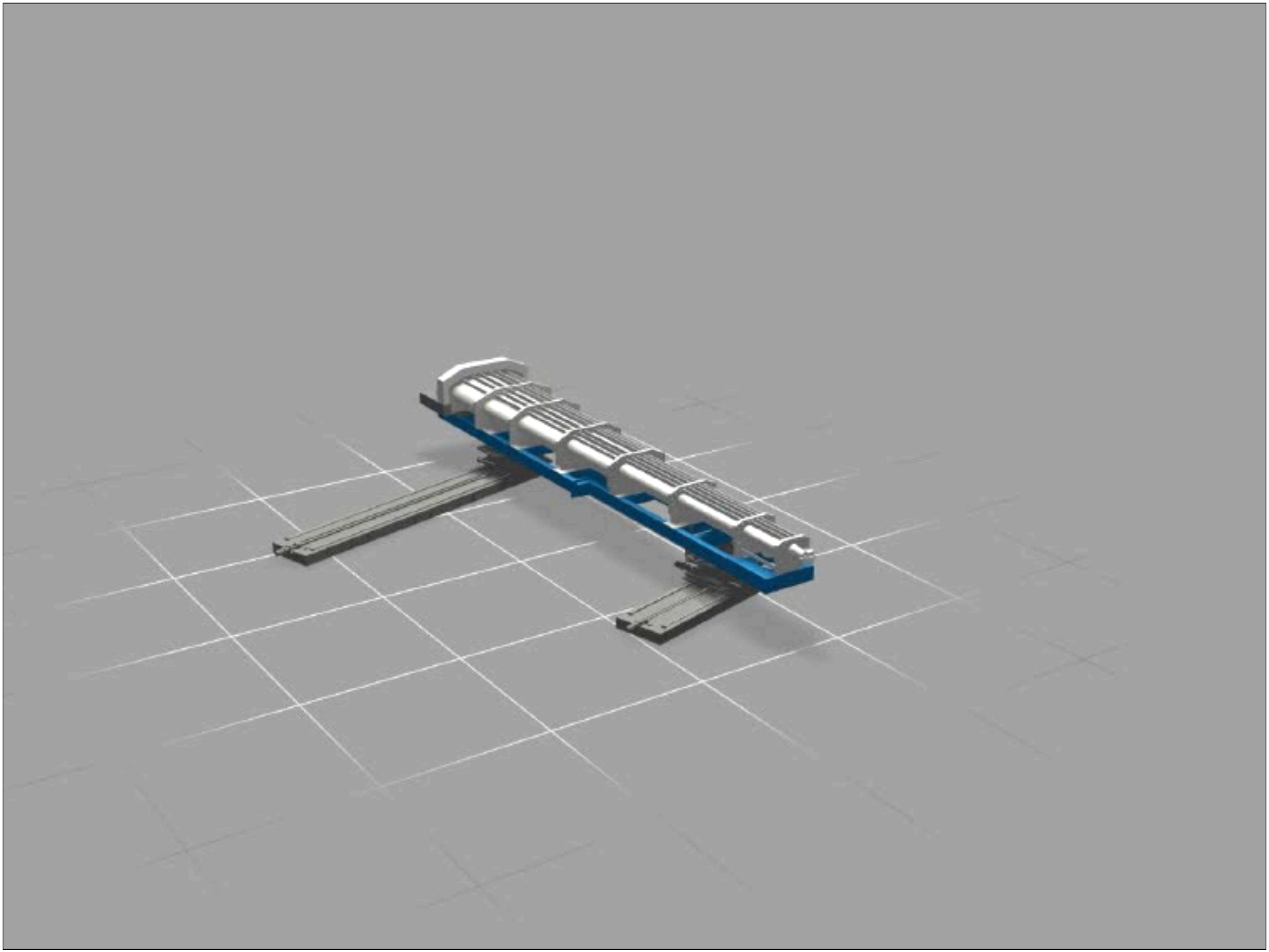

High Melting Point Substances

Lindemann criterion: $mv_{sound}^2 \propto T_{melt}$

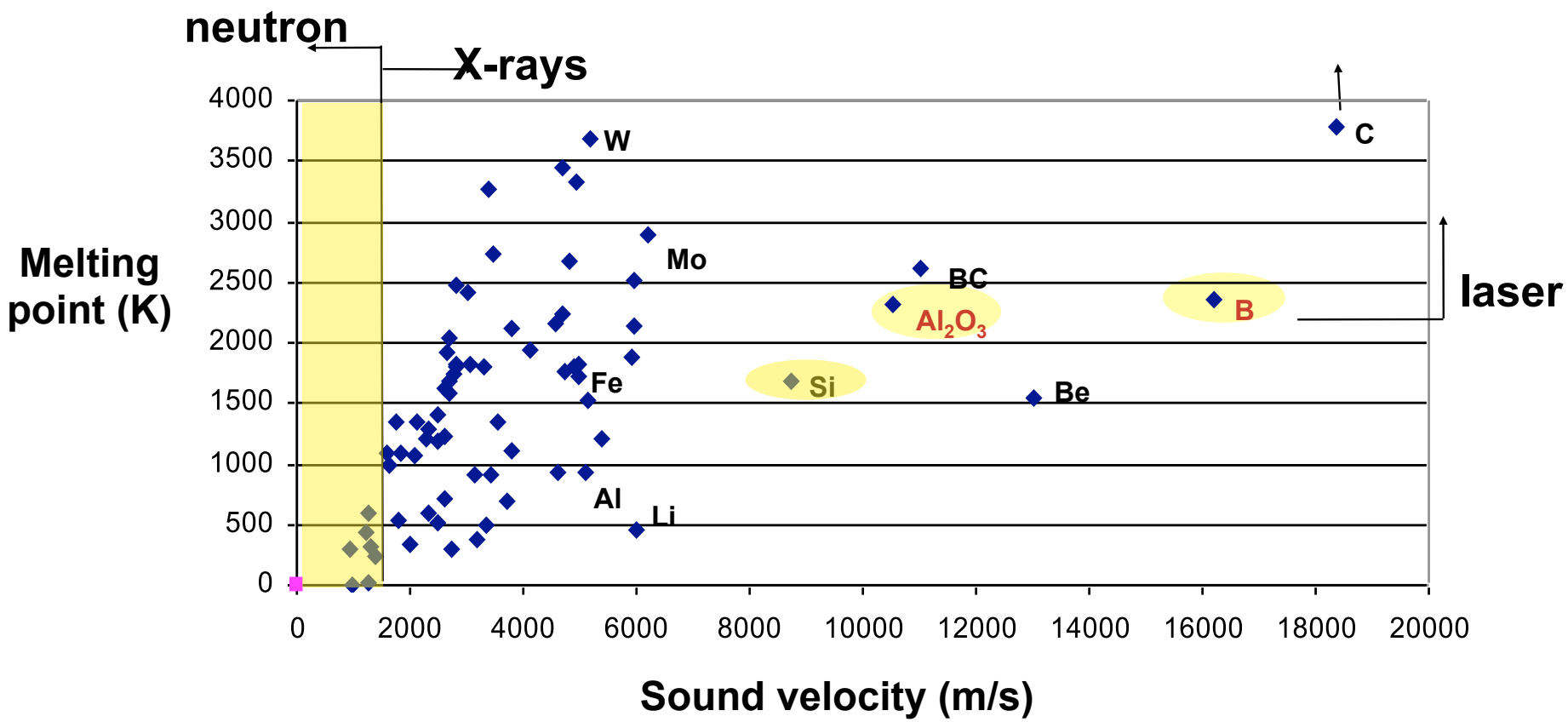

Liquid Al_2O_3

Sapphire
Melting point: 2050°C

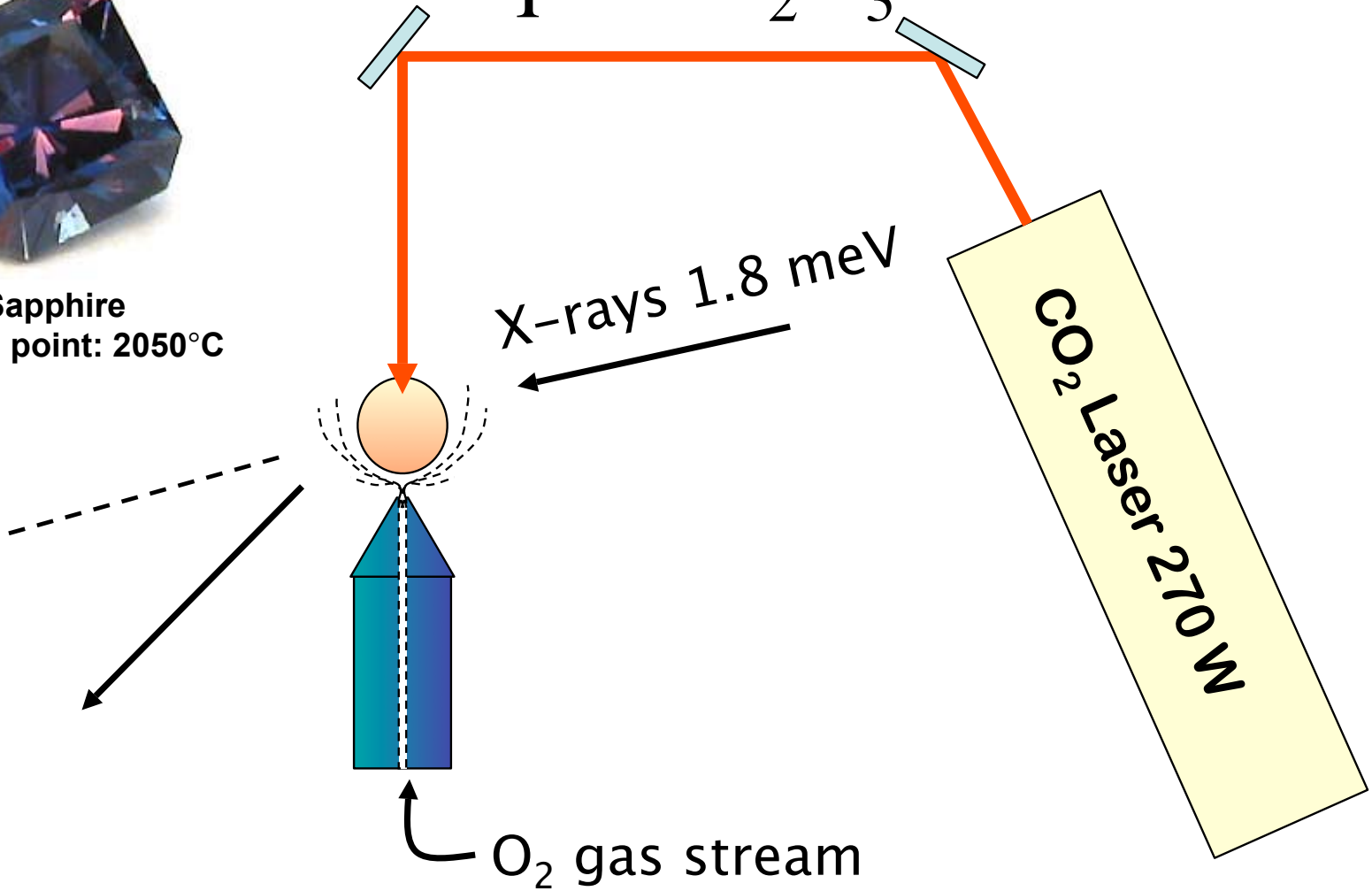

Hydrodynamics: 3 Peaks

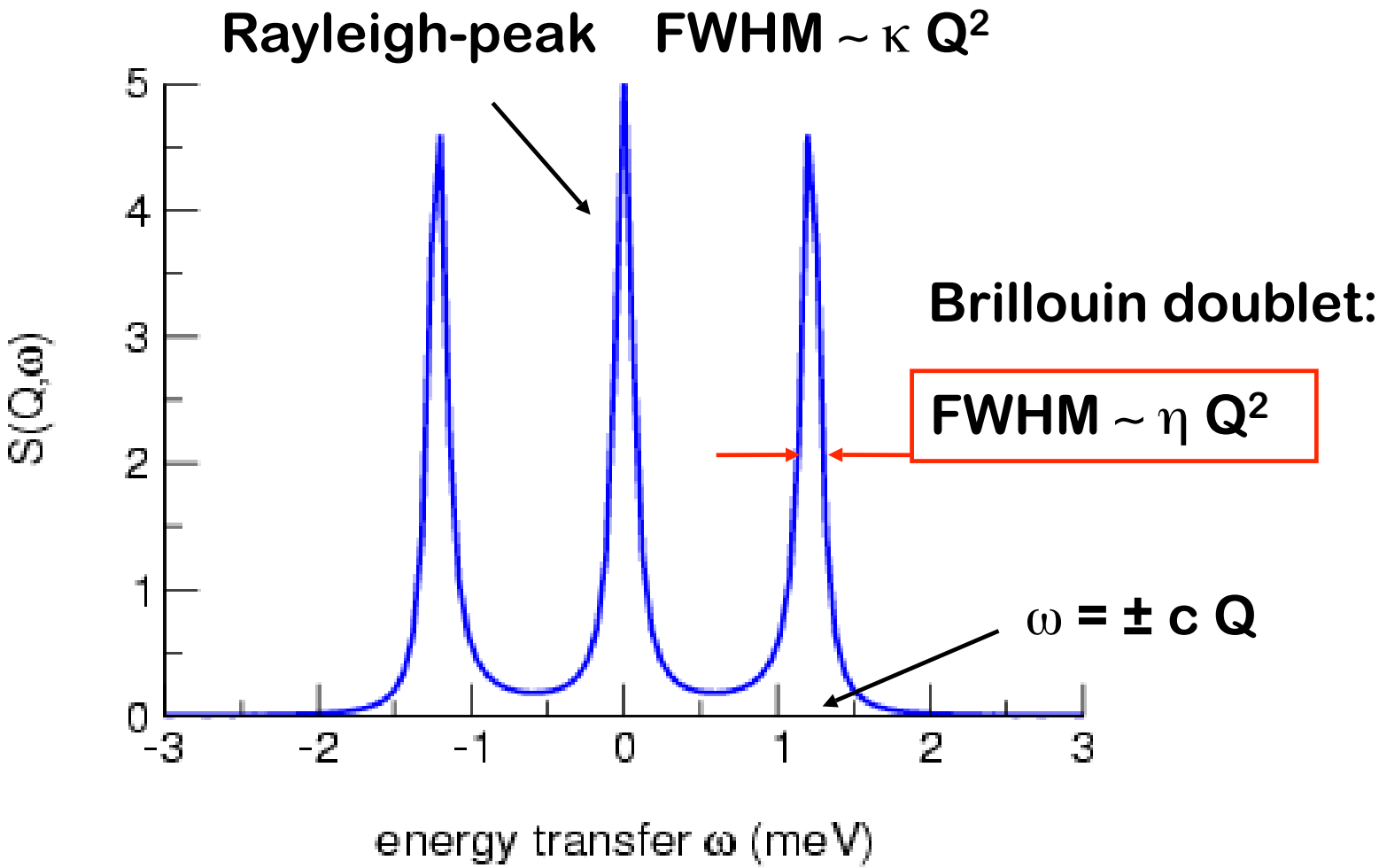

Liquid Al_2O_3 @ 2050°C

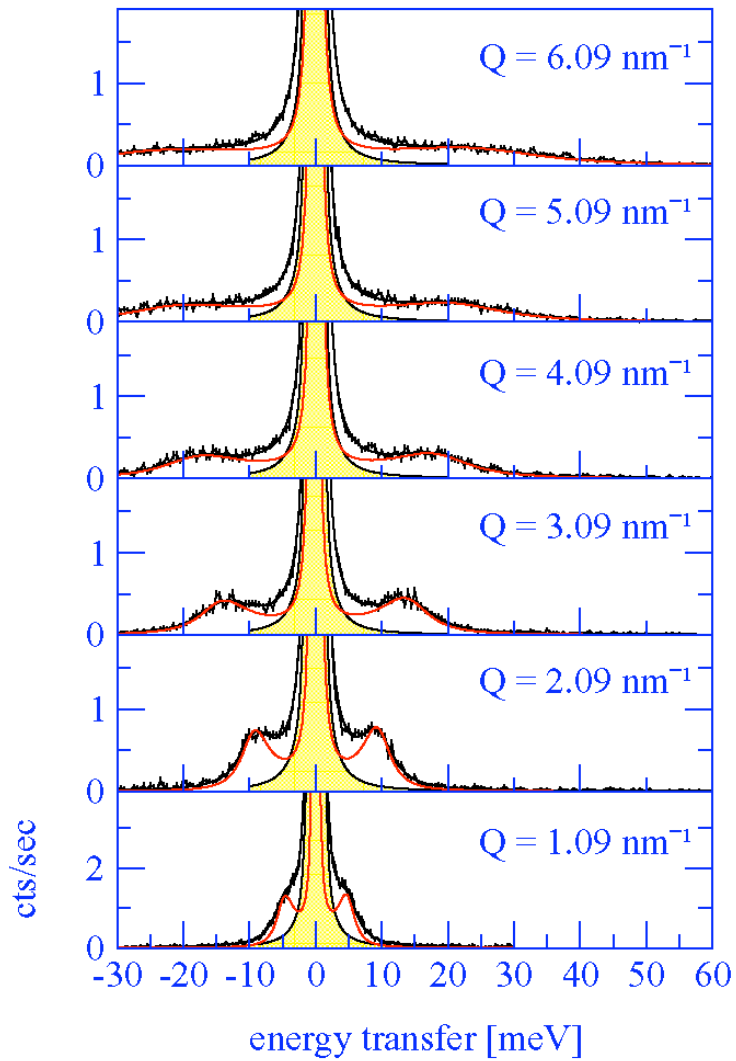

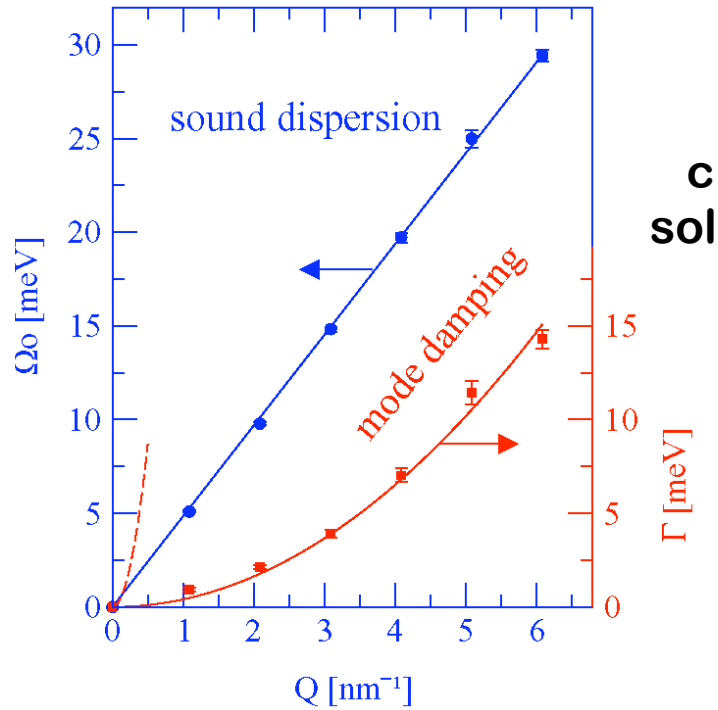

c = 7350 m/s
solid:10500 m/s

Damping is too low by factor 20!

Solid to Liquid Transition in Alumina

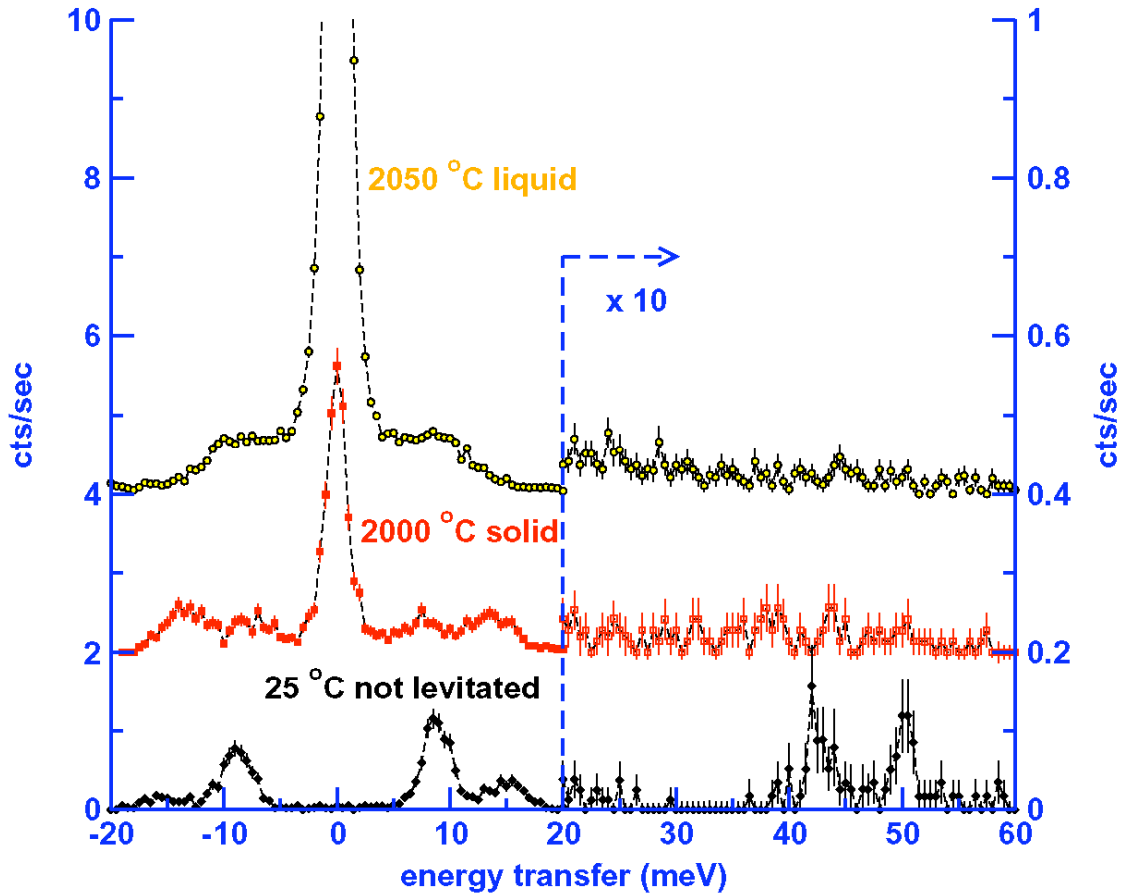

Courtesy, Harald Sinn

Viscoelasticity, $\eta(\omega)$

$$\eta(\omega) = \frac{\eta_0}{1 + i\omega\tau} + \eta_\infty$$

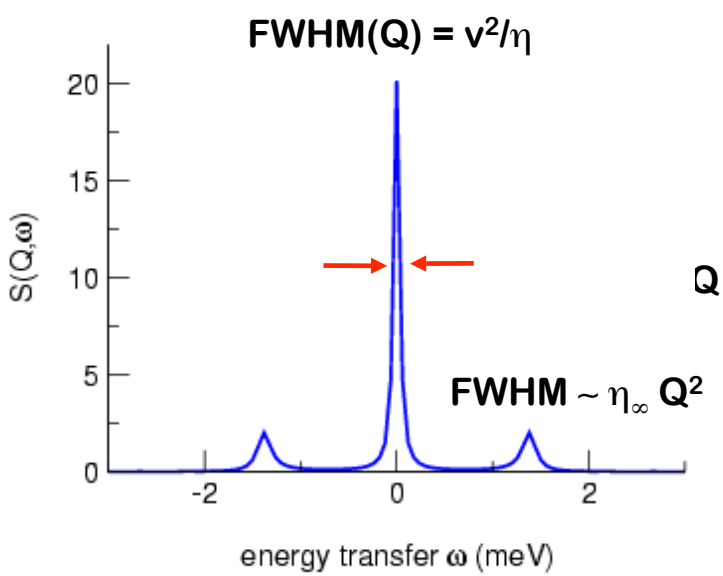

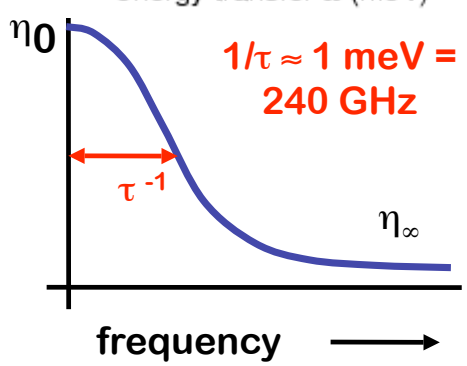

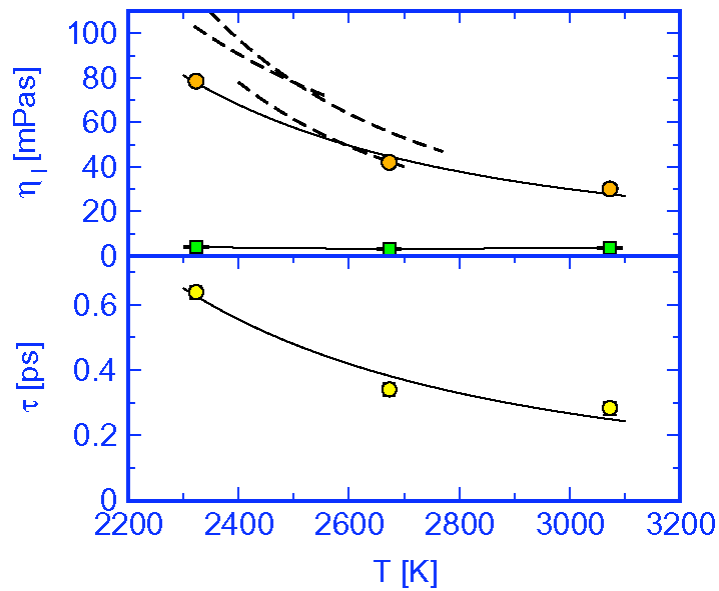

H. Sinn, B. Glorieux, L. Hennet, A. Alatas, M. Hu, E. Alp, F. Bermejo, D. Price, M. Saboungi: Science, 299: 2047, 2003

Viscoelasticity, $\eta(\omega)$

$$\eta(\omega) = \frac{\eta_0}{1 + i\omega\tau} + \eta_\infty$$

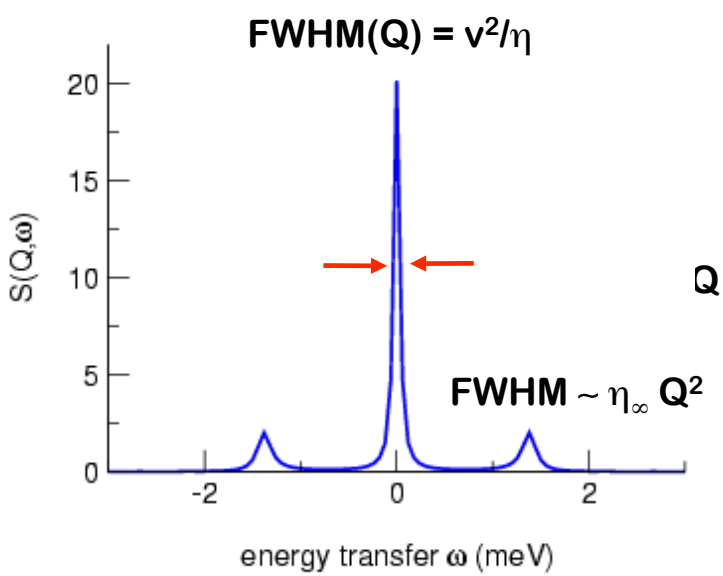

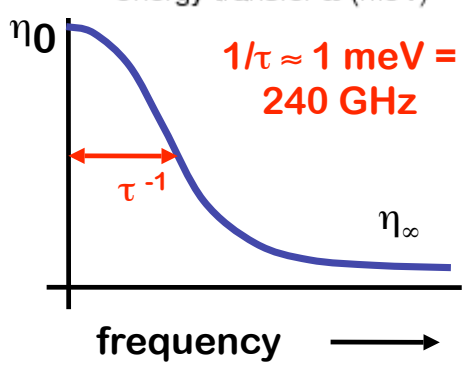

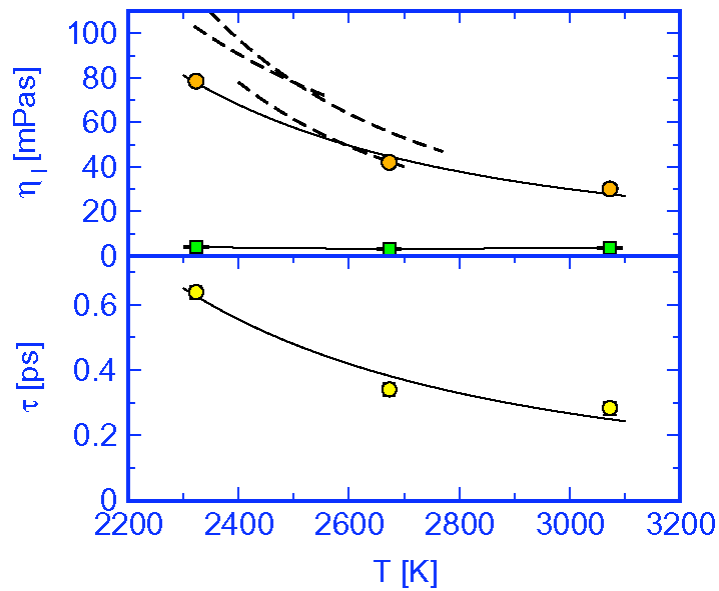

H. Sinn, B. Glorieux, L. Hennet, A. Alatas, M. Hu, E. Alp, F. Bermejo, D. Price, M. Saboungi: Science, 299: 2047, 2003

Silicon - IXS spectra

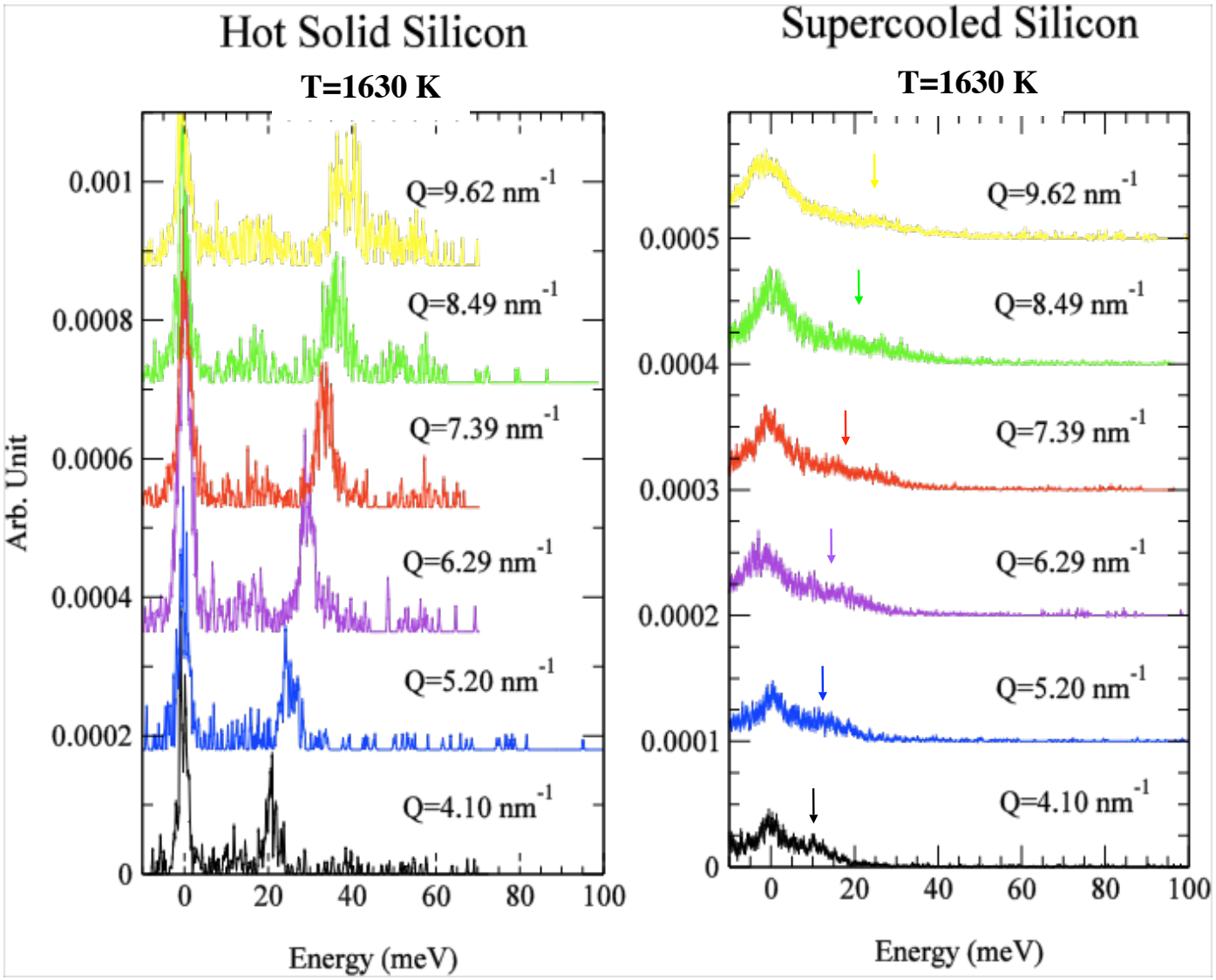

Courtesy: Ahmet Alatas, Ayman Said, &Harald Sinn

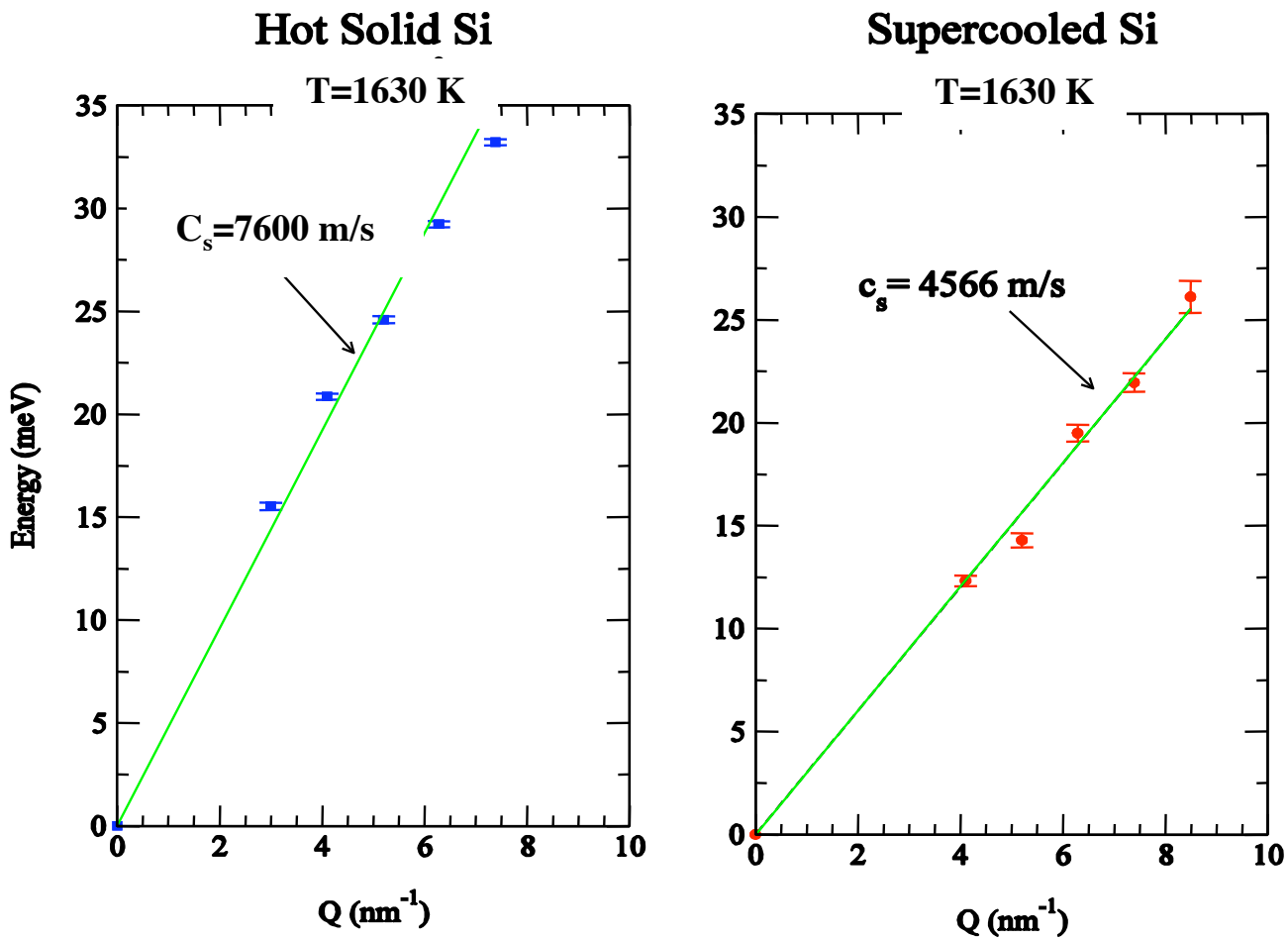
Hot Solid Si
T=1630 K
C_s=7600 m/s
Energy (meV)
Q (nm^{-1})
Supercooled Si
T=1630 K
c_s= 4566 m/s
Q (nm^{-1})

Current-Current Correlation Function, liquid Boron

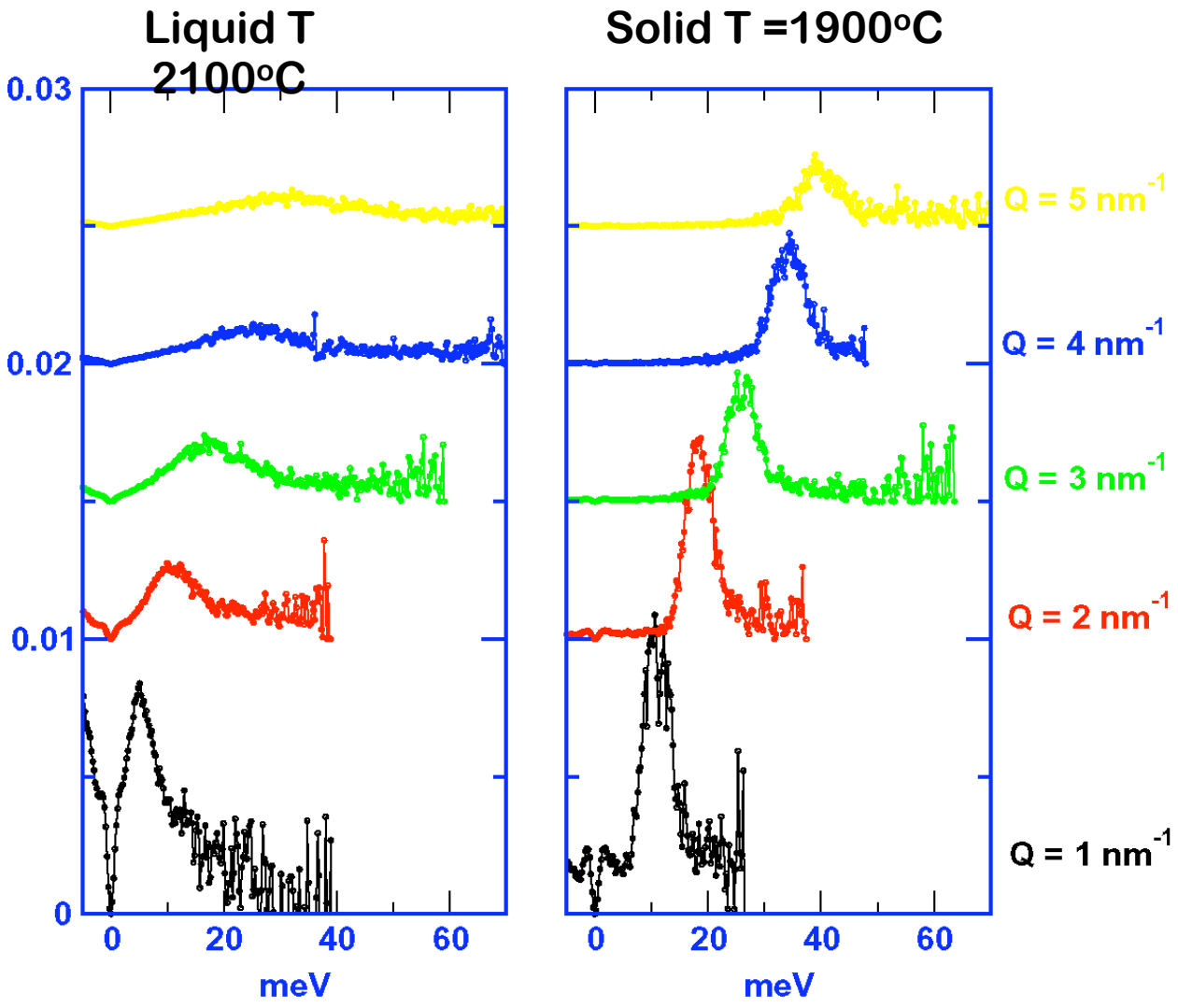

Sound dispersion in boron

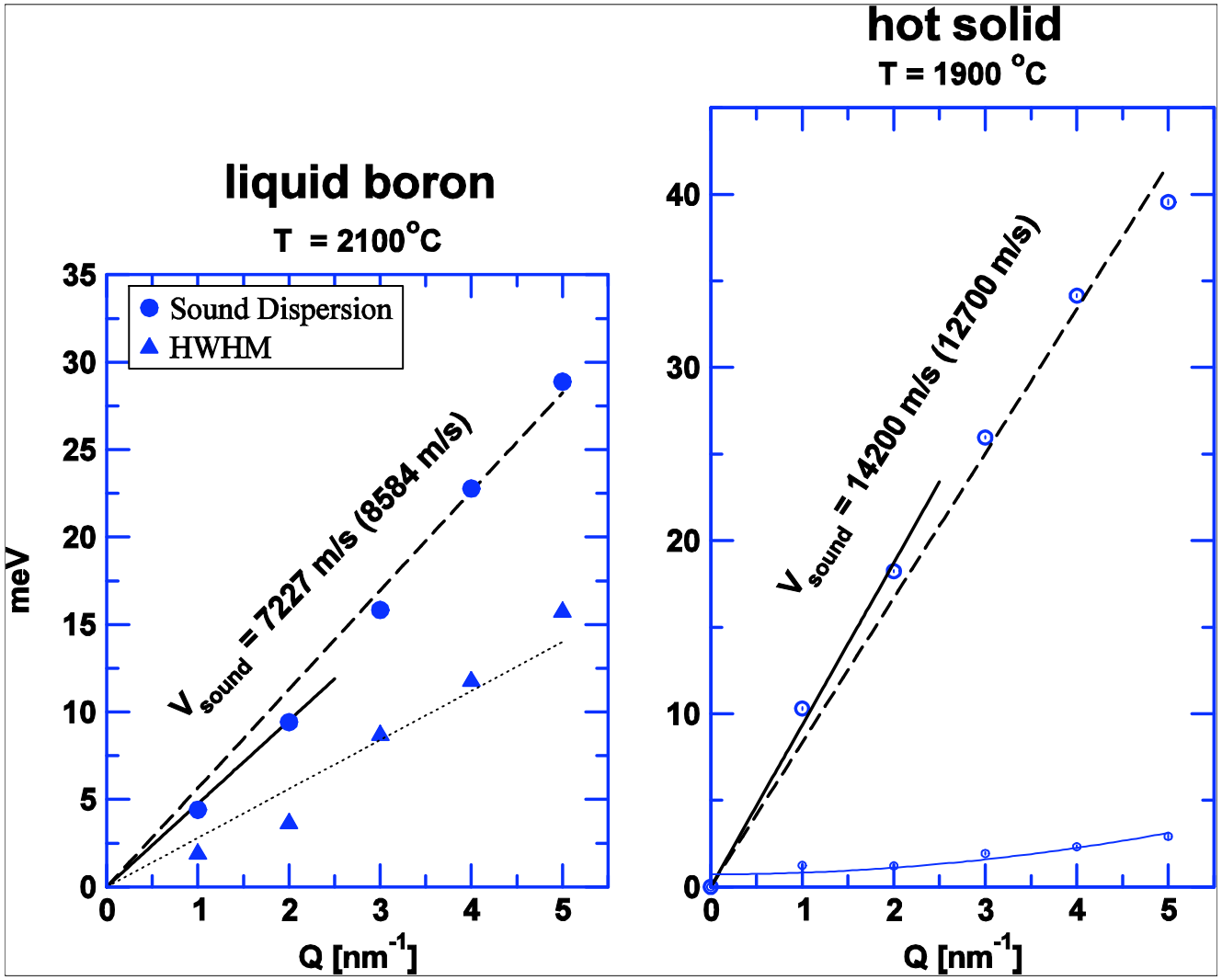

Literature: 14300 - 16000 m/s

49 % reduction in sound velocity upon melting

Si: 47%

Ge: 50 %

η_l (ω=0) = 14 mPas

$\eta_s \approx$ 1.5 mPas (est.)

τ(Q=0) = 0.2 ps

Sound velocity: What's the big deal ?

The sound velocity is directly related to elasticity, which is a function of chemical. and electronic properties materials. In Geosciences, for example, acoustic properties of materials in the Earth's deep interior are of general importance for accurate interpretation of seismic wave observations, geochemical modeling, and geodynamic simulations.

Despite their major roles in the deep Earth, very little is known about the sound velocities and crystal chemistry of these chemically complex phases under the appropriate pressure-temperature conditions.

The results of these IXS measurements under high pressure and temperature may enable a more realistic evaluation of the average mineralogy of Earth's lower mantle by comparing the measured sound velocities and elastic properties with a one-dimensional average Earth model, such as PREM.

The results also give insight into whether observed lateral variations of seismic wave speeds in the lower mantle are due to a chemical origin.

The electronic properties, including the charge and spin states, of iron in silicate perovskite were determined and will be discussed in light of our recent predictions considering the temperature effect on the electronic spin state of iron in dilute iron-bearing materials.

IXS-CDT Beamline: 30-ID

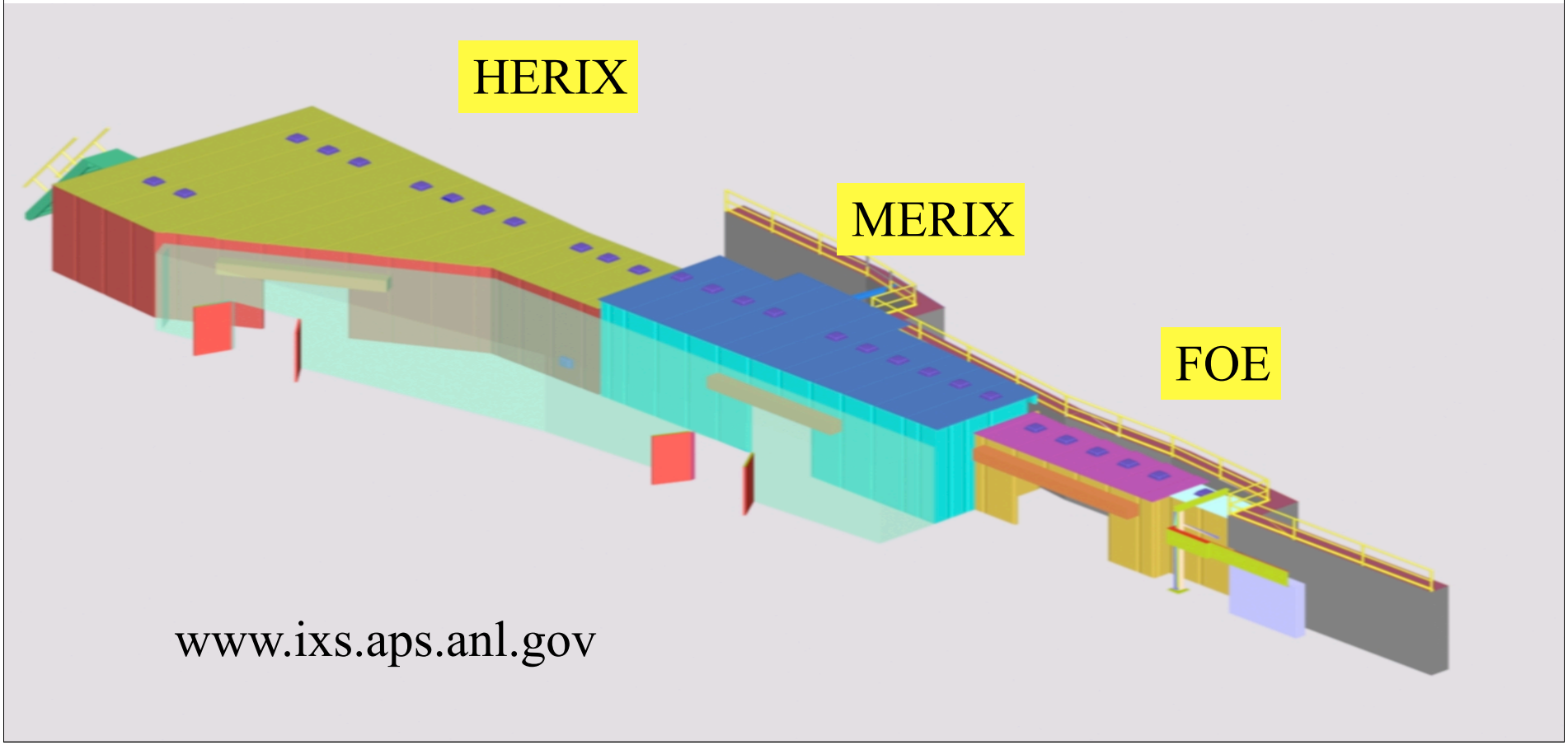

30-ID-B: MERIX Spectrometer

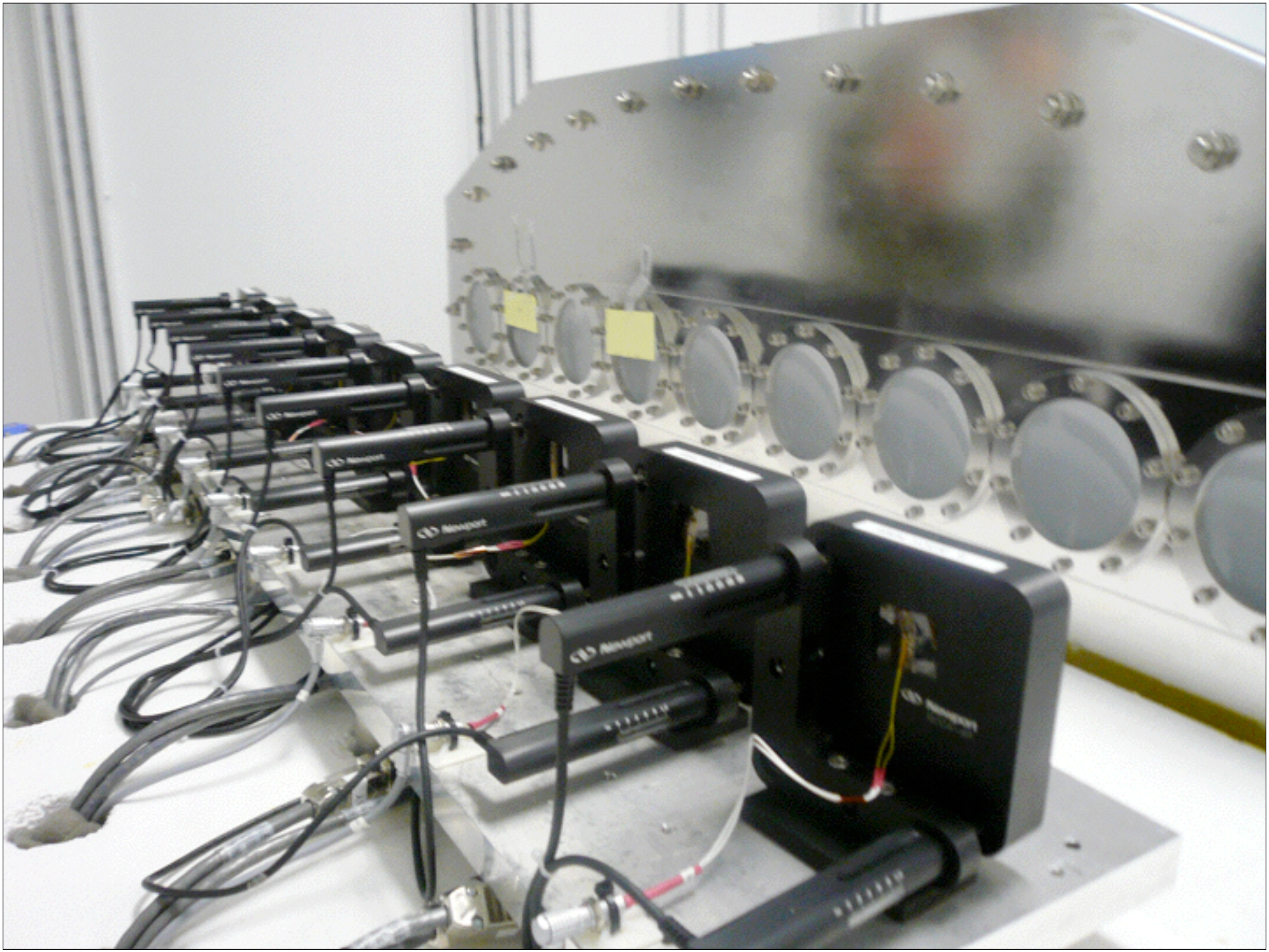

Ercan's dream machine:
SHERI : Super High Energy Resolution Instrument

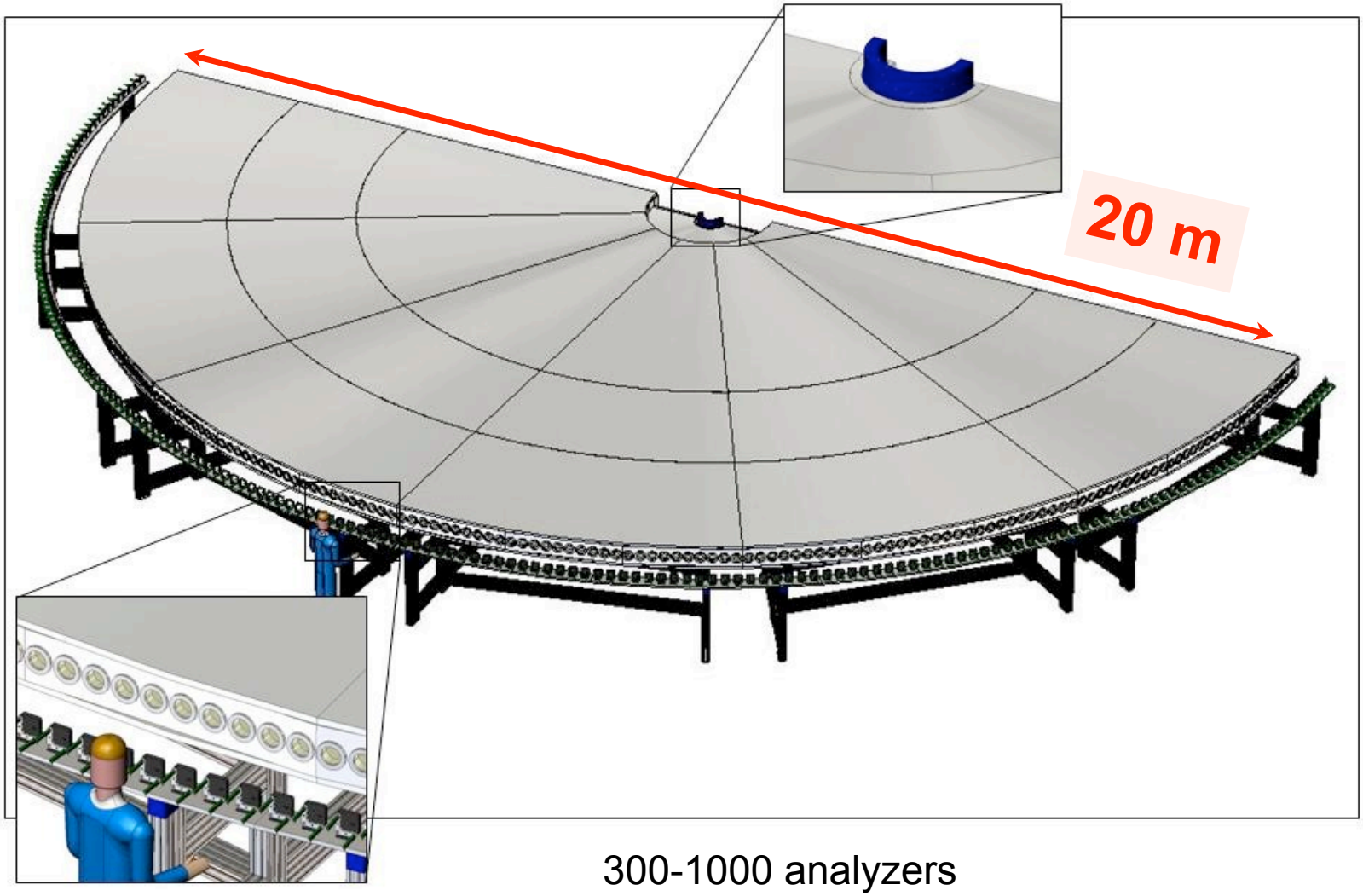

300-1000 analyzers
1% of solid angle, versus 0.01 % today

Why synchrotron radiation for Spectroscopy ?

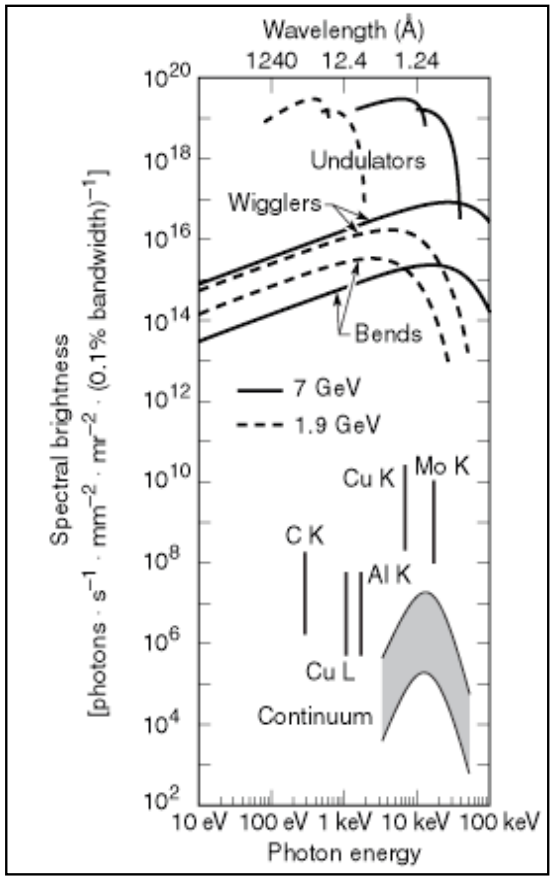

1. Bright and tunable over 100 keV with meV resolution
2. Collimated: good for monochromatization and focussing
3. Polarized; linear or circular with left or right handedness
4. Pulsed: suitable for time domain discrimination
5. Coherent: suitable for speckle and lensless imaging

The distinction between x and γ is historical and relates to the origin of radiation:

electronic transitions : x-rays
nuclear transitions : γ-rays

They overlap in energy

^{181}Ta Mössbauer line: 6.238 keV γ-rays
U $_{K\alpha 1}$ - emission line: 98.439 keV x-rays

Development of the average brightness of X-ray sources

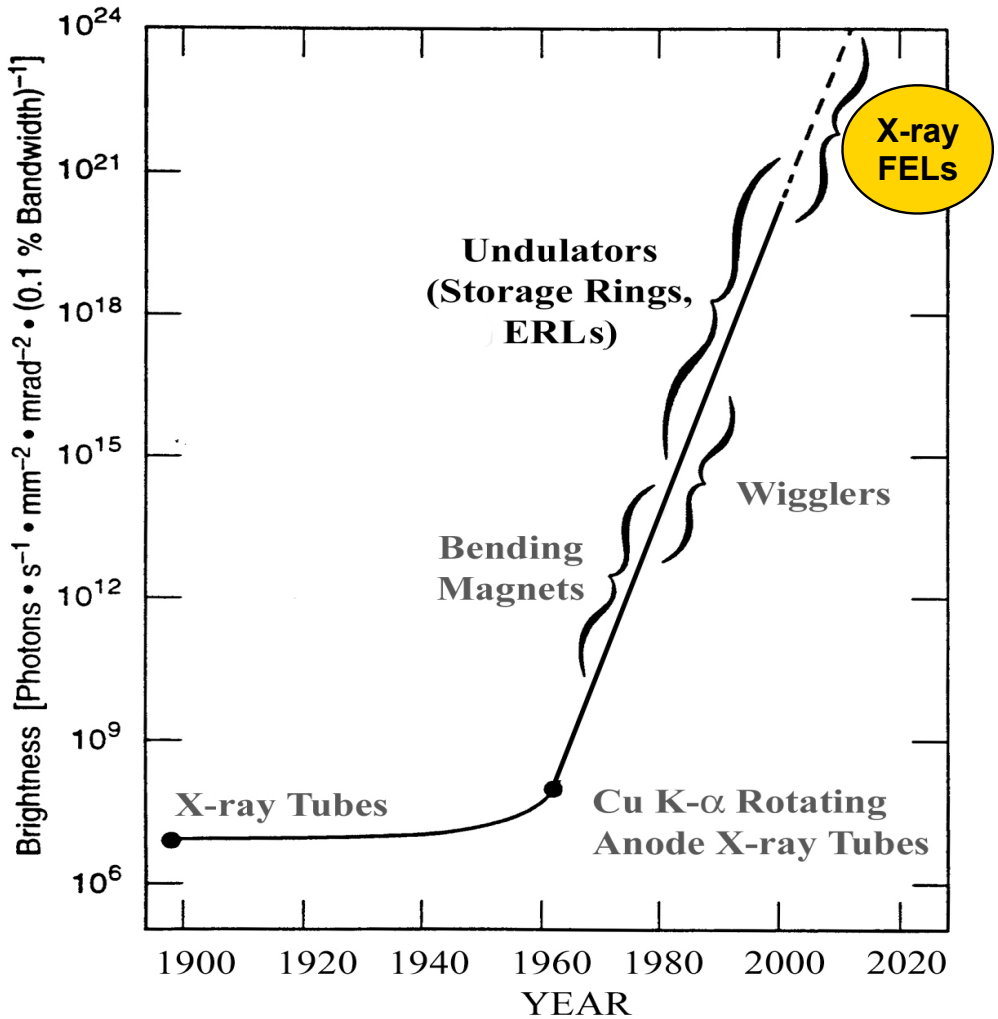

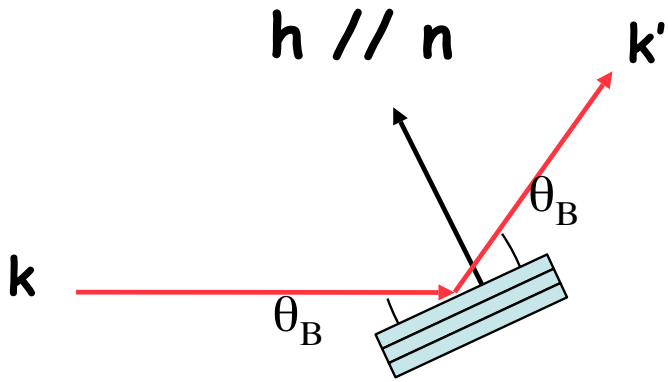

Symmetric: Bragg planes are parallel to the surface of the crystal

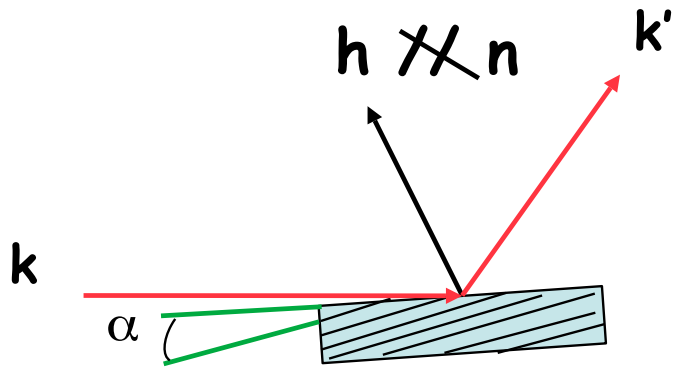

Asymmetric, Bragg planes are not parallel to the surface of the crystal

$$b = -\frac{\sin(\theta_B - \alpha)}{\sin(\theta_B + \alpha)}$$

b < 1	asymmetric,	beam enlarges
b = 1	symmetric,	$\alpha = 0$
b > 1	asymmetric	beam shrinks

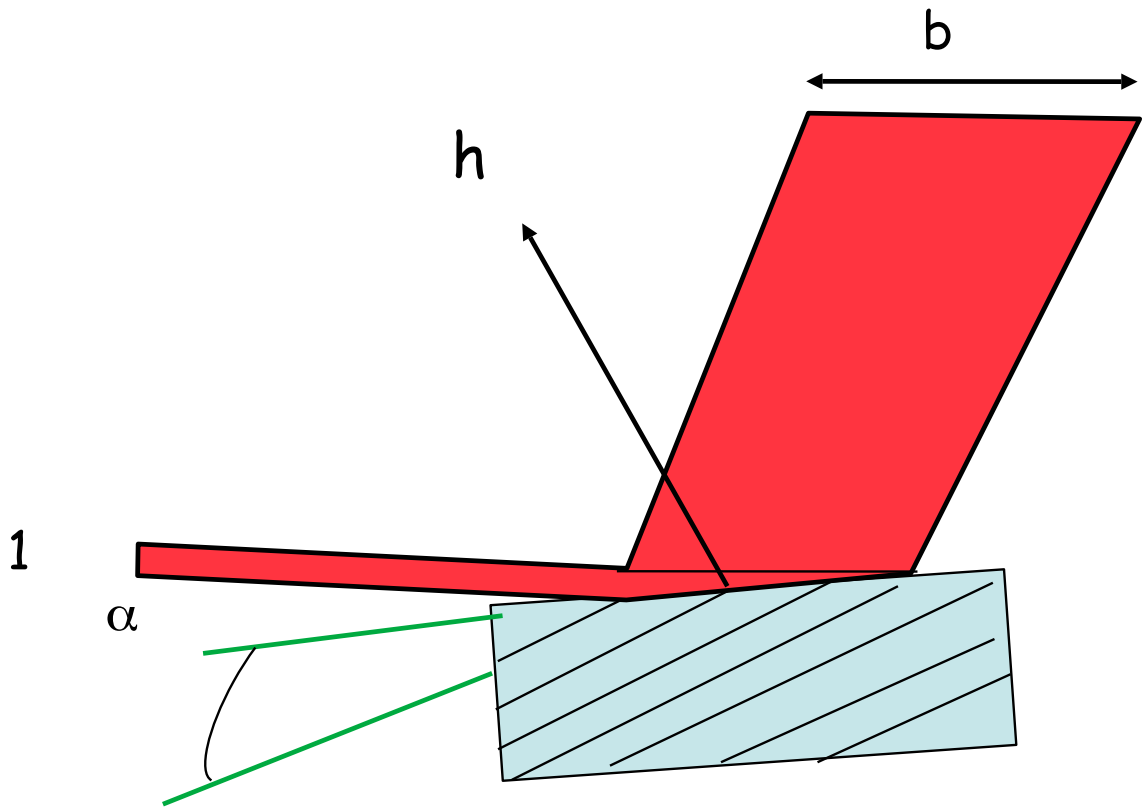

$$b = -\frac{\sin(\theta_B - \alpha)}{\sin(\theta_B + \alpha)}$$

$0.05 < b < 50$

Collimation by asymmetric Bragg diffraction

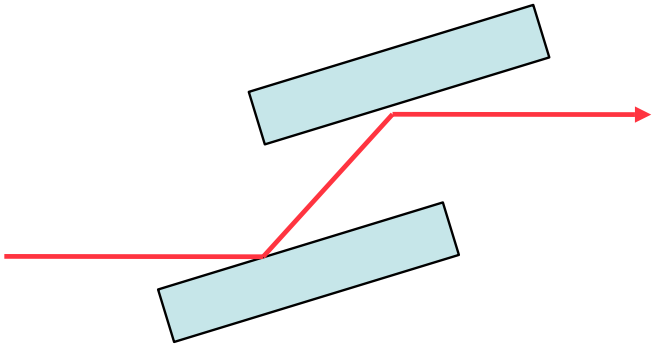

non-dispersive: (+ -)

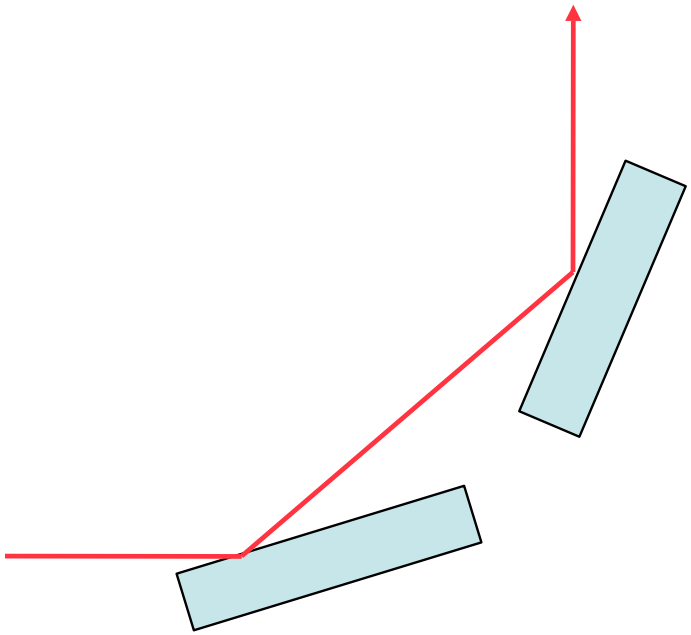

dispersive: (+ +)

Does not select energy per se
Beam leaves in the same direction

energy selective, beam
Leaves in a different direction

Si (800), 4 crystal set for 9.4 keV

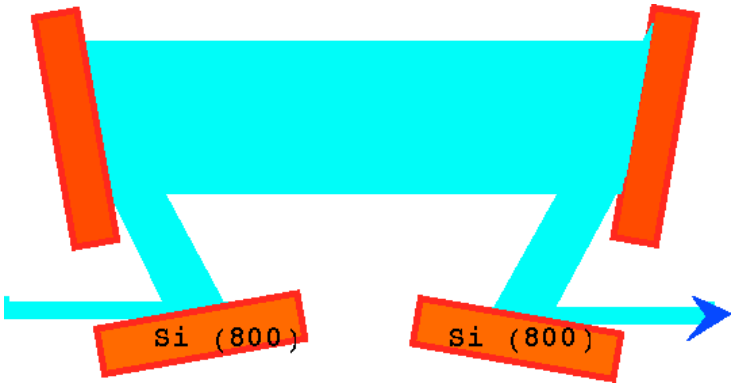

ΔE = 0.97 meV,
$\Delta\Theta$=32 μrad

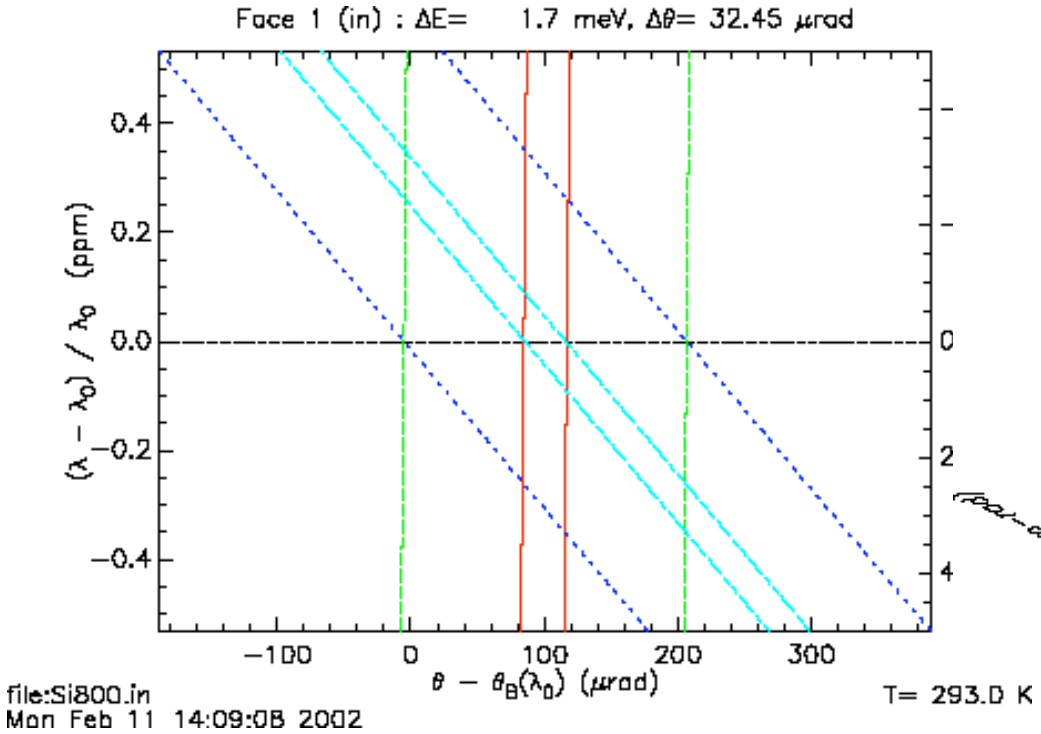

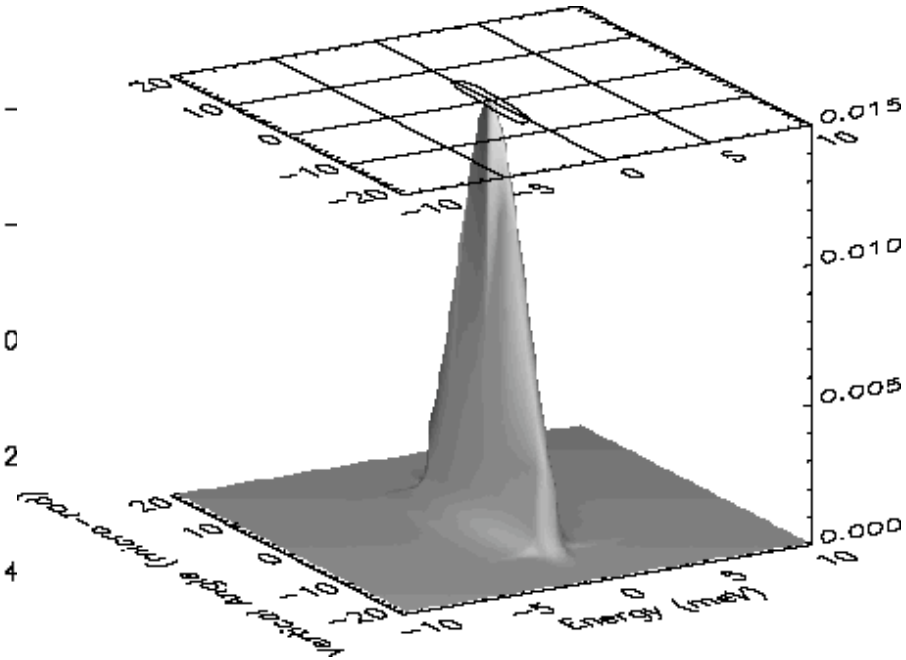

DuMond diagram (J. DuMond, 1932)

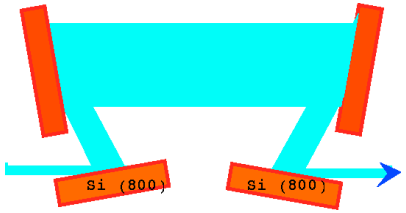

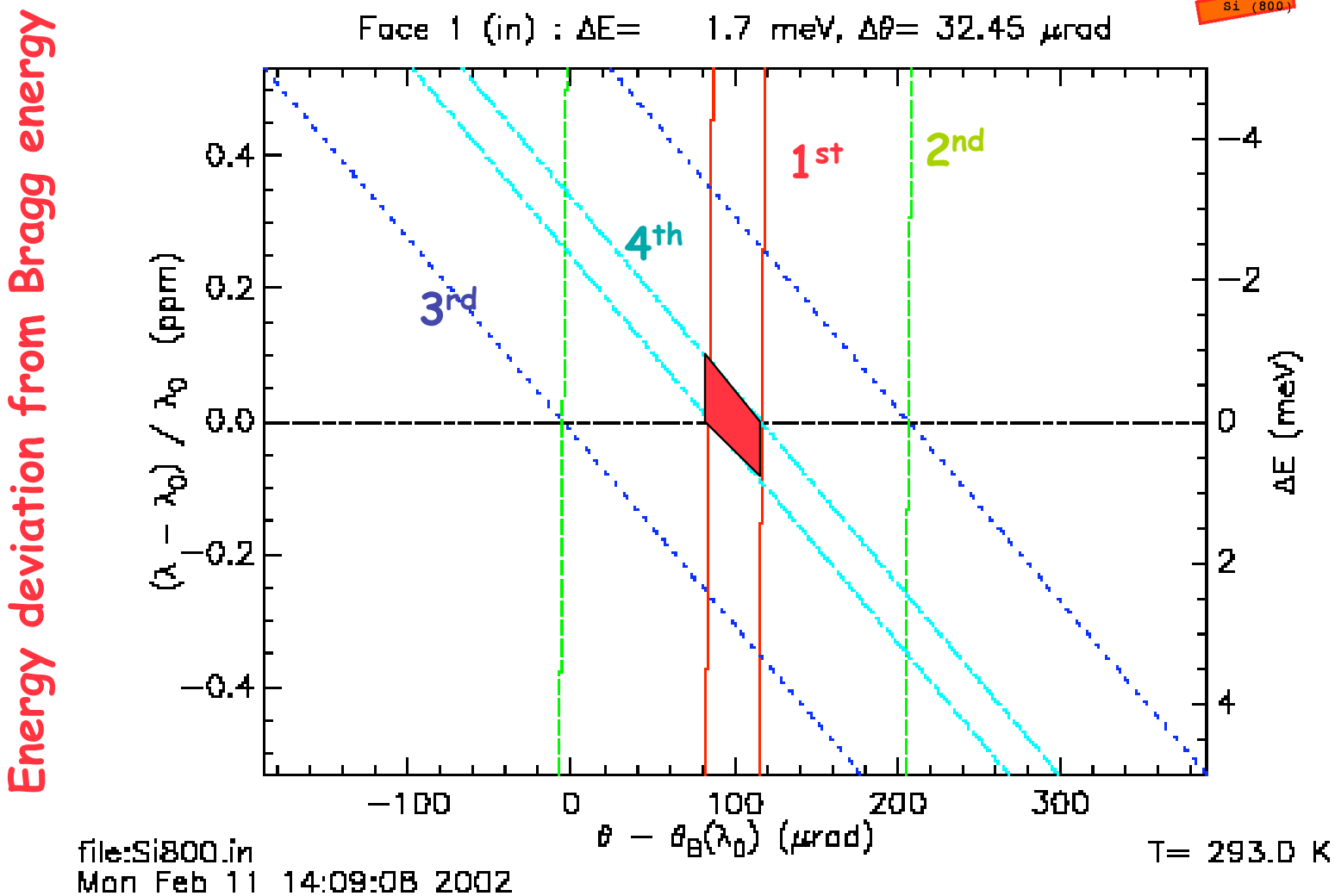

Energy deviation from Bragg energy

Angular deviation from Bragg angle

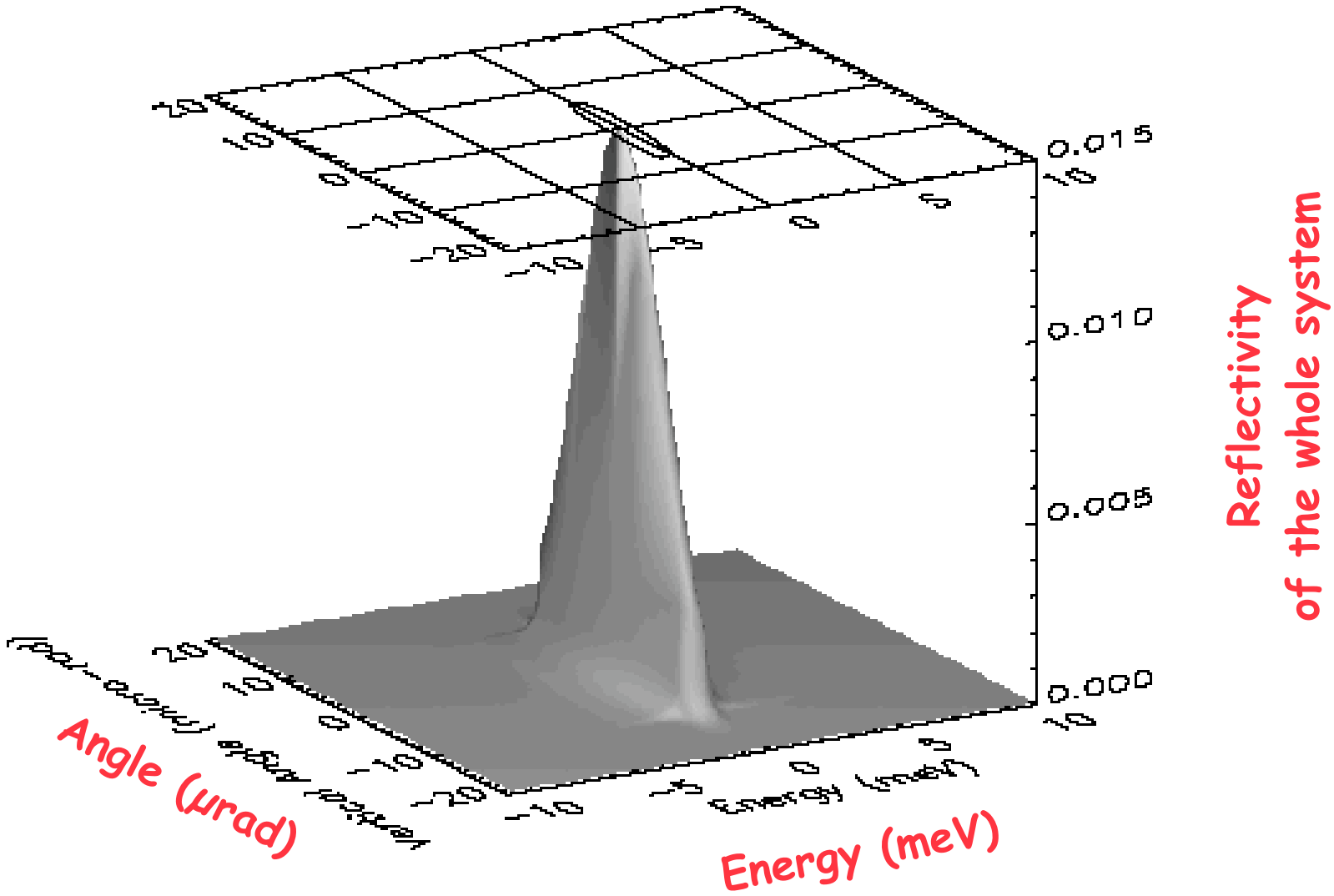
0.015
0.010
0.005
0.000
Reflectivity
of the whole system
Angle (μrad)
Energy (meV)

Si (800), 4 crystal set for 9.4 keV

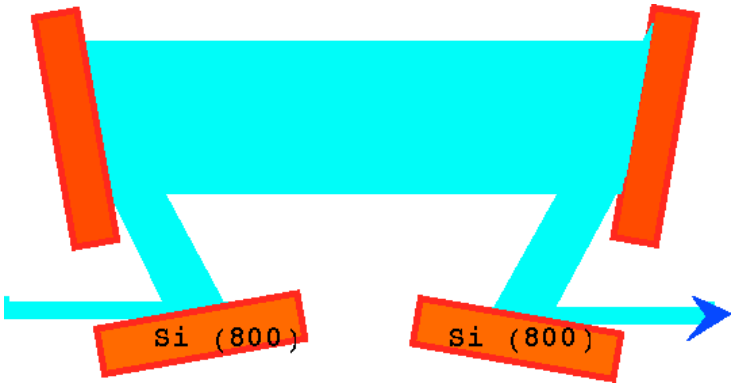

ΔE = 0.97 meV,
$\Delta\Theta$=32 μrad

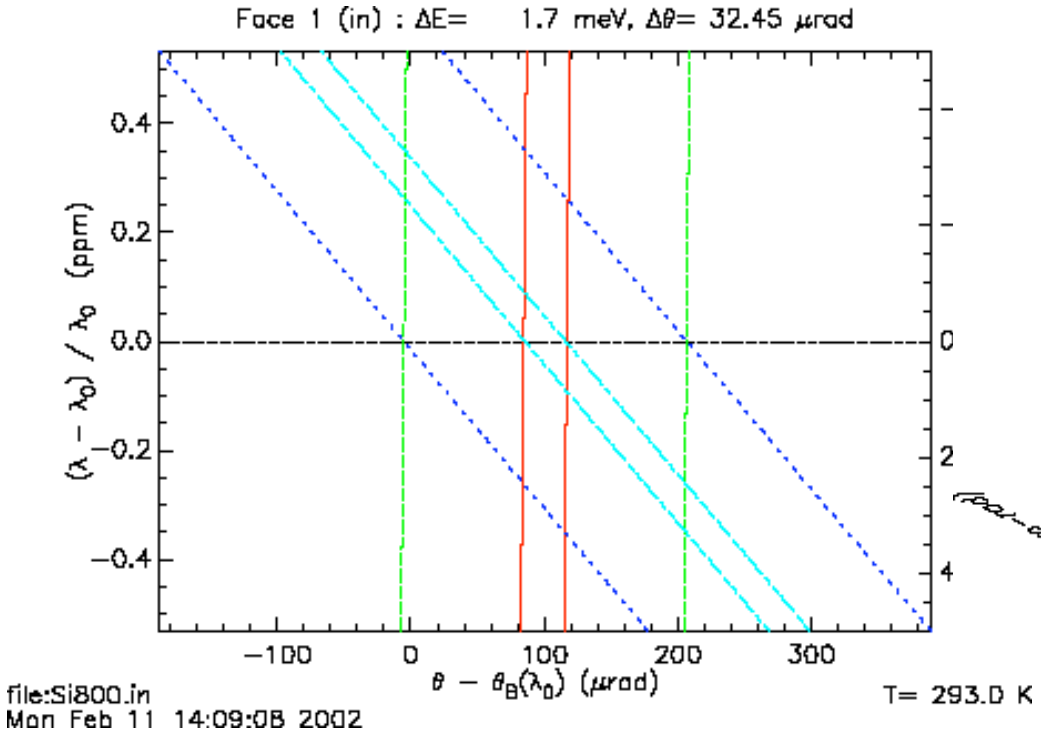

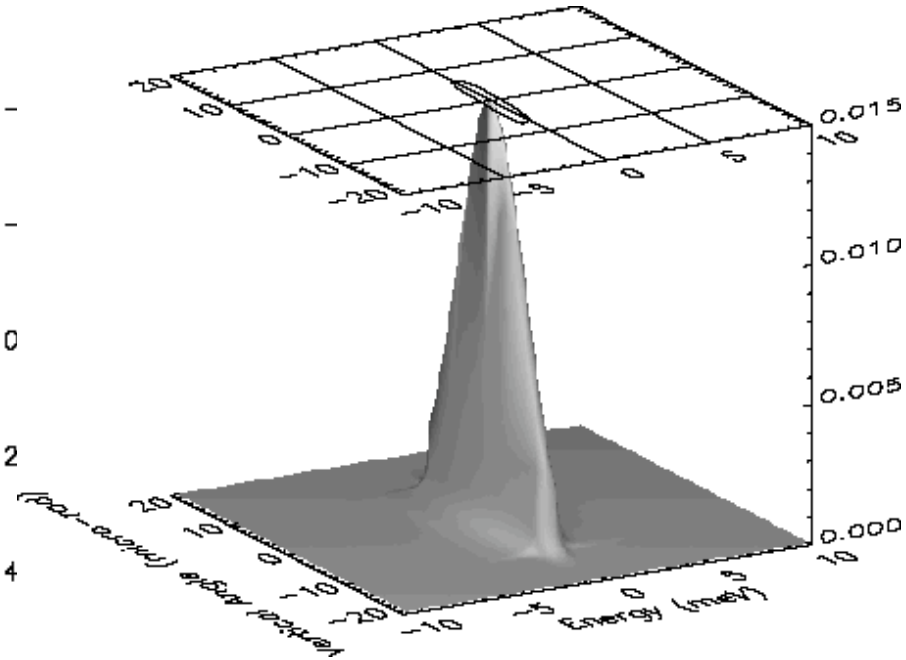

New monochromators with artificially linked, dispersive channel-cut configuration

^{83}Kr, E= 9.401 keV, ΔE= 1.0 meV

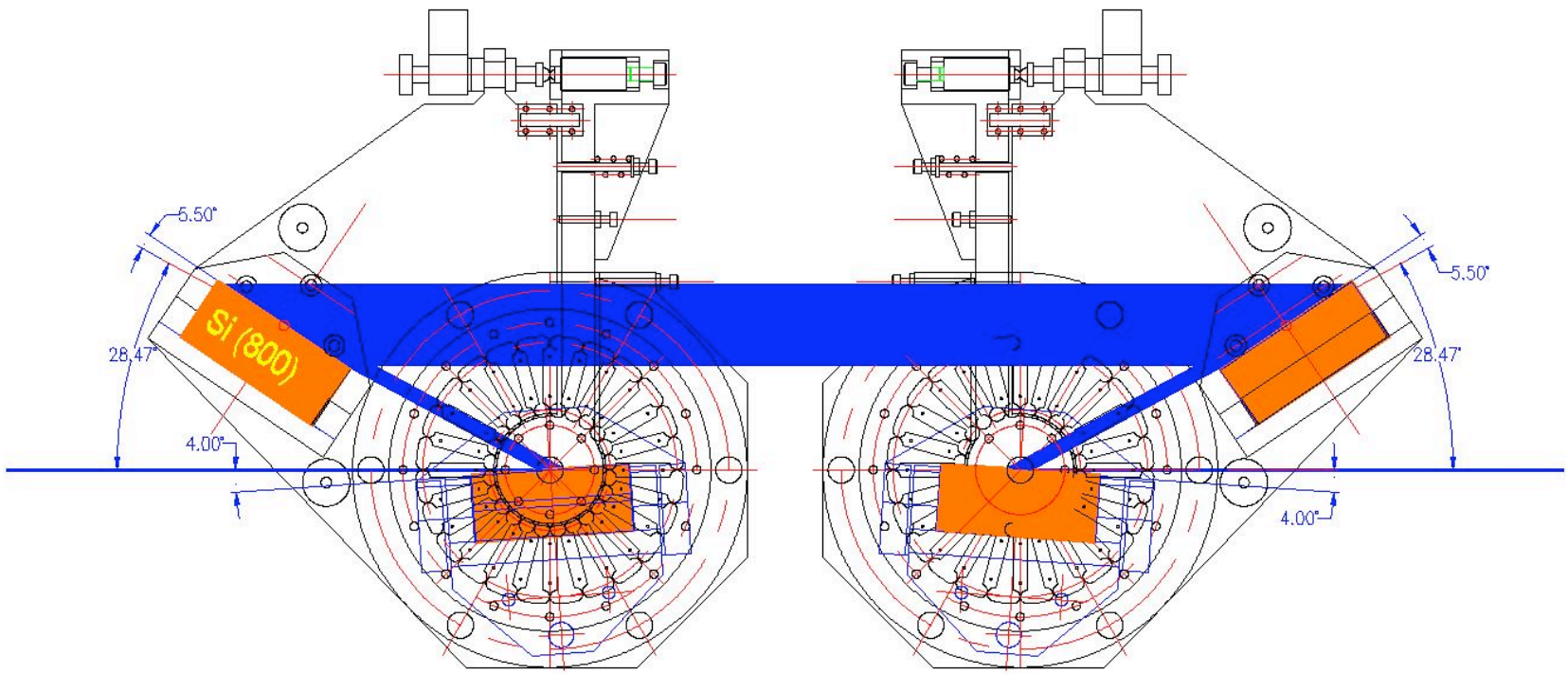

sub-meV mono's between 9-30 keV

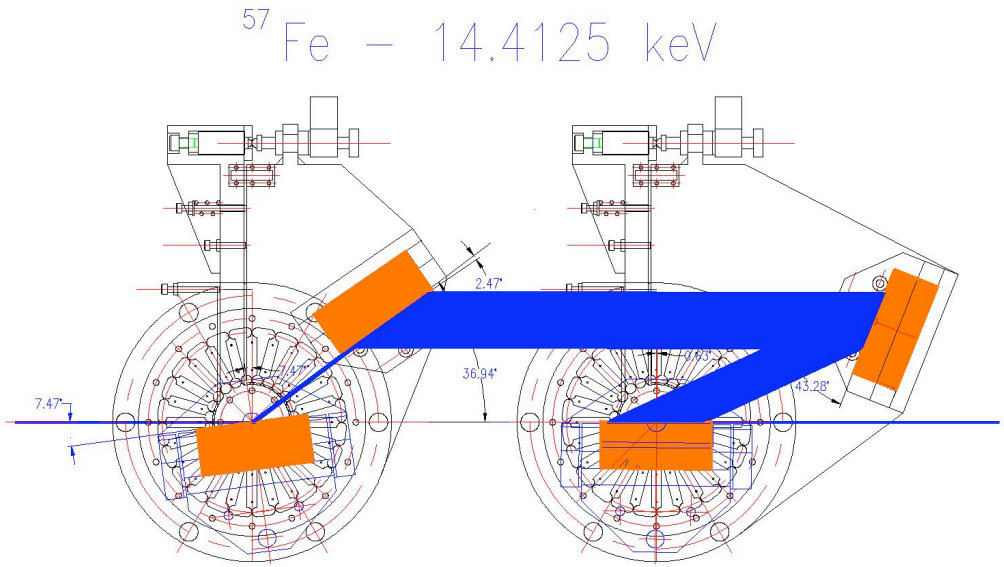

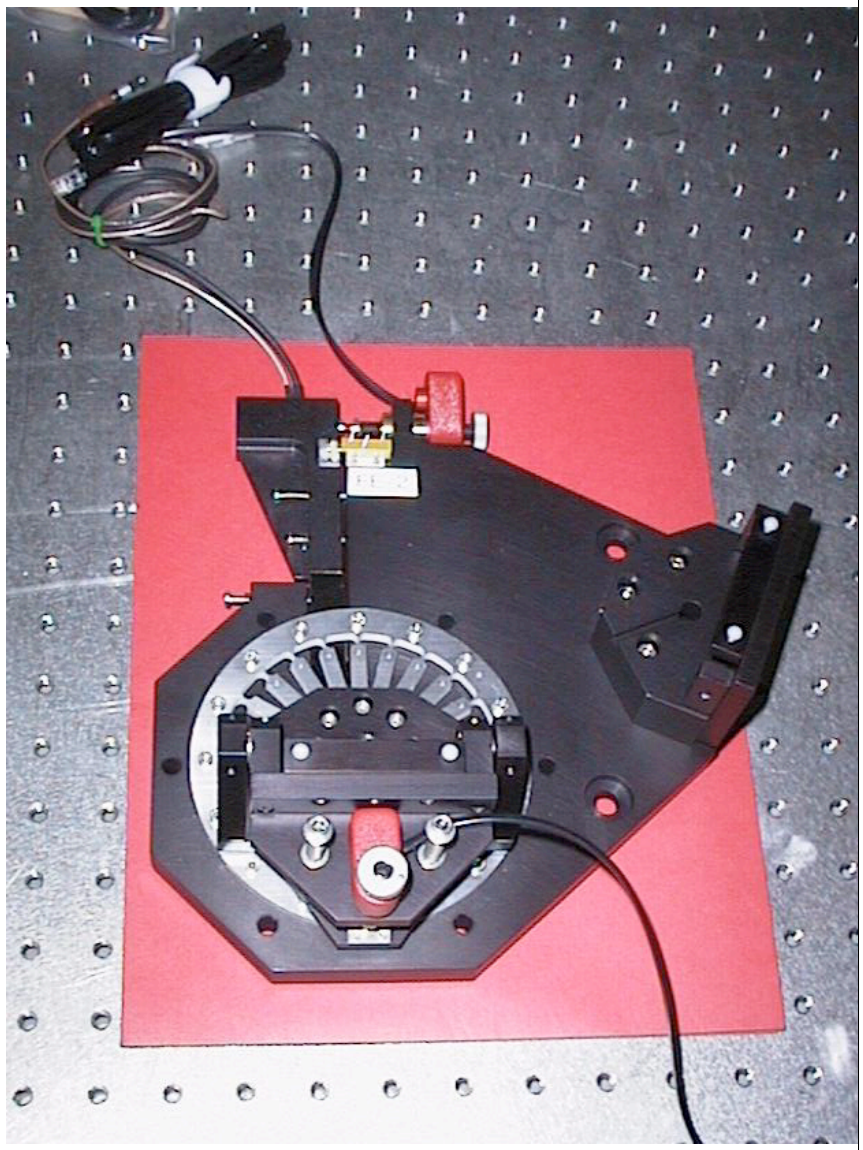

Artificially linked nested mono's

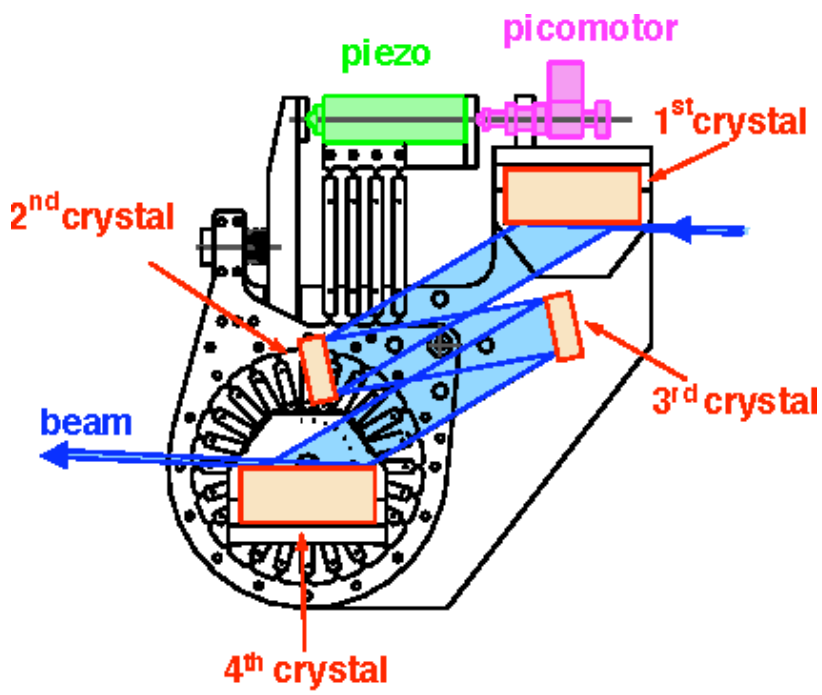

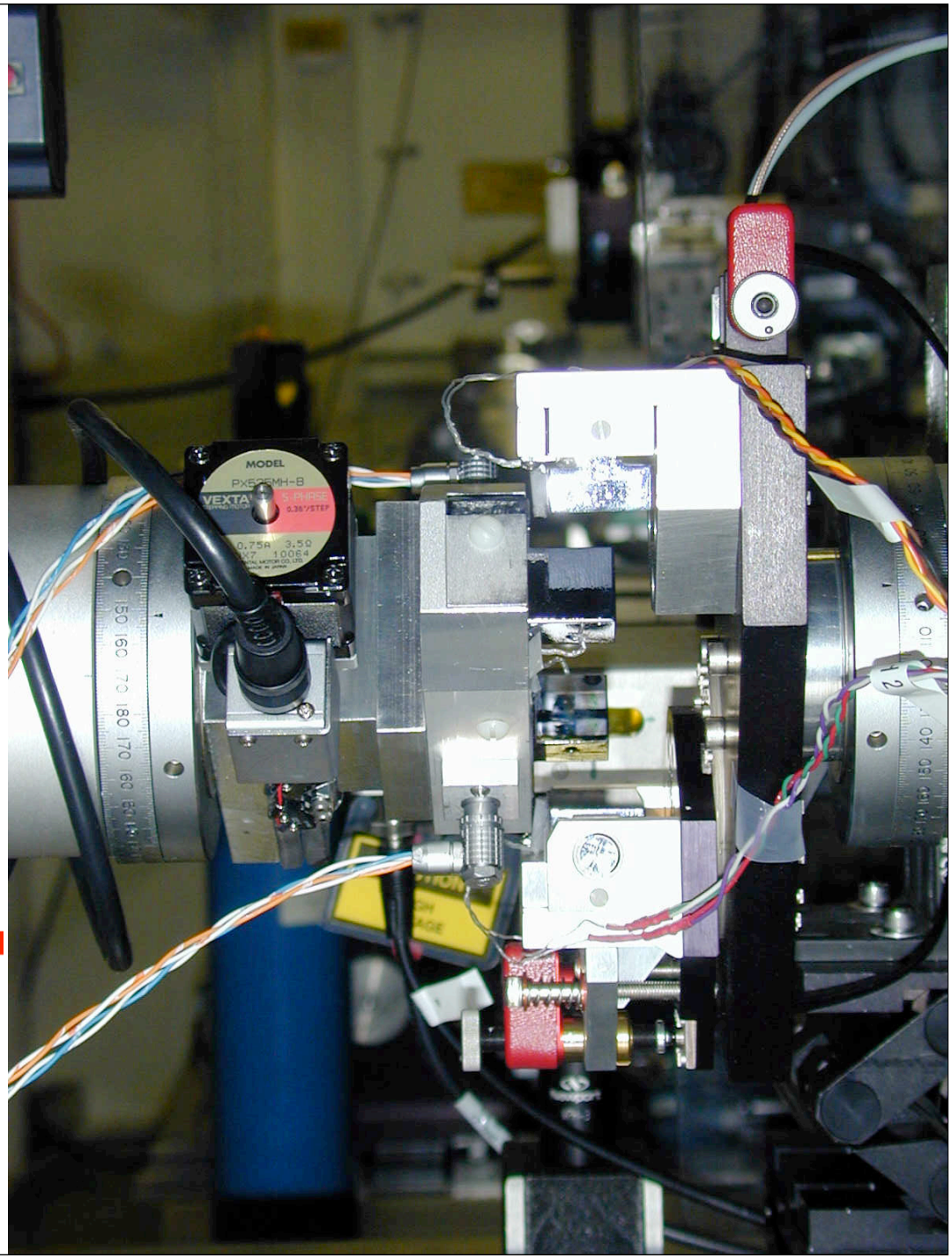

3-ID-B
APS

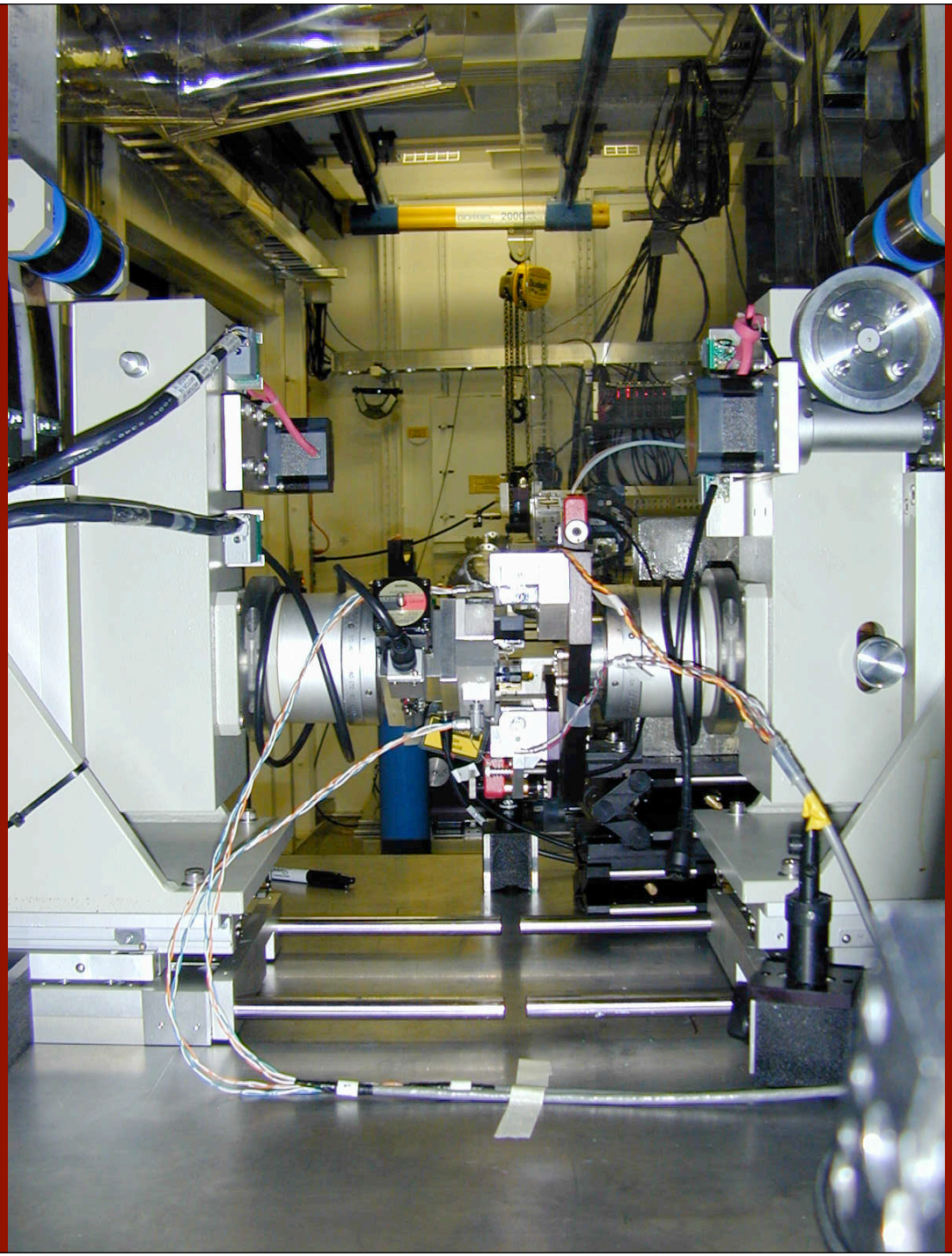

Generations of high-resolution monochromators

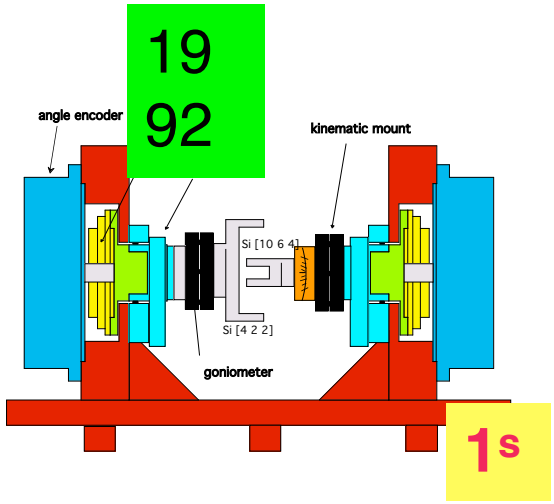

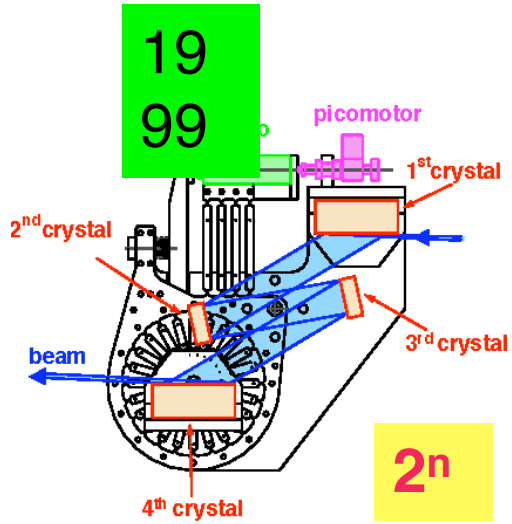

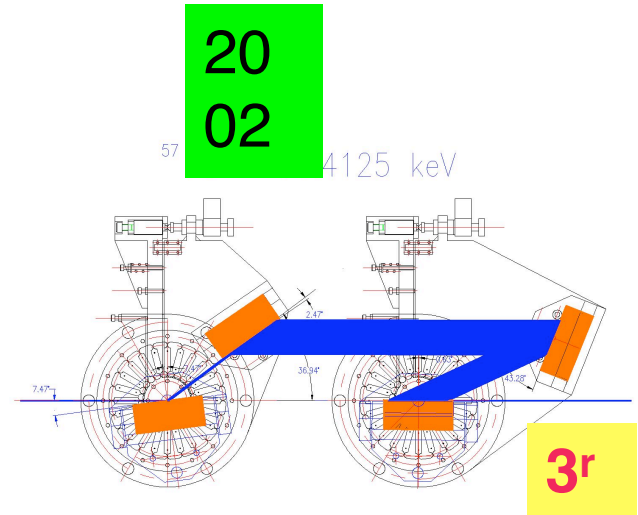

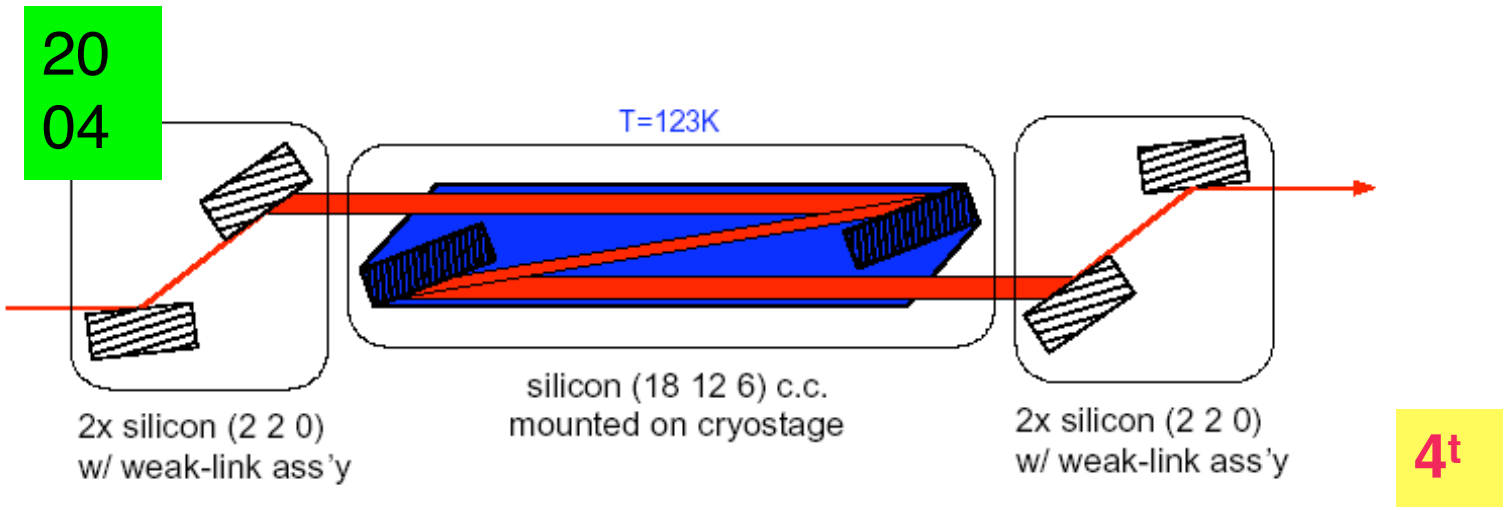

T. Toellner

Record resolution at 23.870 keV
^{119}Sn nuclear resonance
T. Toellner, 2003

$$E/\Delta E = 1.7 \cdot 10^8$$

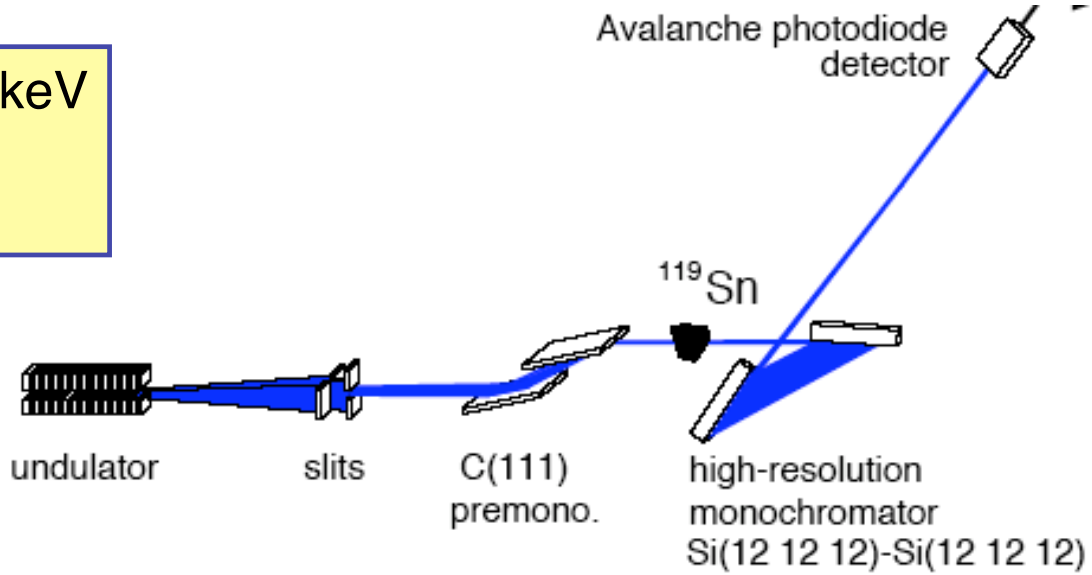

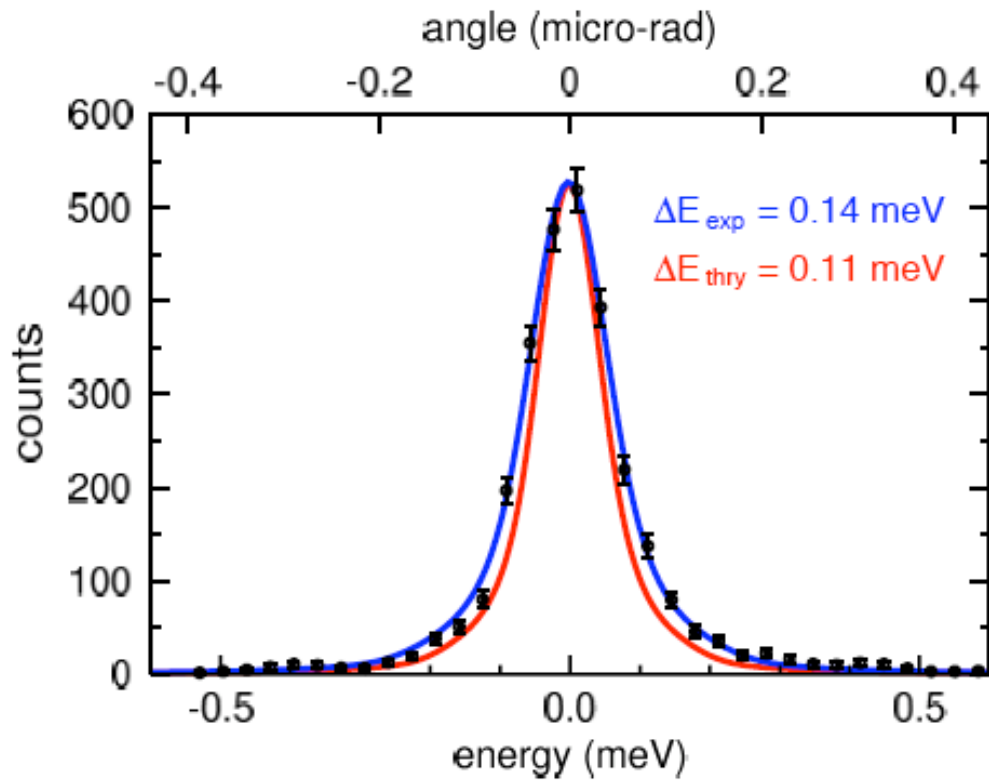

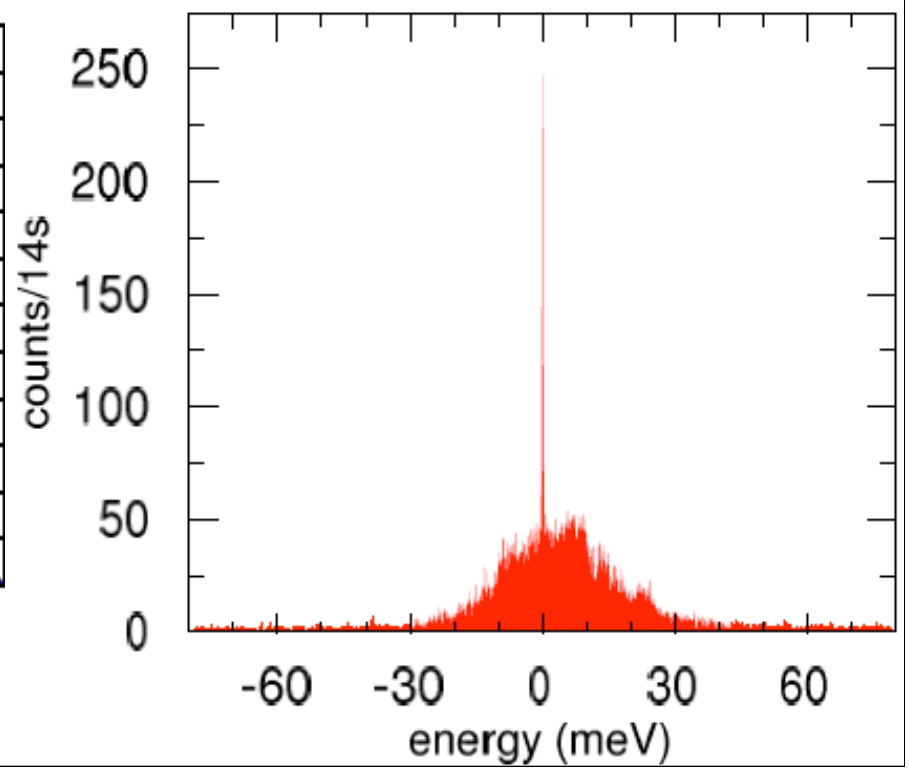

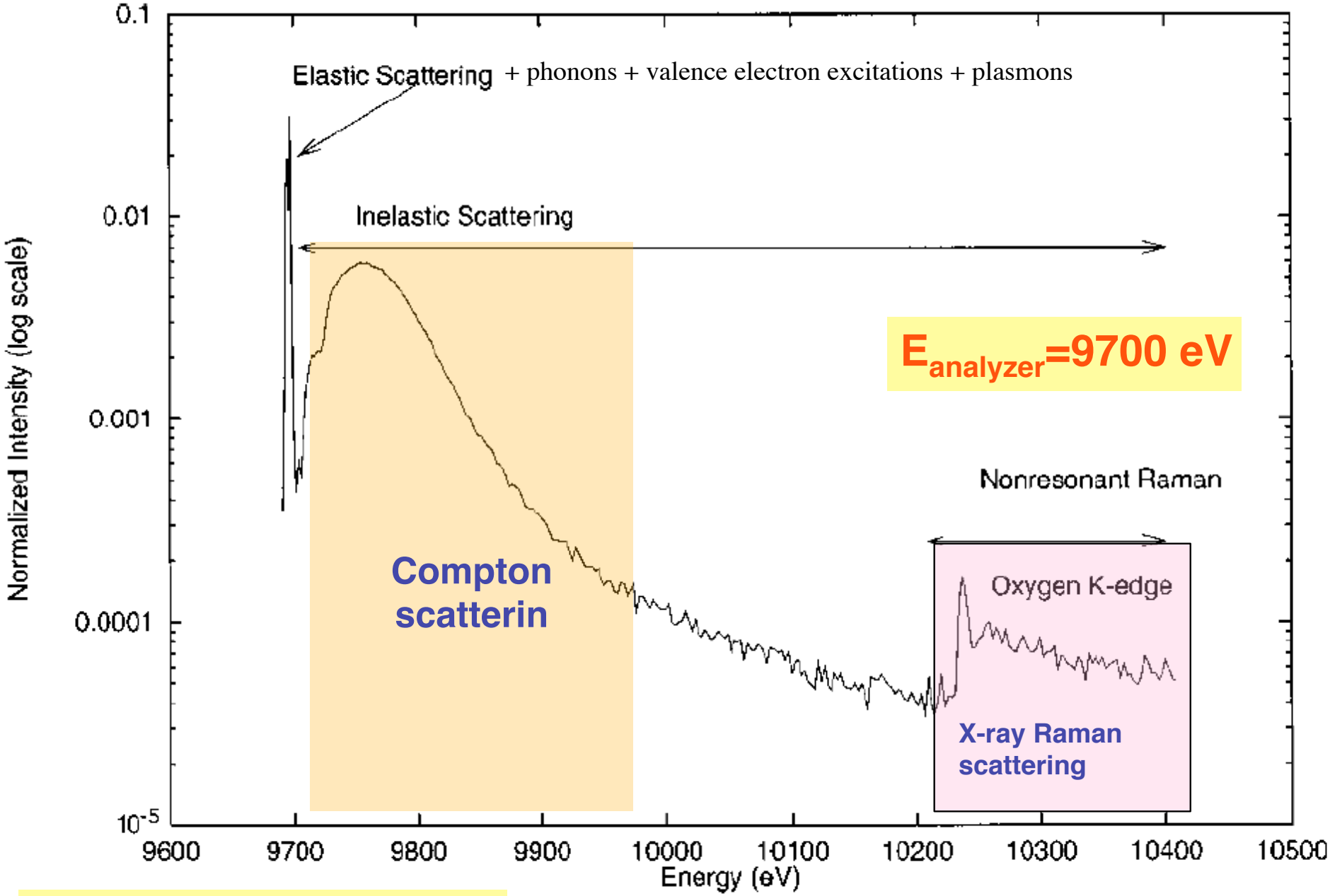

(D.T. Bowron et al, Phys. Rev. B 62 R9223)

Part 3

Nuclear Resonant Inelastic X-Ray Scattering

also known as

Nuclear Inelastic Scattering (NIS)
or

Nuclear Resonant Vibrational Spectroscopy (NRVS)

Argonne NATIONAL LABORATORY

... for a brighter future

Nuclear Resonant Inelastic X-Ray Scattering

W. Sturhahn, J. Zhao, T. S. Toellner, Y. Xiao, B. Leu,
M. Lerche, S. Kharlamova
Advanced Photon Source

T. Sage (Northeastern University)
R. Scheidt, N. Silvernail (Notre Dame)
S. Cramer, Y. Guo, M. Smith (UC, Davis)
S. Durbin (Purdue)
U. Jayasooria (East Anglia University, UK)
W. Keune, (Duisburg)
B. Roldan Cuenya (University of Central Florida)
H. Gieffers, E. Tanis, M. Nicol (UNLV)

4 generation of Mössbauer Spectroscopists (1960-2000) at Argonne

What is it ?

- **Nuclear Resonant Inelastic X-Ray Scattering (NRIXS, NIS,NRVS)**
  - Scattering from PHONONS, detected via exciting a low-lying nuclear resonance
  - **Energy range: 6-100 keV,**
  - **Incident beam: monochromatic to 1 meV level, tunable over several eV,**
  - **Scattered beam: Incoherent, polychromatic over several hundred eV**
  - **Analyzer: Mössbauer resonant nuclei embedded in the sample, nsec time resolved Avalanche Photodiode Detector (APD)**
  - **Energy Resolution : ~ 0.1-10 meV**
  - **Momentum transfer: A momentum integrated method, measuring displacements along the incident beam direction**
- **Main Features:**
  - **Allows determination of phonon density of states, from which many thermodynamic functions can be deduced, element and isotope selective, can be used in crystalline, amorphous materials alike, thin films, buried layers, extreme environments**

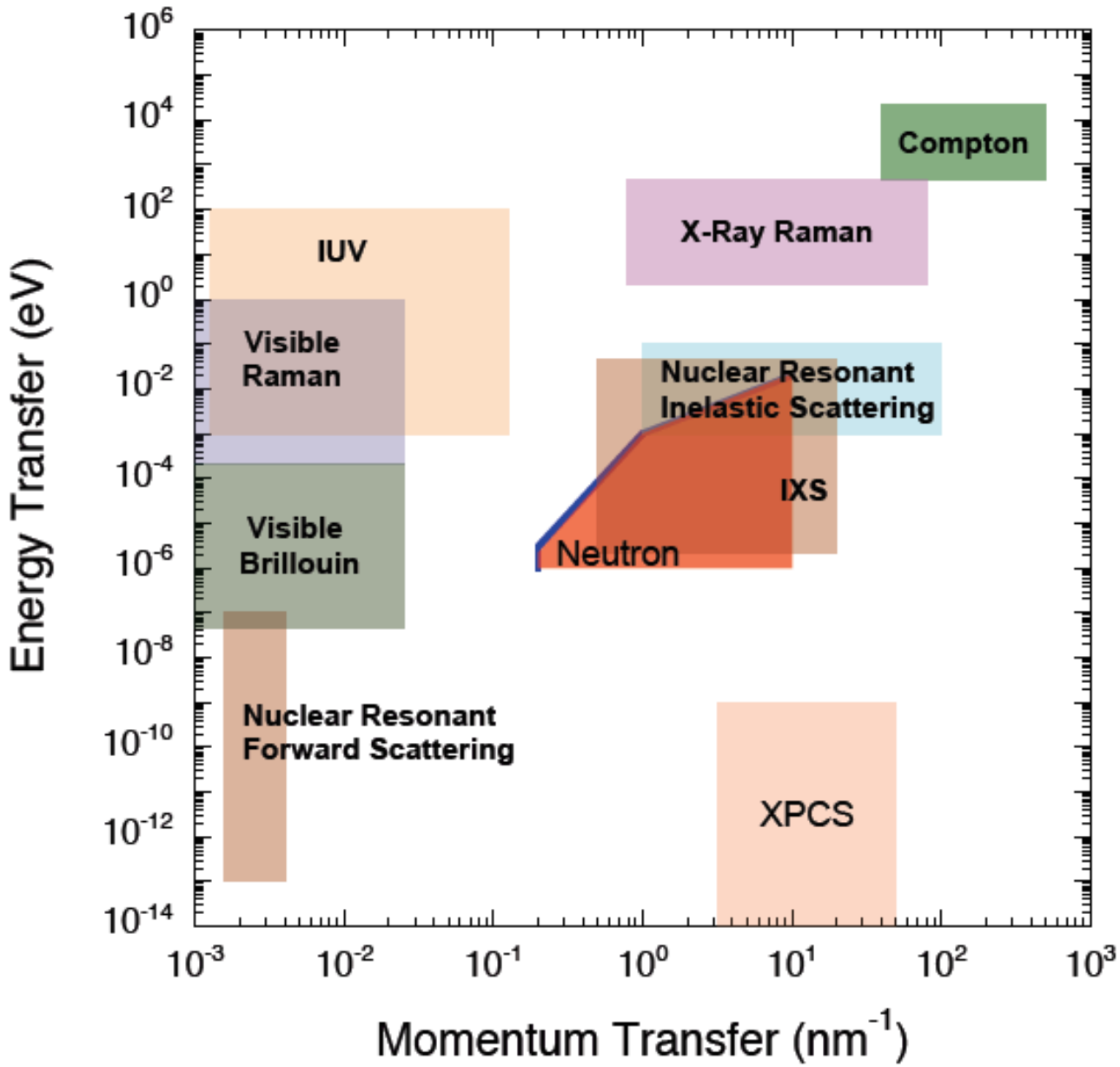
Compton
X-Ray Raman
IUV
Visible
Raman
Nuclear Resonant
Inelastic Scattering
IXS
Visible
Brillouin
Neutron
Nuclear Resonant
Forward Scattering
XPCS
Energy Transfer (eV)
Momentum Transfer (nm^{-1})
10^{6}
10^{4}
10^{2}
10^{0}
10^{-2}
10^{-4}
10^{-6}
10^{-8}
10^{-10}
10^{-12}
10^{-14}
10^{-3}
10^{-2}
10^{-1}
10^{0}
10^{1}
10^{2}
10^{3}

NR-IXS set-up

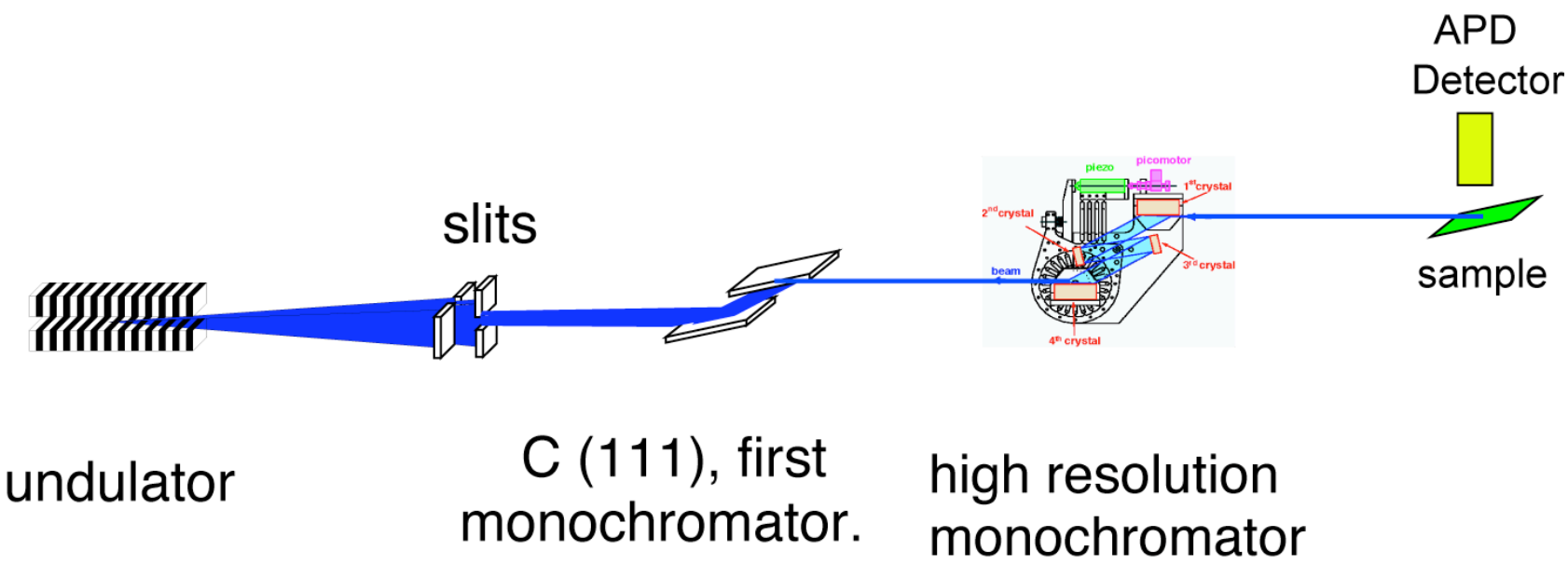
APD
Detector
slits
piezo
picomotor
1st crystal
2nd crystal
3rd crystal
4th crystal
beam
sample
undulator
C (111), first
monochromator.
high resolution
monochromator

Standard Time structure @ APS

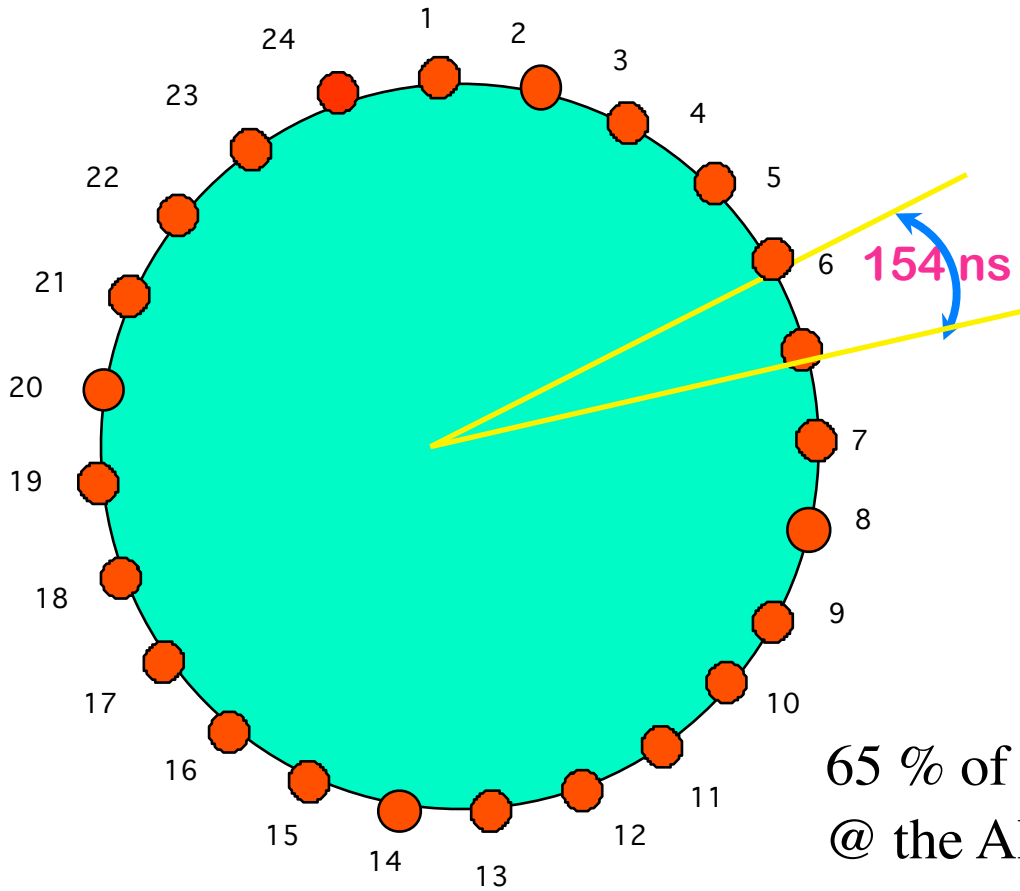

65 % of the time
@ the APS

1 revolution=3.68 μsec =>1296 buckets

Why synchrotron radiation for Mossbauer Spectroscopy ?

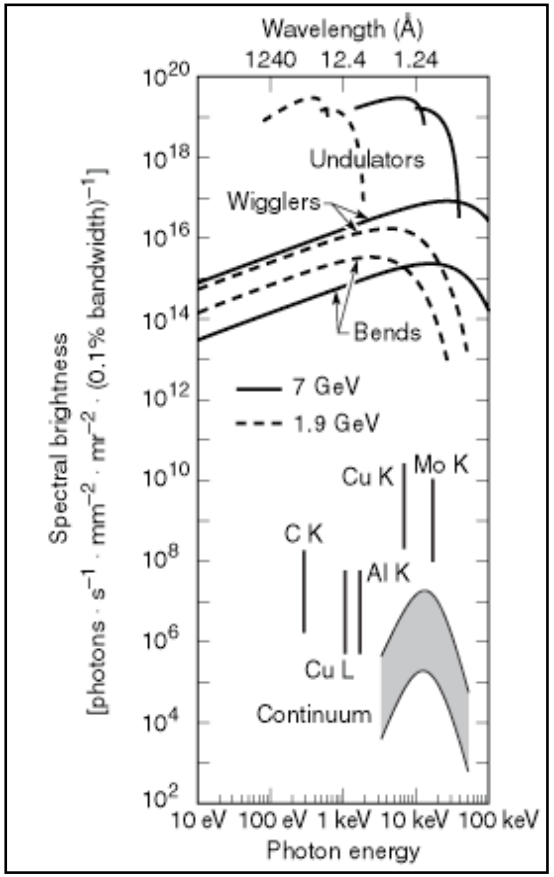

1. Bright and tunable over 100 keV with meV resolution
2. Collimated: good for monochromatization and focussing
3. Polarized; linear or circular with left or right handedness
4. Pulsed: suitable for time domain discrimination
5. Coherent: ? SR-PAC

Recoilless emission and absorption of γ- rays.

The distinction between x and γ is historical and relates to the origin of radiation:

electronic transitions :	x-rays
nuclear transitions :	γ-rays

They overlap in energy

^{181}Ta Mossbauer line:	6.238 keV γ-rays
U $_{K\alpha 1}$ - emission line:	98.439 keV x-rays

Nuclear Resonance and Fallout in ^{57}Fe-decay

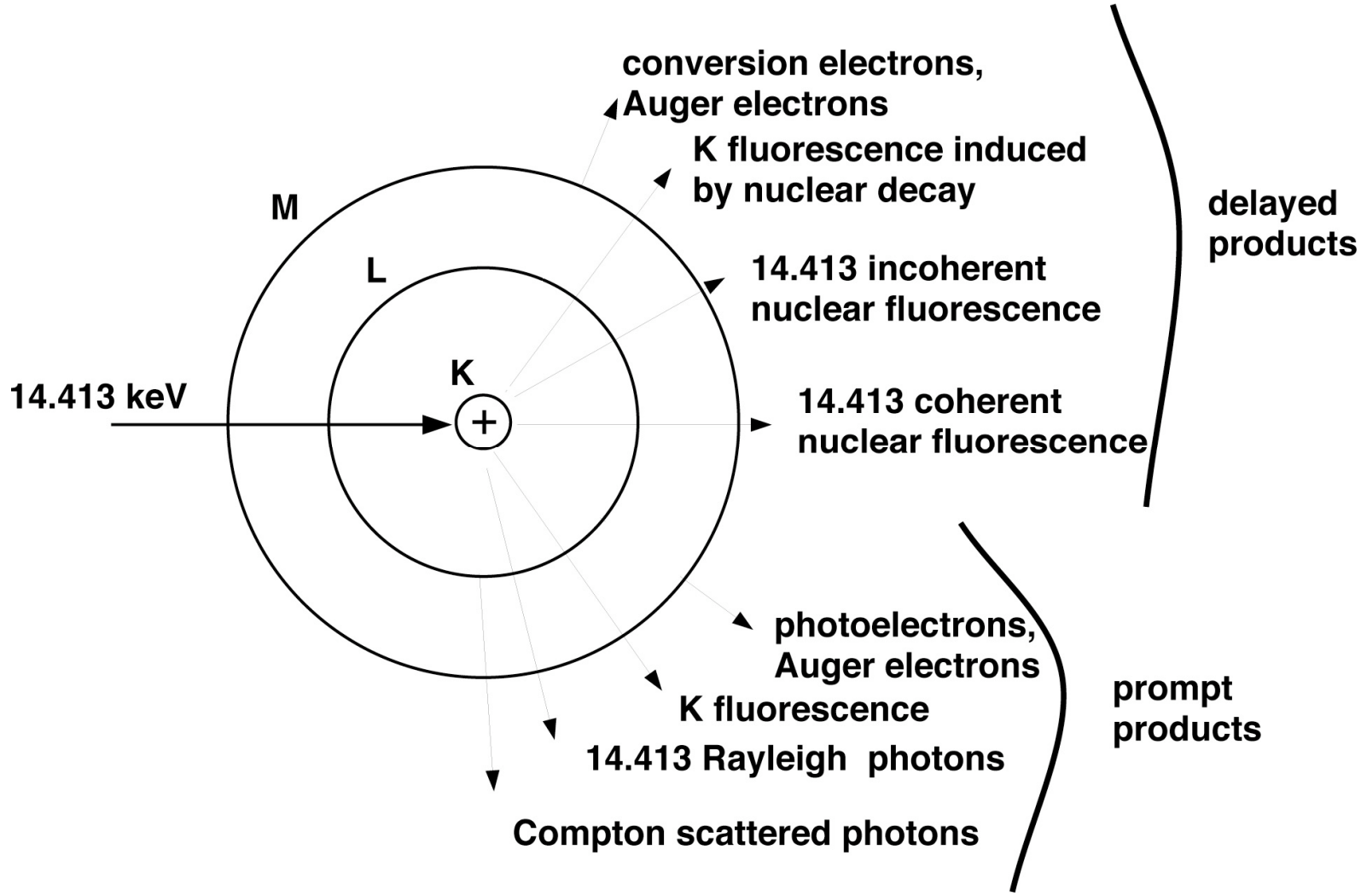

Detection of nuclear decay

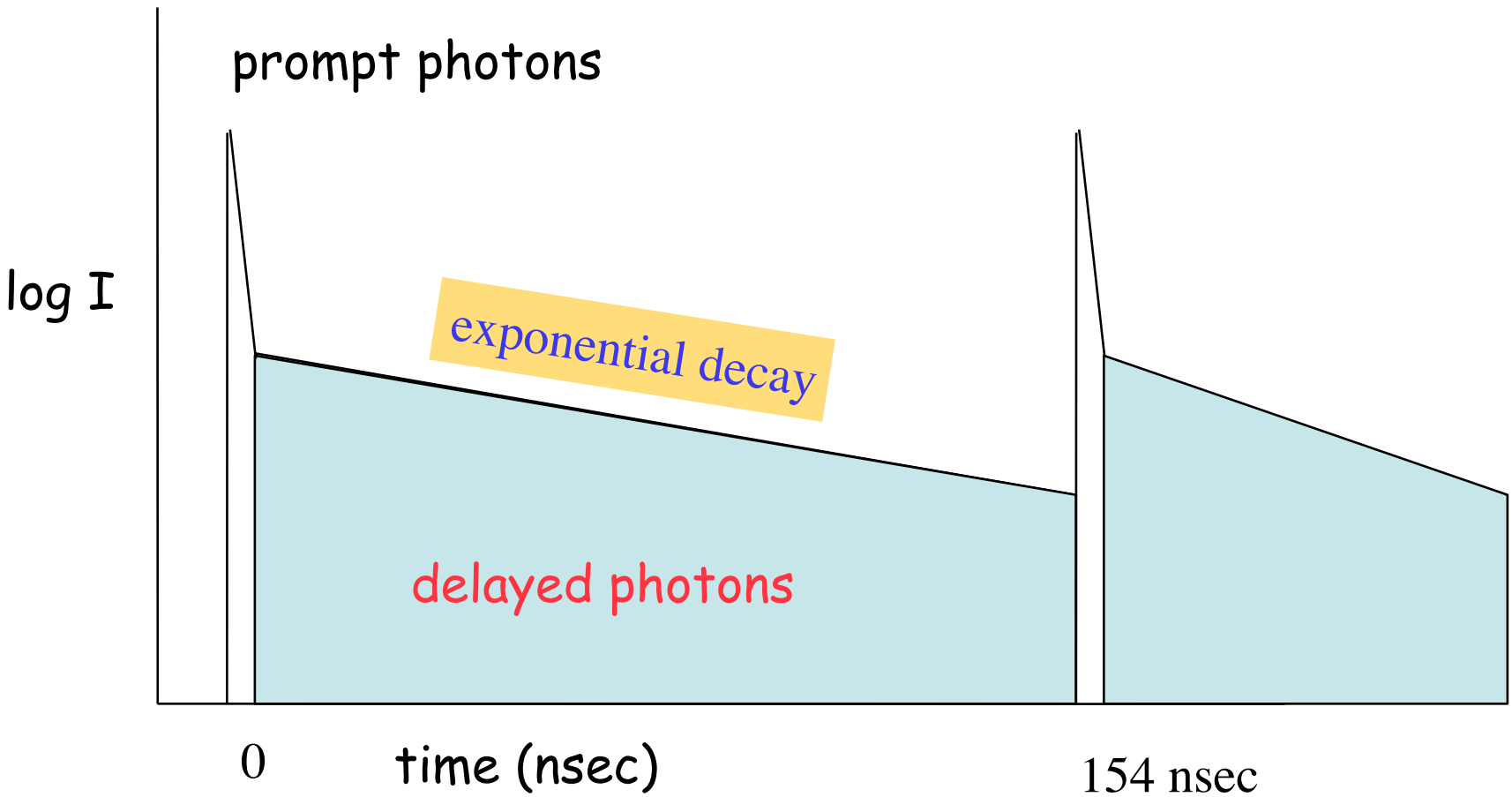

Visualized by Vischer, Singwi and many others but only properly observed after synchrotron radiation based tunable monochromators are realized in 1995

Seto et al, PRL, 74 (1995) p. 3828
Sturhahn et al, PRL , 74 (1995) p. 3832

H. Frauenfelder, *The Mössbauer Effect (1963)*

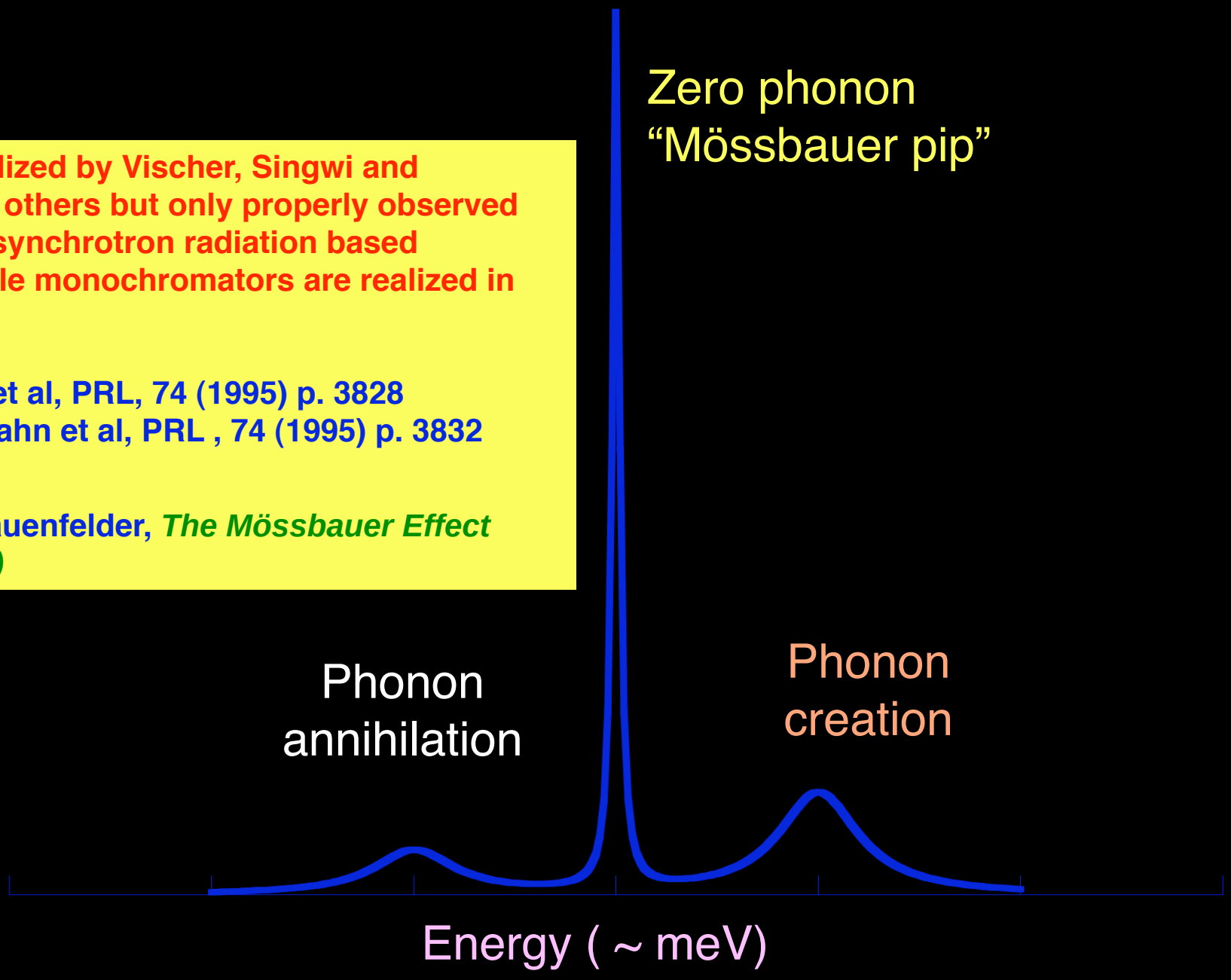

NRIXS on polycrystalline Fe (bcc):

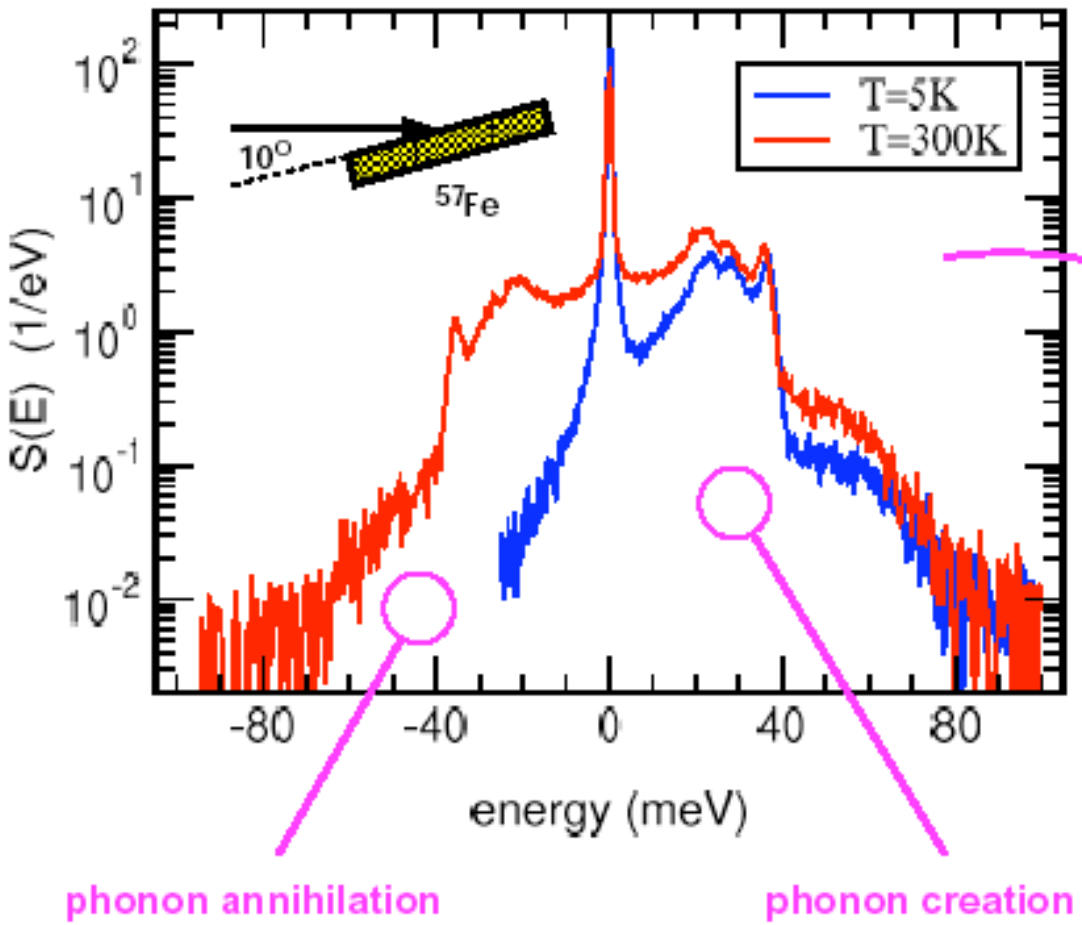

☆ the partial phonon DOS is extracted from the spectrum

M.Hu et al., Nucl.Intrum.Methods A 428 (1999)

W.Sturhahn, Hyperfine Int. 125 (2000)

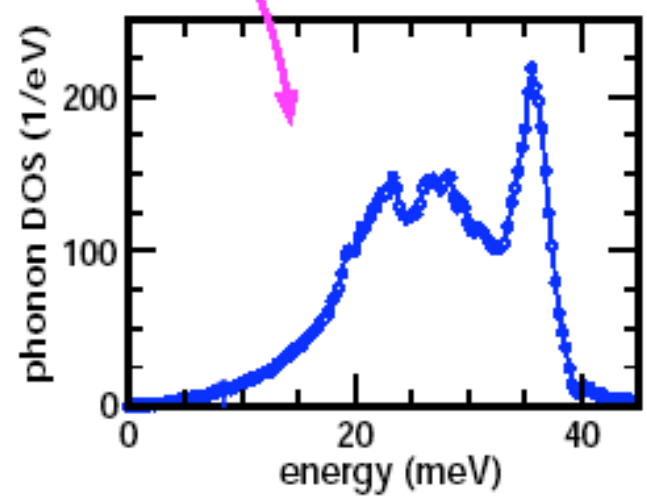

Crystalline and amorphous Fe_2Tb, raw data

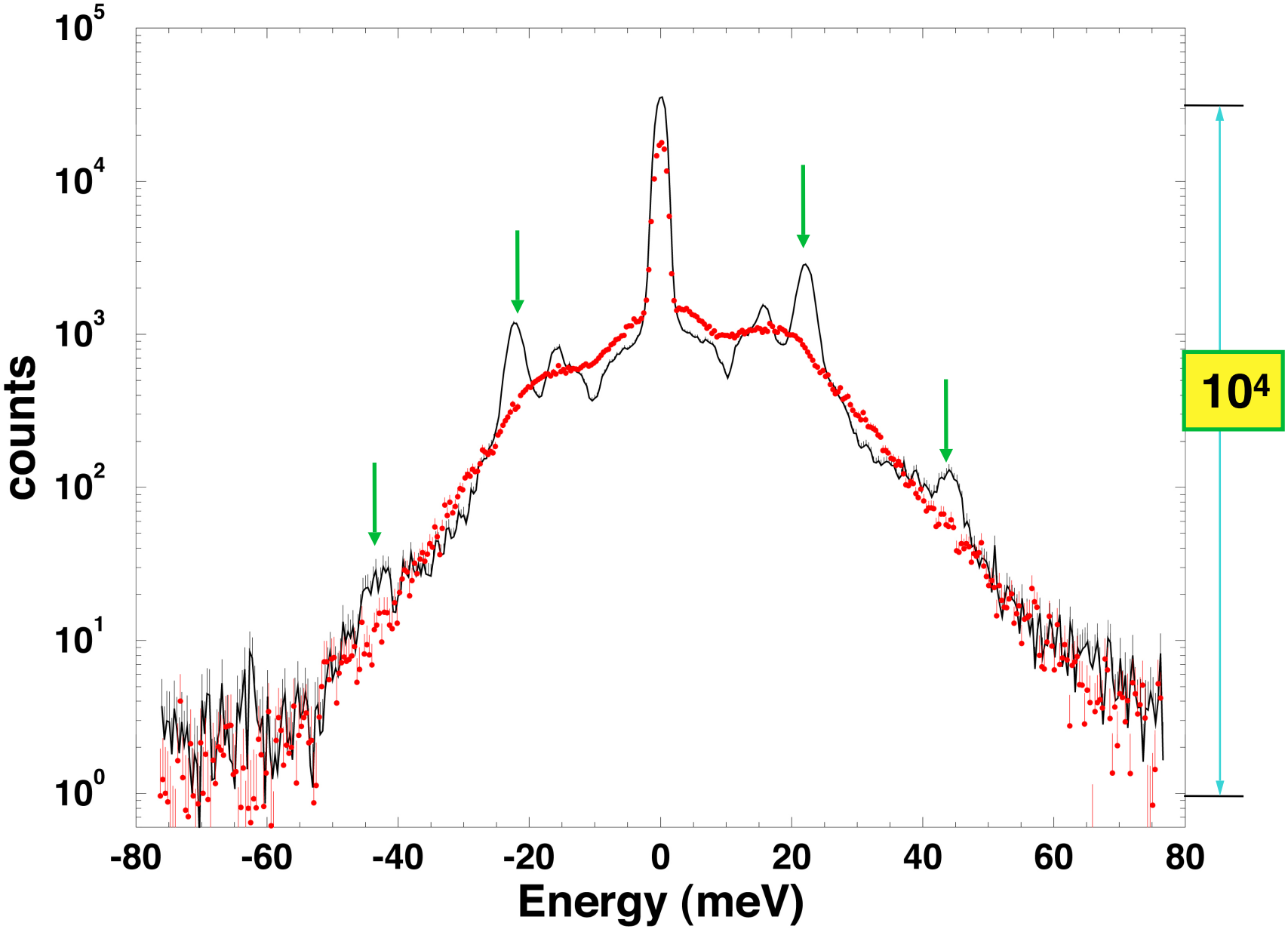

Crystalline-amorphous transformation

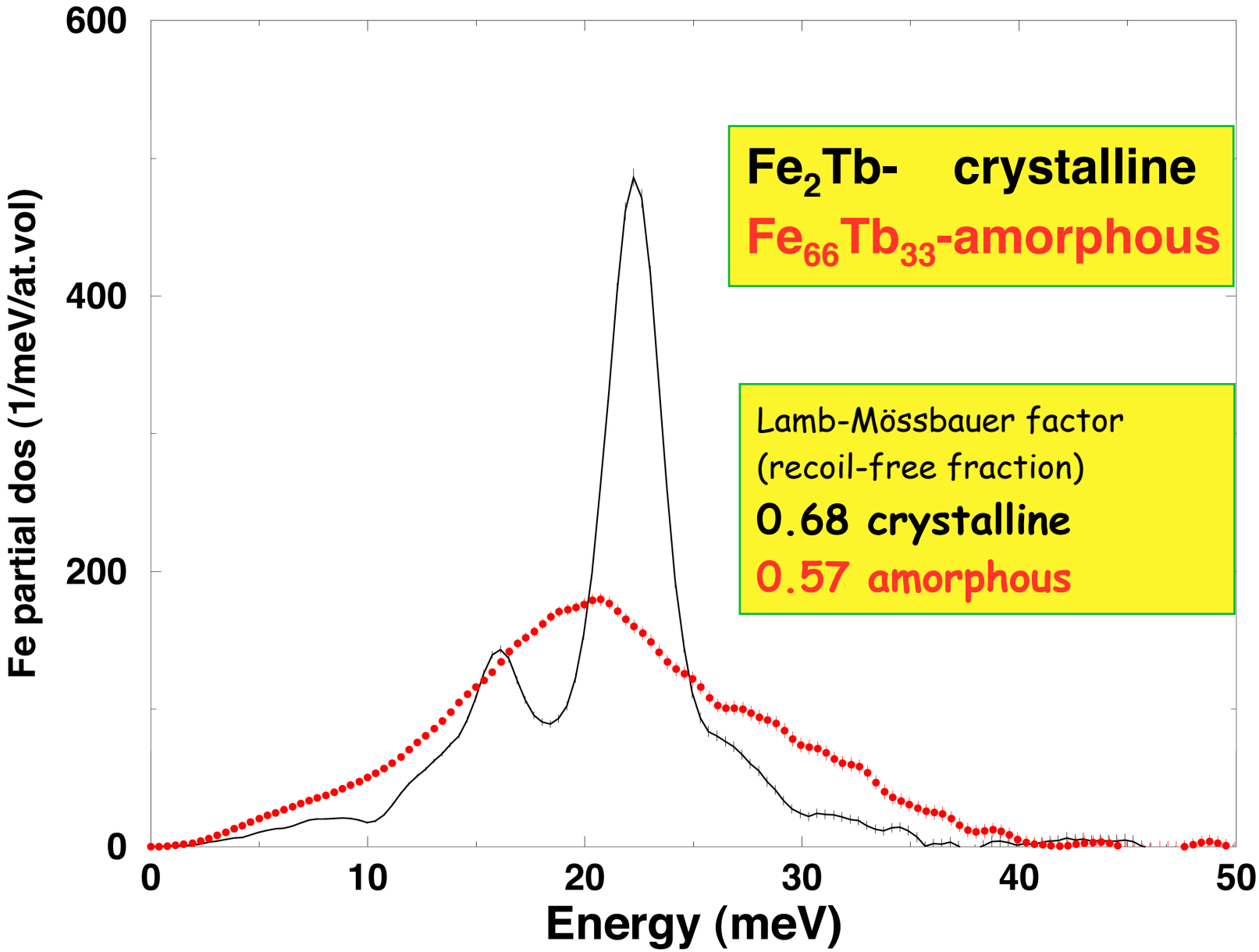

NRIXS: The method and its information content

$$\sigma(\mathbf{k},E) = \frac{\pi}{2}\sigma_0 \Gamma S(\mathbf{k},E)$$

Interaction cross-section

$$S(\mathbf{k},E) = \frac{1}{2\pi}\int dt d^3\mathbf{r} e^{i(\mathbf{kr}-\omega t)} G_s(\mathbf{r},t))$$

space-time Fourier transform of self correlation function

$$S_1(E) = \frac{E_R \cdot g(E)}{E(1-e^{-E/kT})}$$

One-phonon term $S_1(E)$ & phonon density of states, $g(E)$

$$g(\mathbf{s},\omega) = \frac{1}{N}\sum_{m\kappa}\left|\mathbf{s}\cdot\mathbf{e}_{pm}^{(\kappa)}\right|^2 \delta(\omega-\omega_m^{(\kappa)})$$

s: x-ray direction, **e**:polarization vector
ω_m: phonon energy in mode m

$$G_s(\mathbf{r},t) = \left\langle e^{-ik\mathbf{r}(t)} e^{ik\mathbf{r}(0)} \right\rangle \ :$$

Self-correlation of the phase of the scattering amplitude

$$S(\mathbf{k},E) = \frac{1}{N}\sum_{j=1}^{N} S^j(\mathbf{k},E)$$

Inelastic absorption probability

Iron phonon dispersion relations and phonon density of states

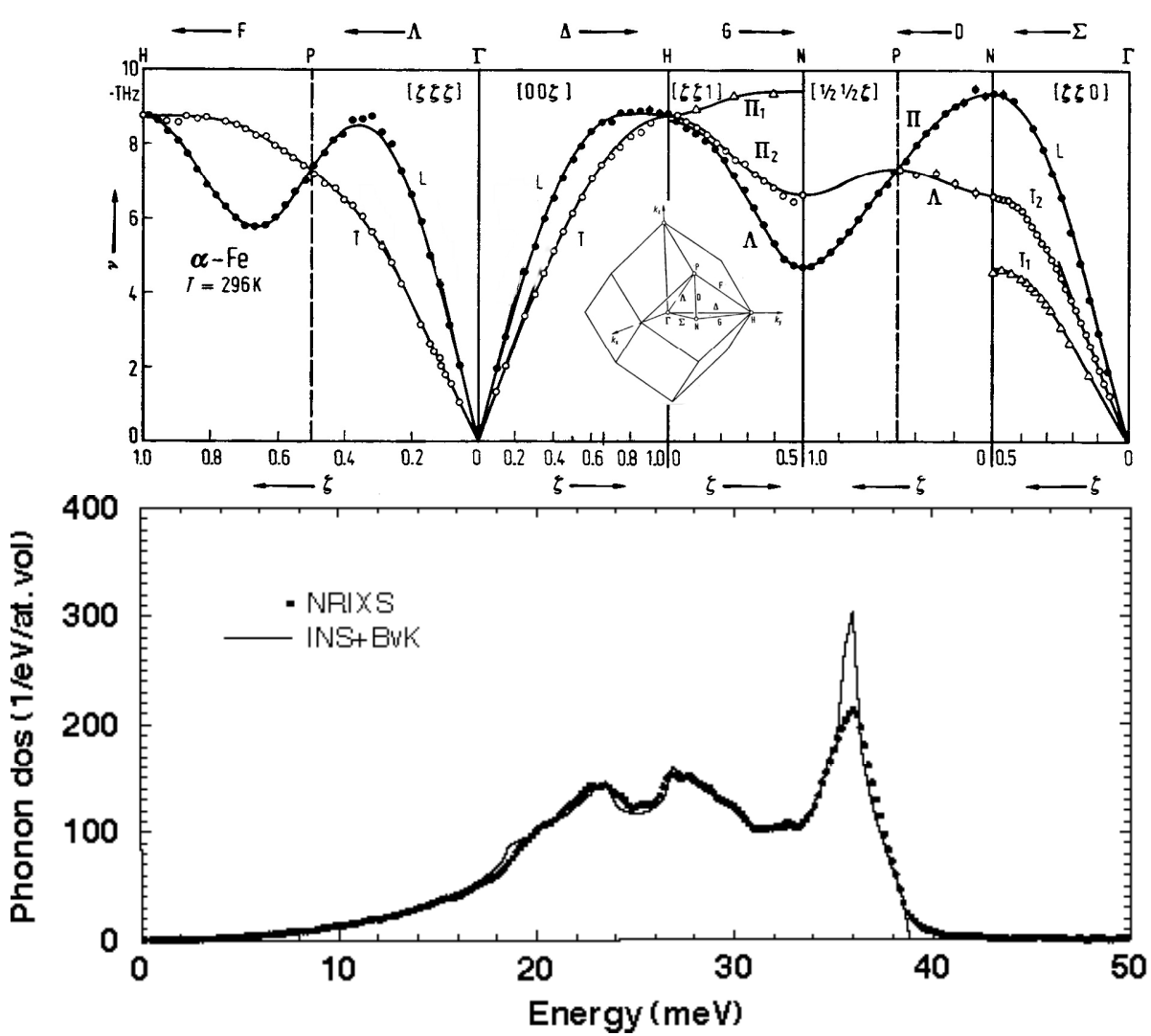

Nuclear resonance and brightness of synchrotron radiation

Undulator based SR

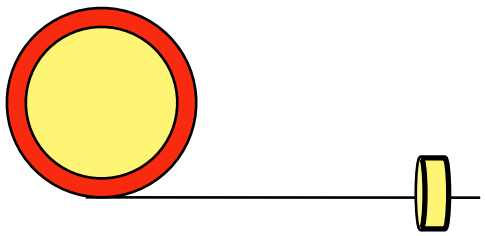

10^{23} photons / sec / eV / sr

10 mCi ^{57}Co source

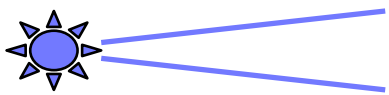

10^{11} photons /sec / eV / sr

Characteristics of nuclear excitation and decay

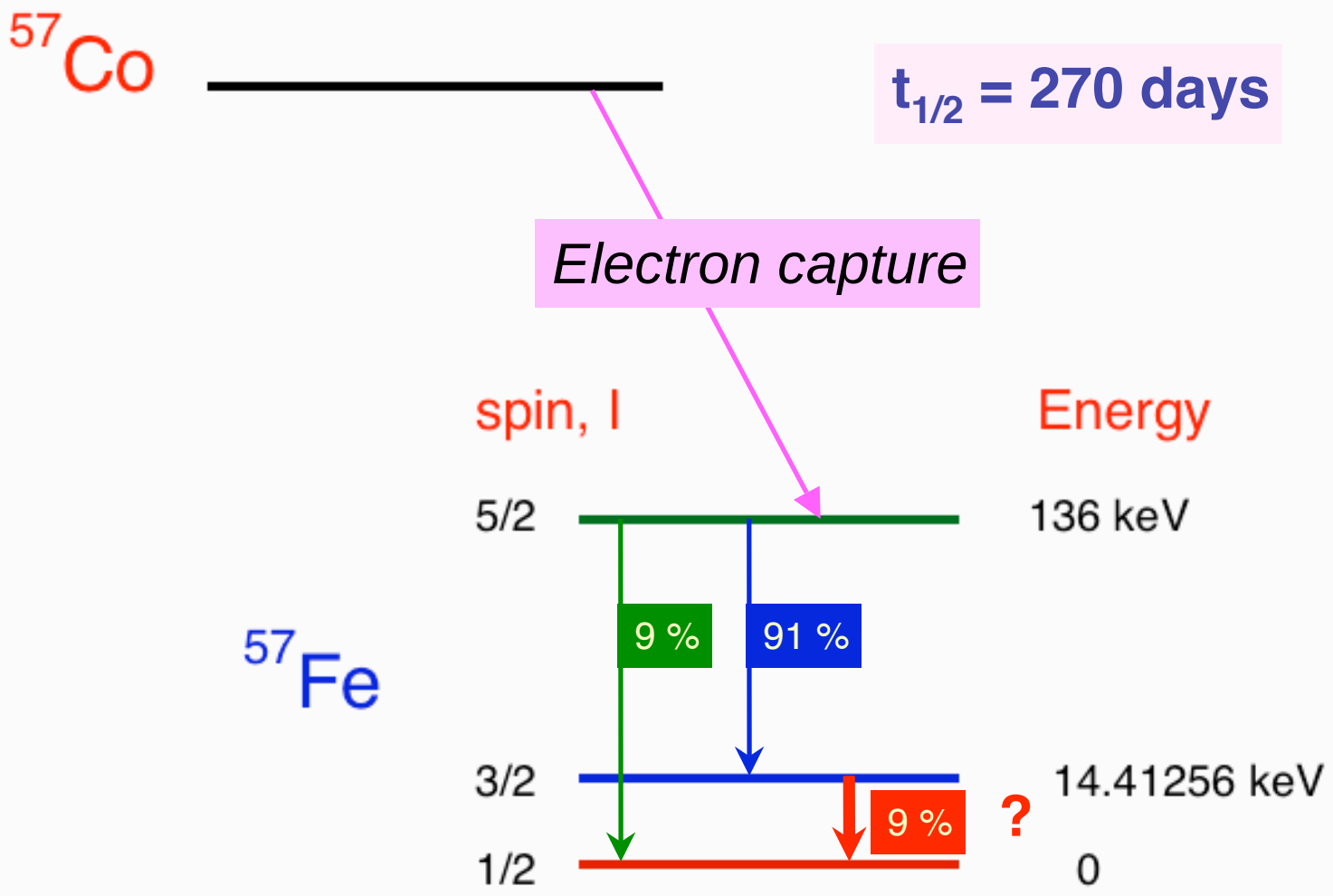

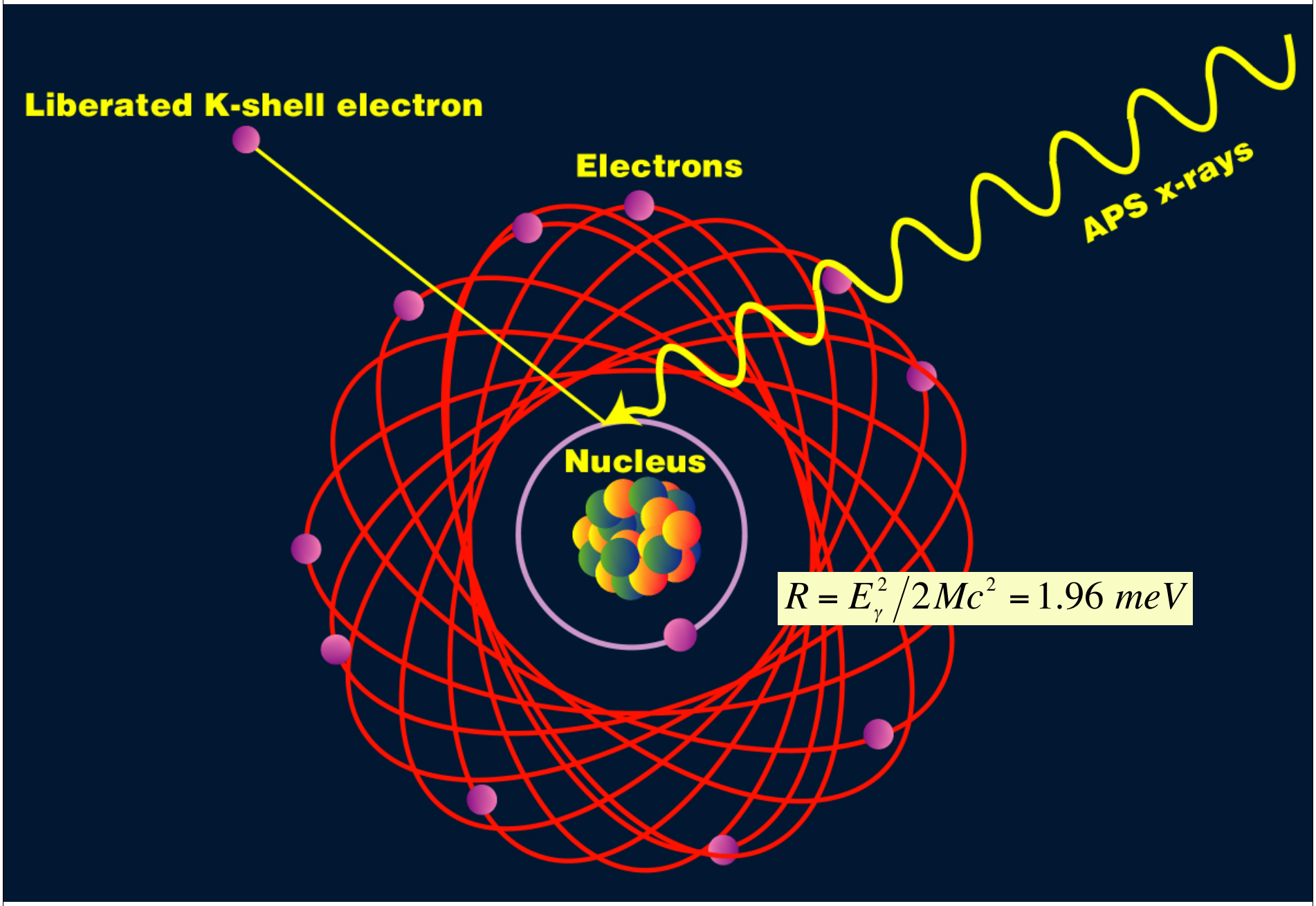
Liberated K-shell electron
Electrons
APS x-rays
Nucleus
$R = E_\gamma^2 / 2Mc^2 = 1.96\ meV$

absorption-emission & recoil

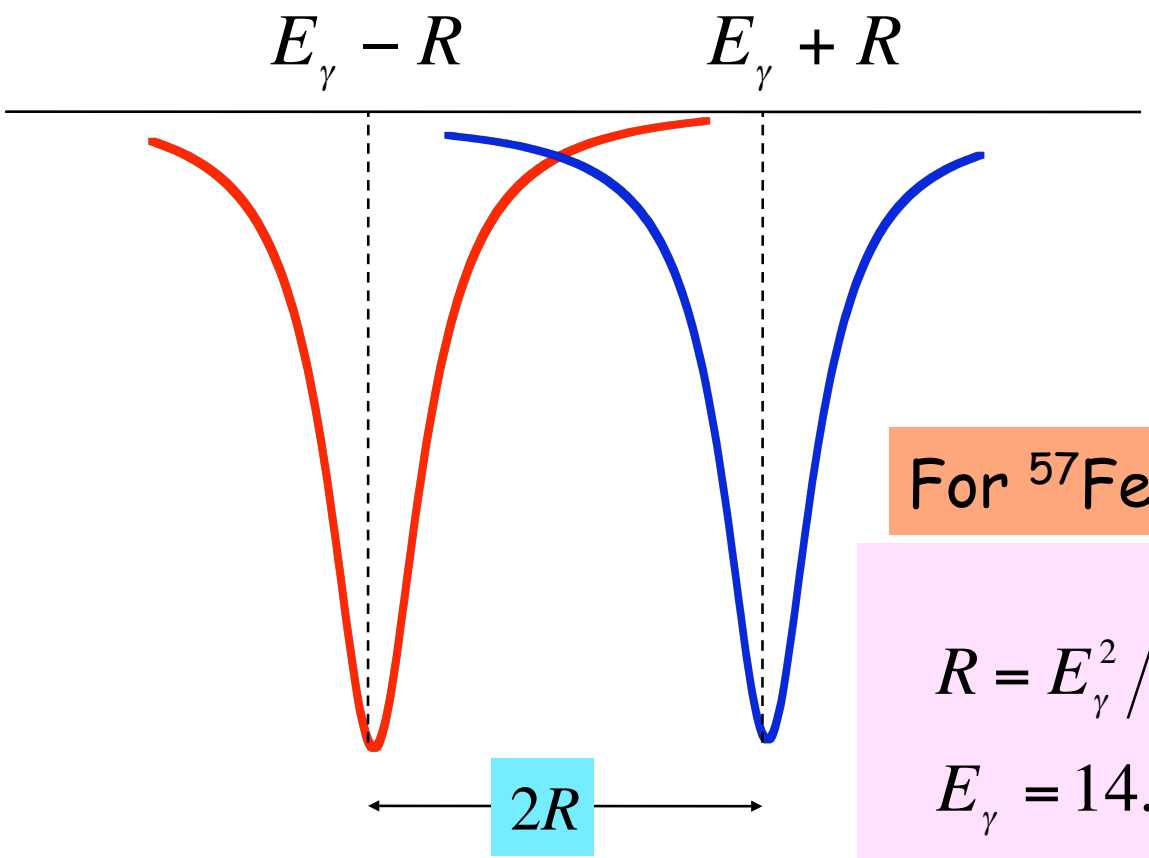

For ^{57}Fe:

$$R = E_\gamma^2 / 2Mc^2 = 1.96 \cdot 10^{-3} \text{ eV}$$

$$E_\gamma = 14.4 \cdot 10^{+3} \text{ eV}$$

$$\Gamma = 4.8 \cdot 10^{-9} \text{ eV}$$

absorption-emission & recoil

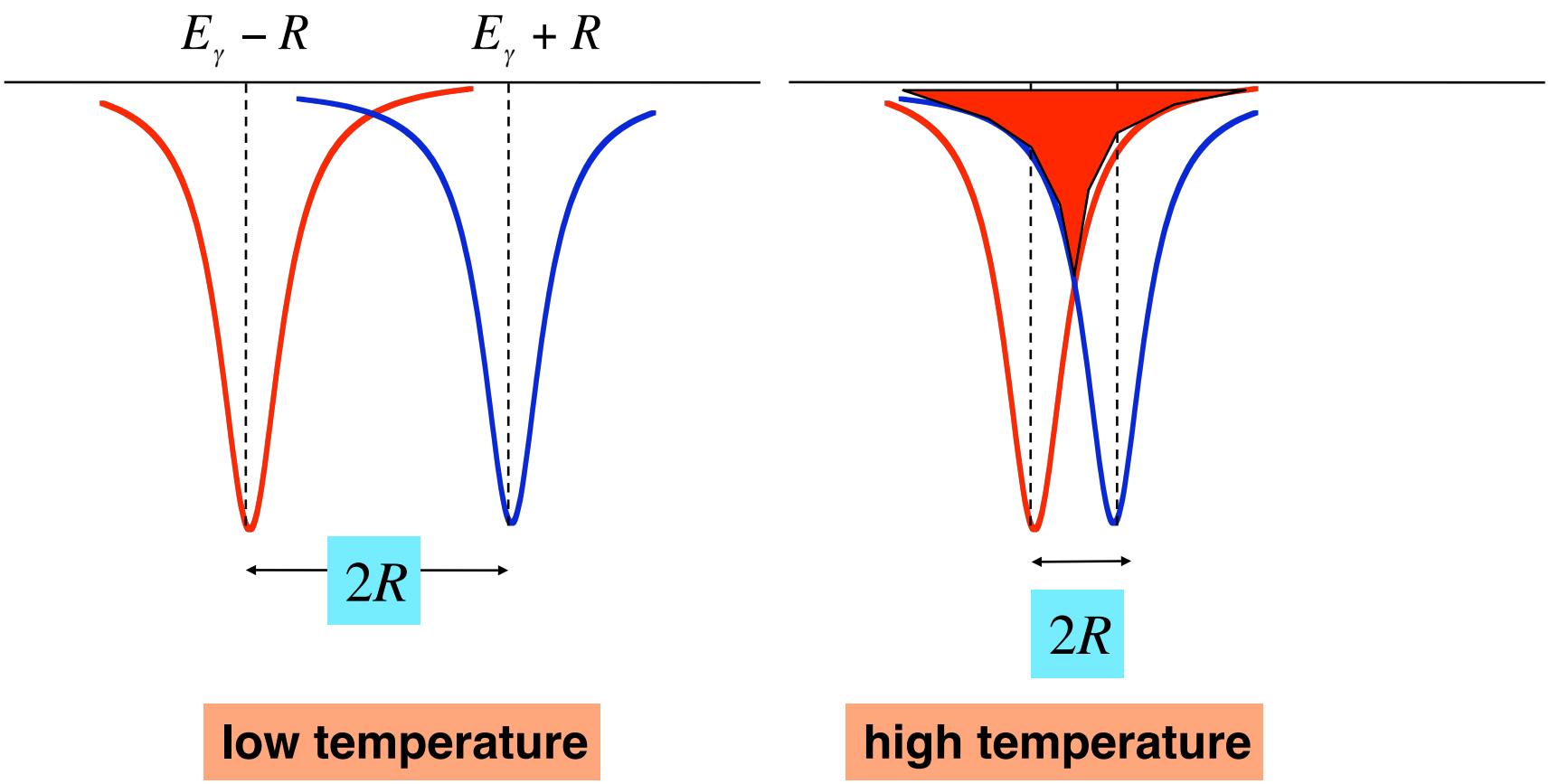

intuitive expectation: large resonance absorption at high temperature

Mossbauer's observation: less absorption at high temperature

Properties extracted from NRIXS data

Property	Information content
Lamb-Mössbauer Factor, or recoil-free fraction	f_{LM}, recoil free fraction obtained from density of states, $g(E)$: $f_{LM} = \exp\left(-E_R \int \frac{g(E)}{E} \cdot \coth\frac{\beta E}{2} dE\right)$
Second order Doppler shift	$\delta_{SOD} = -E_0 \frac{<v^2>}{2c^2}$
Average kinetic energy	Extracted from second moment of energy spectrum: $T = \frac{1}{4E_R}\left\langle (E - E_R)^2 \right\rangle$
Average force constant	Extracted from third moment of energy spectrum: $\frac{\partial^2 U}{\partial z^2} = \frac{m}{2\hbar^2}\left\langle E^3 \right\rangle$
Phonon density of states	Extracted one-phonon absorption probability, $S_1(E)$: $g(E) = \frac{E}{E_R}\tanh(\beta E/2)(S_1(E) + S_1(-E))$
Specific heat (vibrational part only)	$C_V = 3k_B \int_0^\infty (\beta E/2)^2 \operatorname{csch}(\beta E)\, g(E) dE$
Vibrational entropy	$S_V = 3k_B \int_0^\infty \left\{\frac{\beta E}{2}\coth(\beta E) - \ln\left[2\sinh(\beta E)\right]\right\} g(E) dE$
Debye sound velocity (aggregate sound velocity)	From low-energy portion of the density of states: $g(E) = \frac{3V}{2\pi\hbar^3 v_D^3} E^2$
Mode specific vibrational amplitude	Contribution of mode α of atom j to zero-point fluctuation [11,12]: $\left\langle r_{j\alpha}^2 \right\rangle_0 = \frac{\hbar^2}{2m_j\omega_\alpha^2} e_{j\alpha}^2$
Mode specific Gruneisen constant	From pressure dependence of phonon frequencies ω_α of acoustic or optical modes: $\gamma_\alpha = -\frac{\partial \ln \omega_\alpha}{\partial \ln V}$
Temperature of the sample	From detailed balance between phonon occupation probability

The Mössbauer isotopes

Isotope	Energy (eV)	Half-life (ns)	ΔE (neV)
• ^{181}Ta	6238.	9800.	0.067
• ^{169}Tm	8401	4.	114.0
• ^{83}Kr	9400.	147.	3.1
^{73}Ge	13263.	2953.	0.15
• ^{57}Fe	14413.	97.8	4.67
• ^{151}Eu	21532.	9.7	47.0
• ^{149}Sm	22490.	7.1	64.1
• ^{119}Sn	23870.	17.8	25.7
• ^{161}Dy	25655.	28.2	16.2
• ^{40}K	29560.	4.25	107.0
•^{121}Sb	37130.	5.0	131.6
^{145}Nd	67100.	67.1	6.8
• ^{61}Ni	67400.	5.1	89.0
^{193}Ir	73000.	6.3	72.3
^{133}Cs	81000.	6.4	71.5
^{67}Zn	93300.	9200.	0.049

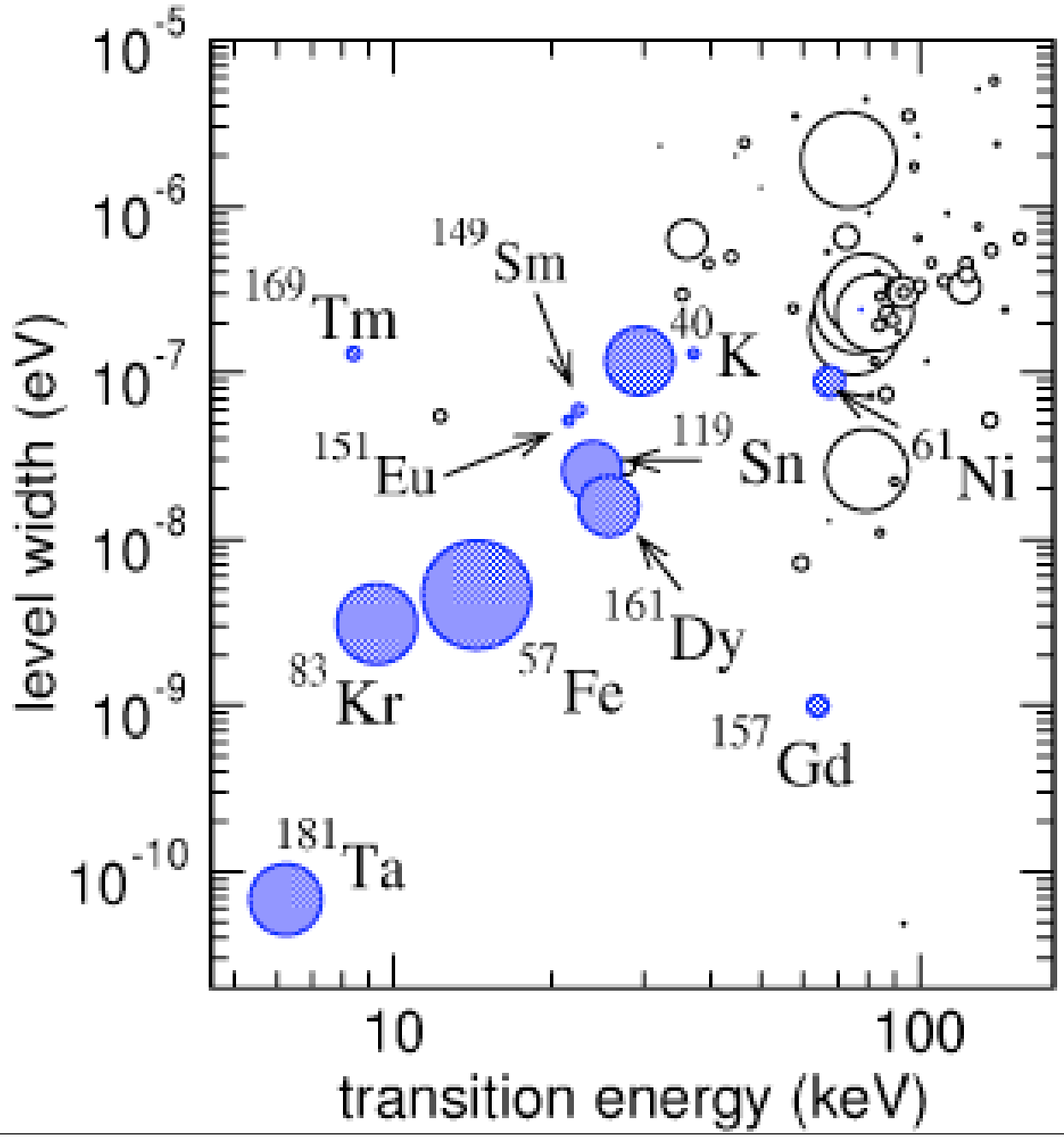
level width (eV)
transition energy (keV)
10
100
10^{-5}
10^{-6}
10^{-7}
10^{-8}
10^{-9}
10^{-10}
^{169}Tm
^{149}Sm
^{40}K
^{151}Eu
^{119}Sn
^{61}Ni
^{161}Dy
^{83}Kr
^{57}Fe
^{157}Gd
^{181}Ta

Generations of high-resolution monochromators

1992

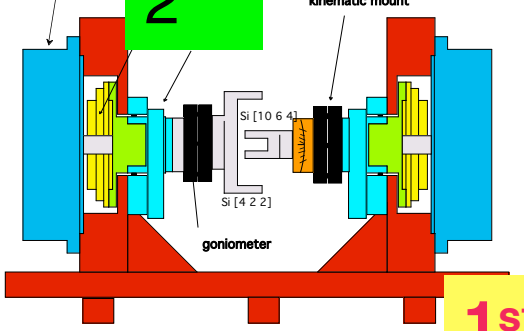

1st

1999

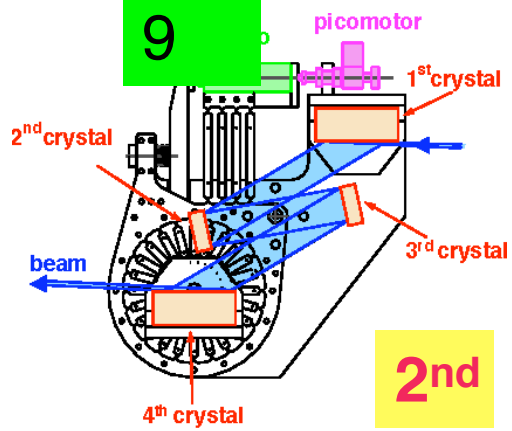

2nd

2002

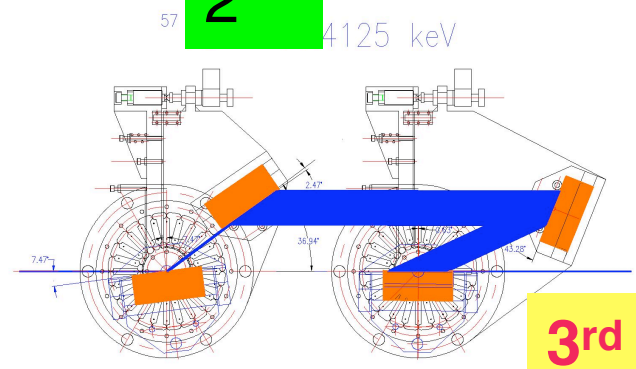

3rd

2004

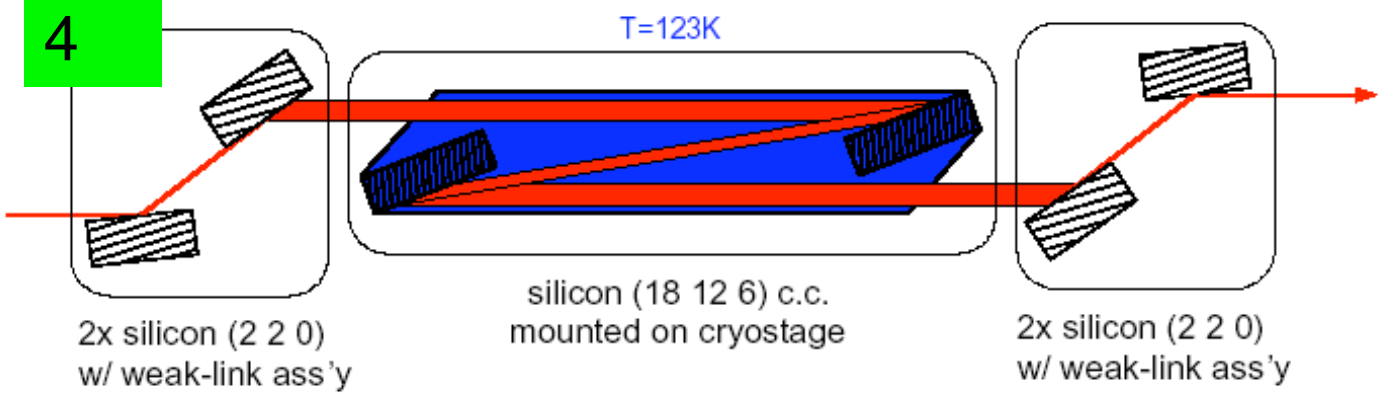

4th

T. Toellner

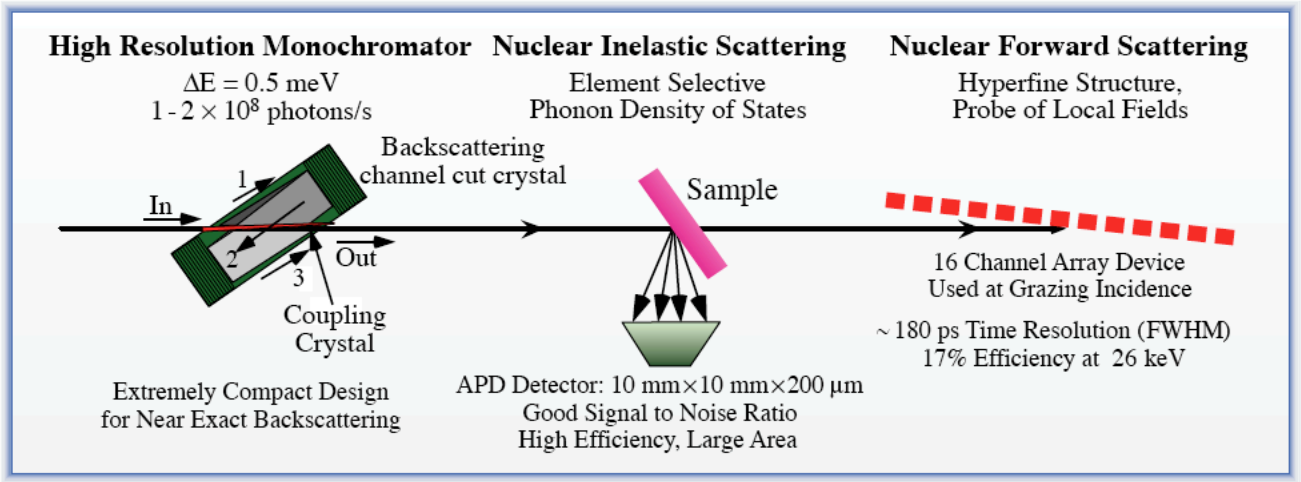

A. Baron, et al, J. Sync. Rad. 8 (2001) 1127

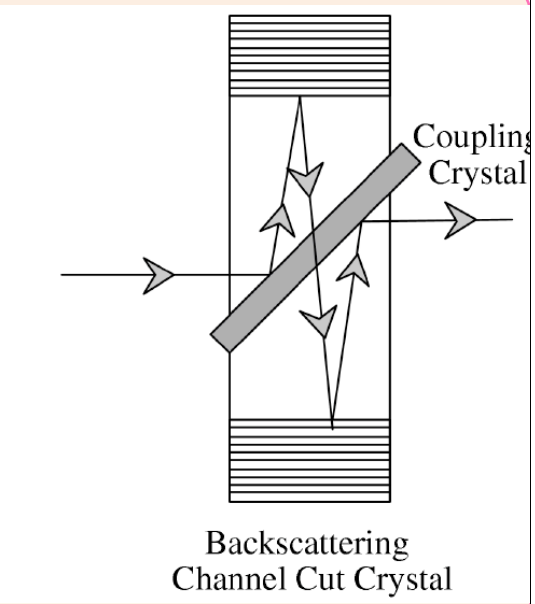

M. Yabashi, et al,

Rev. Sci. Instrum., Vol. 72, No. 11, November 2001

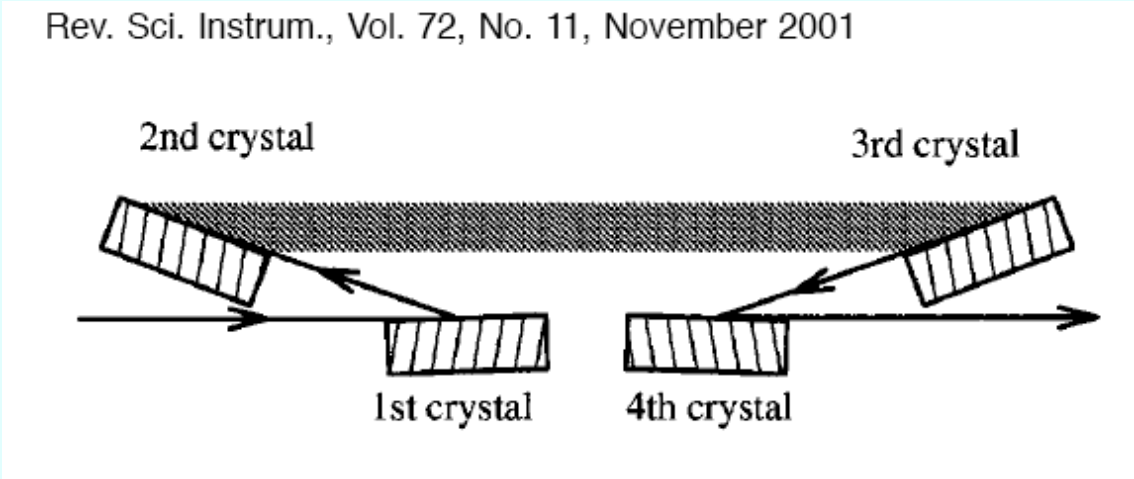

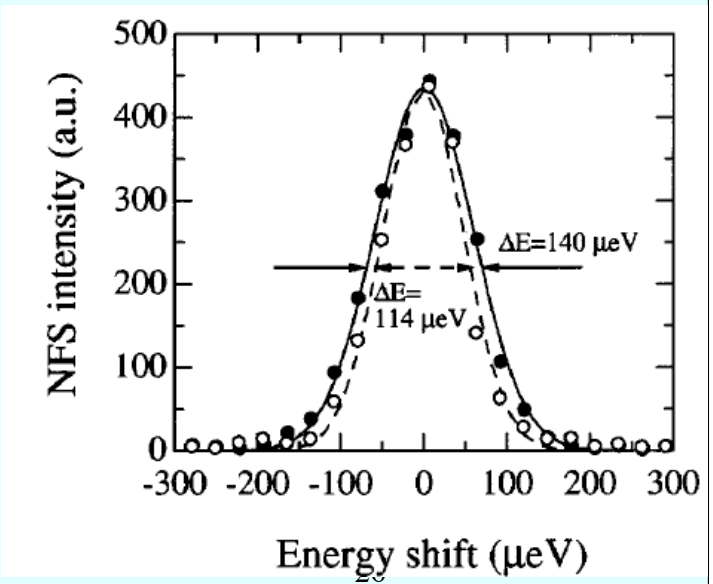

Observation of ^{121}Sb nuclear resonance with sapphire backscattering monochromator

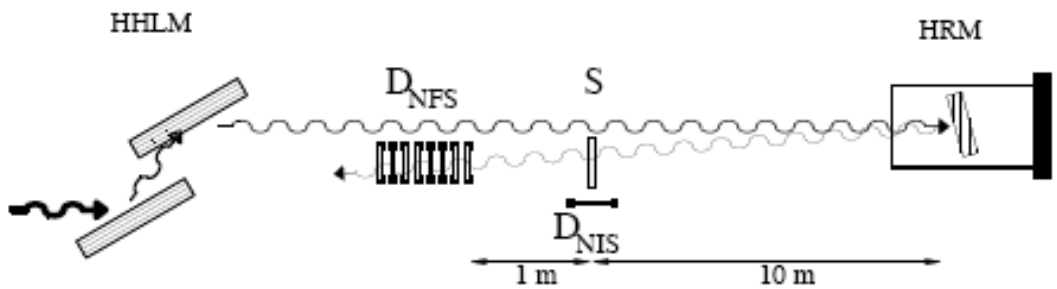

H.-C. Wille, Y. Shvyd'ko, E. E. Alp, H. D. Rüter, O. Leupold, I. Sergueev, R. Rüffer, A. Barla, and J. P. Sanchez, **Europhys. Lett. 74, 170 (2006).**

Al_2O_3 (15 13 $\overline{28}$ 14)

Bragg angle of 89.92 to separate the direct and backscattered beam.

T_0 = 146.54(95) K,
dE/dT = 59.6 meV/K

E= 37.1298(2) keV.

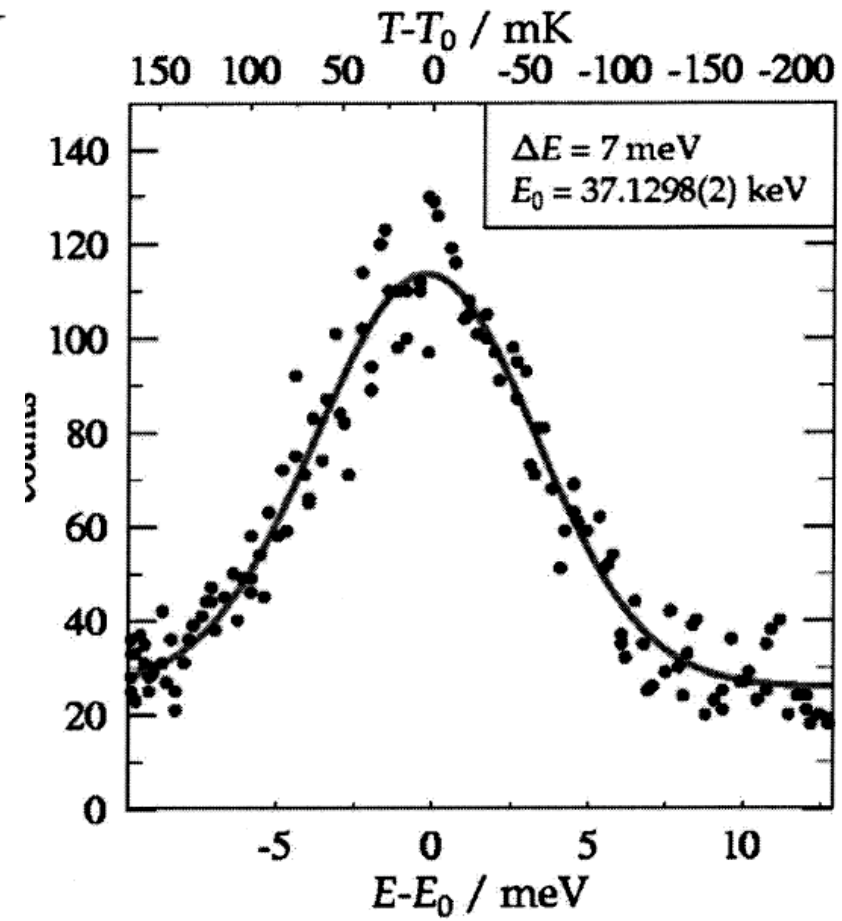

$EuFe_4Sb_{12}$

Maybe the first sample to be studied partially and completely

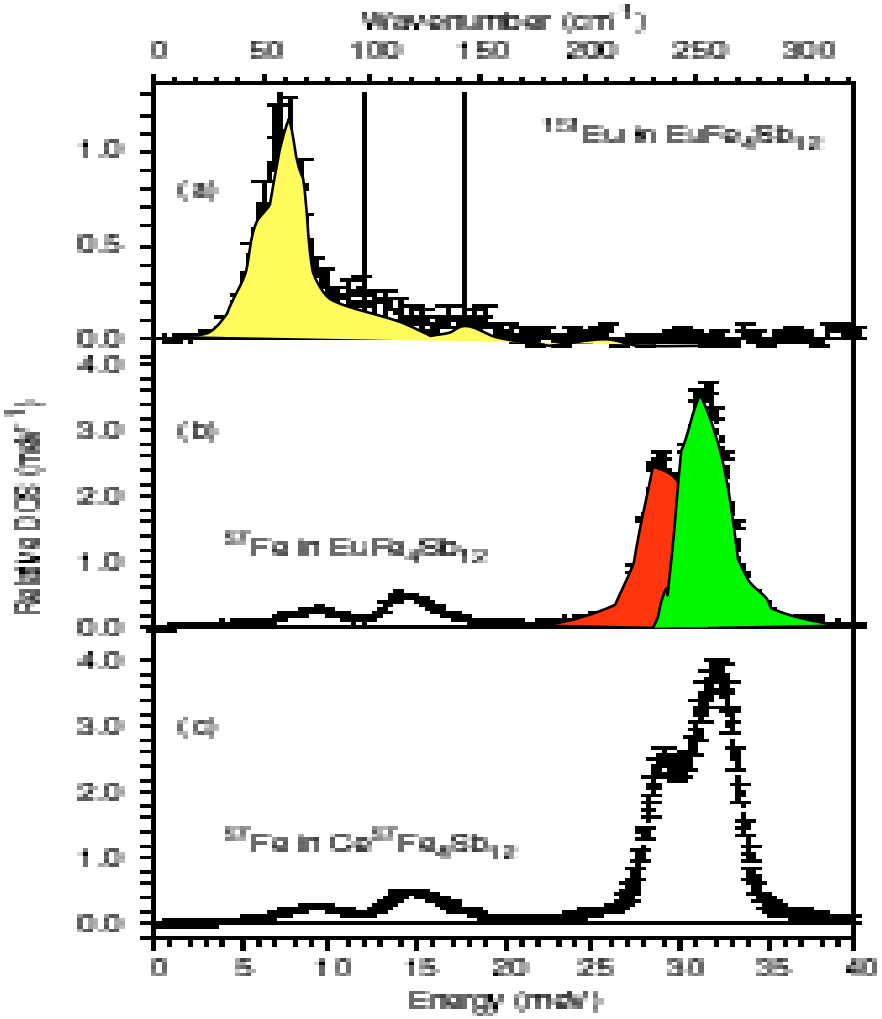

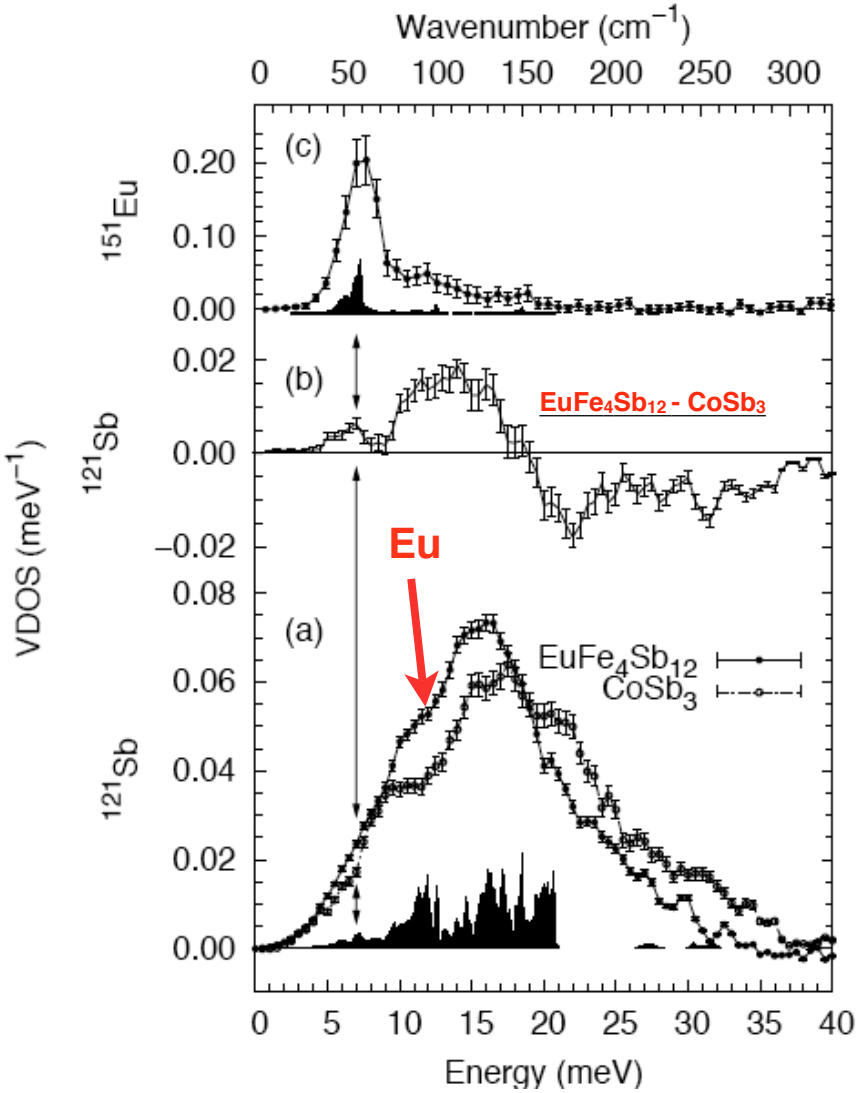

Filled skutterudite: $EuFe_4Sb_{12}$

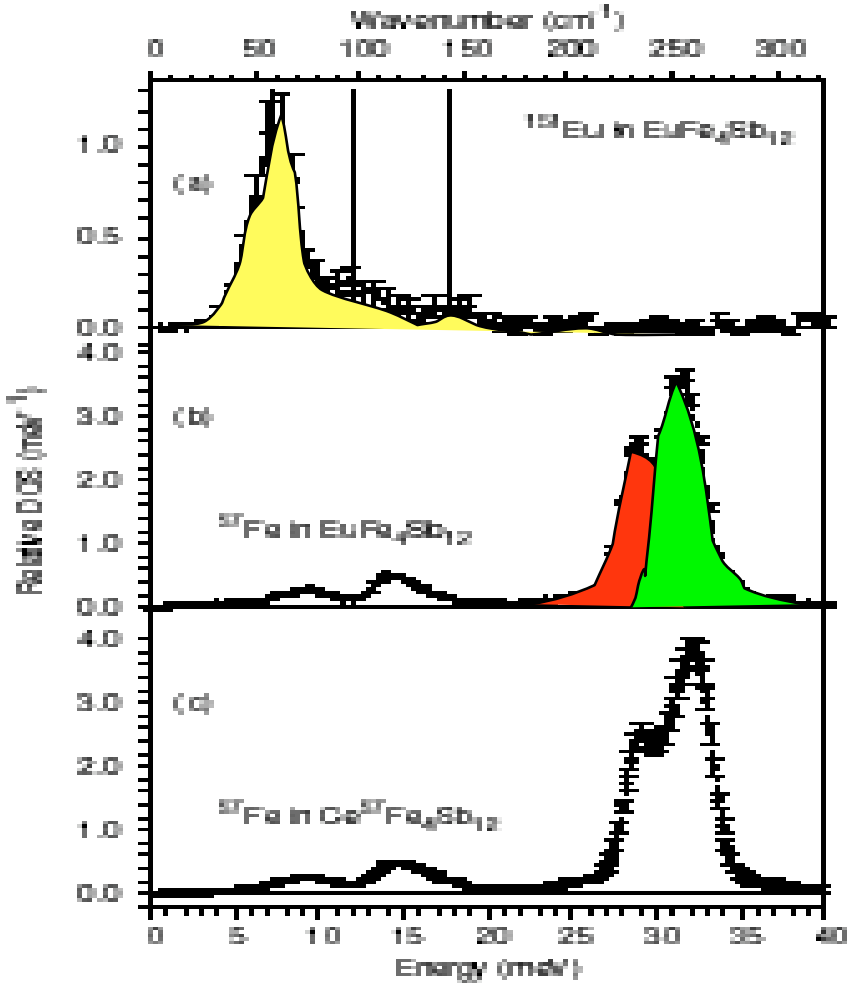

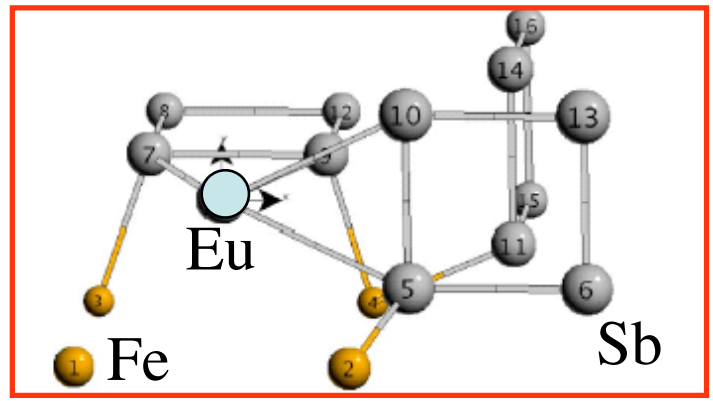

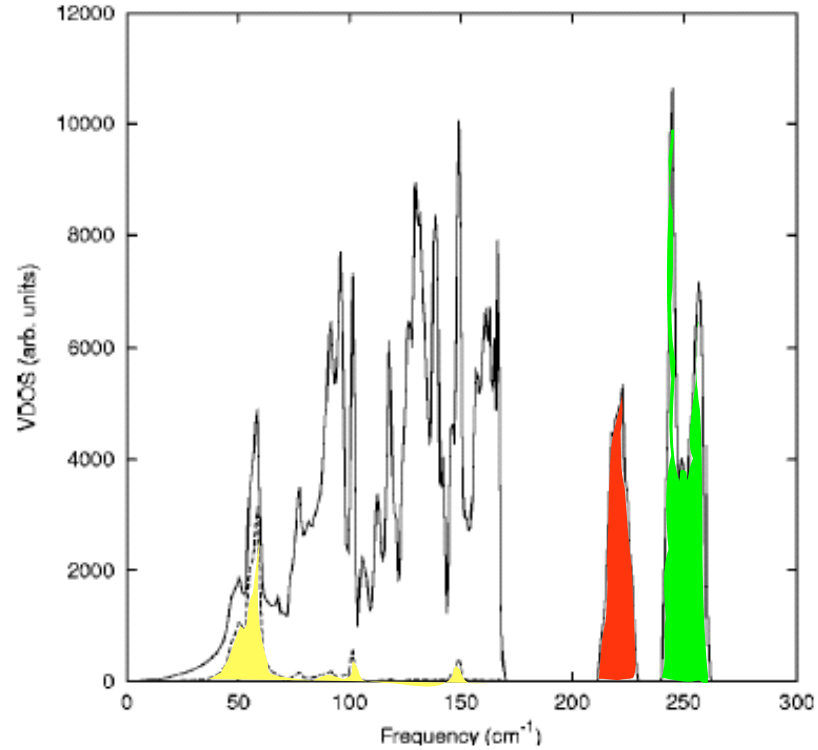

FIG. 4. Calculated vibrational density of states (VDOS): Total VDOS (solid) and La projected VDOS (dashed).

G. Long et al (Phys Rev B, 71 (2005) 140302

Feldman, et al, Phys Rev B 68 (2003) 94301

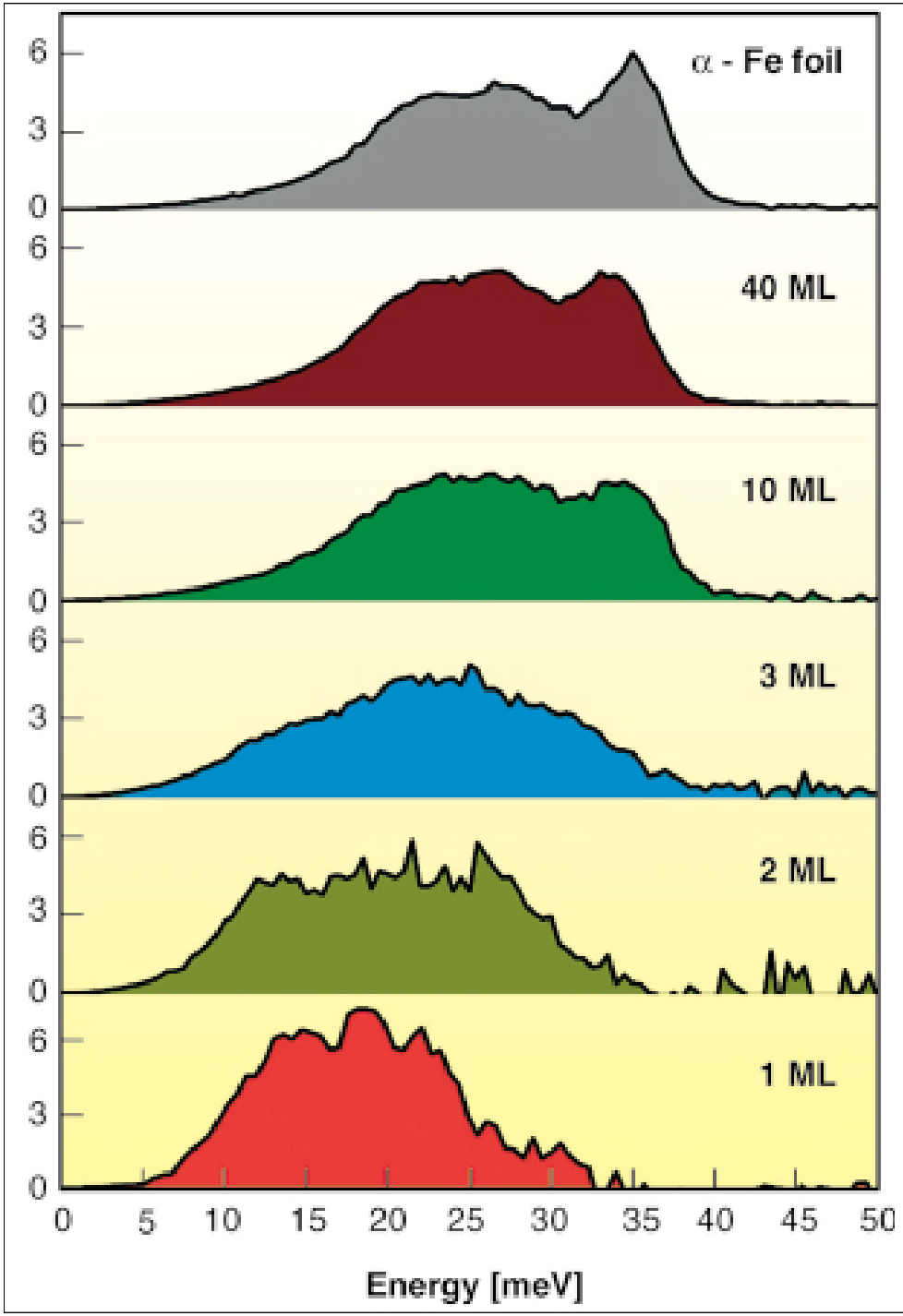

Fe films deposited on W(110)

Transition from the bulk to a single iron monolayer

S. Stankov, R. Röhlsberger, T. Slezak, M. Sladecek, B. Sepiol, G. Vogl, A. I. Chumakov, R. Rüffer, N. Spiridis, J. Lazewski, K. Parlinski, and J. Korecki,

ESRF Highlights 2006

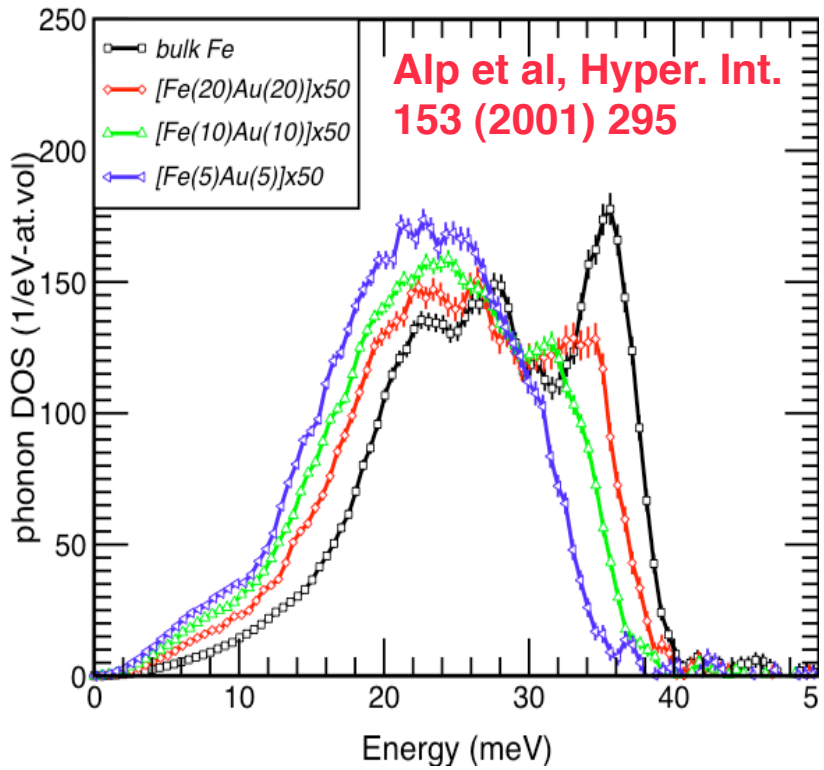

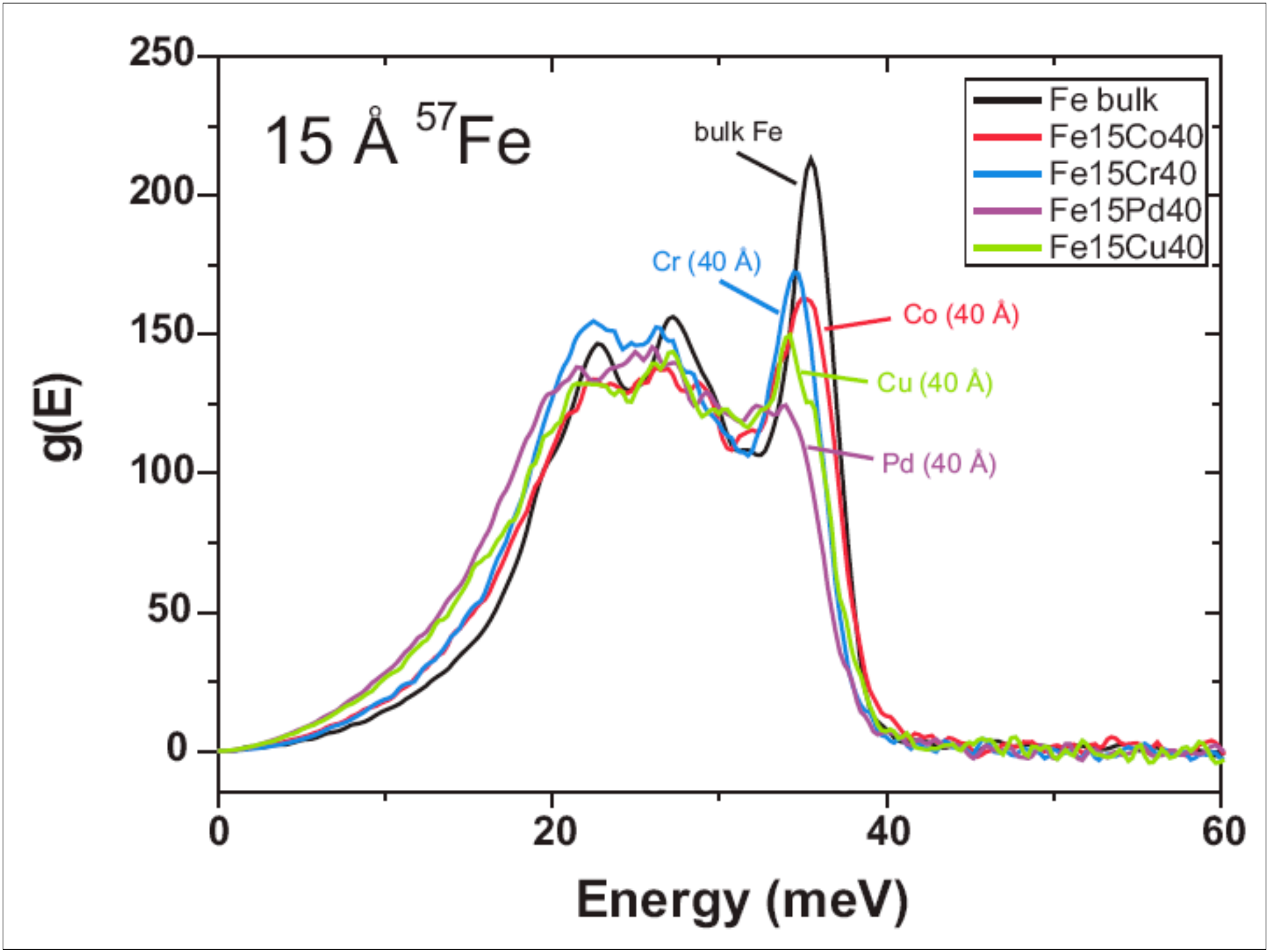
15 Å ^{57}Fe
bulk Fe
Cr (40 Å)
Co (40 Å)
Cu (40 Å)
Pd (40 Å)
Fe bulk
Fe15Co40
Fe15Cr40
Fe15Pd40
Fe15Cu40
g(E)
Energy (meV)
0
50
100
150
200
250
0
20
40
60

Fe_xMg_{1-x} amorphous alloys, Sahoo & Keune, JPCM (2005)

BOSON PEAK

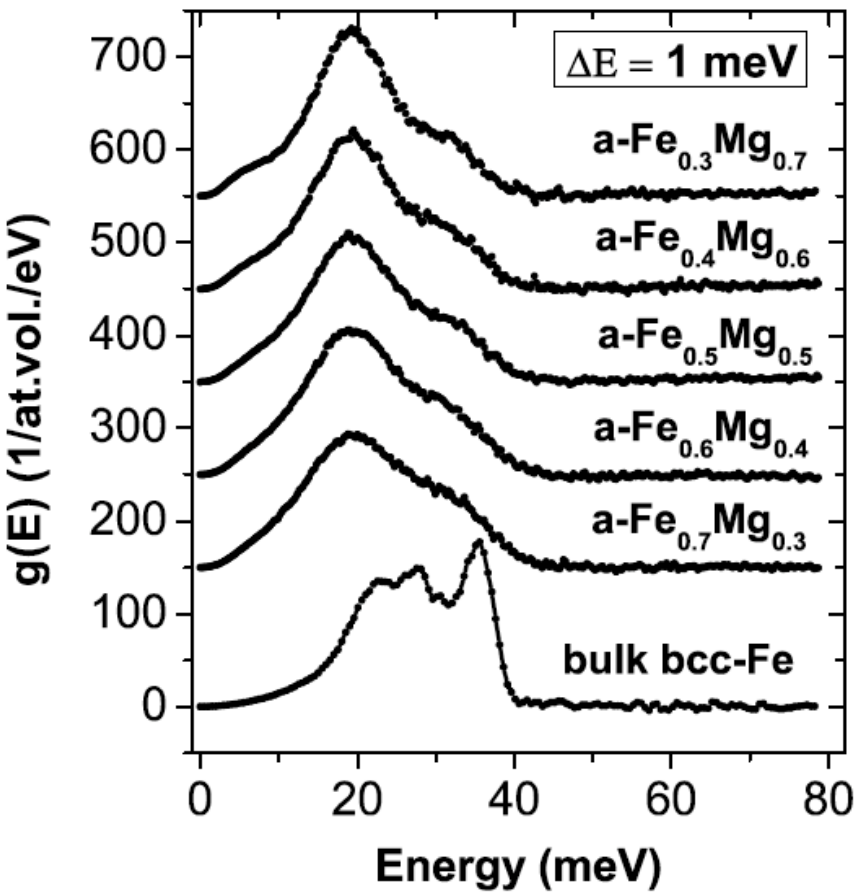

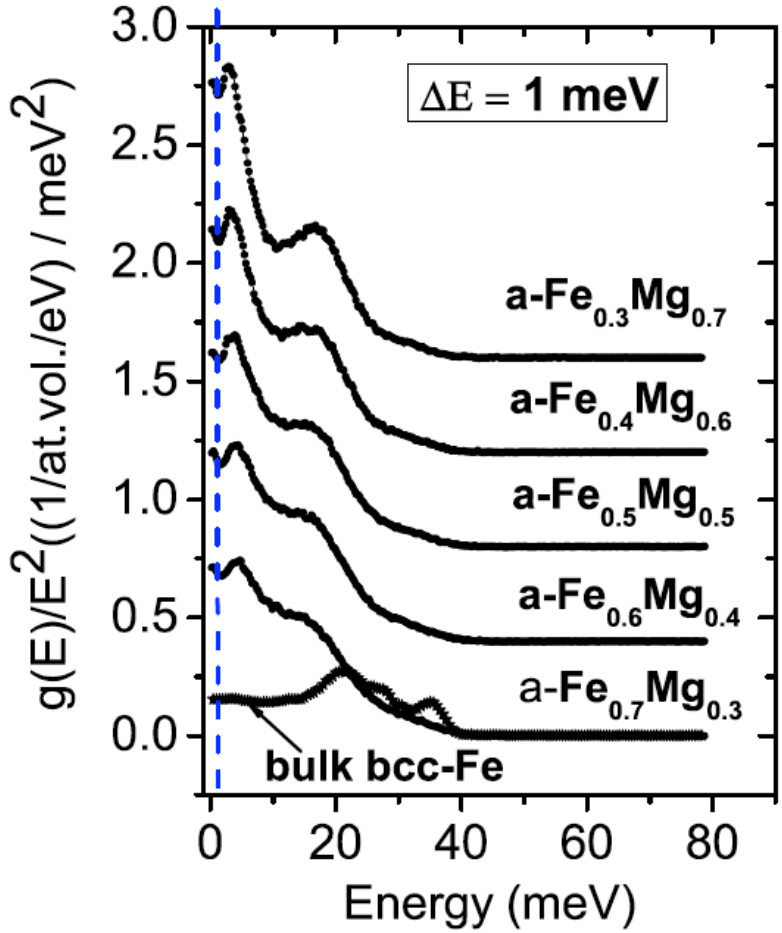

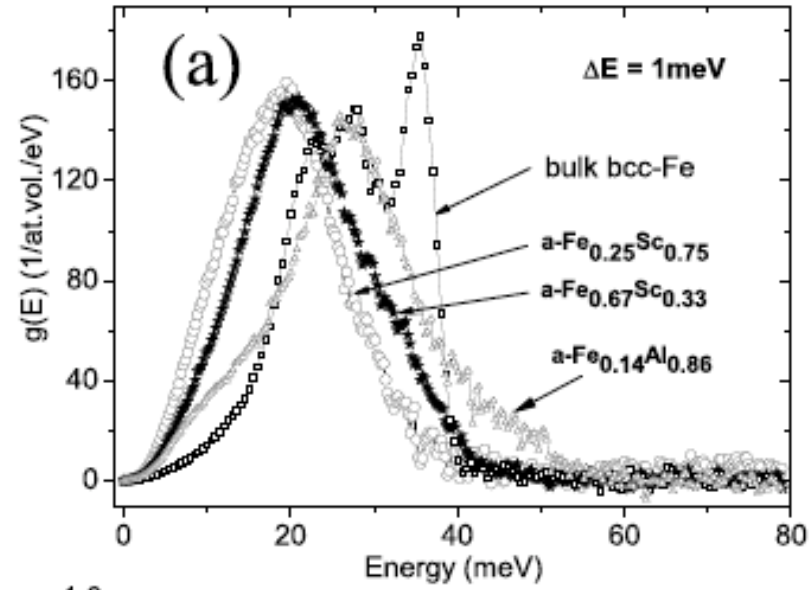

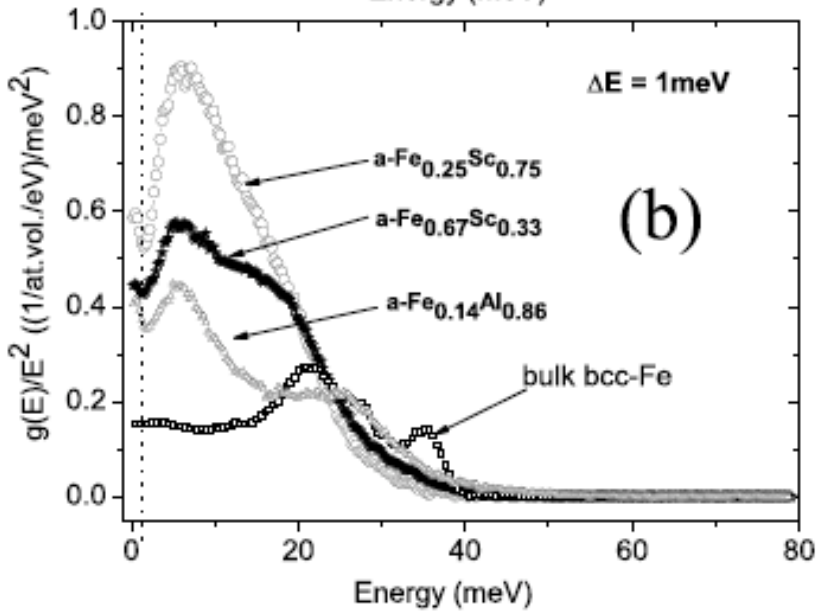

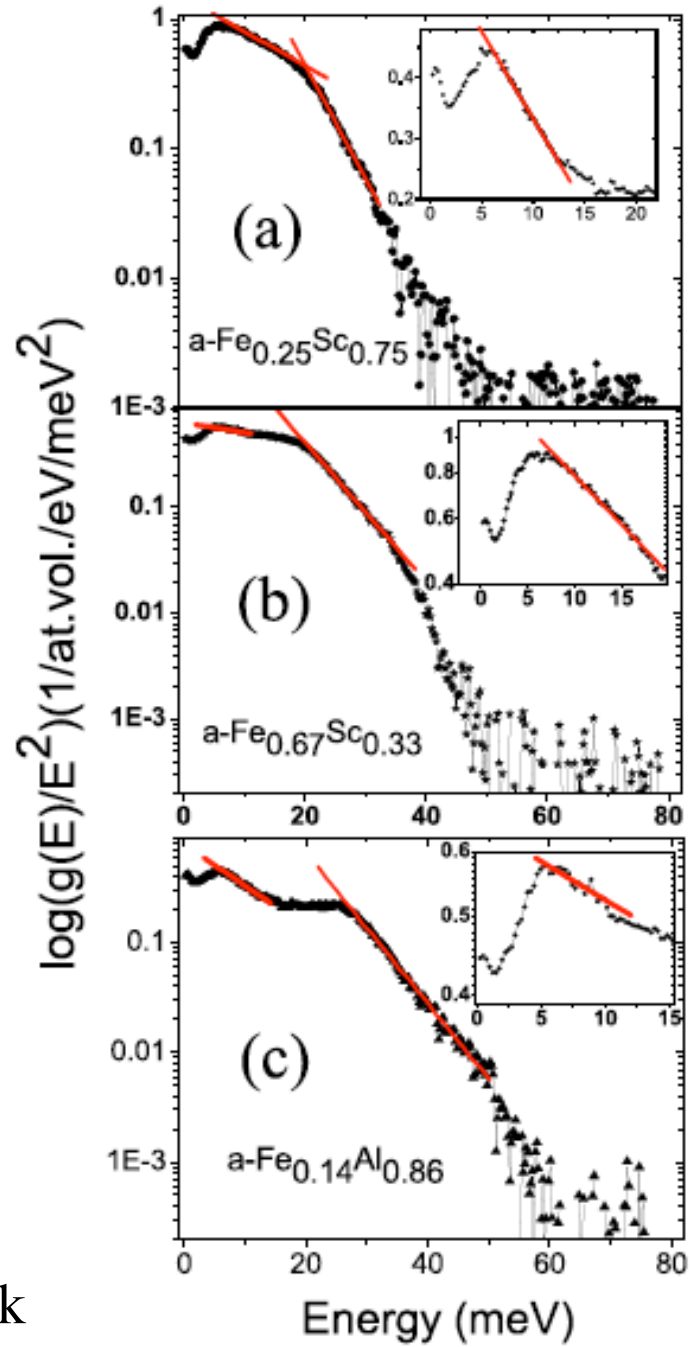

$g(E)/E^2 \propto exp(-E/E_0)$, E_0 boson peak

Porphyrin 101

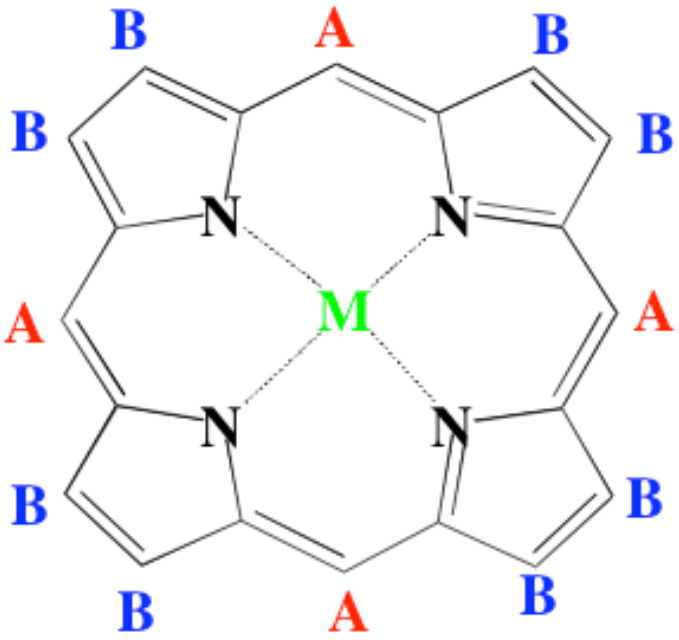

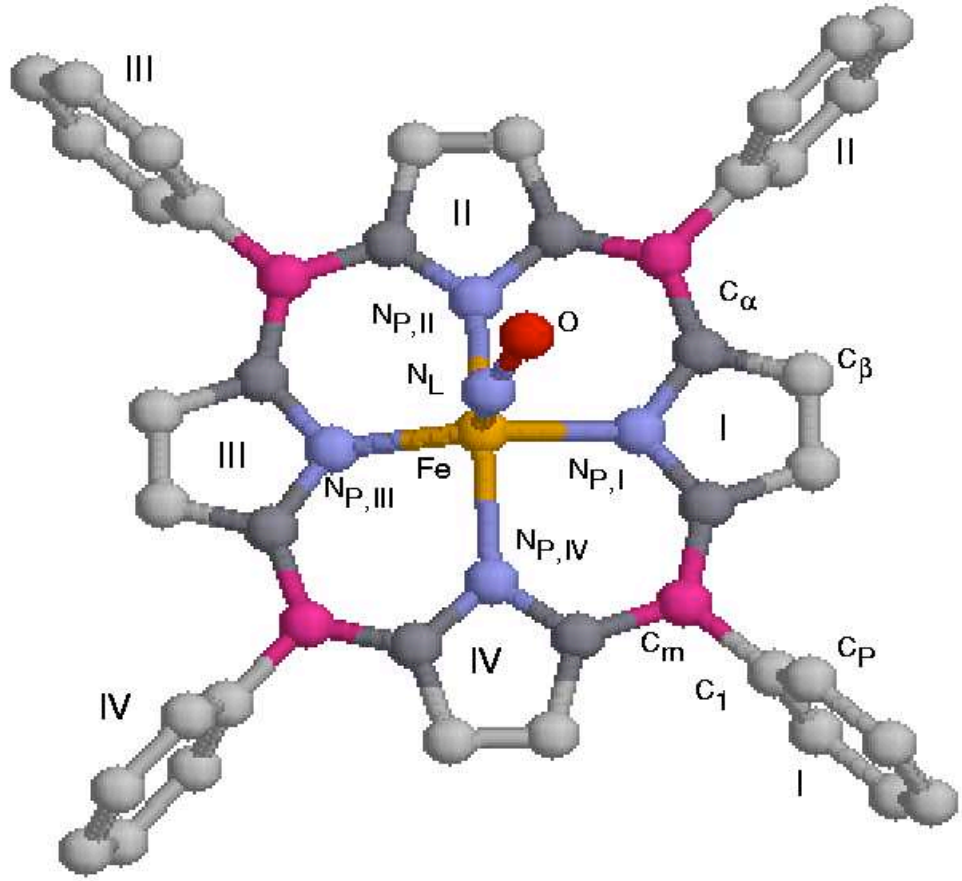

Porphyrins:	A	B
Tetraphenylporphyrin (TPP)	Phenyl	H
Octaethylporphyrin (OEP)	H	Ethyl

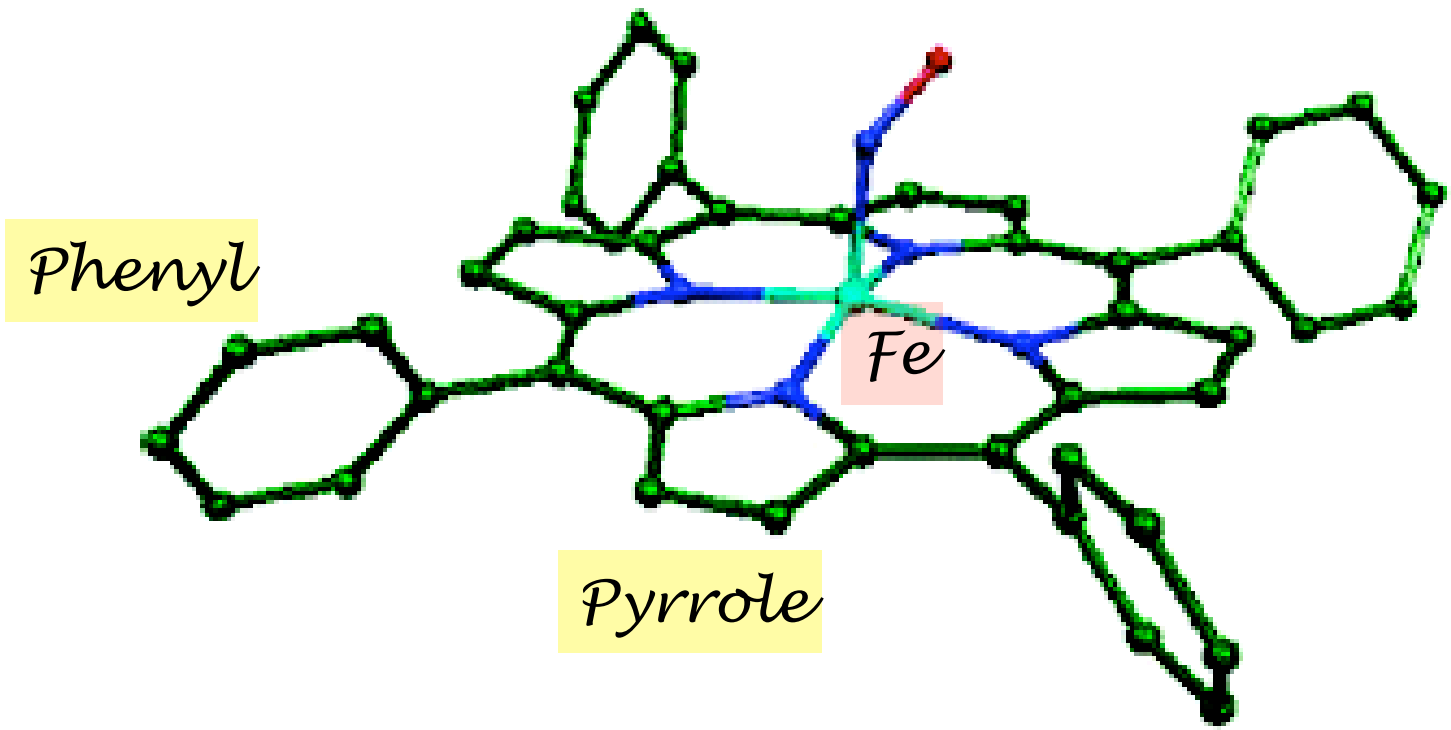

Figure 1. Calculated structure of ferrous nitrosyl tetraphenylporphyrin,

In-plane vibrations of heme Fe have not been identified in Raman spectra due to lack of electric dipole moment in D_{4h} symmetry.

Solvent absorption limit IR studies below 125 meV (1000 cm^{-1}).

Low frequency reactive modes are rarely identified with Raman or IR.

Why another vibrational technique for bio-inorganic and organic compounds ?

The general utility of vibrational spectroscopy is well understood.

However, site-selective techniques are needed to obtain vibrational information for **active sites** for complex molecular systems such as proteins and enzymes.

Resonance Raman, difference infrared, and femtosecond coherence spectroscopy may provide some site selectivity. However, relevant active-site vibrational information is not directly available with these techniques.

Selection rules for both infrared and Raman spectroscopy may restrict the observation of some functionally important vibrations.

For example, in-plane vibrations of the heme iron, which is related to the strength of the Fe-pyrrole bonds, have not been identified by resonance Raman method.

Also, reactive modes which would illuminate the energetics of chemical reactions lie at low frequencies that are difficult to get with traditional methods. For example, heme doming is very interesting to study.

Elastic properties such as velocity of sound, Gruneisen constant, and Debye Temperature can all be measured using NUCLEAR RESONANT INELASTIC-X-RAY SCATTERING

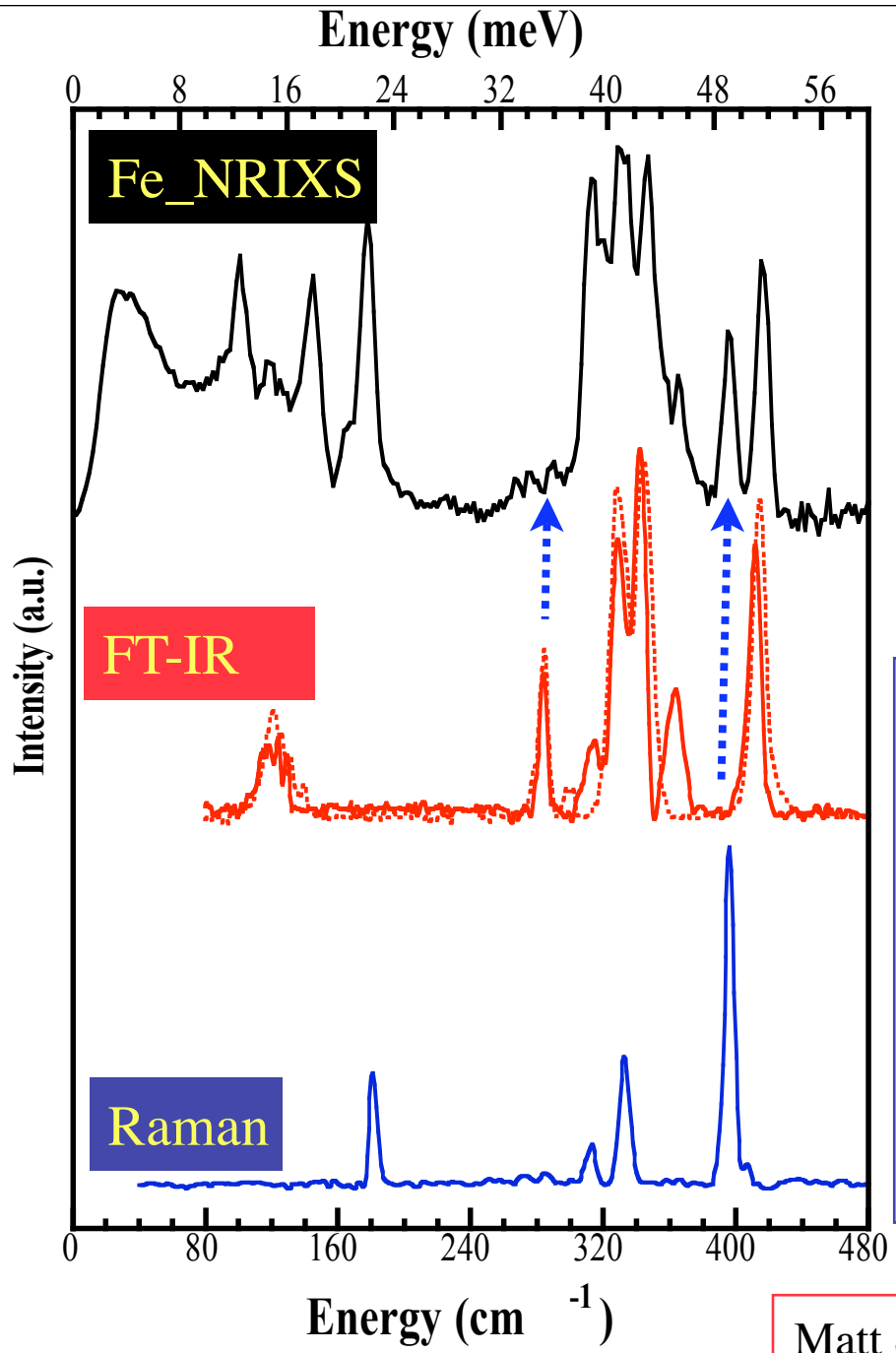

$[NEt_4]_2[Fe_2S_2Cl_4]$.

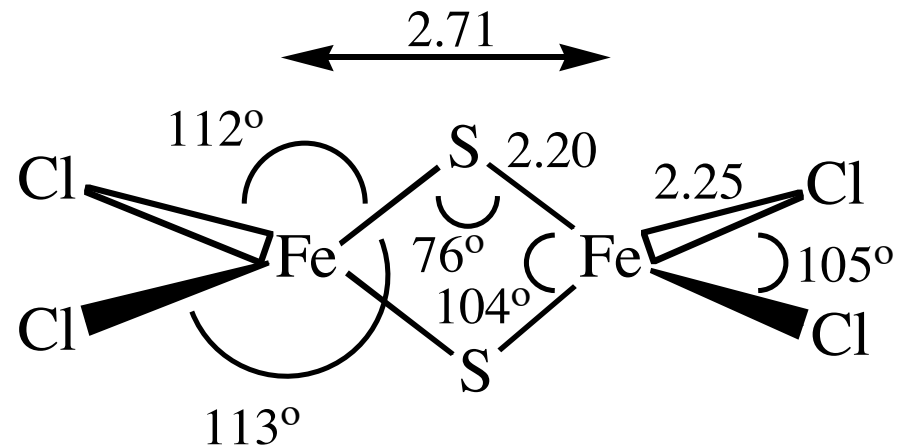

Some unique advantages of NRIXS

- Low frequency motions
2. No selection rule except motion of atoms along x-ray propagation
3. Peak intensity ~ mode participation ~ actual displacement
4. No matrix effects or limitations
5. Element and isotope selective
6. No unpredictable cancellations in scattering terms

Matt Smith, et al, Inorganic Chemistry, 2005, 44,5562

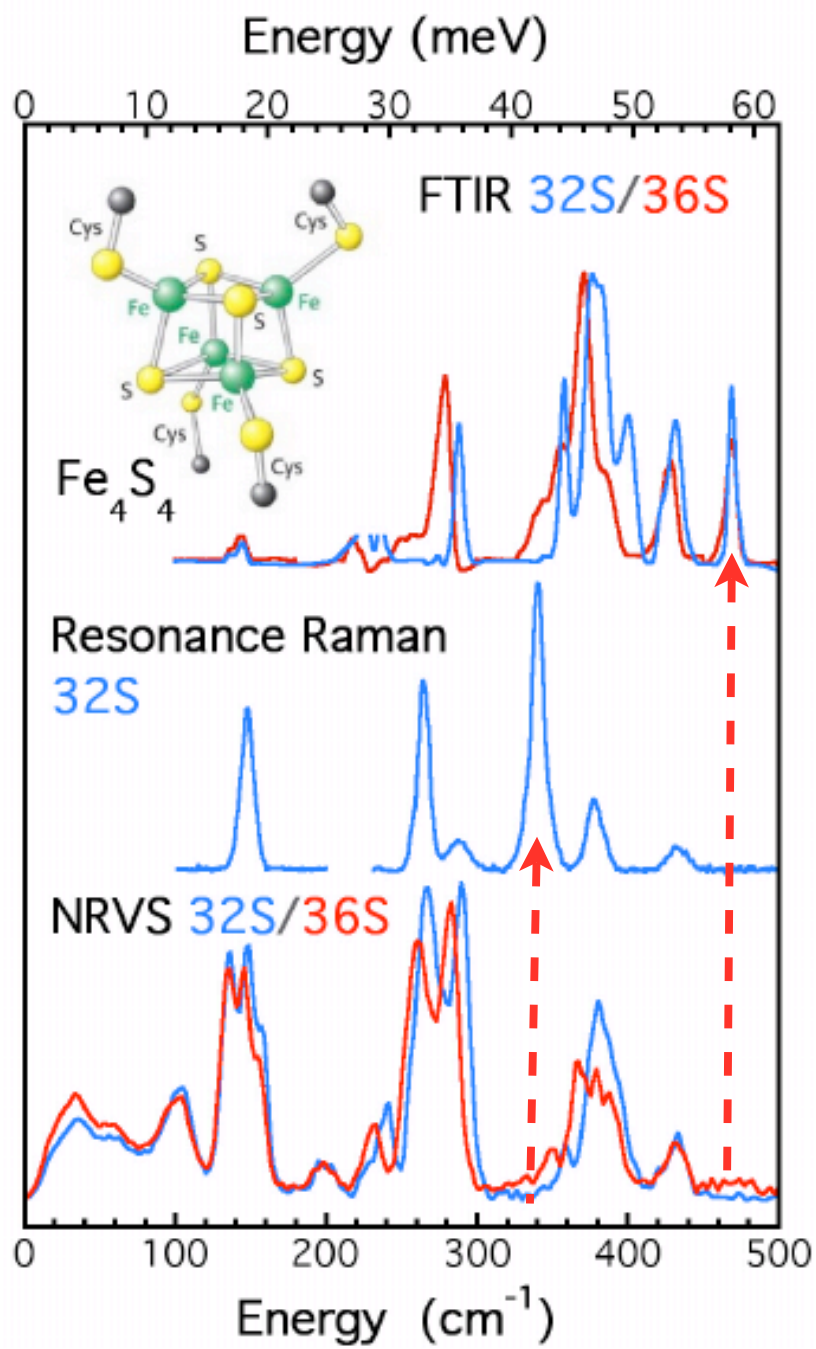

$[Fe_4S_4(SPH_4)]^{-2}$

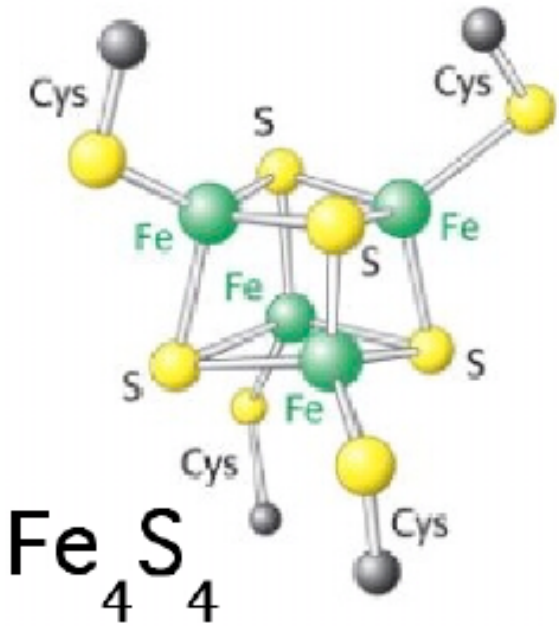

Some unique advantages of NRIXS

- Low frequency motions
2. No selection rule except motion of atoms along x-ray propagation
3. Peak intensity ~ mode participation ~ actual displacement
4. No matrix effects or limitations
5. Element and isotope selective
6. No unpredictable cancellations in scattering terms

Iron-sulfur cubane compounds

- **Reduced {4Fe4S}$^{+}$ has not been possible to observe with resonant Raman technique, in contrast to oxidized {4Fe4S}$^{2+}$**

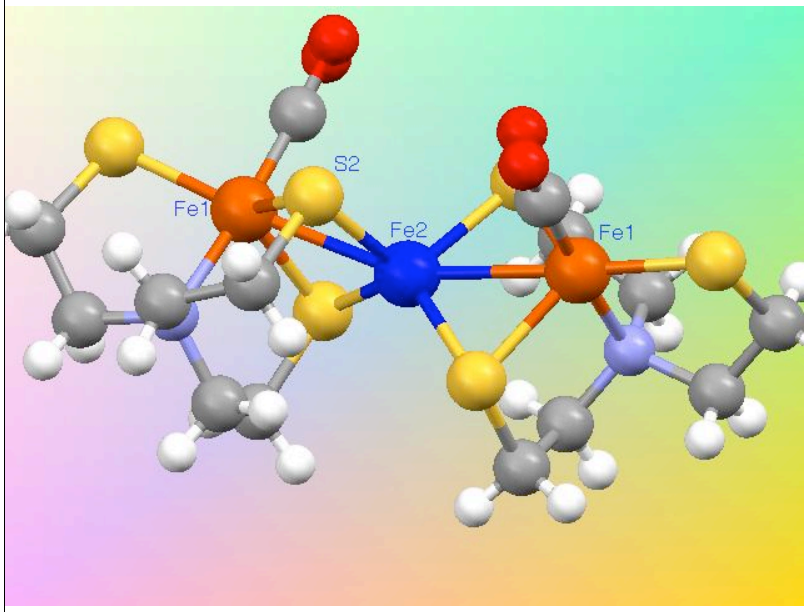

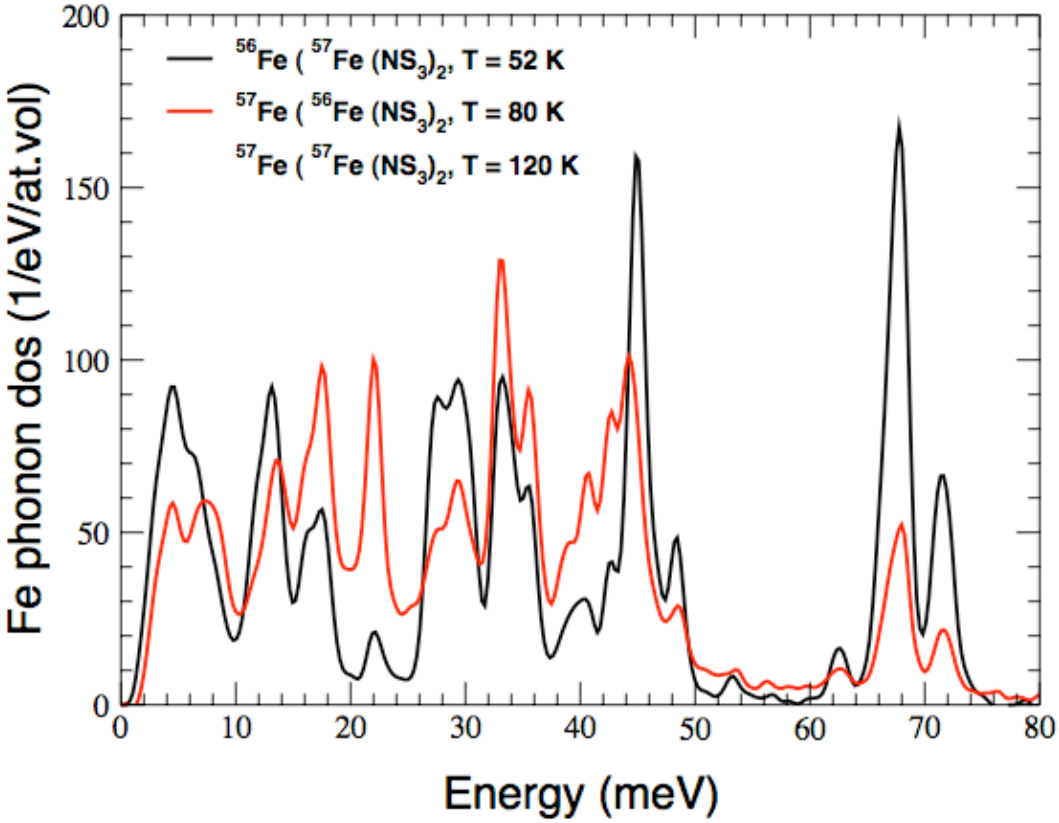

U. Jayasooriya et al, unpublished

Why model compounds ?

Model porphyrins are capable of reversible oxygen binding and thus can serve as a model for some proteins.

e.g. 1,2 Dimethyl imidazole --> T-state (deoxy) hemoglobin
picketfence porphyrins --> R-state: liganded to O_2

Lower oxygen affinity of T-state is attributed to spatial constraint posed by proximal histidine. In this state, Fe is 0.5 Å out-of-porphyrin plane, and drags the proximal histidine with it.

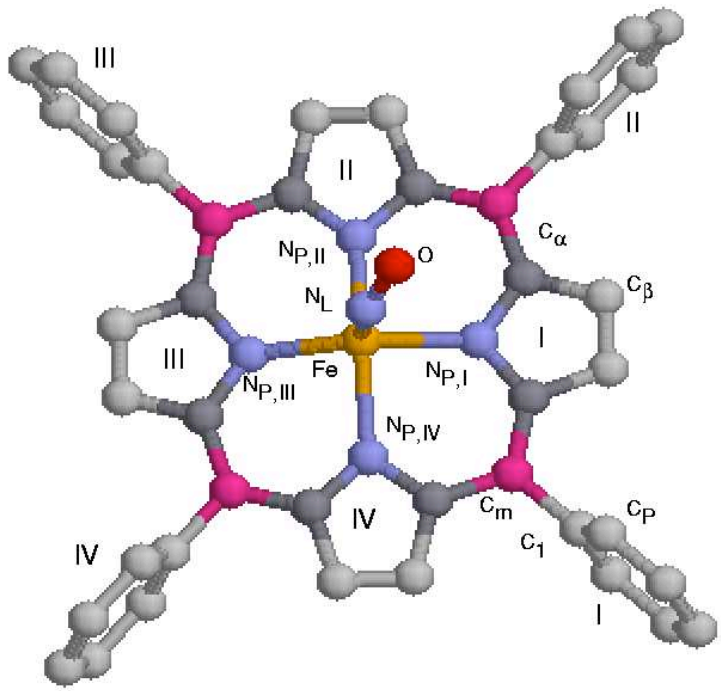

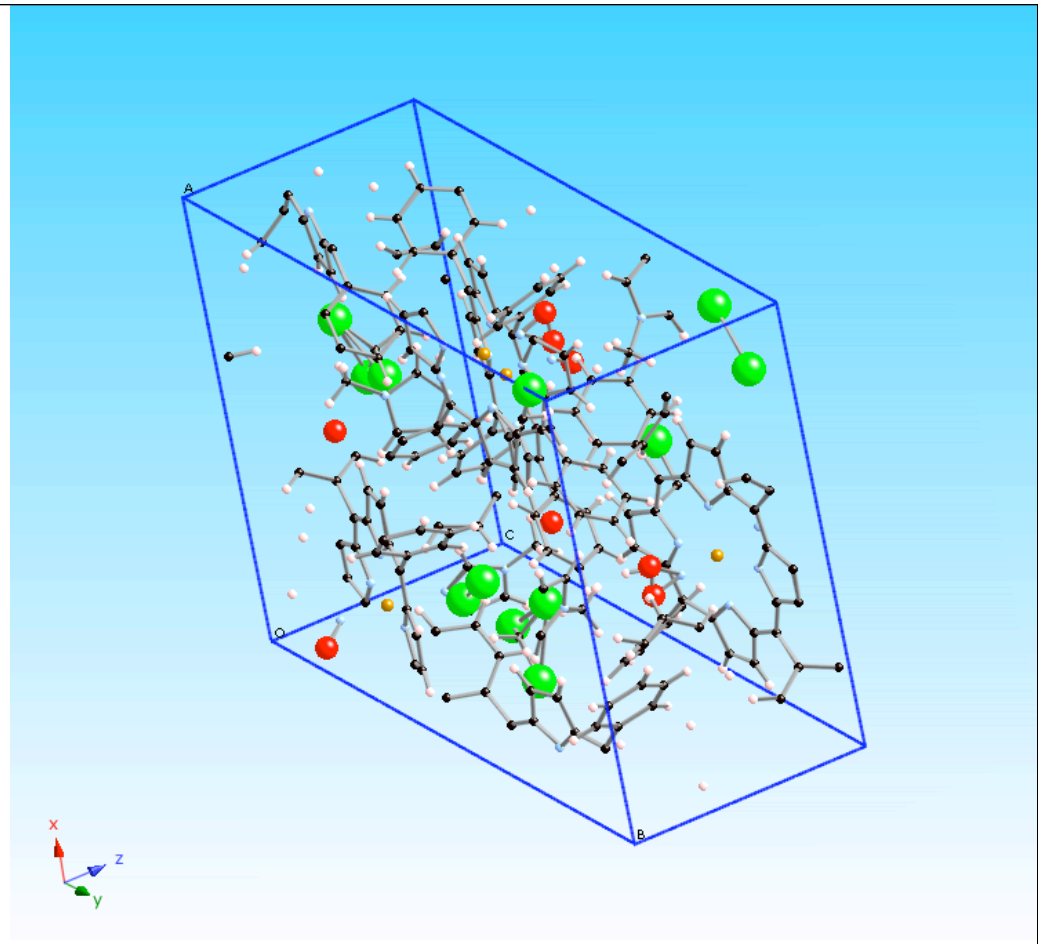

Porphyrins:	A	B
Tetraphenylporphyrin (TPP)	Phenyl	H
Octaethylporphyrin (OEP)	H	Ethyl

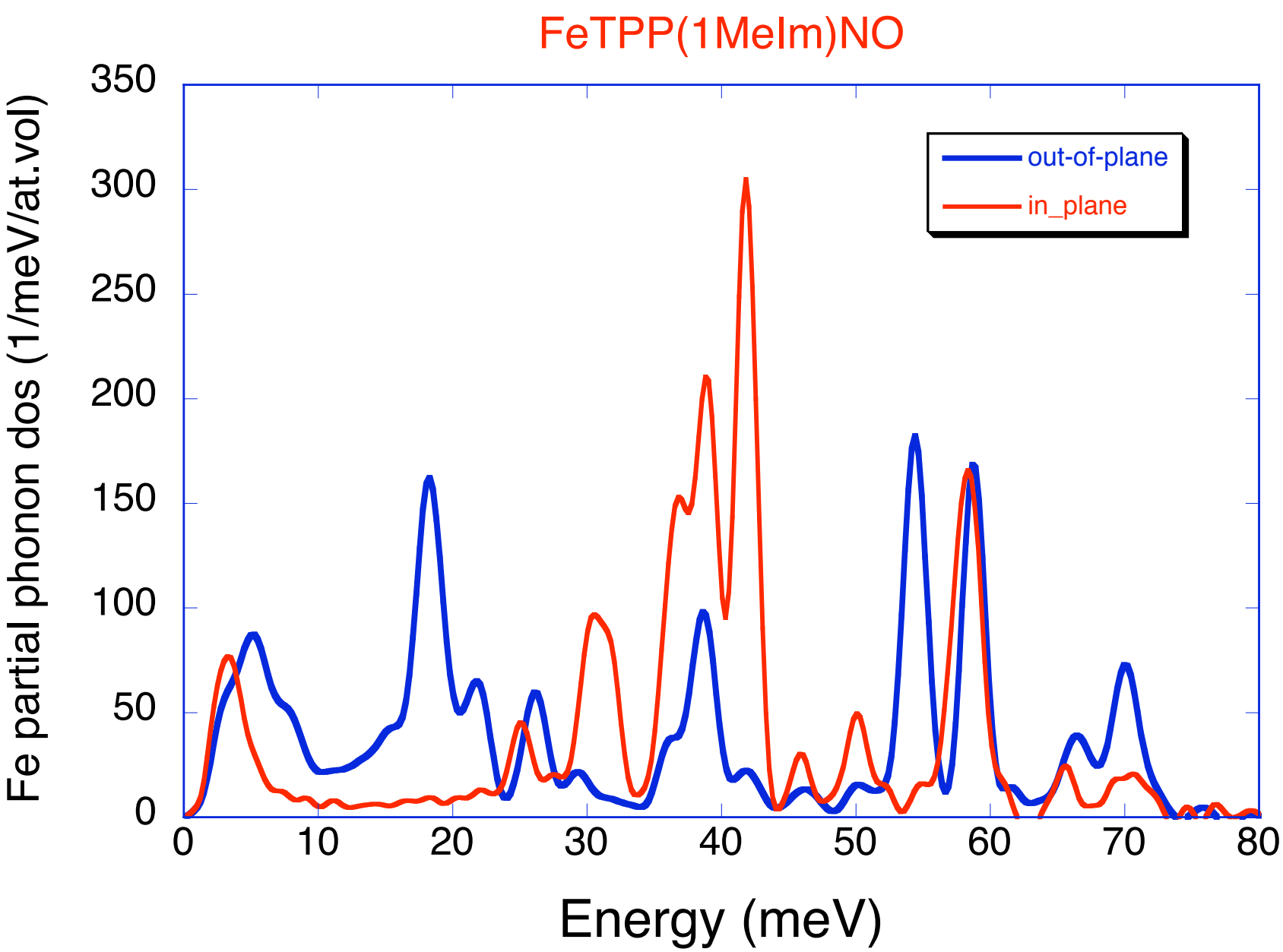
FeTPP(1MeIm)NO
Fe partial phonon dos (1/meV/at.vol)
350
300
250
200
150
100
50
0
0
10
20
30
40
50
60
70
80
Energy (meV)
out-of-plane
in_plane

Scheidt, Durbin, Sage, J. Inorganic Biochemistry, 99 (2005) 60.

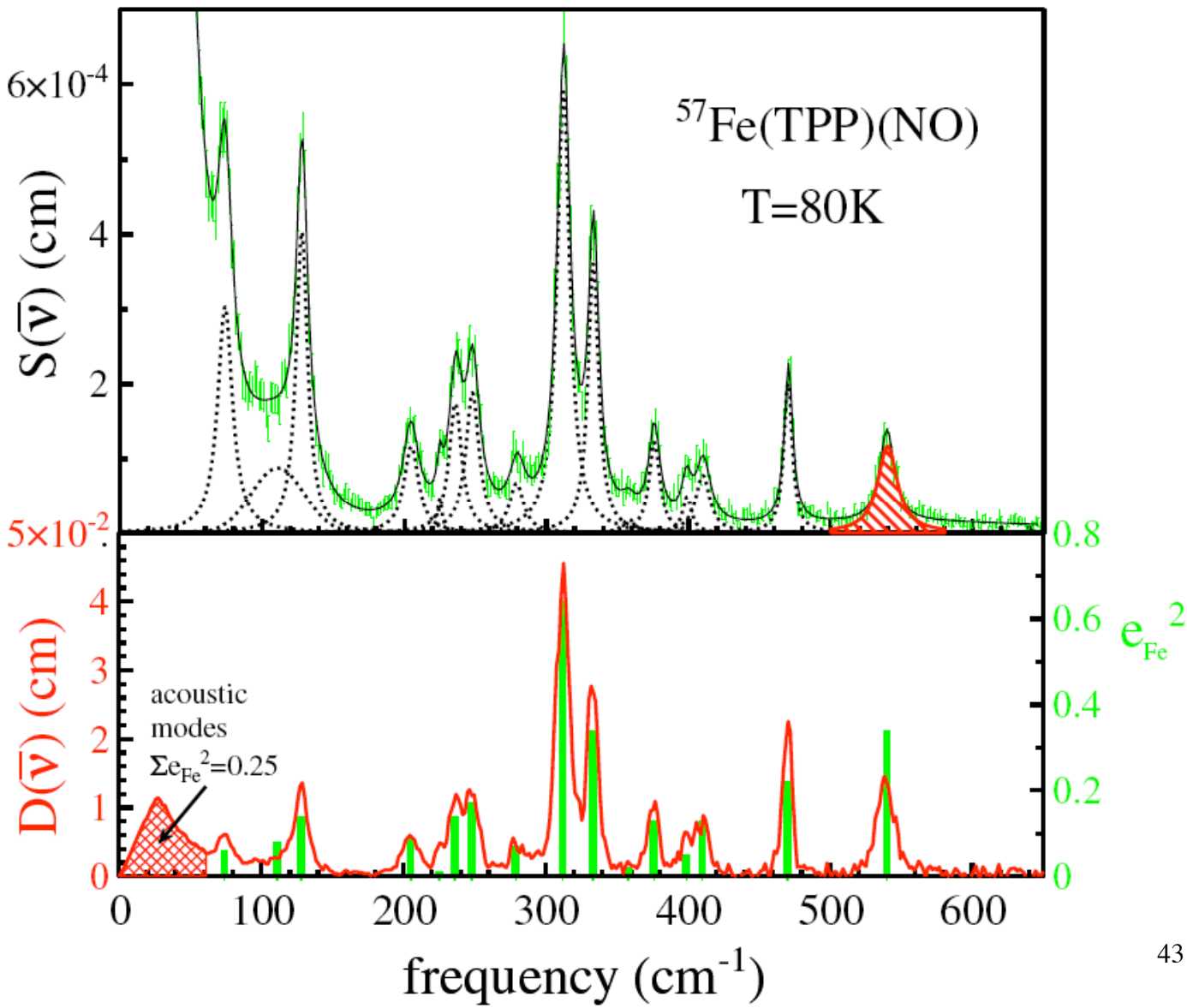

Dynamics of Molecules with Nuclear Resonant Scattering

A. Chumakov, R. Rüffer, O. Leupold, and I. Sergueev, Structural Chemistry, 14 (2003) 109

$$\breve{g}(E,\vec{s}) = \frac{V_0}{(2\pi)^3}\sum_j \int d\vec{q}\,\delta\left(E - \hbar\omega_j(\vec{q})\right)\left|\vec{s}\cdot\vec{e}_j(\vec{q})\right|^2$$

Orientational (projected) density of states, $\vec{e}_j(\vec{q})$ is the phonon polarization vector.

$$\breve{g}_j(\vec{s}) = \left|\vec{s}\cdot\vec{e}_j(\vec{q})\right|^2$$

Fraction of dos belonging to *j* th vibrational mode for non-interacting modes like Einstein modes or optical modes (no or little momentum dependence)

$$g_j = \frac{1}{3}e_j^2$$

randomly oriented powder

$$e_j^2 = \frac{r_{j,res}^2 m_{res}}{\sum_{k=1}^{N} r_{j,k}^2 m_k}$$

polarization vector of vibrations in the *j* th mode

$$e_{acoustic}^2 = m_{res}/M_{total}$$

For acoustic modes, mean square displacements are the same

Modes

1. Stretch internal coordinate is defined by a variation in the bond length.

2. Angle bend internal coordinate describes a variation in the angle between two bonds which have one atom in common.

3. Torsion internal coordinate involves a variation in the dihedral angle of two planes which are defined by three consecutive bonds connecting four atoms.

4. Out-of-plane Bend internal coordinate is defined by a variation in the angle between a bond and a plane defined by two bonds.

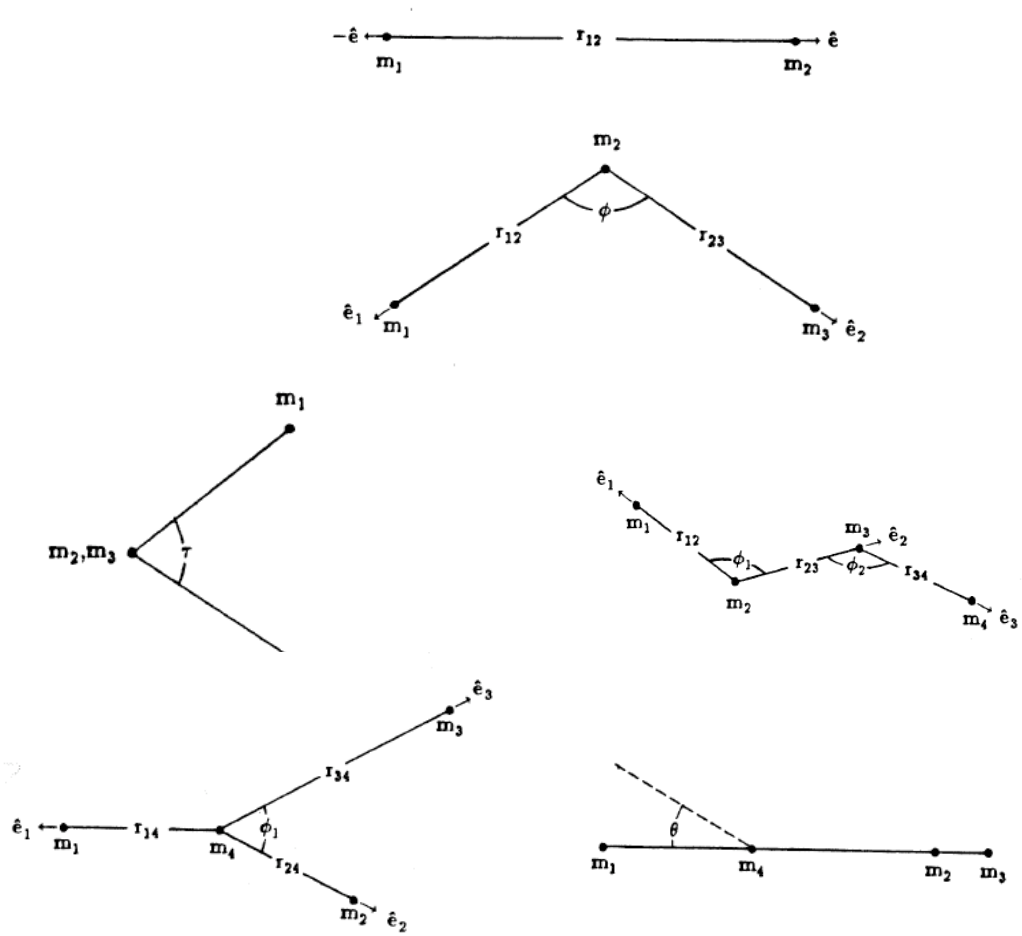

Top view

Side view

doming

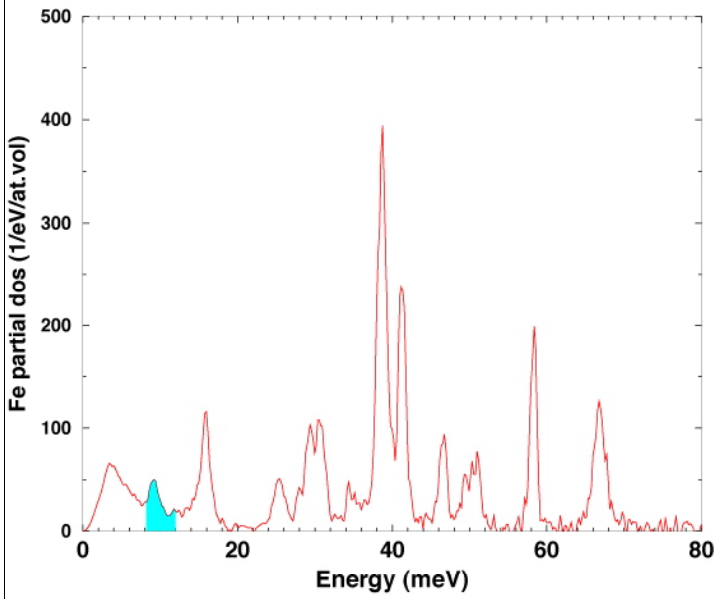

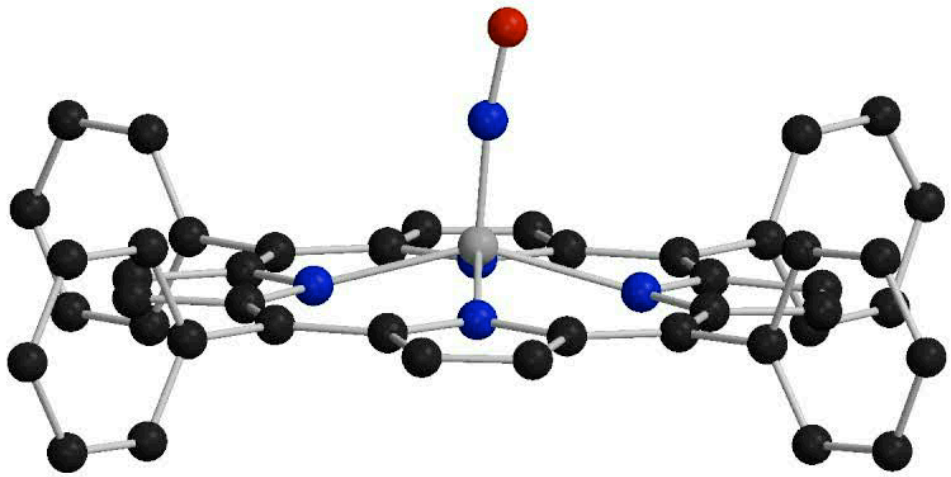

B. Rai, S. Durbin, W. Sturhahn, et al, Biophysics Journal, 2002

in-plane

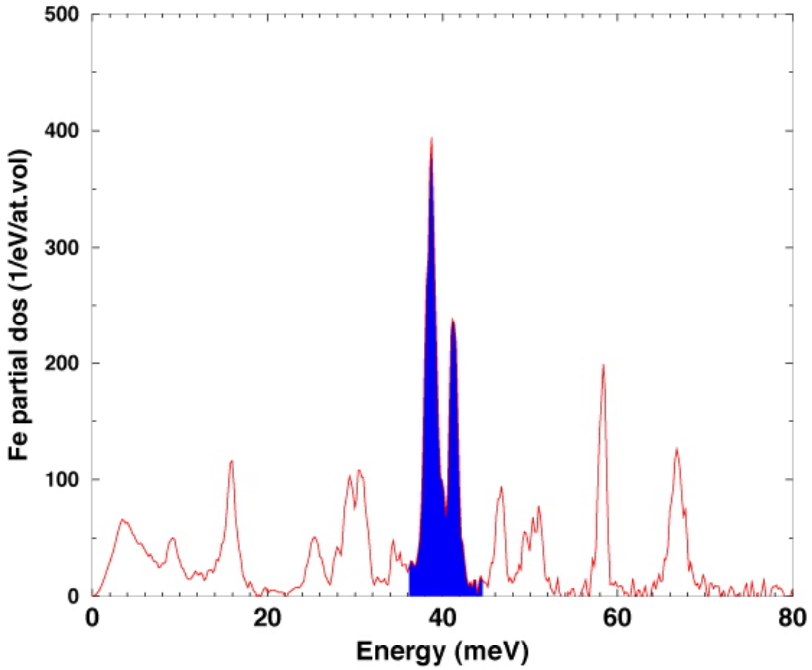

B. Rai, S. Durbin, W. Sturhahn, et al, Biophysics Journal, 2002

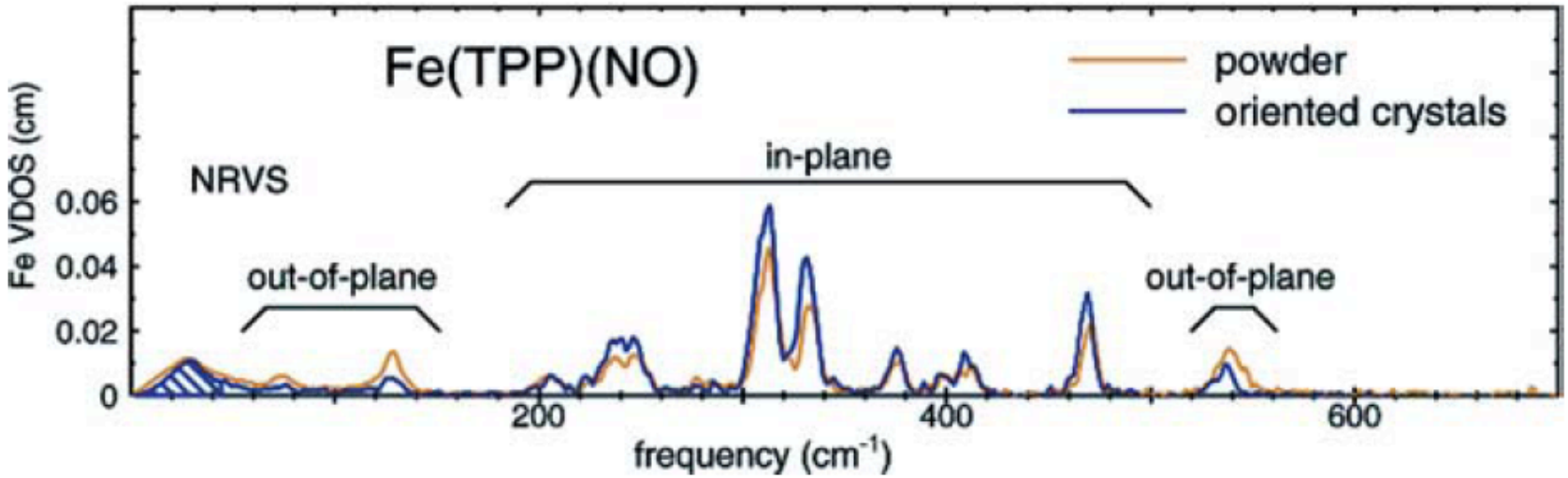
Fe(TPP)(NO)
powder
oriented crystals
NRVS
in-plane
out-of-plane
out-of-plane
Fe VDOS (cm)
0.06
0.04
0.02
0
200
400
600
frequency (cm-1)

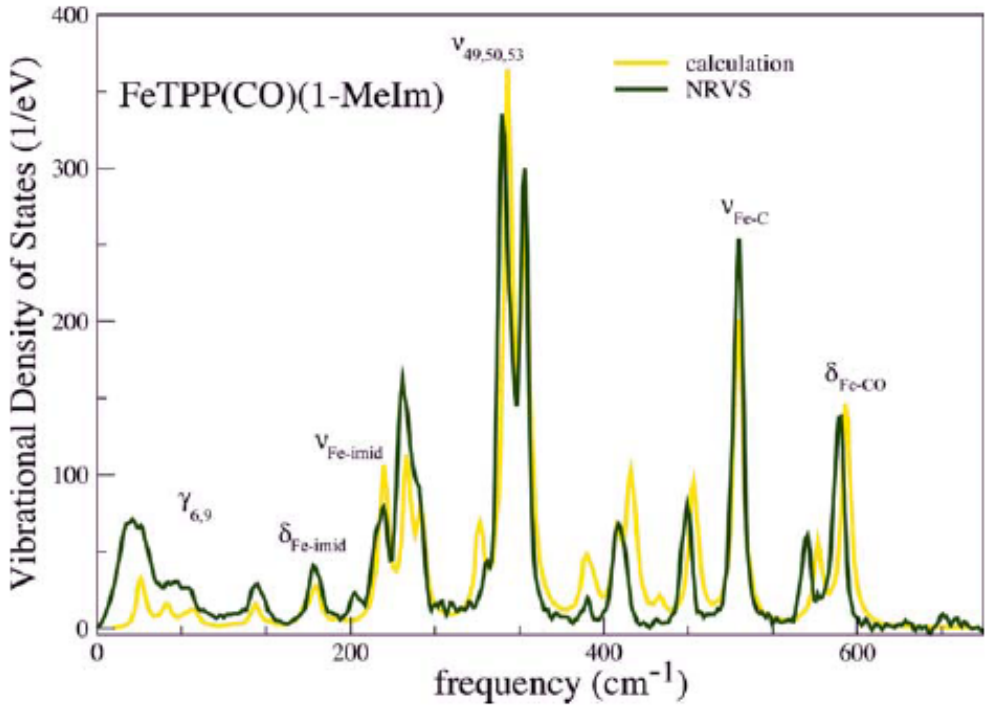
FeTPP(CO)(1-MeIm)
calculation
NRVS
ν49,50,53
νFe-C
δFe-CO
νFe-imid
γ6,9
δFe-imid
Vibrational Density of States (1/eV)
400
300
200
100
0
0
200
400
600
frequency (cm-1)

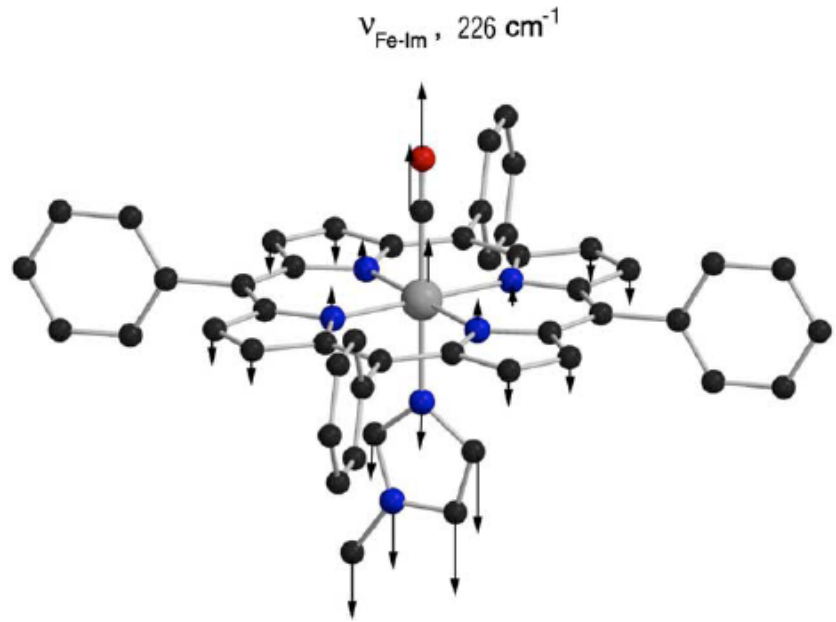
νFe-Im , 226 cm-1

Temperature dependence of dos

From the shift in the position of the phonon line, it may be possible to discern the total mass involved in that particular mode, while from the change in the linewidth an idea of phonon damping can be learned.

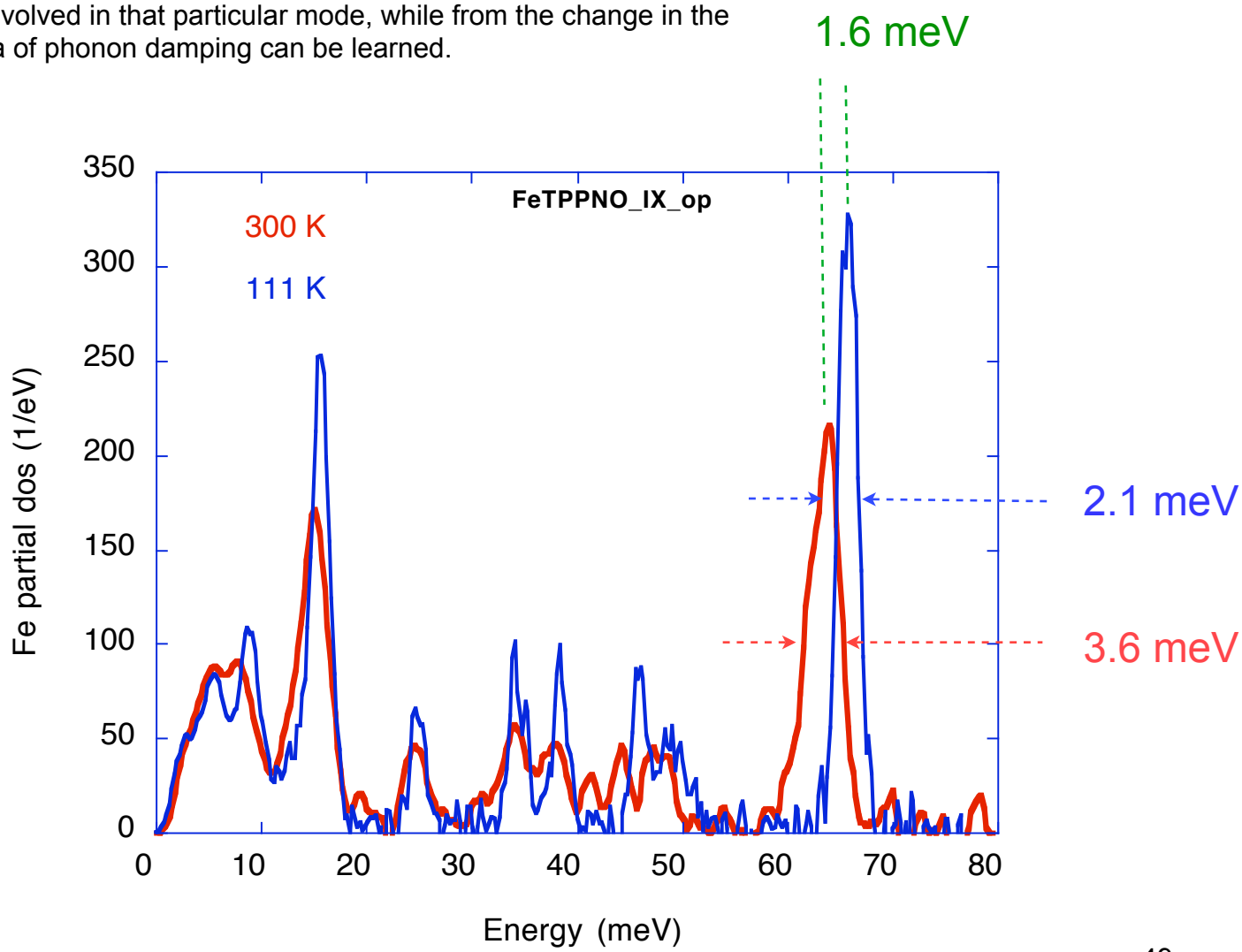

1.6 r

Temperature dependence of dos

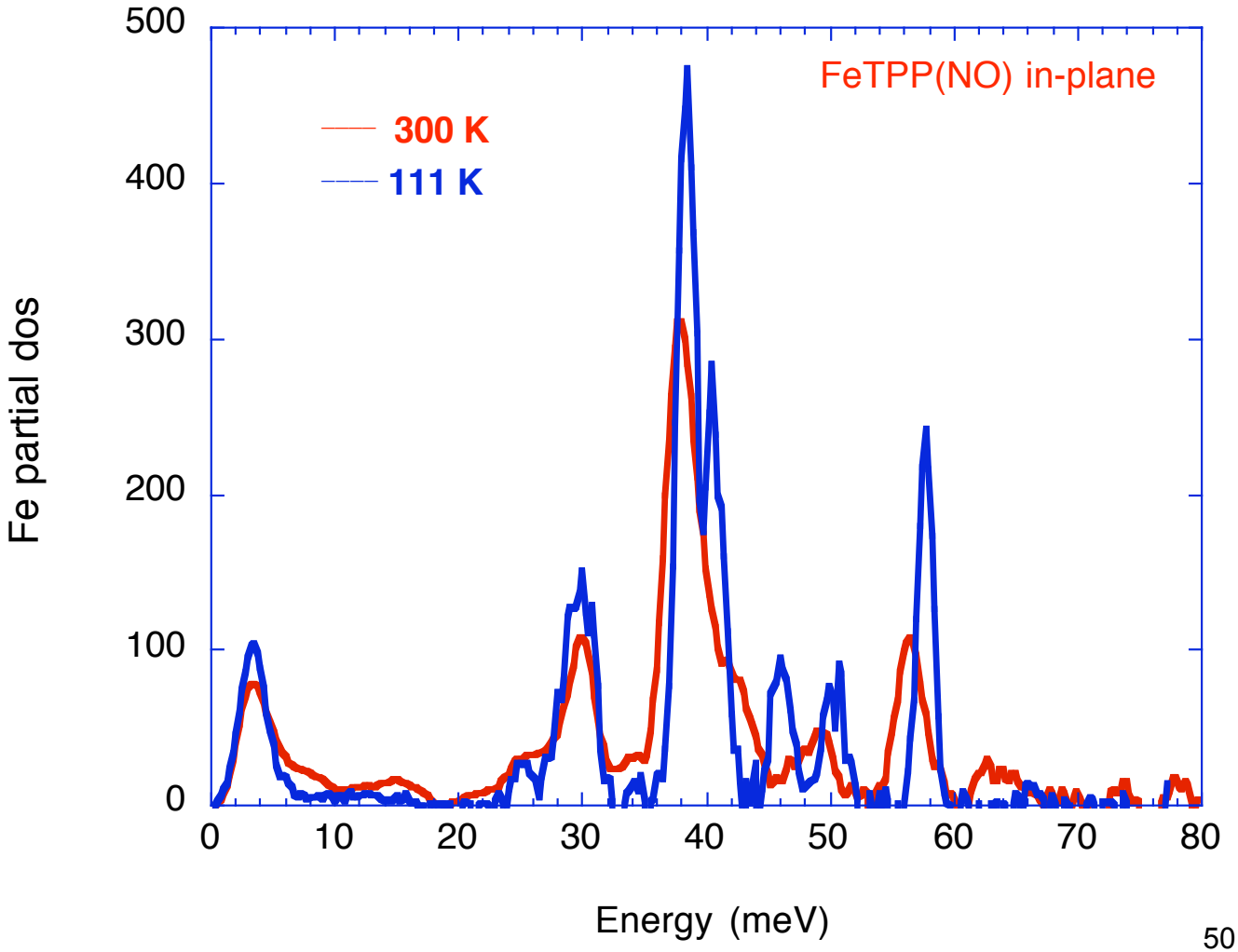

Pressure dependence of dos

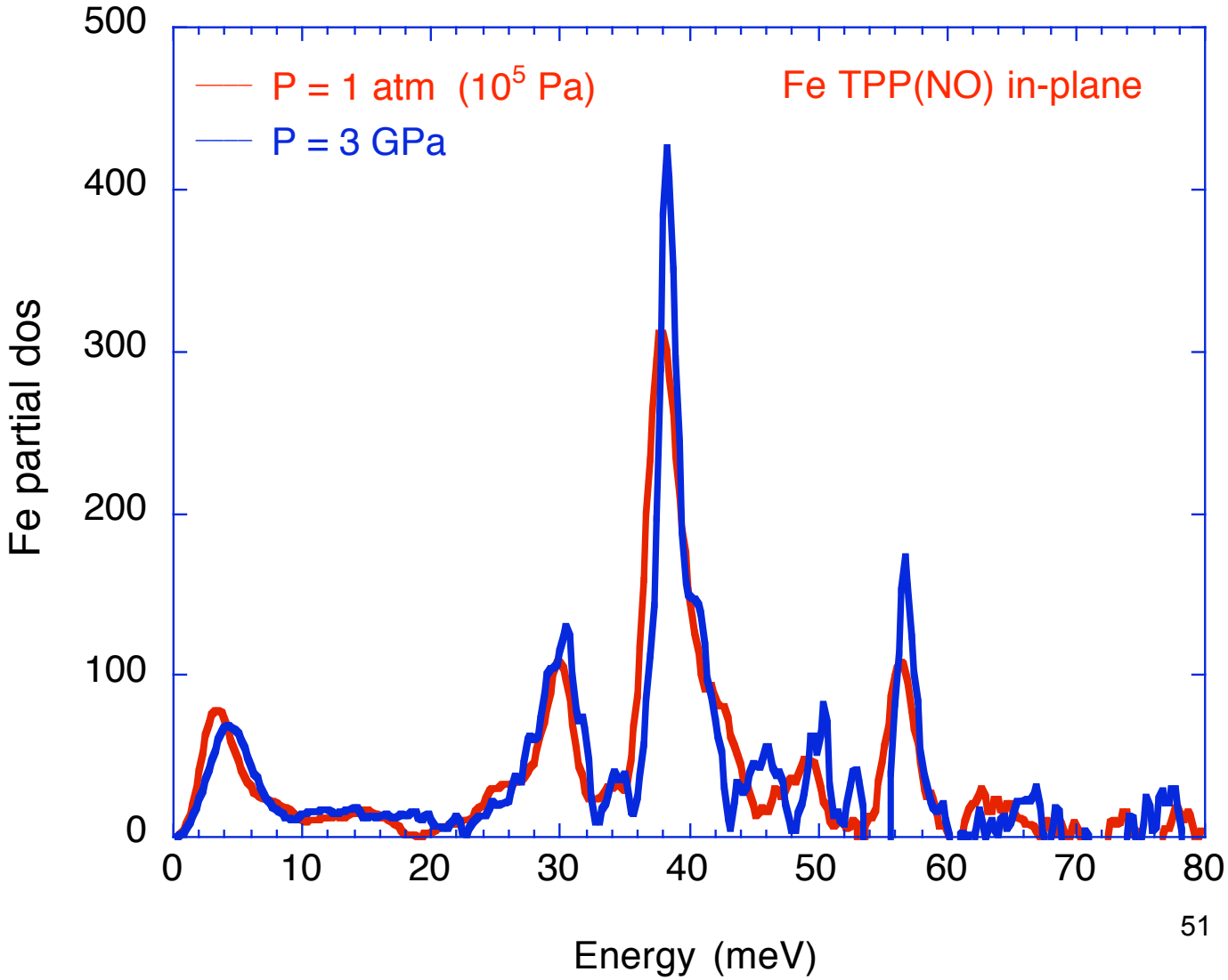

Pressure dependence of dos

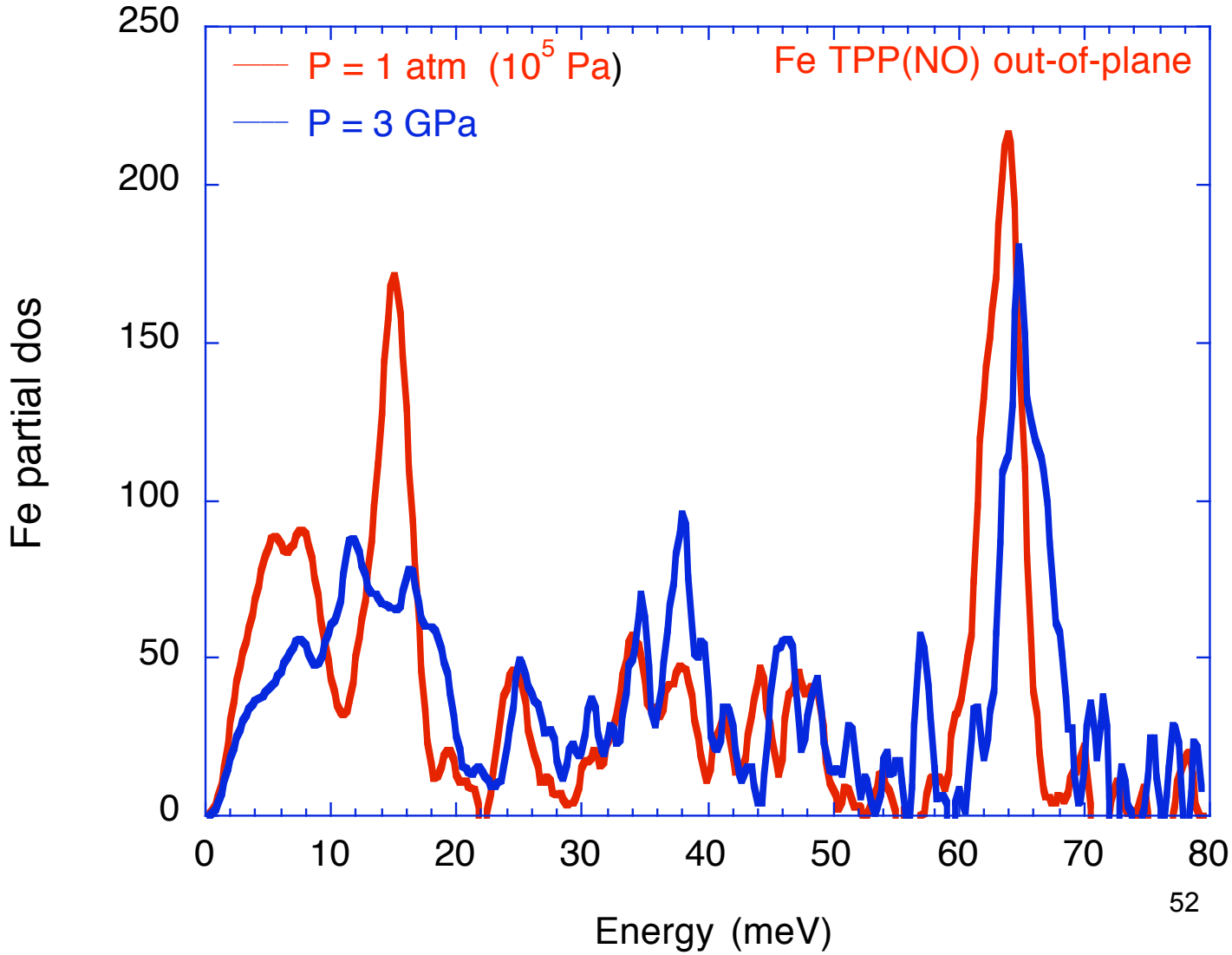

Anisotropy of pressure dependence of dos

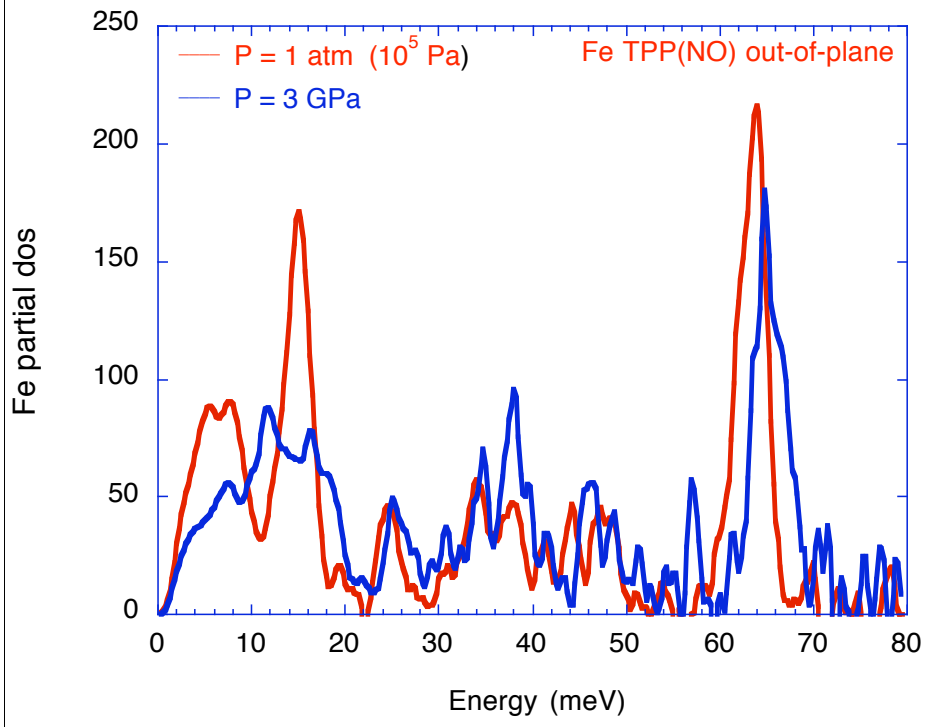

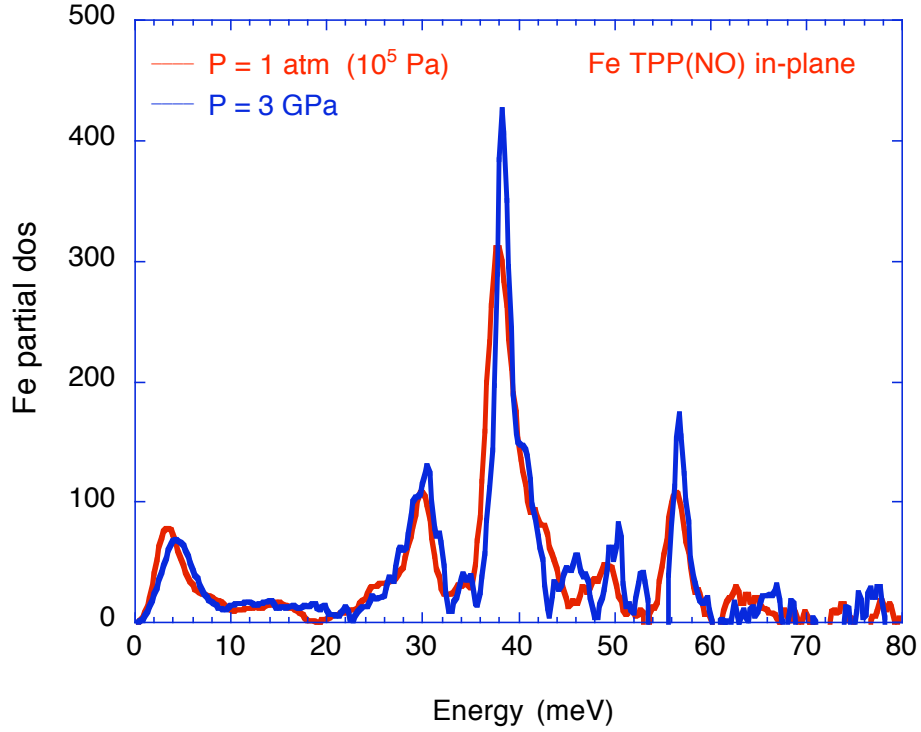

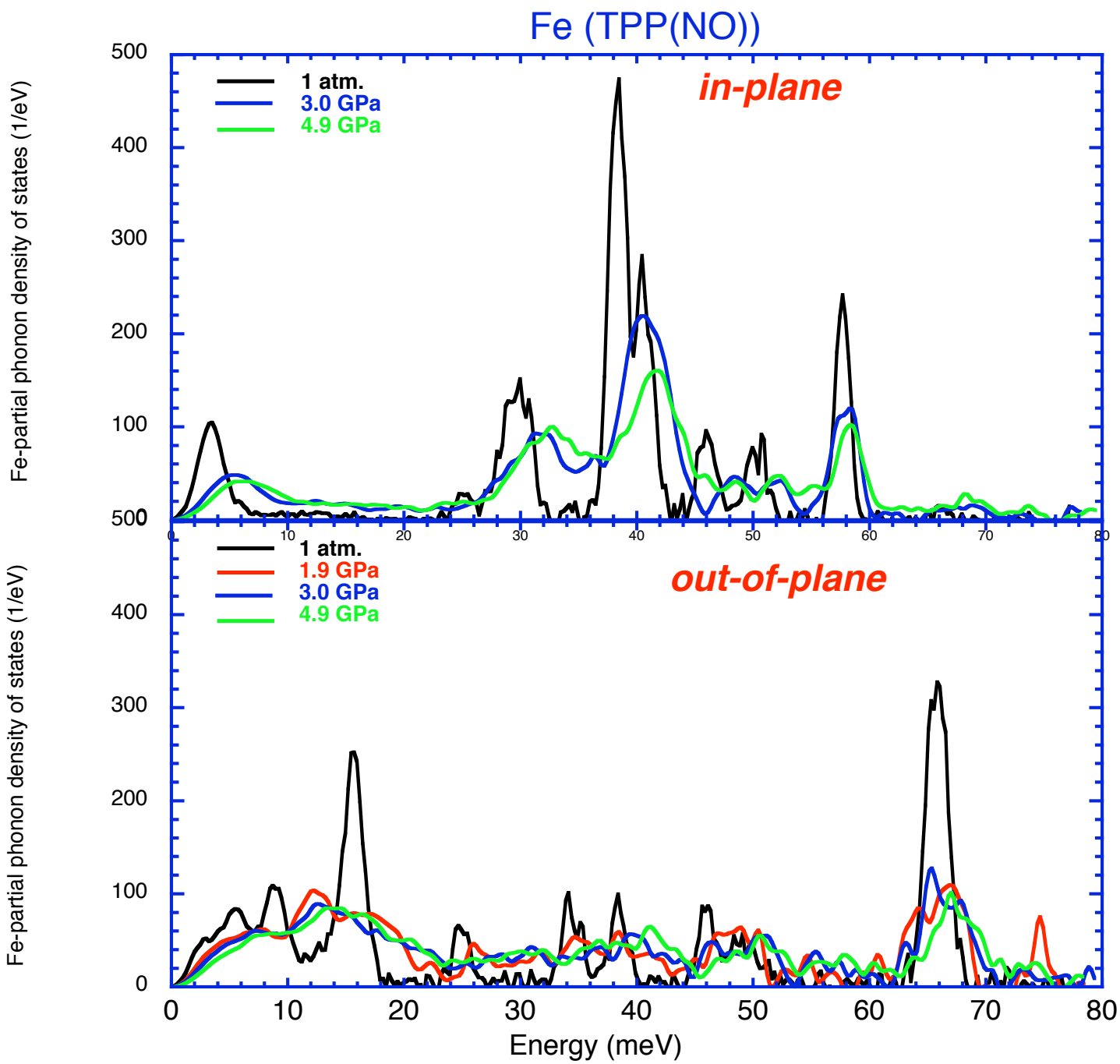
Fe (TPP(NO))
in-plane
1 atm.
3.0 GPa
4.9 GPa
out-of-plane
1 atm.
1.9 GPa
3.0 GPa
4.9 GPa
Fe-partial phonon density of states (1/eV)
Fe-partial phonon density of states (1/eV)
Energy (meV)
0
10
20
30
40
50
60
70
80
100
200
300
400
500

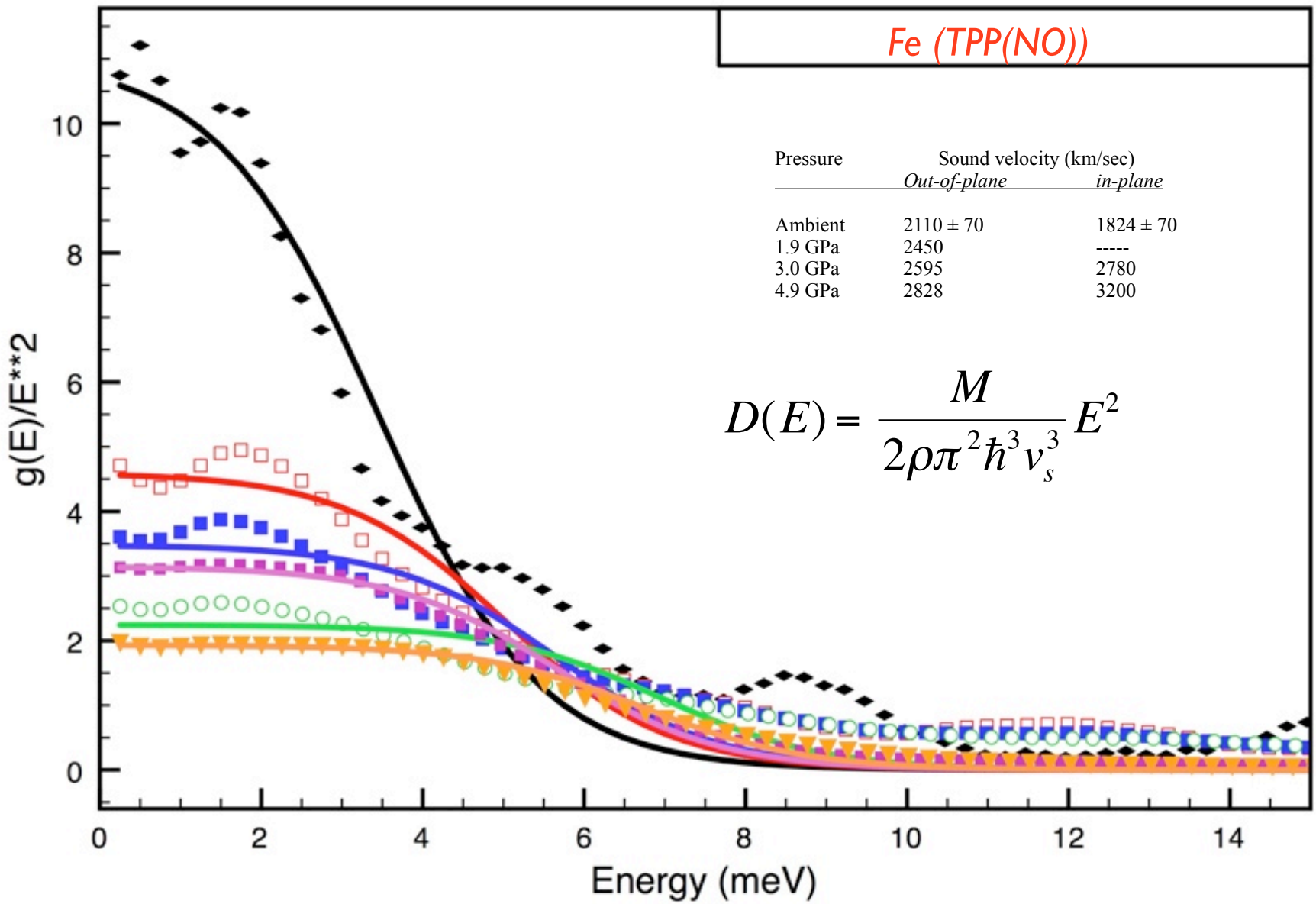

Pressure	Sound velocity (km/sec) *Out-of-plane*	*in-plane*
Ambient	2110 ± 70	1824 ± 70
1.9 GPa	2450	-----
3.0 GPa	2595	2780
4.9 GPa	2828	3200

$$D(E) = \frac{M}{2\rho\pi^2\hbar^3 v_s^3} E^2$$

Porphyrin model compounds

J. T. Sage, et al, J. Phys. Cond. Matt, 13 (2001) 7707

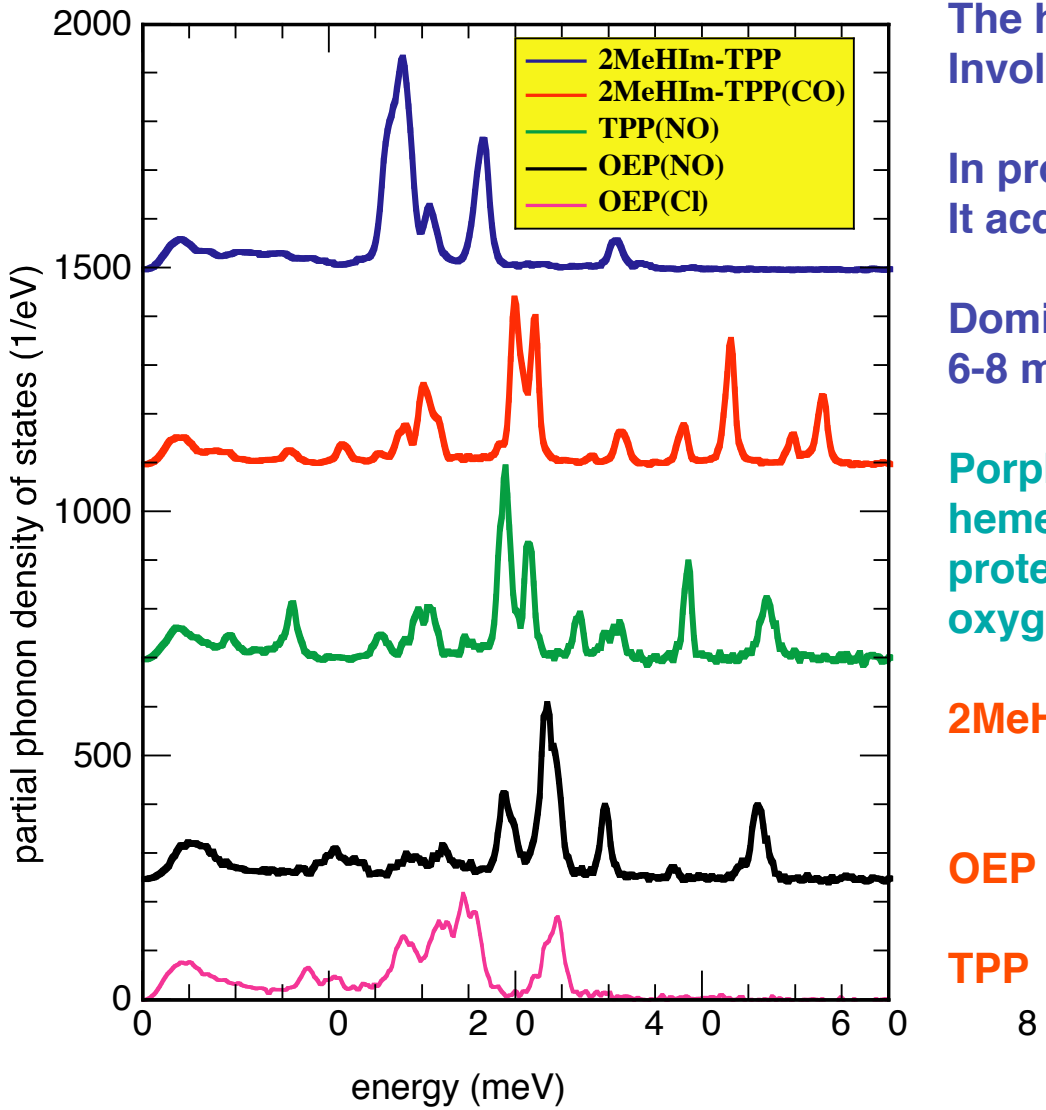

The heme doming coordinate is directly Involved in oxygen-binding reaction.

In proteins, it is important to know whether It acquires a global character.

Doming modes are expected in the range of 6-8 meV.

Porphyrin model compounds mimic the heme group found at the active site of many proteins involved in biological usage of oxygen and nitric oxide.

2MeHIm-TPP: Methyl-Hydrogen-Imidazole tetra phenyl porphyrin

OEP : Octo ethyl porphyrin

TPP : Tetra phenyl porphyrin

Cramer, S, et al **Nuclear Resonance Vibrational Spectroscopy (NRVS) of Fe-S model compounds, Fe-S proteins, and nitrogenase**. Hyperfine Interactions (2007), 170(1-3), 47-54.

Starovoitova, V. et al **Vibrational Spectroscopy and Normal-Mode Analysis of Fe(II) Octaethylporphyrin.** Journal of Physical Chemistry B (2006), 110(26), 13277-13282.

Adams, K. et al s. **Fe Vibrational Spectroscopy of Myoglobin and Cytochrome f.** Journal of Physical Chemistry B (2006), 110(1), 530-536.

Xiao, Y. et al **How Nitrogenase Shakes - Initial Information about P-Cluster and FeMo-cofactor Normal Modes from Nuclear Resonance Vibrational Spectroscopy (NRVS).** Journal of the American Chemical Society (2006), 128(23), 7608-7612.

Xiao, Y. et al **Dynamics of an [Fe4S4(SPh)4]2- cluster explored via IR, Raman, and nuclear resonance vibrational spectroscopy (NRVS)-analysis using 36S substitution, DFT calculations, and empirical force fields.** Dalton Transactions (2006), (18), 2192-2201.

Scheidt, W. R. et al. **Nuclear resonance vibrational spectroscopy - NRVS.** Journal of Inorganic Biochemistry (2005), 99(1), 60-71.

Zeng, W. et al **Direct Probe of Iron Vibrations Elucidates NO Activation of Heme Proteins.** Journal of the American Chemical Society (2005), 127(32), 11200-11201.

Leu, B. et al. **Vibrational dynamics of biological molecules Multi-quantum contributions.** Journal of Physics and Chemistry of Solids (2005), 66(12), 2250-2256.

Xiao, . et al P**. Normal Mode Analysis of Pyrococcus furiosus Rubredoxin via Nuclear Resonance Vibrational Spectroscopy (NRVS) and Resonance Raman Spectroscopy. J**ournal of the American Chemical Society (2005), 127(42), 14596-14606.

Smith, M et al**. Normal-Mode Analysis of FeCl4- and Fe2S2Cl42- via Vibrational Moessbauer, Resonance Raman, and FT-IR Spectroscopies.** Inorganic Chemistry (2005), 44 (16), 5562-5570.

Leu, B. et al. **Quantitative Vibrational Dynamics of Iron in Nitrosyl Porphyrins**. Journal of the American Chemical Society (2004), 126(13), 4211-4227.

Starovoitova, V; **Vibrational spectroscopy and normal-mode analysis of Fe(II) octaethylporphyrin** JOURNAL OF PHYSICAL CHEMISTRY B, 110 (26) 13277-13282 JUL 6 2006

Xiao, YM; et al **How nitrogenase shakes - Initial information about P-cluster and FeMo-cofactor normal modes from nuclear resonance vibrational Spectroscopy (NRVS)** JOURNAL OF THE AMERICAN CHEMICAL SOCIETY, 128 (23) 7608-7612 JUN 14 2006

Rai, BK; Prohofsky, EW; Durbin, SM **Single-atom test of all-atom empirical potentials Fe in myoglobin** JOURNAL OF PHYSICAL CHEMISTRY B, 109 (40) 18983-18987 OCT 13 2005

Smith, MC; et al **Normal-mode analysis of FeCl4- and Fe2S2Cl42- via vibrational Mossbauer, resonance Raman, and FT-IR spectroscopies** INORGANIC CHEMISTRY, 44 (16) 5562-5570 AUG 8 2005

Scheidt, WR; Durbin, SM; Sage, JT **Nuclear resonance vibrational spectroscopy - NRVS** JOURNAL OF INORGANIC BIOCHEMISTRY, 99 (1) 60-71 JAN 2005

Leu, B. et al **Quantitative vibrational dynamics of iron in nitrosyl porphyrins** JOURNAL OF THE AMERICAN CHEMICAL SOCIETY, 126 (13) 4211-4227 APR 7 2004

alp @ anl.gov

Geophysics applications

Geophysics applications of NRS

P vs. depth for Earth

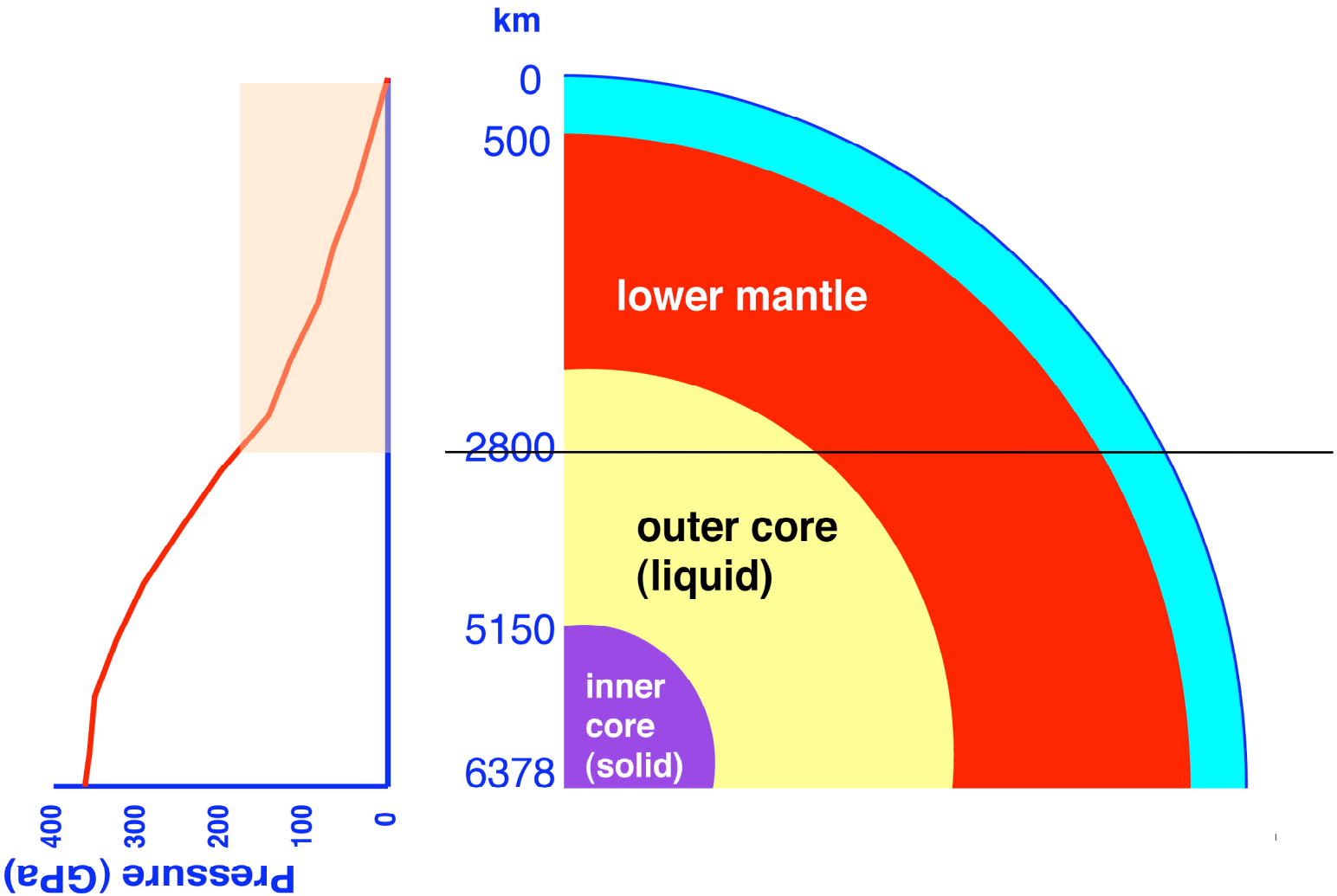

Earth's Interior (simplified)

Earth's seismic structure

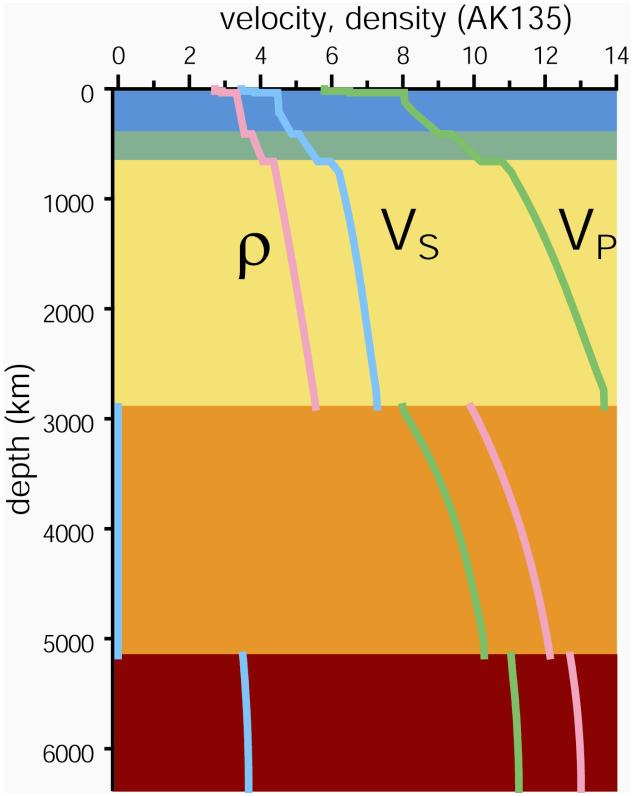

Earth's stratification

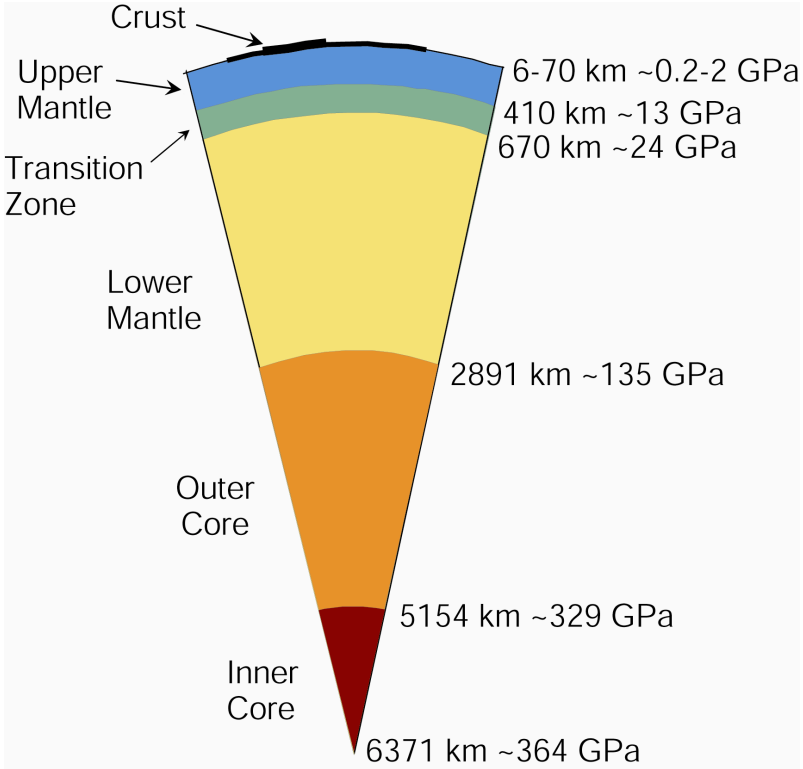

Earth's composition

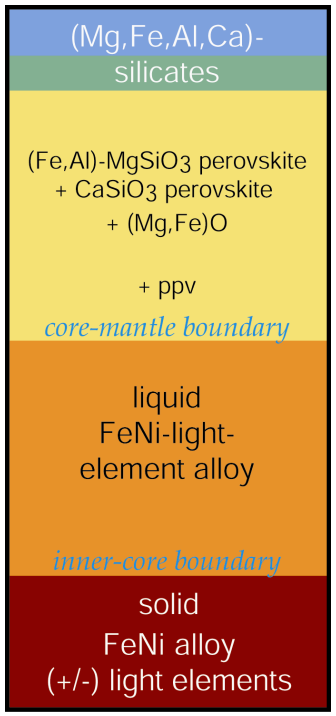

Sound velocity: What's the big deal ?

The sound velocity is directly related to elasticity, which is a function of chemical. and electronic properties materials. In Geosciences, for example, acoustic properties of materials in the Earth's deep interior are of general importance for accurate interpretation of seismic wave observations, geochemical modeling, and geodynamic simulations.

Despite their major roles in the deep Earth, very little is known about the sound velocities and crystal chemistry of these chemically complex phases under the appropriate pressure-temperature conditions.

The results of these IXS measurements under high pressure and temperature may enable a more realistic evaluation of the average mineralogy of Earth's lower mantle by comparing the measured sound velocities and elastic properties with a one-dimensional average Earth model, such as PREM.

The results also give insight into whether observed lateral variations of seismic wave speeds in the lower mantle are due to a chemical origin.

The electronic properties, including the charge and spin states, of iron in silicate perovskite were determined and will be discussed in light of our recent predictions considering the temperature effect on the electronic spin state of iron in dilute iron-bearing materials.

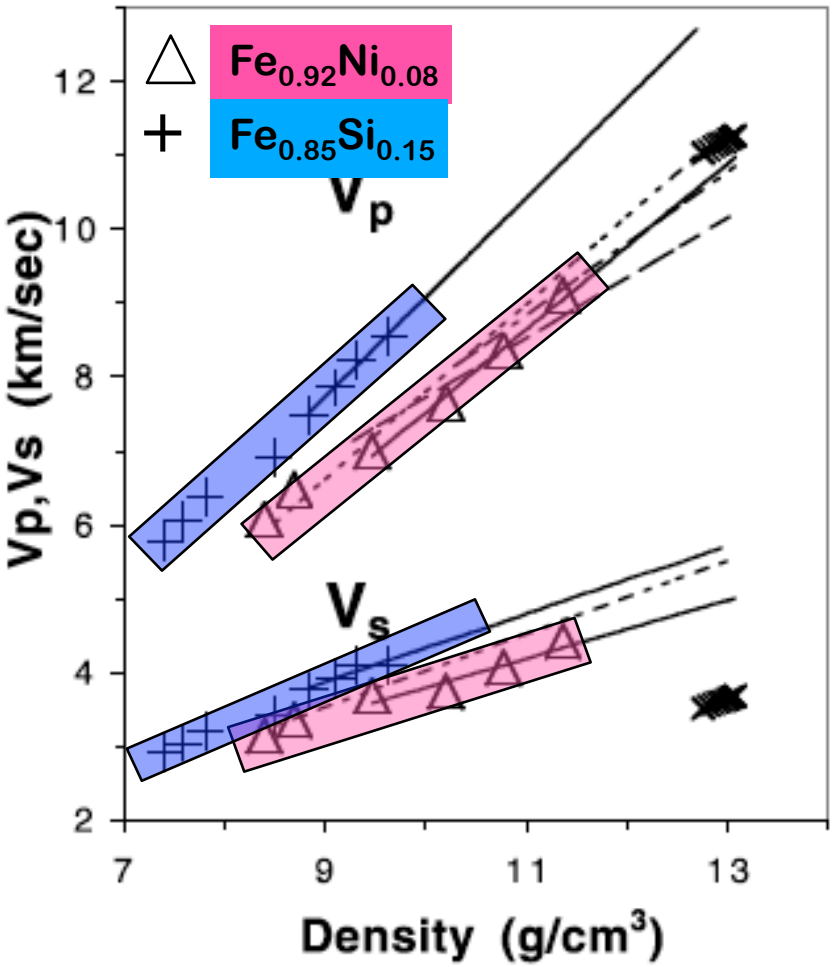

$$\frac{K_S}{\rho} = V_P^2 - \frac{4}{3}V_S^2$$

$$\frac{G}{\rho} = V_S^2$$

$$\frac{3}{V_D^3} = \frac{1}{V_P^3} + \frac{2}{V_S^3}$$

K_S : adiabatic bulk modulus

G : shear modulus

V_P : compression wave velocity

V_S : shear wave velocity

V_D : Debye sound velocity

P : density

Alloying effects of Ni and Si on density, Vp, Vs of hcp-Fe by NRIXS study

PDOS of $Fe_{0.92}Ni_{0.08}$

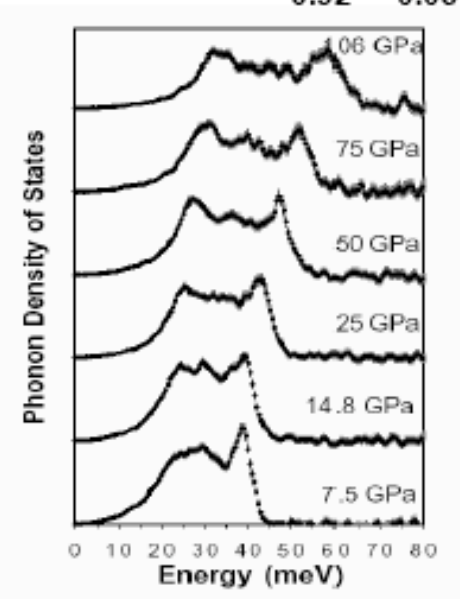

PDOS of $Fe_{0.85}Si_{0.15}$

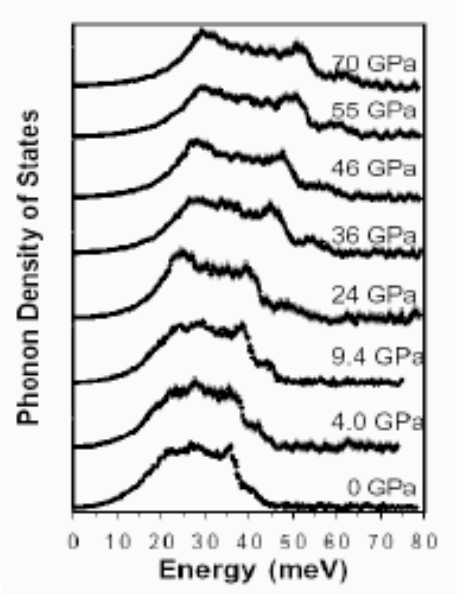

Lin et al., GRL, 2003

$Fe_{0.92}Ni_{0.08}$ and $Fe_{0.85}Si_{0.15}$ alloys

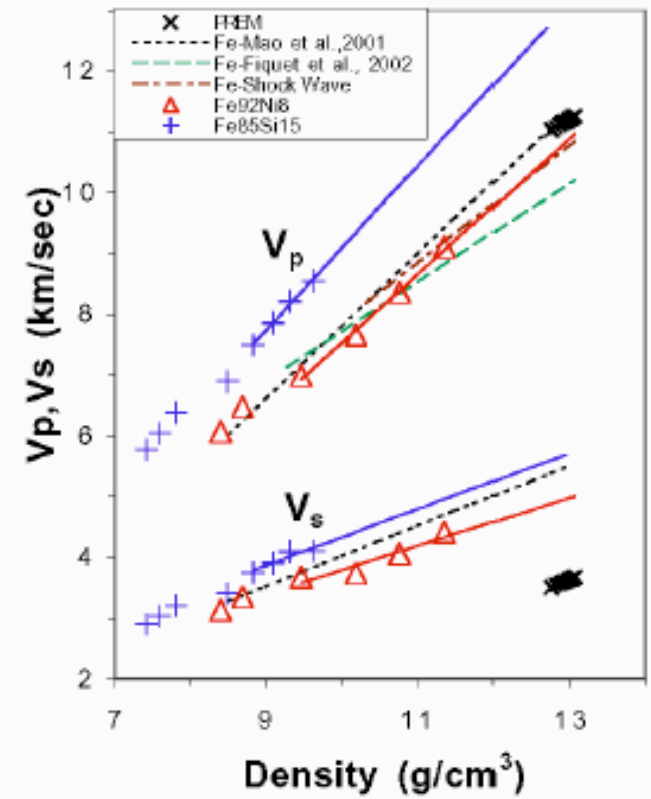

$$\frac{K_S}{\rho} = V_P^2 - \frac{4}{3} V_S^2$$

$$\frac{G}{\rho} = V_S^2$$

Addition of Ni slightly decreases the compression wave velocity and shear wave velocity of Fe under high pressures. Substitution of Si in Fe increases the compressional wave velocity and shear

A geotherm together with accessible *P-T* ranges by static techniques

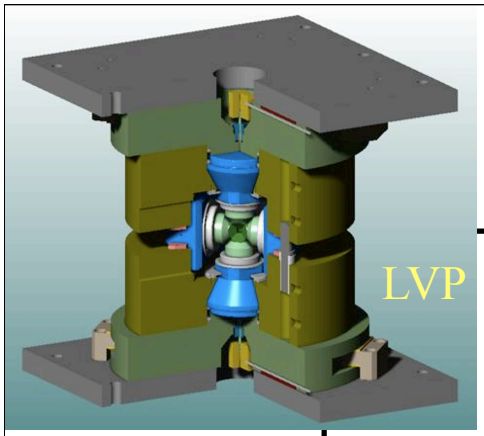

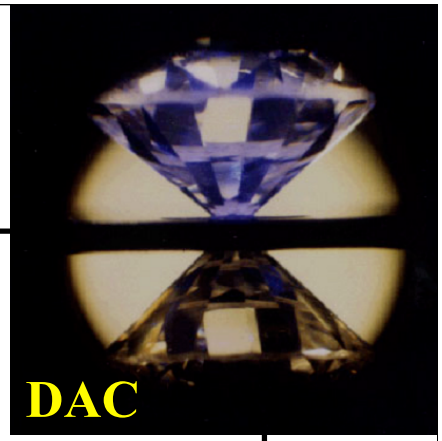

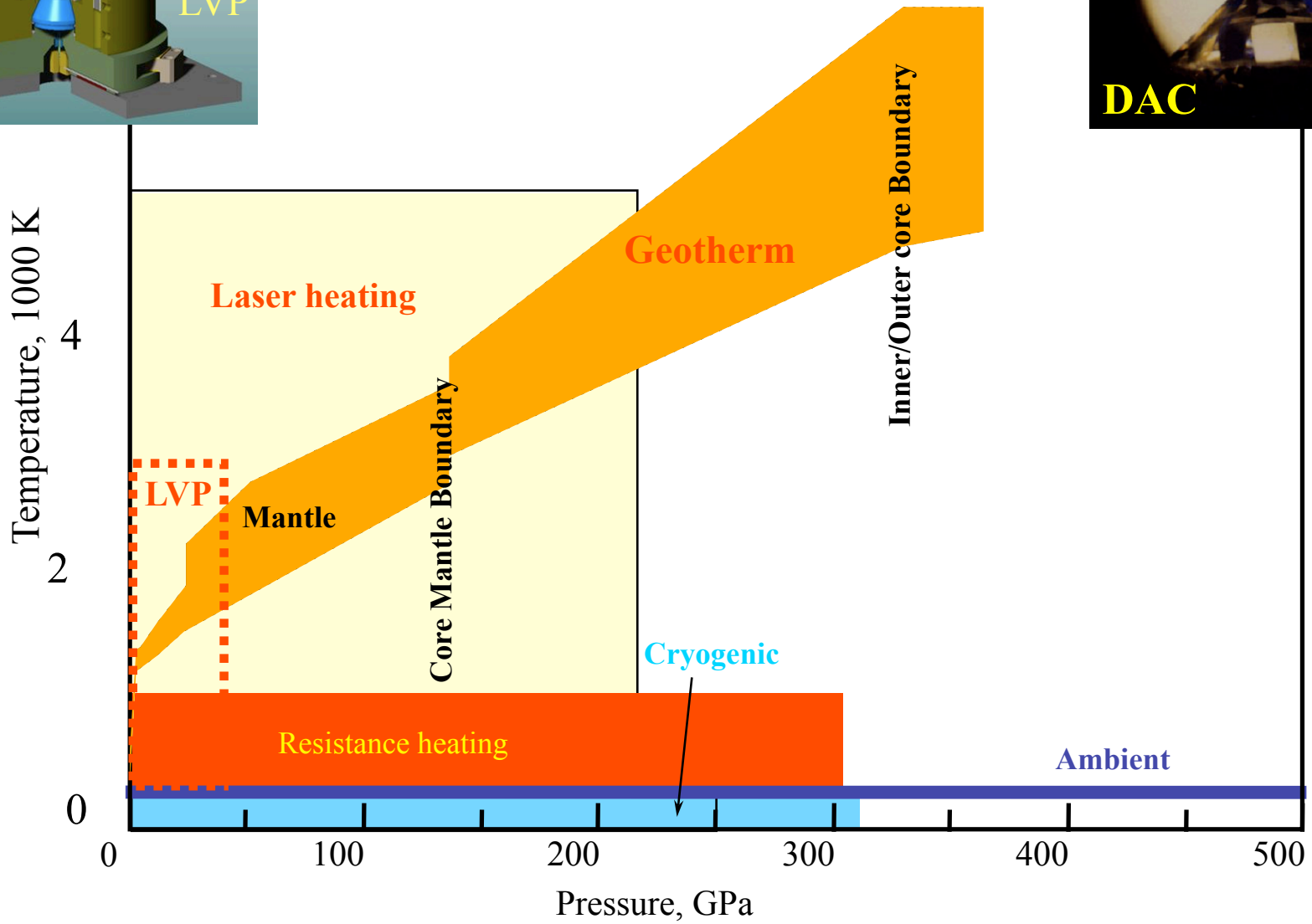

Earth's Interior (simplified)

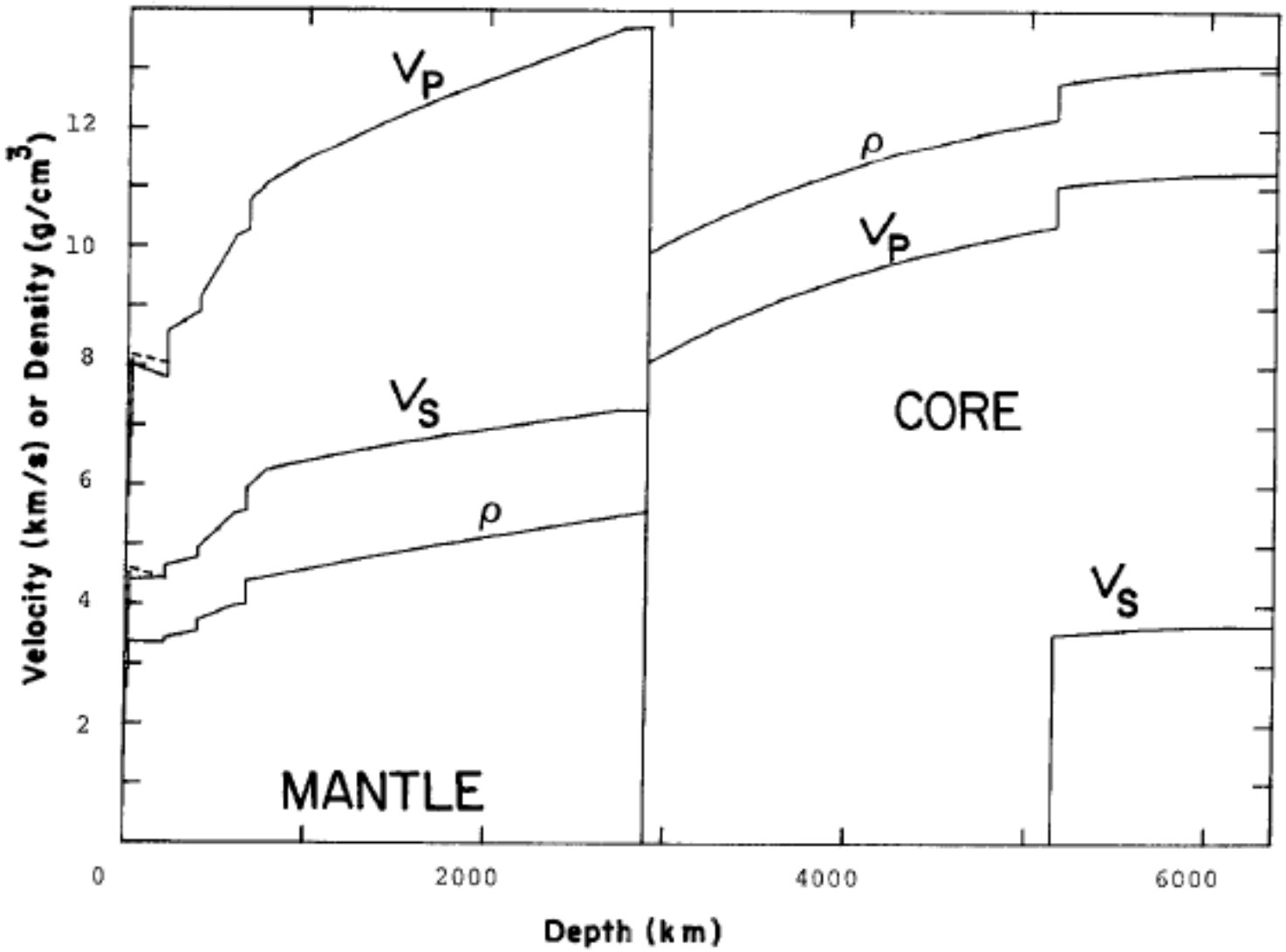

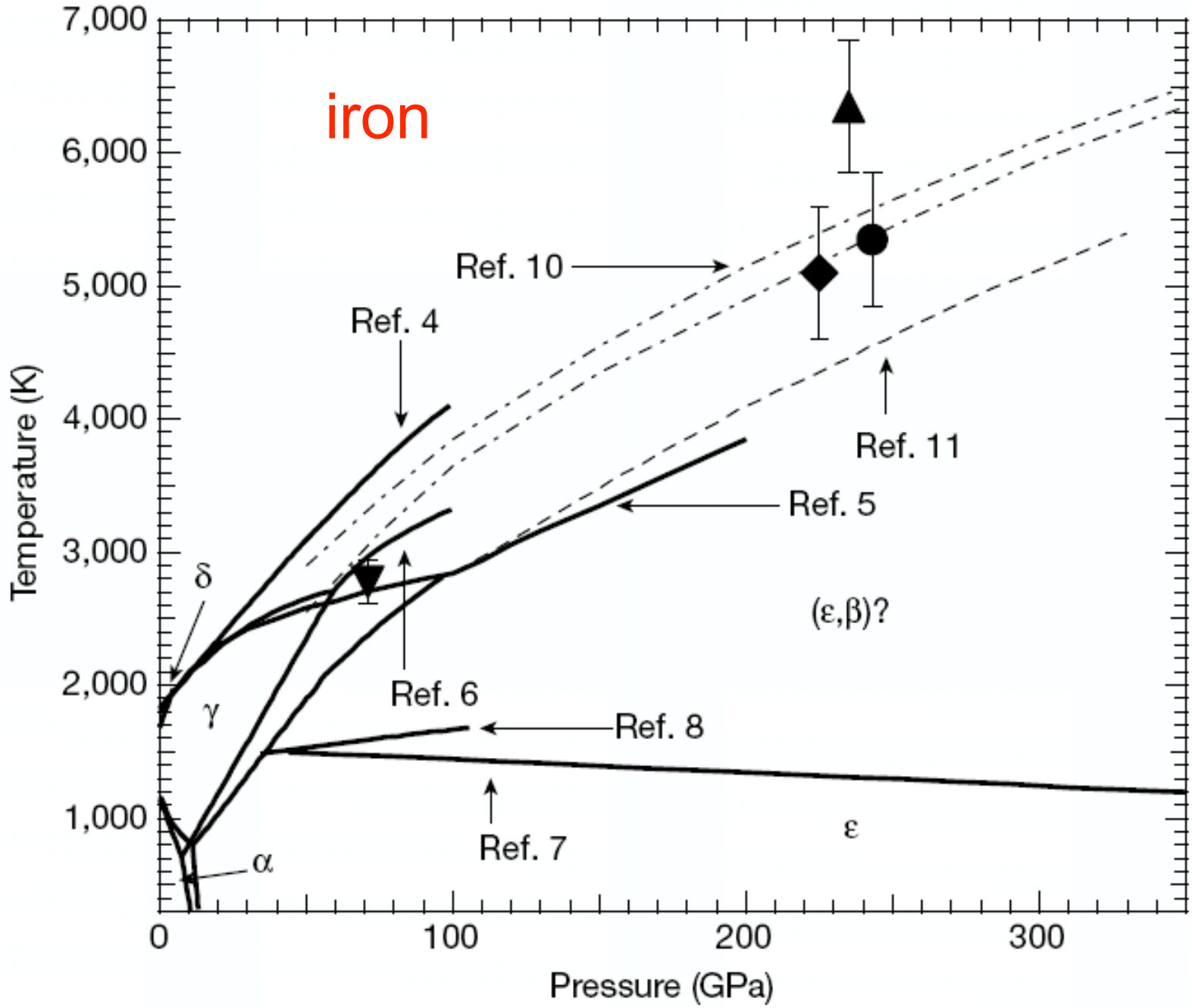

Nguyen and Holmes, Nature, 427, 339, 2004

Nuclear resonant in a laser-heated diamond cell

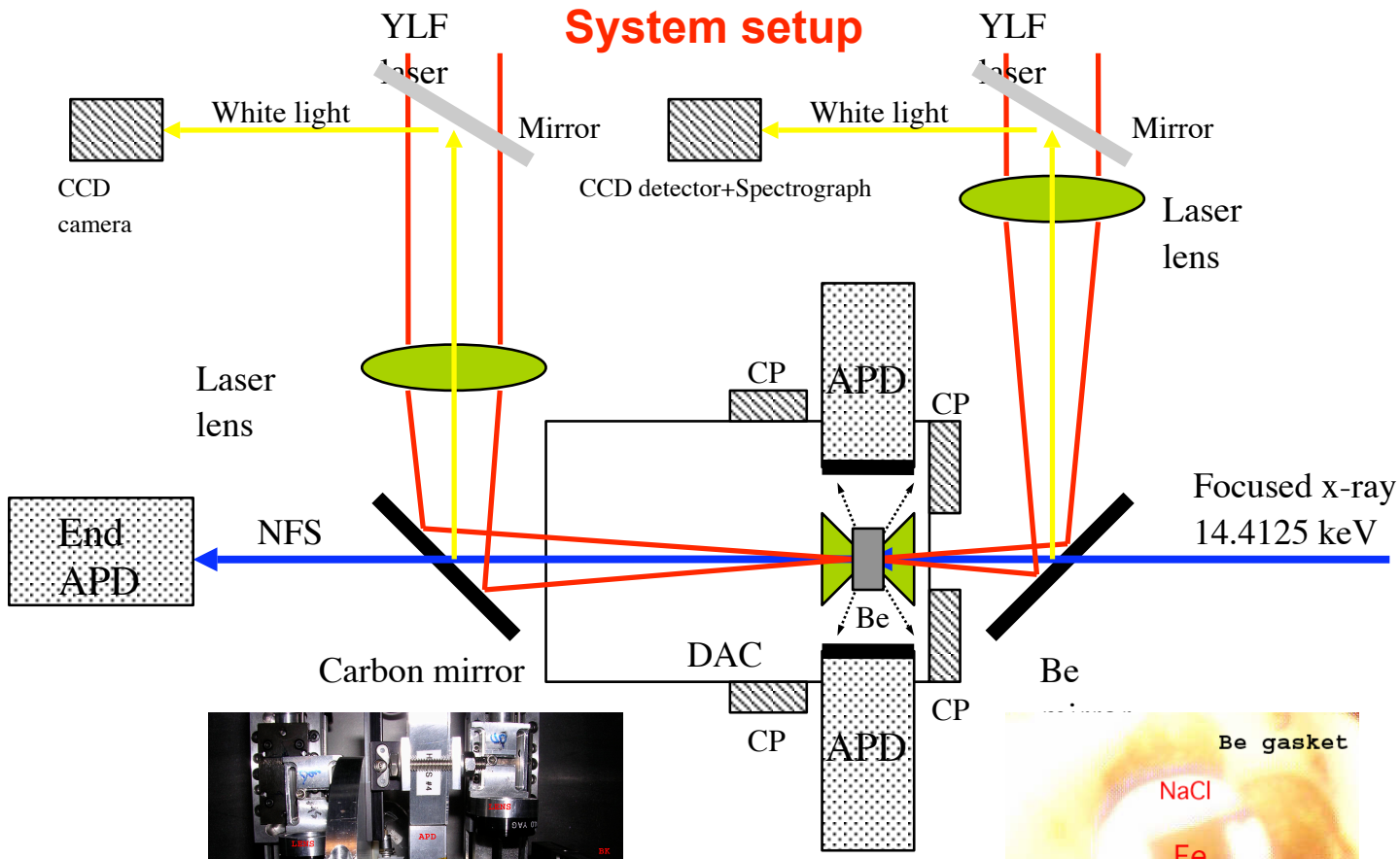

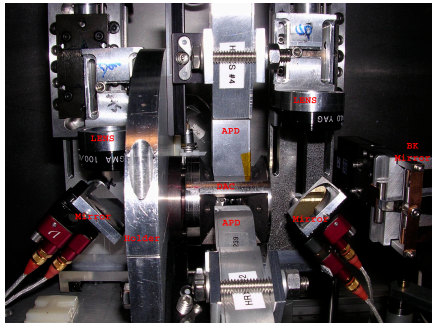

System setup
XOR-3, APS
(Lin et al., in press)

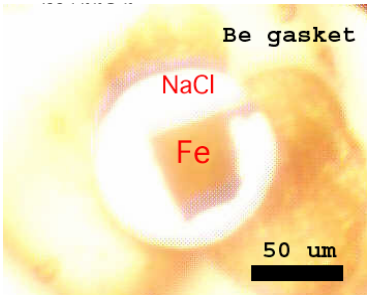

Fe sample in a diamond cell

Temperature: spectroradiometry and detailed balance principle of the energy spectra
Pressure: ruby pressure scale, EoS of NaCl, and thermal EoS of hcp-Fe

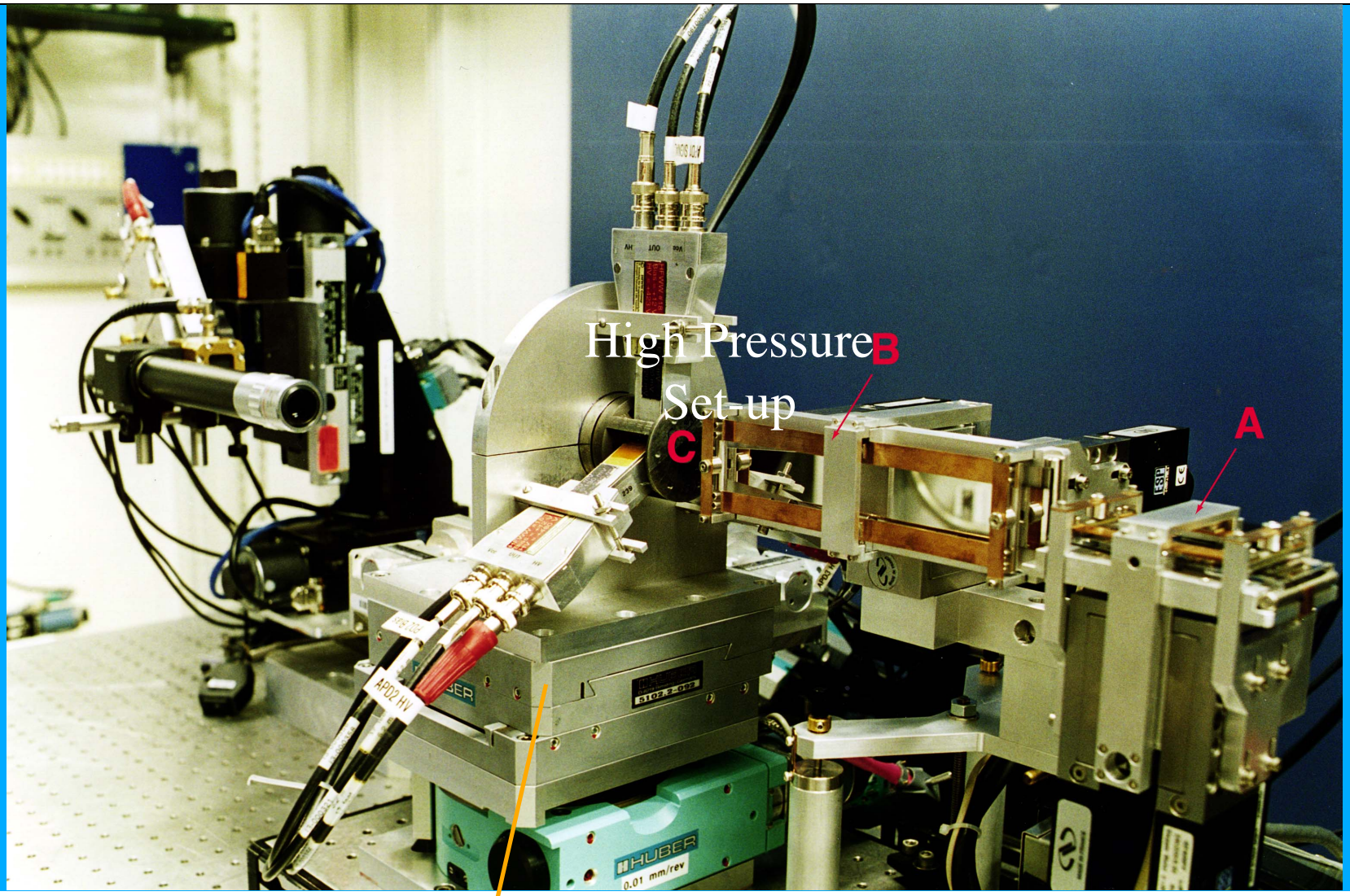
High Pressure
Set-up
A
B
C
HUBER
0.01 mm/rev
APD2 HV

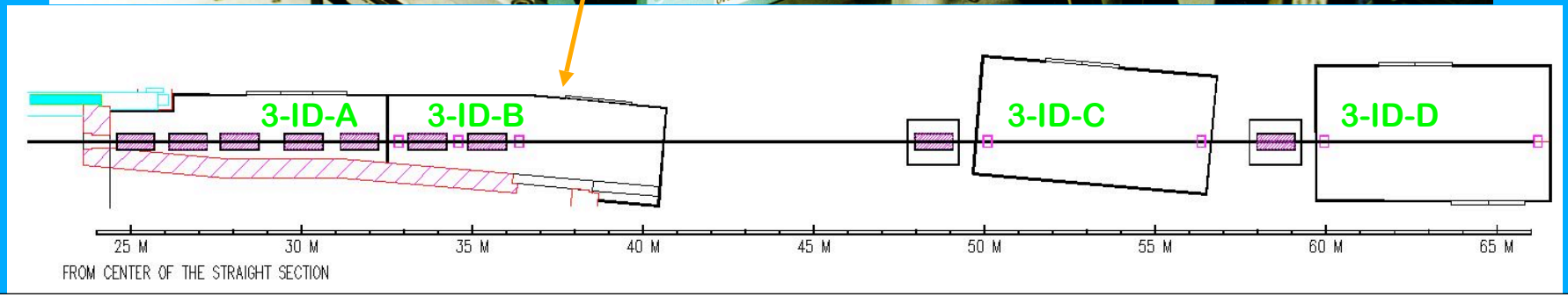
3-ID-A
3-ID-B
3-ID-C
3-ID-D
25 M
30 M
35 M
40 M
45 M
50 M
55 M
60 M
65 M
FROM CENTER OF THE STRAIGHT SECTION

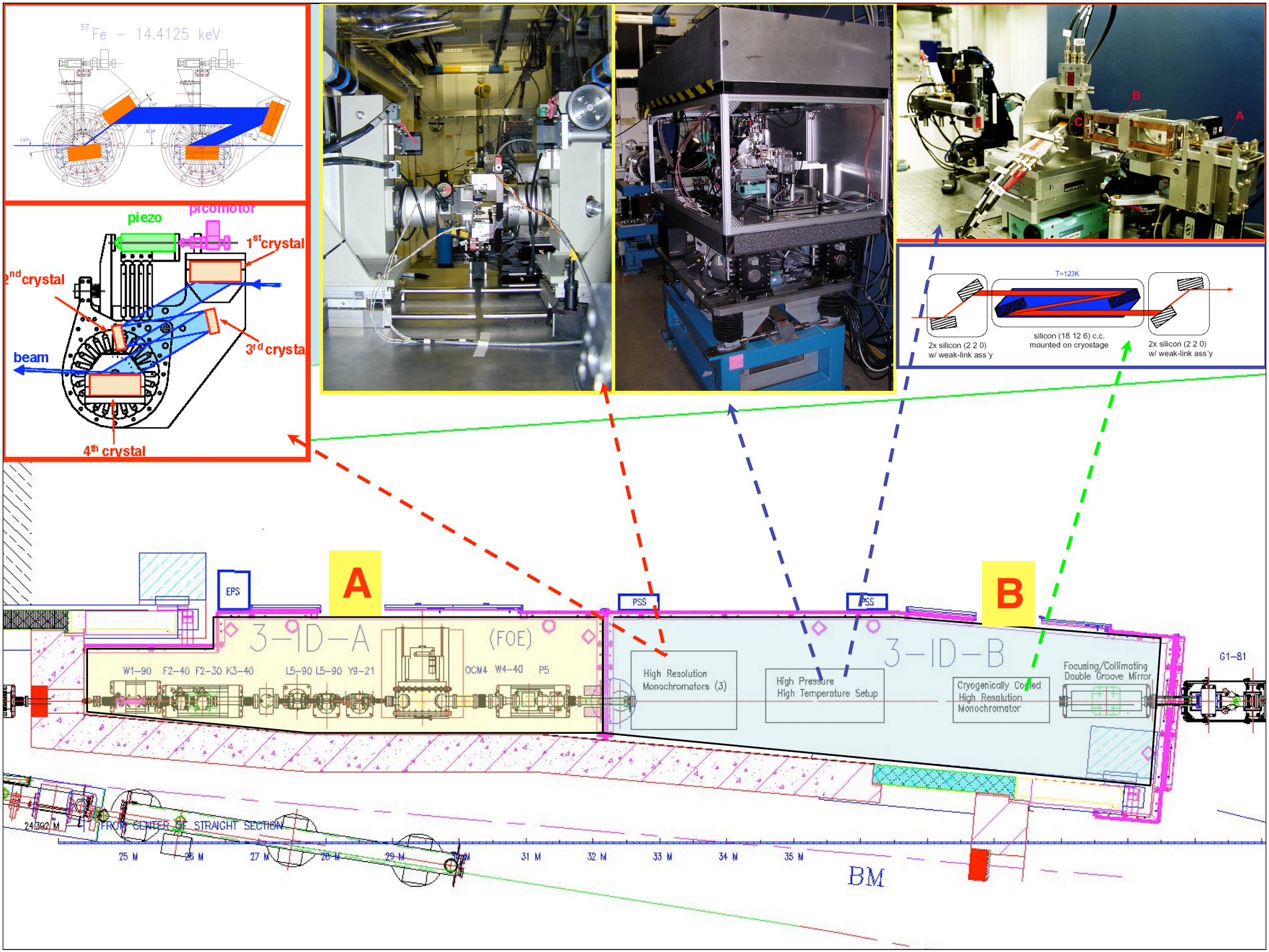
57Fe – 14.4125 keV
piezo
picomotor
1st crystal
2nd crystal
3rd crystal
beam
4th crystal
A
B
C
T=123K
2x silicon (2 2 0)
w/ weak-link ass'y
silicon (18 12 6) c.c.
mounted on cryostage
2x silicon (2 2 0)
w/ weak-link ass'y
EPS
PSS
PSS
3-ID-A
(FOE)
W1-90 F2-40 F2-30 K3-40
L5-90 L5-90 Y9-21
OCM4 W4-40 P5
3-ID-B
High Resolution
Monochromators (3)
High Pressure
High Temperature Setup
Cryogenically Cooled
High Resolution
Monochromator
Focusing/Collimating
Double Groove Mirror
G1-81
24392 M
FROM CENTER OF STRAIGHT SECTION
25 M
26 M
27 M
28 M
29 M
31 M
32 M
33 M
34 M
35 M
BM

Determination of Debye velocity of sound from phonon density of states

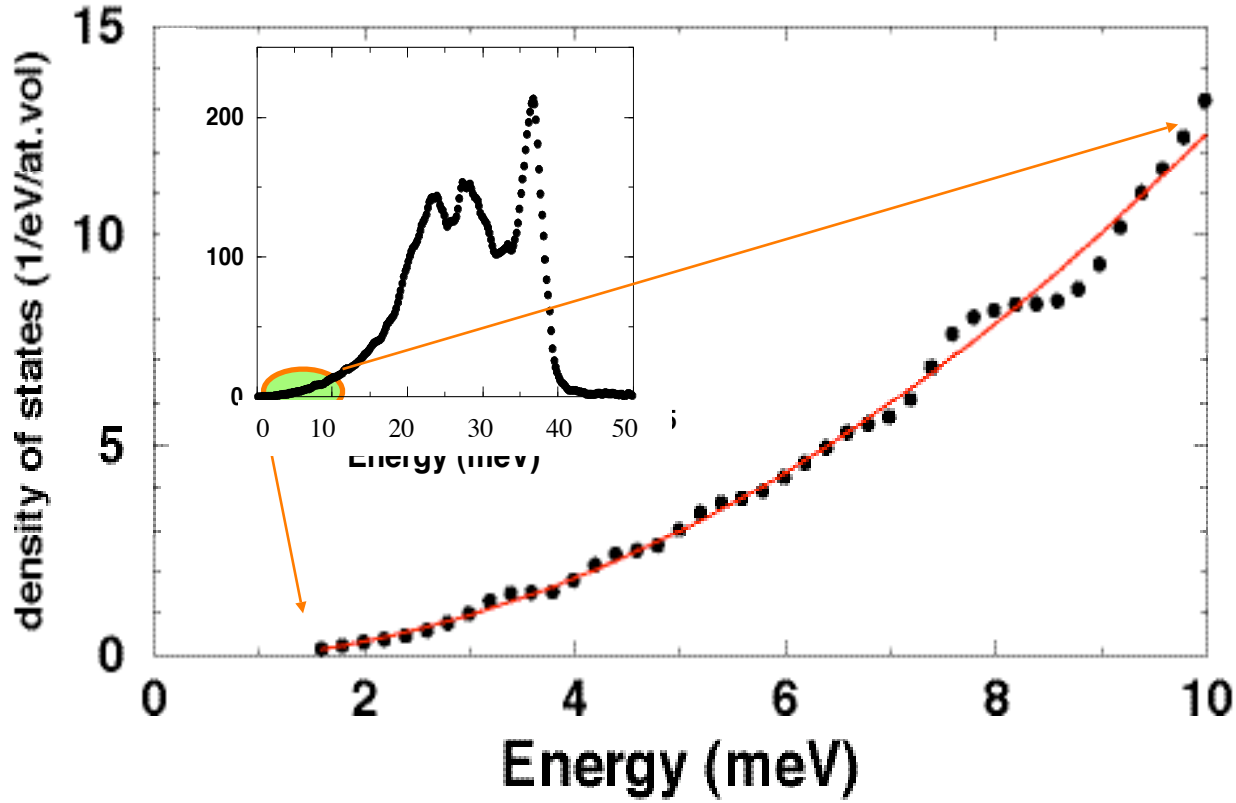

$$D(E) = \frac{V}{2\pi h^3 c_s^3} E^2$$

PHYSICAL REVIEW B **67**, 094304 (2003)

Measuring velocity of sound with nuclear resonant inelastic x-ray scattering

Michael Y. Hu,[1,*] Wolfgang Sturhahn,[2] Thomas S. Toellner,[2] Philip D. Mannheim,[3] Dennis E. Brown,[4] Jiyong Zhao,[2] and E. Ercan Alp[2]

Speed of sound of Iron at high pressure/temperatures

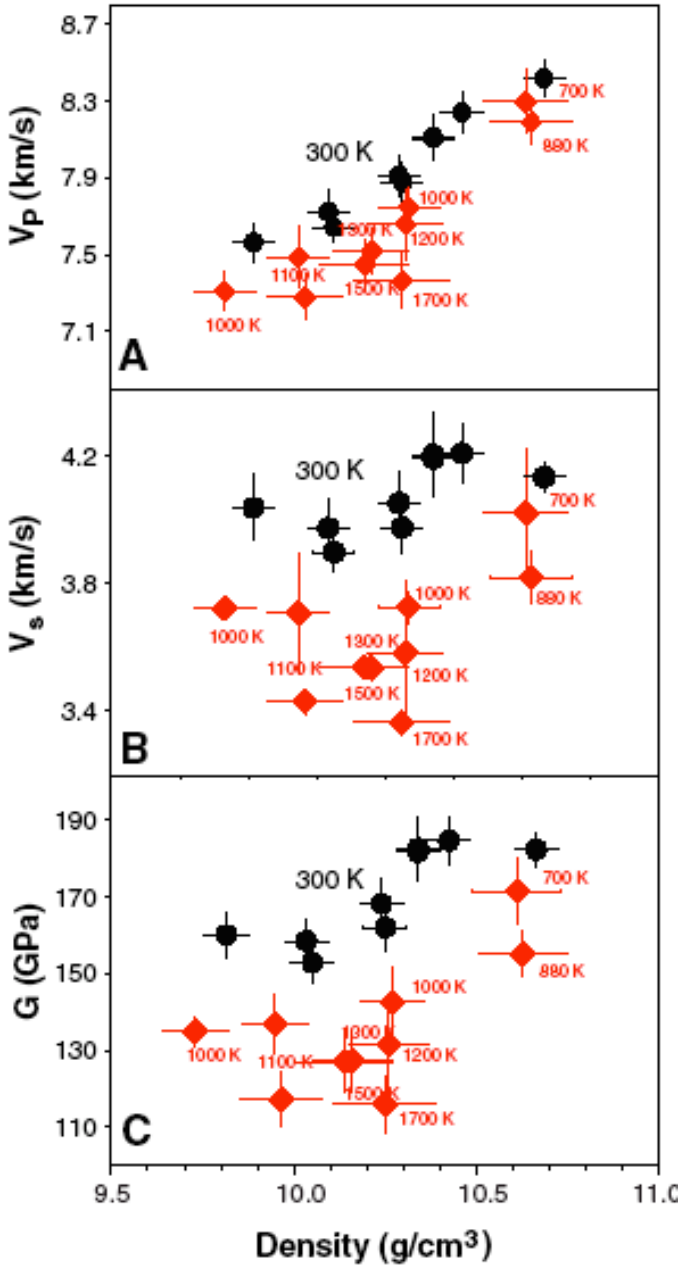

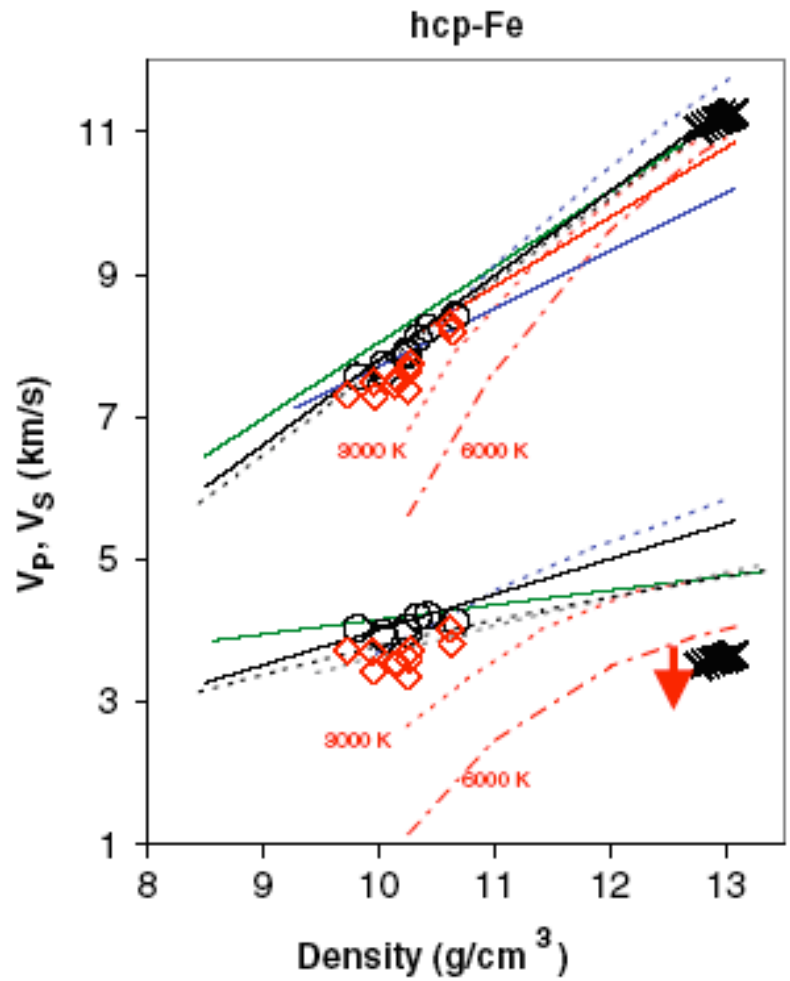

Lin, Sturhahn, Zhao, Shen, Mao, Hemley, Science, 308, (2005) 1892

Phonon density of states of iron under high pressure

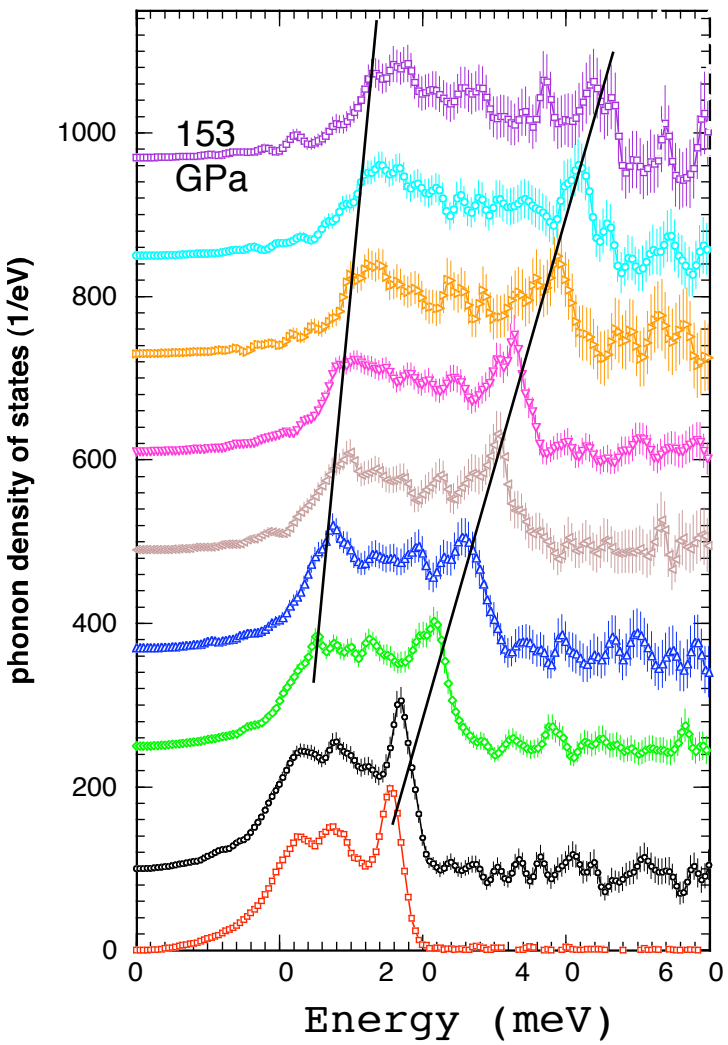

H.K. Mao, et al, Science, 292 (2001) 914

Magneto-elastic coupling in FeO under high pressure

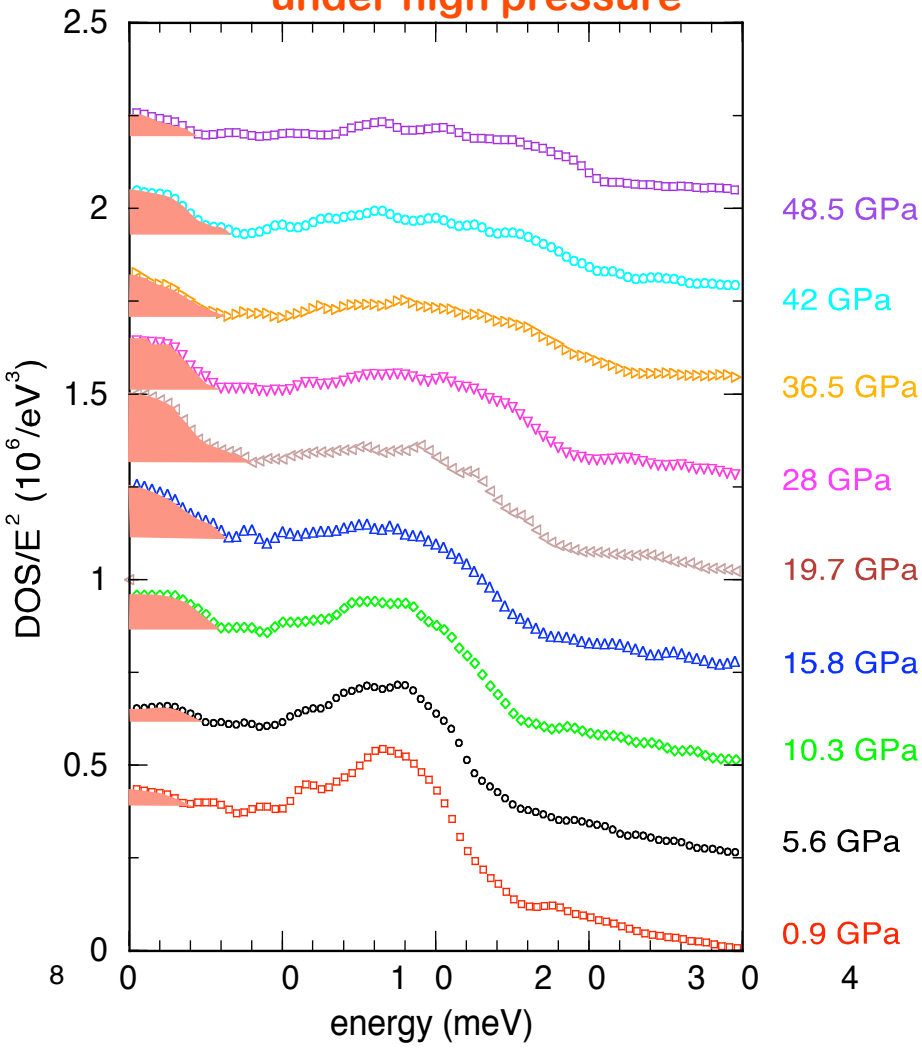

V. Struzhkin, et al, PRL 87 (2001) 255501

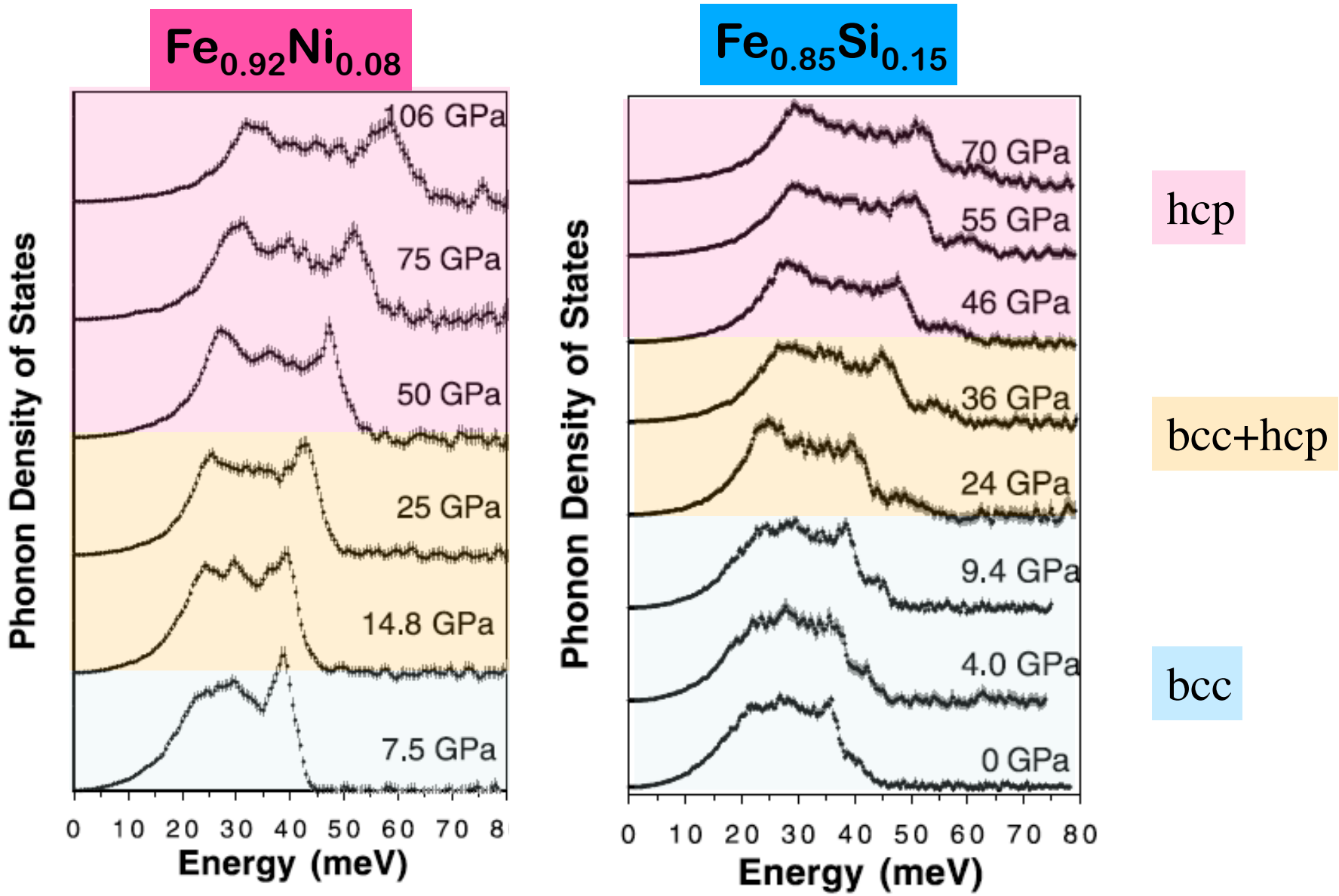

J.F. Lin, et al, Geophys. Res. Lett., 30 (2003) 2112

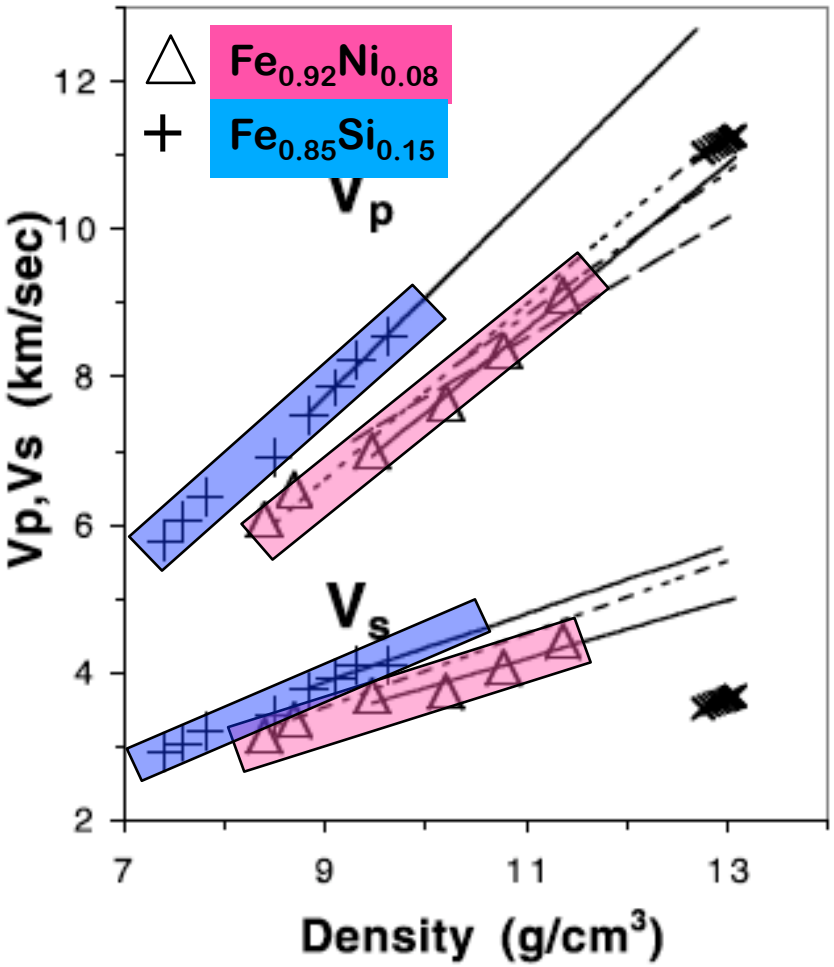

$$\frac{K_S}{\rho} = V_P^2 - \frac{4}{3}V_S^2$$

$$\frac{G}{\rho} = V_S^2$$

$$\frac{3}{V_D^3} = \frac{1}{V_P^3} + \frac{2}{V_S^3}$$

K_S : adiabatic bulk modulus
G : shear modulus
V_P : compression wave velocity
V_S : shear wave velocity
V_D : Debye sound velocity
P : density

J. F. Lin, W. Sturhahn, et al

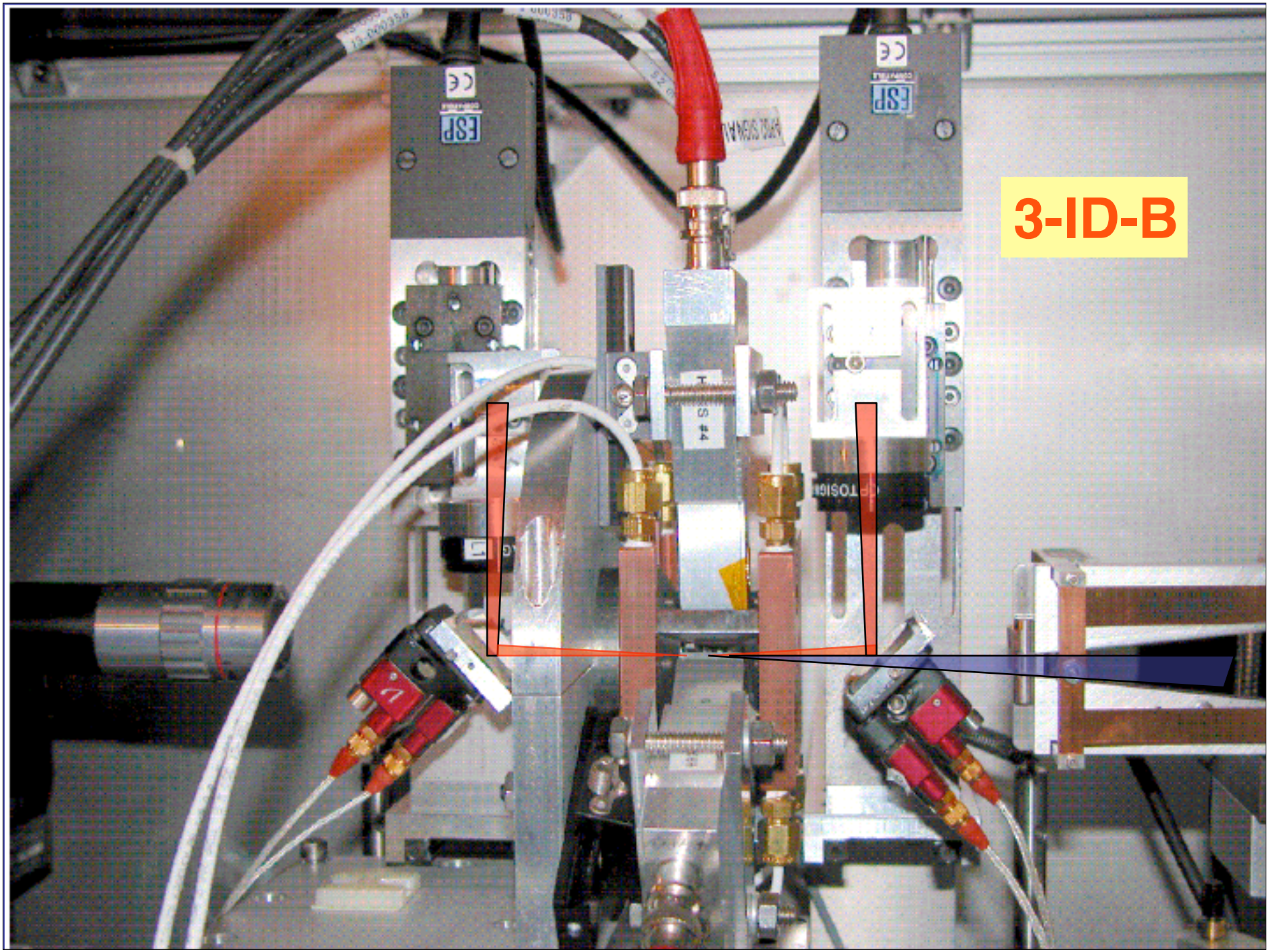
3-ID-B

Classical thermodynamical quantities and phonon density of states

In the Harmonic Approximation (i.e. interatomic forces are linear in atomic displacement) the thermodynamic functions are additive functions of the normal mode frequencies. Thus, they are expressible as averages over frequency distribution function, **g**(ω), or phonon density of states.

1.Helmholtz Free Energy

$$F_V = 3RNk_BT\int \ln\left\{2\sinh\left(\frac{\hbar\omega}{k_BT}\right)\right\}\mathbf{g}(\omega)\mathbf{d}\omega$$

2.Vibrational Energy

$$F_V = 3RN\frac{\hbar}{2}\int \ln\left\{\coth\left(\frac{\hbar\omega}{k_BT}\right)\right\}\omega\cdot\mathbf{g}(\omega)\mathbf{d}\omega$$

3. Specific heat

$$C_P = 3RNk_B\int\left(\frac{\hbar\omega}{2k_BT}\right)^2 \operatorname{csch}\left(\frac{\hbar\omega}{k_BT}\right)\mathbf{g}(\omega)\mathbf{d}\omega$$

4.Entropy

$$S = 3RNk_B\int\left\{\left(\frac{\hbar\omega}{2k_BT}\right)\coth\left(\frac{\hbar\omega}{k_BT}\right) - \ln\left[2\sinh\left(\frac{\hbar\omega}{k_BT}\right)\right]\right\}\mathbf{g}(\omega)\mathbf{d}\omega$$

What do Nuclear Resonant Spectroscopy need?

- Bunch-to-bunch separation > 150 nsec up to 300 nsec
- clean bunches (purity < 10^{-10})
- lower emittance / top-up
- Brilliance >> 10^{20}, 6-30 keV
- Higher current / bunch (30 mA/bunch, 80 ps or longer)

What does Nuclear Resonant Spectroscopy deliver in return ?

- Phonon dynamics via NRIXS
  - Monolayers, buried layers, spin dynamics
  - Nanoscale materials
  - Dynamics at pressures exceeding 2 Mbar, 3000 K
  - Dilute systems to extend the applicability of the method
  - Applications in astrophysics, geophysics, biophysics, and condensed matter & materials physics

- Structural, magnetic and electronic structure via Synchrotron Mössbauer Spectroscopy
  - Element and isotope selective magnetometry
  - Melting temperature at high pressures
  - In-situ oxidation/reduction kinetics for environmental problems
  - Mössbauer microscope

- Optics development
  - Monochromators, new alternative crystals,

- Novel ideas
  - X-ray wavelength standards

BOSON PEAK: $Fe_{1-x}Tb_x$

J. Phys.: Condens. Matter 16 (2004) S379–S393

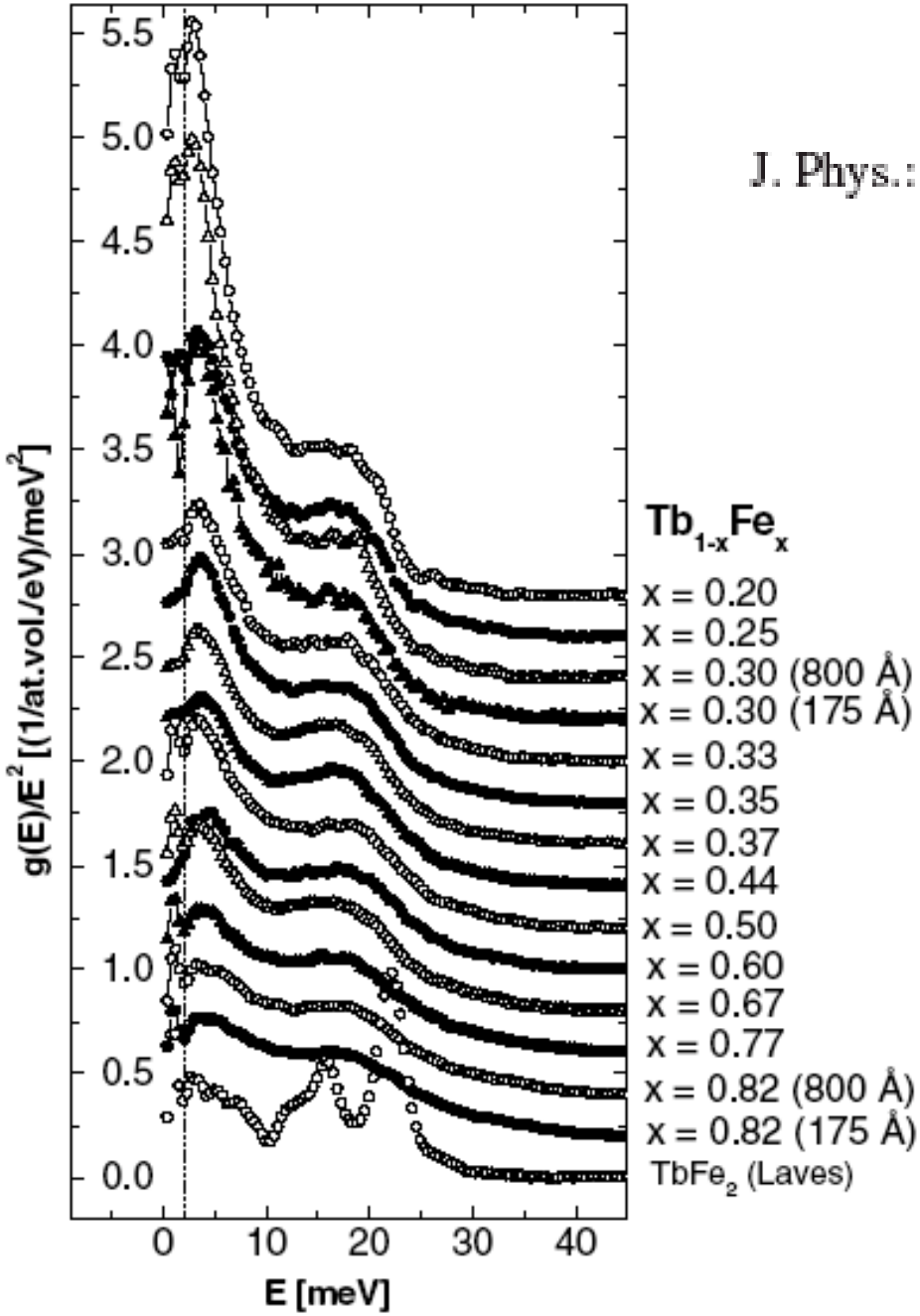

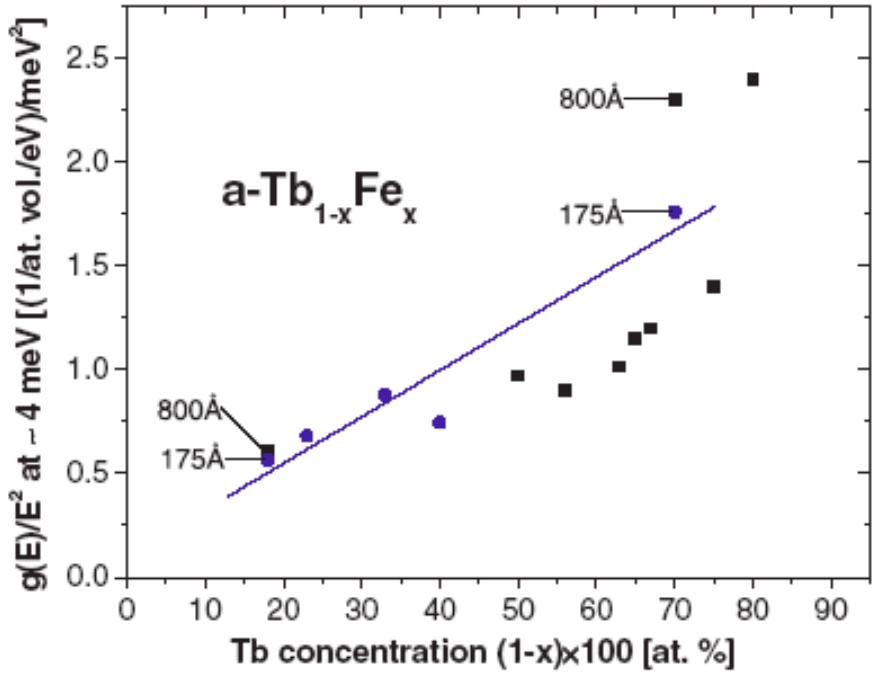

BOSON PEAK : $Fe_{1-x}Mg_x$

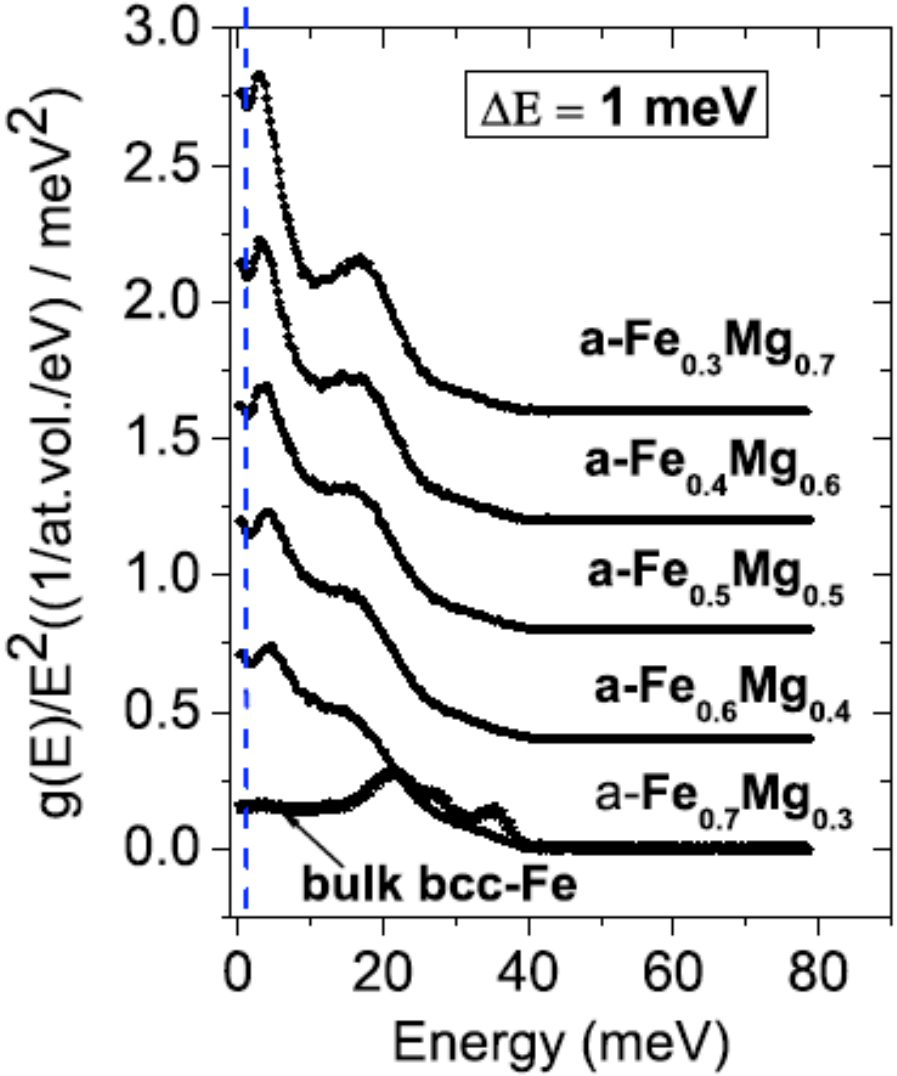

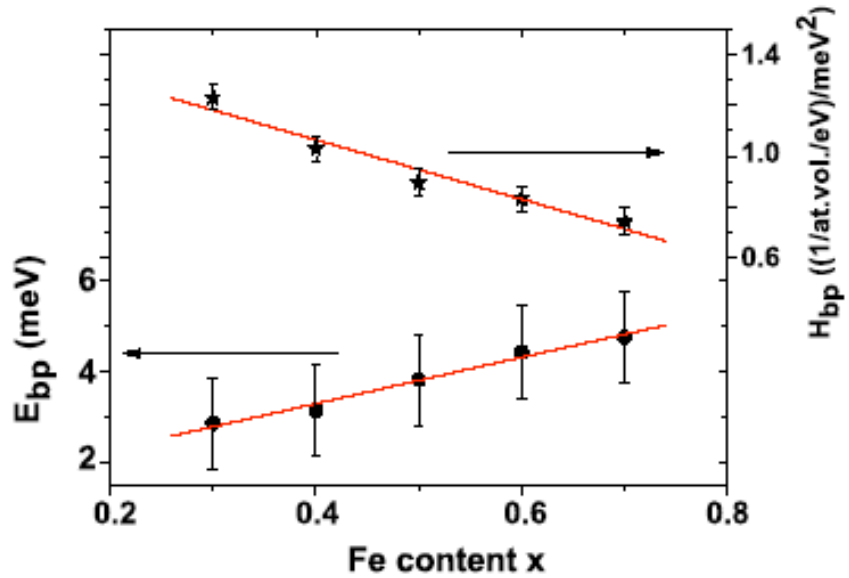

Phonon density of states of iron under high pressure

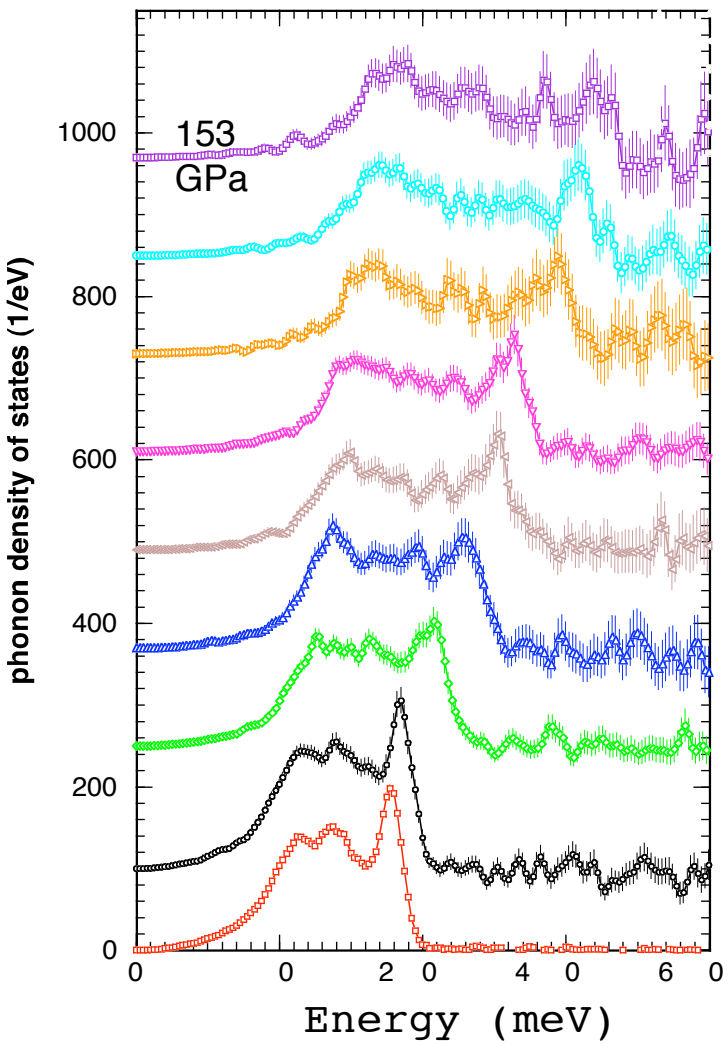

H.K. Mao, et al, Science, 292 (2001) 914

Magneto-elastic coupling in FeO under high pressure

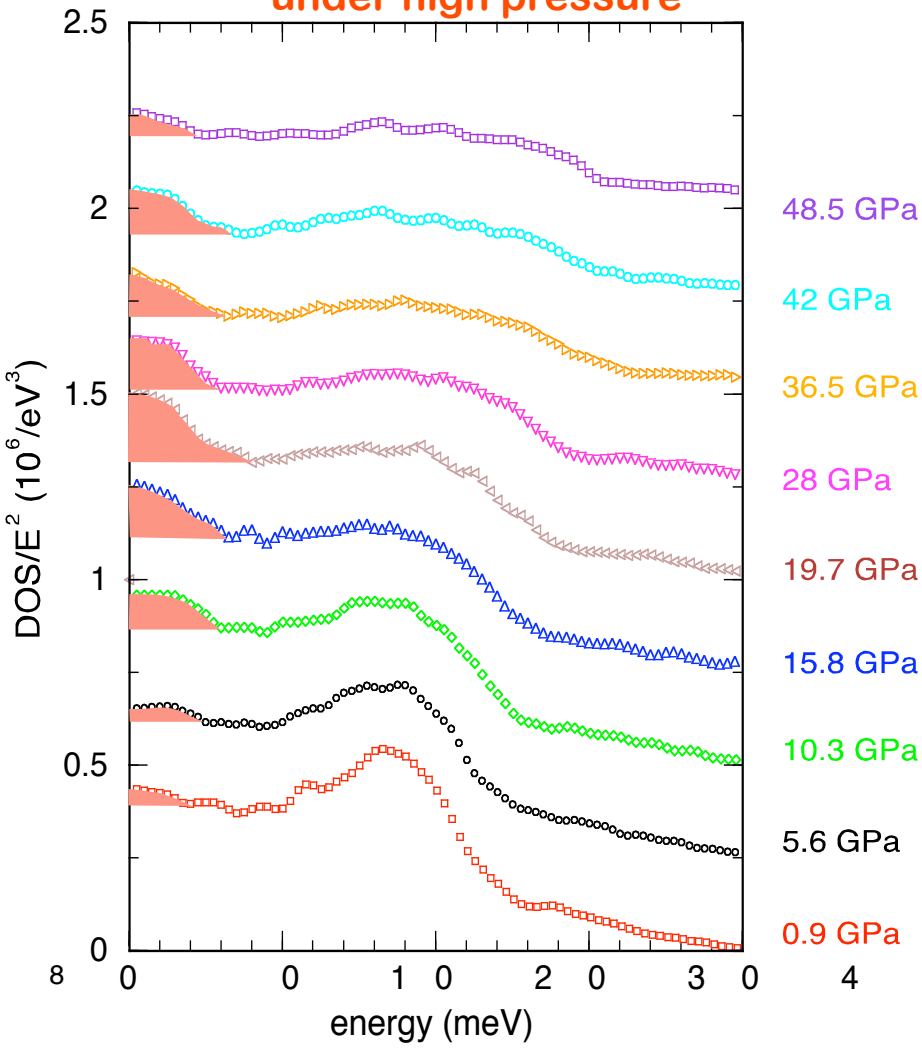

V. Struzhkin, et al, PRL 87 (2001) 255501

Werner Keune, Duisburg
Phonon confinement in multilayers

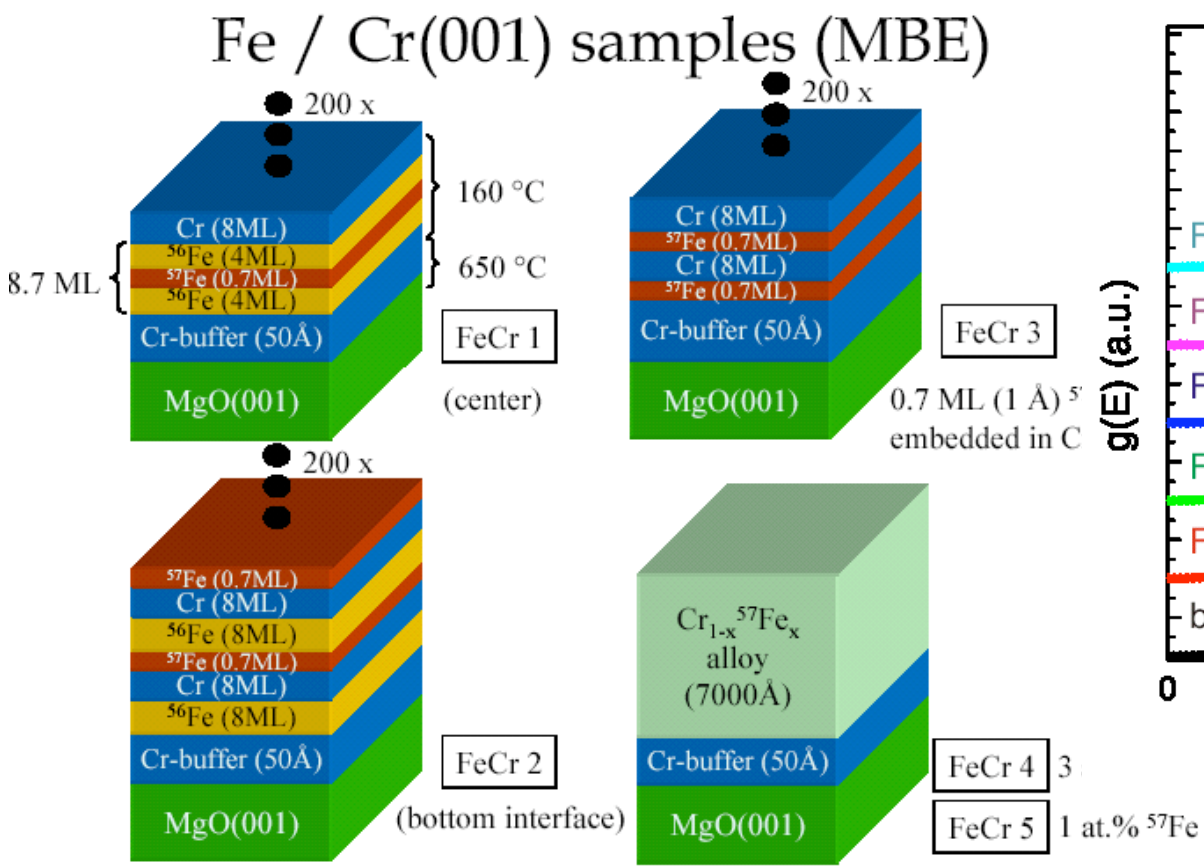

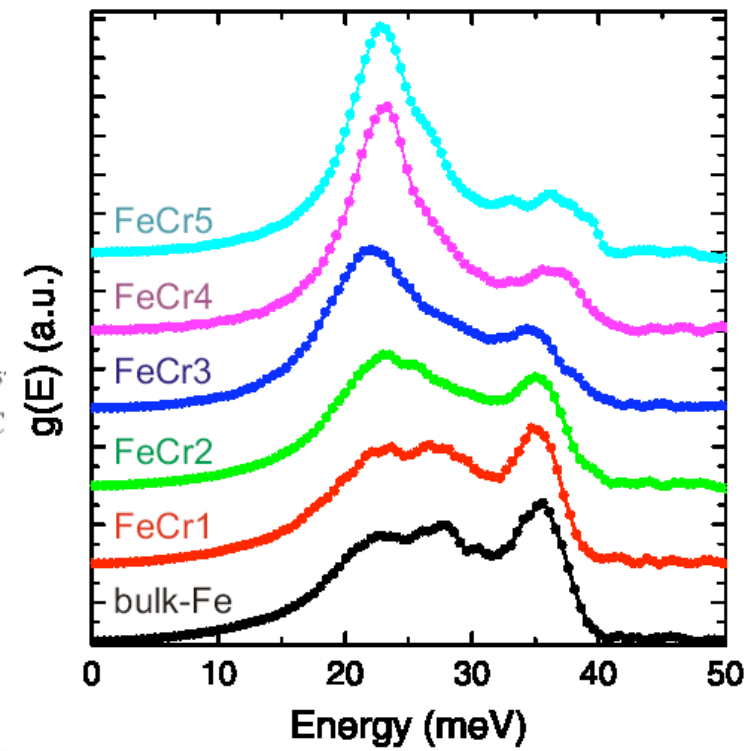

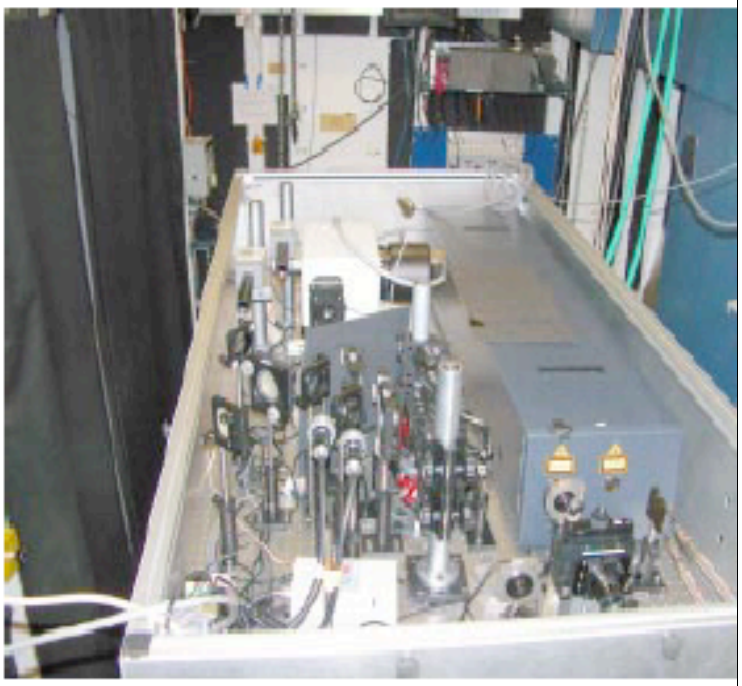

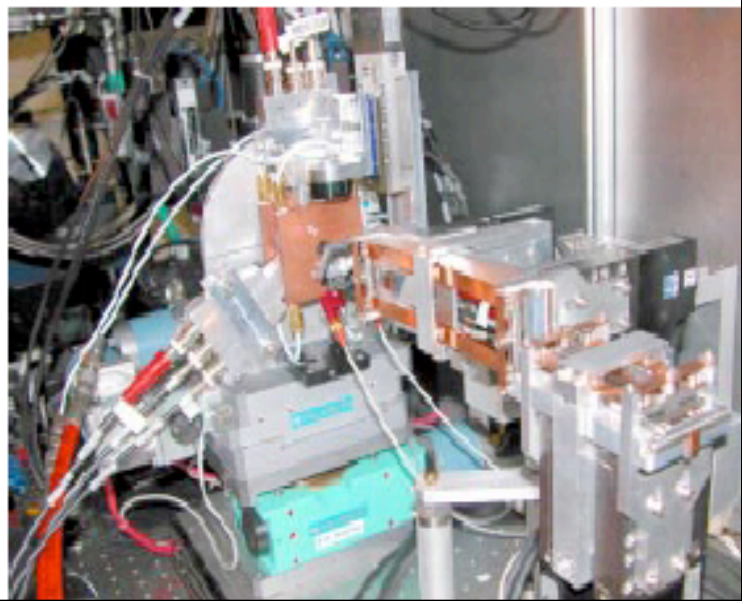

Sn-metal: (alfa_Sn: diamond (T>287 K), beta_Sn: bct with 4 at/unit cell, P > 9GPa: 2 at/unit cell, P > 45GPa bcc

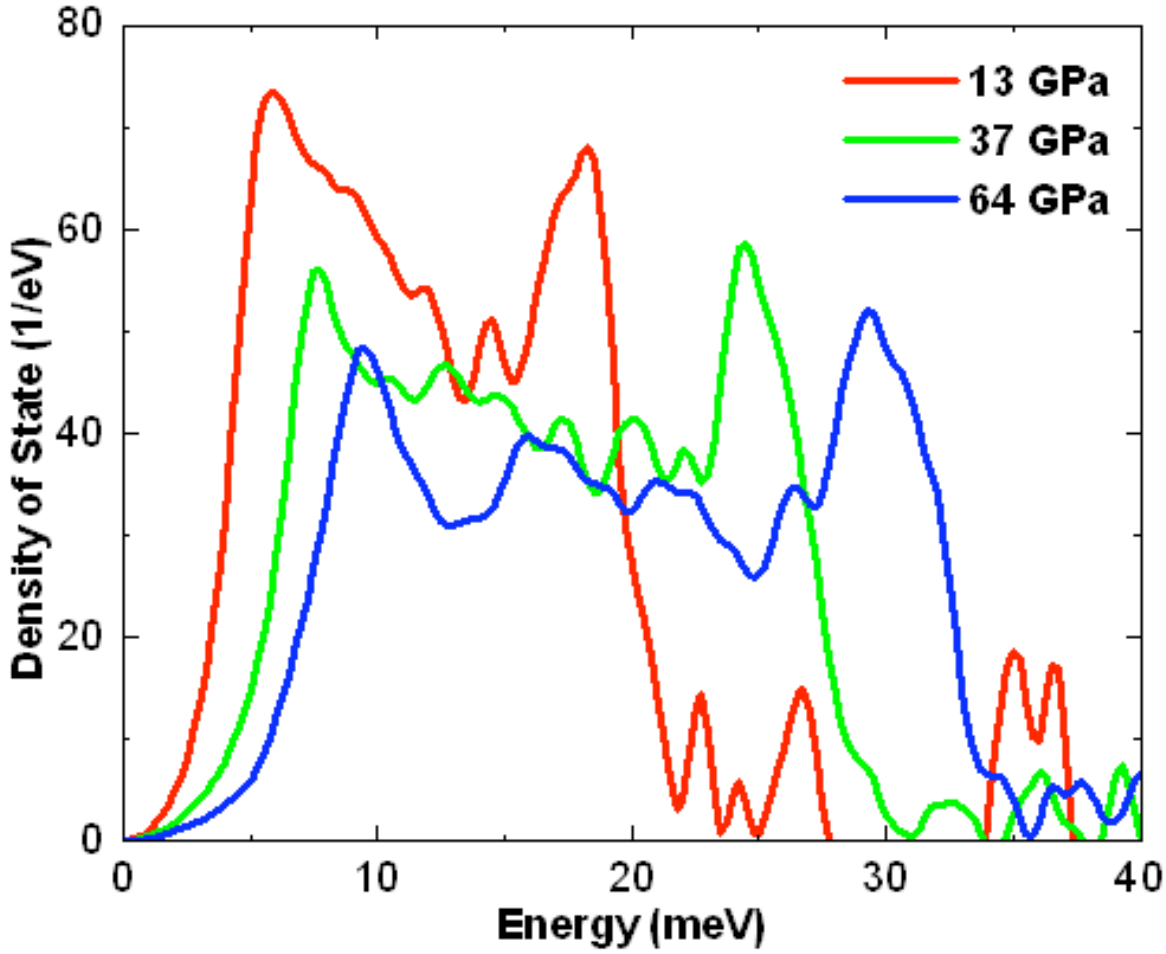

Elizabeth Tanis, et al, Poster P41

Part 4

X-Ray Raman Scattering
X-Ray Emission Spectroscopy
RIXS
Compton Scattering

A SHORT SUMMARY OF CURRENT INELASTIC X-RAY SCATTERING TECHNIQUES

Technique	Source of interaction	Typical resolution	Deetection method	Location at the APS
Momentum-resolved, high energy resolution IXS: HERIX	Collective excitations of atoms, ions, molecules, PHONONS	1-3 meV	Back-scattering, curved and diced crystal analyzer	3-ID
Momentum-resolved, medium energy resolution resonant IXS: MERIX	Valence electrons near Fermi level	100-500 meV	Near-back-scattering, curved and diced crystal analyzer	9-ID, 12-ID, 33-ID
Momentum-integrated, nuclear resonant IXS: NRIXS	Collective excitations monitored through a nuclear resonance	0.5-2 meV	Nano-second time resolved detectors monitoring nuclear level decay	3-ID, 16-ID
High resolution Compton scattering: CS	Core and valence electrons	1 eV	Triple Laue crystal analyzer, PSD detector	
Magnetic Compton scattering: MCS	Spin polarized electrons	100 eV	Solid state detector	11-ID
X-ray Raman spectroscopy: XRS	Core electron excitations of low-Z elements	1 eV	Back-scattering curved flat analyzers	13-ID, 16-ID
X-ray emission spectroscopy: XES	X-ray fluorescence by incident photons: photon-in/photon-out	0.5 eV	Back-scattering curved flat analyzers	10-ID
Soft-X-ray IXS : PEEM	x-ray induced photoemission: photon-in/electron-out	5 meV	Electron spectrometer	4-ID

What is it ?

- **High Resolution Inelastic X-Ray Scattering (IXS)**
  - Scattering from spatially localized or dispersed collective atomic or ionic excitations like PHONONS.
  - **Energy range: 15-30 keV,**
  - **Incident beam: monochromatic to 1 meV level, tunable over several eV,**
  - **Scattered beam: Incoherent, polychromatic over several hundred meV**
  - **Analyzer: Bent, diced or Si, crystal analyzer, temperature stabilized to 10 mK**
  - **Energy Resolution : ~ 1-2 meV**
  - **Momentum transfer: Relevant to distinguish localized versus spatially dispersed excitations, sound velocity, phonon dispersion curves**
- **Main Features:**
  - **Allows determination of phonon dispersion relations without any kinematic limitation that is suffered by neutrons, works for most elements, liquids and solid alike, suitable for extreme conditions**

What is it ?

- **Nuclear Resonant Inelastic X-Ray Scattering (NRIXS, NIS,NRVS)**
  - Scattering from PHONONS, detected via exciting a low-lying nuclear resonance
  - **Scattering from phonons**
  - **Energy range: 6-100 keV,**
  - **Incident beam: monochromatic to 1 meV level, tunable over several eV,**
  - **Scattered beam: Incoherent, polychromatic over several hundred meV**
  - **Analyzer: Mössbauer resonant nuclei embedded in the sample, nsec time resolved Avalanche Photodiode Detector (APD)**
  - **Energy Resolution : ~ 0.1-10 meV**
  - **Momentum transfer: A momentum integrated method, measuring displacements along the incident beam direction**
- **Main Features:**
  - **Allows determination of phonon density of states, from which many thermodynamic functions can be deduced, element and isotope selective, can be used in crystalline, amorphous materials alike, thin films, buried layers, extreme environments**

What is it ?

- **X-ray Raman Scattering (XRS)**:
  - Indirect emission of photons from inner core energy levels via absorption of the incident photon, when the transferred energy matches the energy level between core levels. XRS enables measurement of light element XANES or EXAFS using hard x-rays.
  - **Energy range: 6-10 keV,**
  - **Incident beam: monochromatic, tunable over 1000 eV,**
  - **Scattered beam: Incoherent, polychromatic,**
  - **Analyzer: Bent, undiced Si or Ge crystal analyzer,**
  - **Energy Resolution : ~ 1 eV**
  - **Momentum transfer: Relevant to distinguish dipole transitions from higher order terms**
- **Main Features:**
  - **Allows determination of XANES or EXAFS for low Z-elements in mixtures or complex environments**

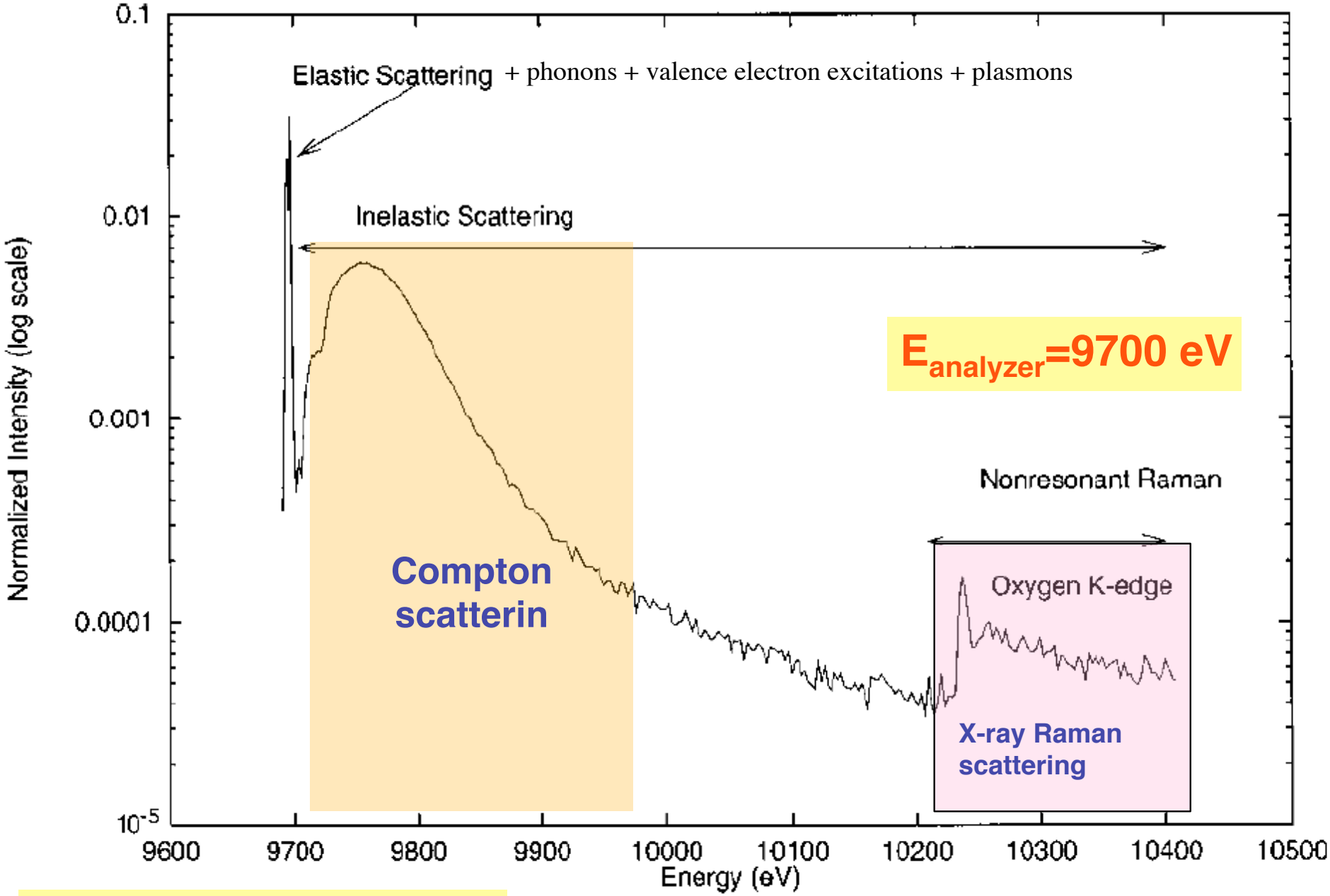

(D.T. Bowron et al, Phys. Rev. B 62 R9223)

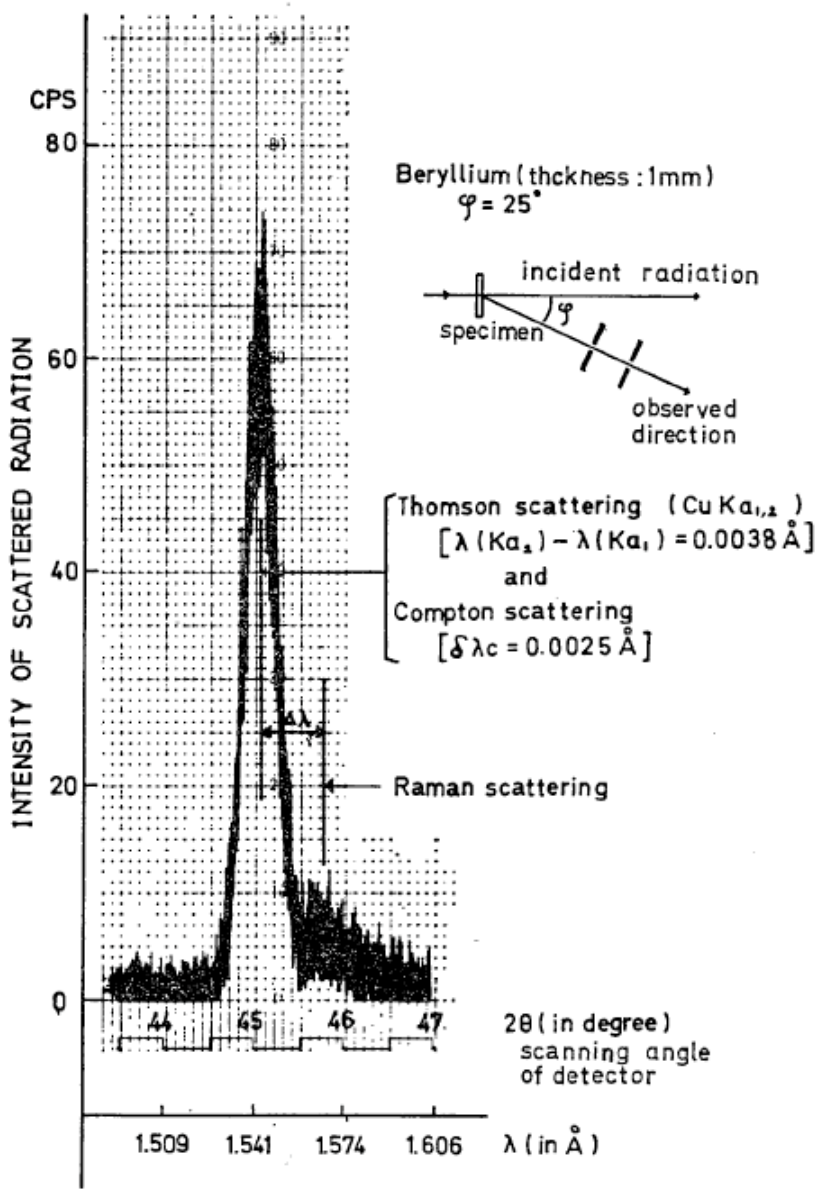

J. PHYS. SOC. JAPAN **21** (1966) 2087

X-Ray Raman Scattering

Tadasu SUZUKI

Faculty of Science and Technology, Sophia University, Chiyoda-ku, Kioi-cho 7, Tokyo.

(Received July 30, 1966)

In order to verify this effect experimentally, beryllium, boron and carbon were examined. Incident X-rays were generated from a rotating copper target. This X-ray source was operated at 50 kV and 80 mA. The usual X-ray diffractomerer with a LiF single crystal cut parallel to (100) plane was used for the energy analysis. One of the results obtained for beryllium is shown in Fig. 1. When the scattering angle is increased, the peak of Compton scattering shifts to the longer wave length side and overlaps the Raman scattering, which seems scarcely to change its position. Quantitative measurements were performed by a fixed-time counting method. The observed wave length differences ($\Delta\lambda$) are $0.02_3 A$, $0.03_8 A$ and $0.05_8 A$ for beryllium, boron and carbon and correspond to 115eV, 180eV and 290eV, respectively. These values are nearly equal to the 1s electron energies of each atom.

$$H = H_1 + H_2$$

$$H = -\frac{e}{m}\vec{p}\cdot\vec{A} + \frac{e^2}{m}\vec{A}^2$$

$$w = \frac{2\pi}{h}\left|\left\langle f, j\middle|H_1(2) + H_2(1)\middle|0, i\right\rangle\right|^2 * \delta\left(E_f - E_i - h\left(\nu_i - \nu_j\right)\right)$$

$H_1(2)$: Linear in A, 2nd order perturbation
$H_2(1)$: Quadradtic in A, 1st order perturbation

$<f,j|$: Electronic final state $<f|$, photon final state $<j|$

$<f,j|$: Electronic initial state $<0|$, photon initial state $<i|$

In visible Raman scattering, $H_2(1) << H_1(2)$ because

$\lambda >> a$: wavelength longer than electron radius

This is also true for K-shell electrons of the high Z elements. However, for low-Z elements, $H_1(2)$ diminishes,

$$w = \frac{4\pi^3 e^4 h}{m^2 \nu_i \nu_j}\left(1+\cos^2\theta\right)\left|\left\langle f \;\left|e^{i\left(k_j - k_f\right)\cdot\vec{r}}\right|\; 0 \right\rangle\right|^2 * \delta\left(E_f - E_i - h\left(\nu_i - \nu_j\right)\right)$$

It can be shown that the transition probability can be reduced to:

$$w = \frac{64\pi^5 e^4 h}{m^2 c^2}\left(1+\cos^2\theta\right)\sin^2(\theta/2)\left|\left\langle i \;\left|\vec{r}\right|\; f \right\rangle\right|^2$$

This is similar to matrix elements describing the EXAFS equation, providing the formal basis that either experimental approaches can benefit from the same interpretation.

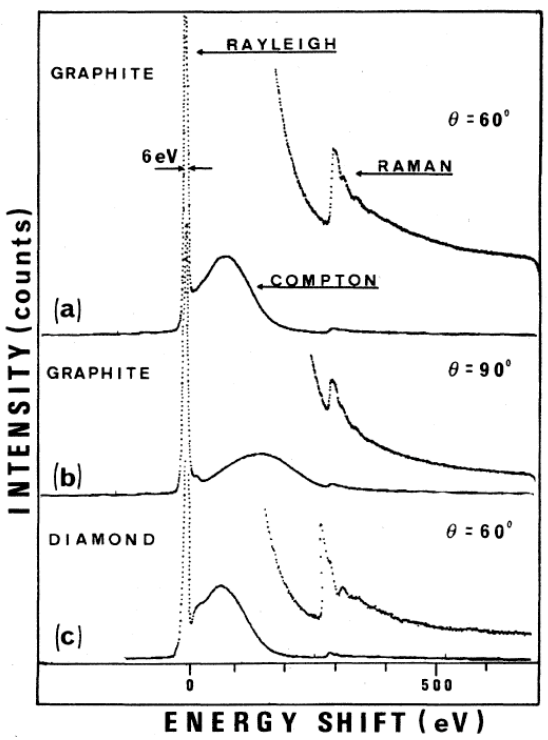

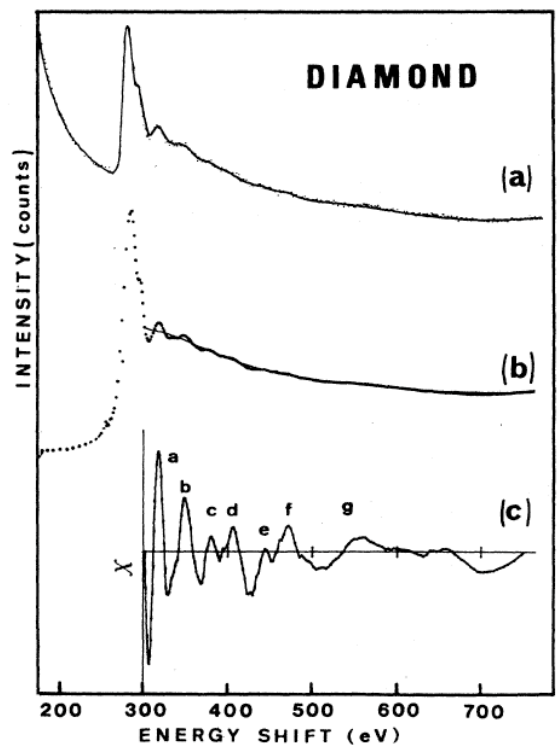

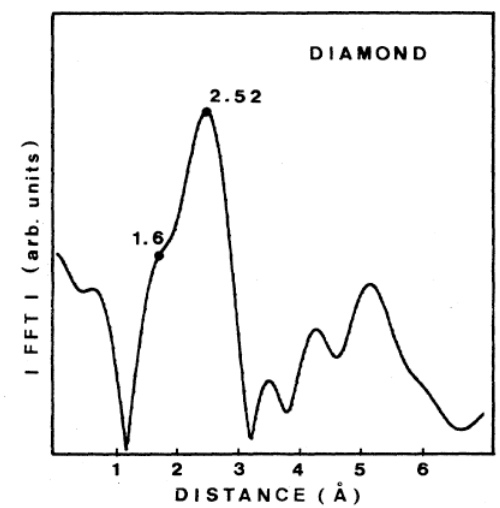

Bulk-sensitive XAS characterization of light elements: from X-ray Raman scattering to X-ray Raman spectroscopy

Uwe Bergmann[a,b,*], Pieter Glatzel[b], Stephen P. Cramer[a,b]

Microchemical Journal 71 (2002) 221–230

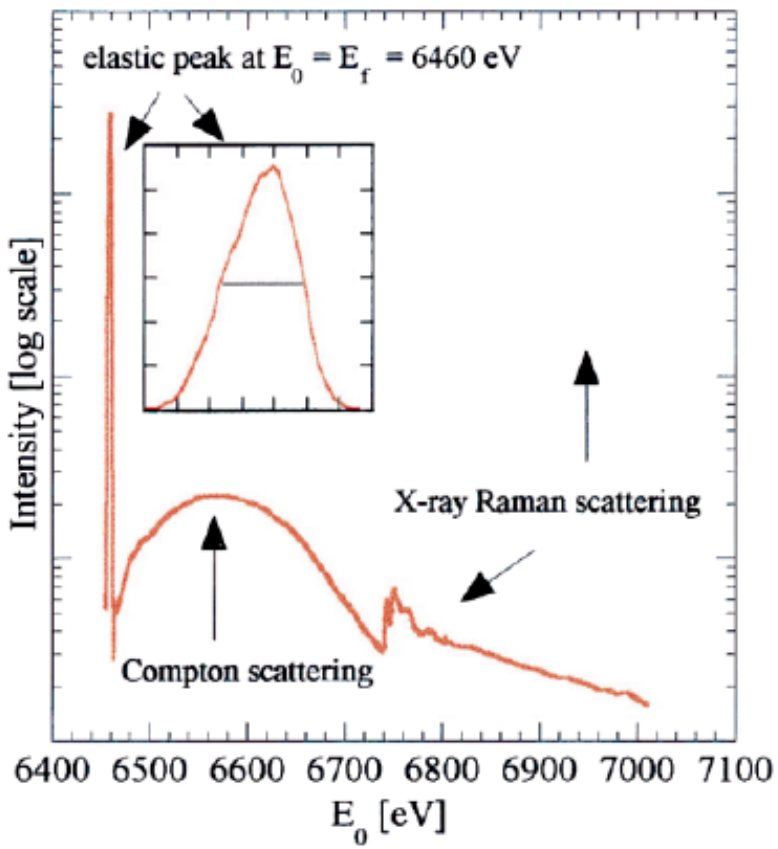

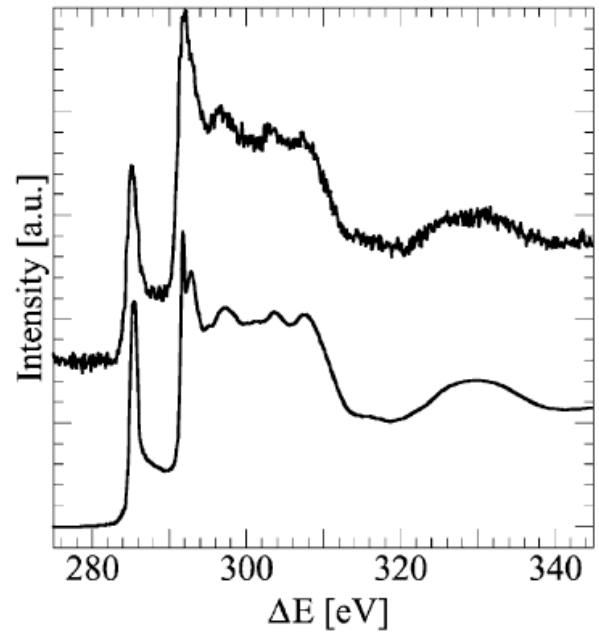

Fig. 2. Comparison of graphite K-edge XANES taken by XRS (top) with 1 eV FWHM resolution and by conventional XAS in electron yield mode (bottom) at 0.15 eV FWHM resolution. The analyzer energy was set to $E_f = 6.46$ keV, at an incident intensity of some 10^{13} photons/s.

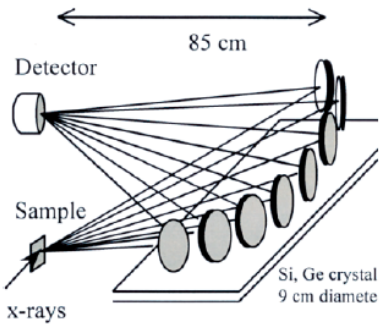

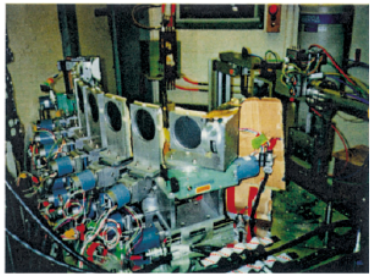

U. Bergmann, et al,
Microchemical Journal, 71 (2002) 221

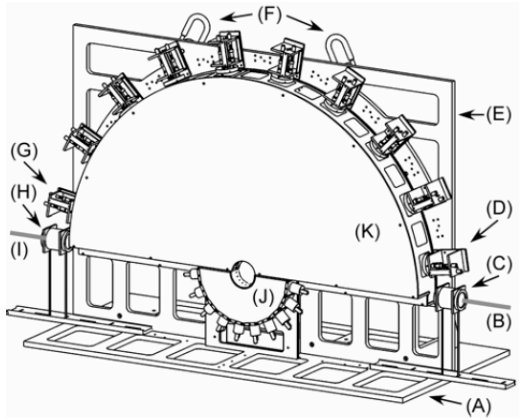

T. T. Fister, G. Seidler, et al,
Rev. Sci. Instr. 77 (2006) 063901

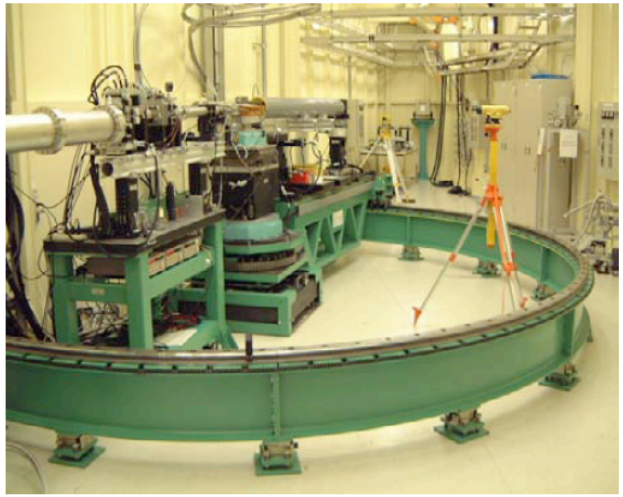

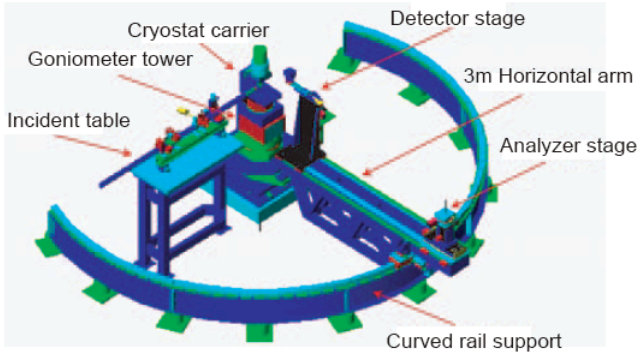

Optical System & Performance

- **Optical system and spectrometer for non-resonant inelastic x-ray scattering**

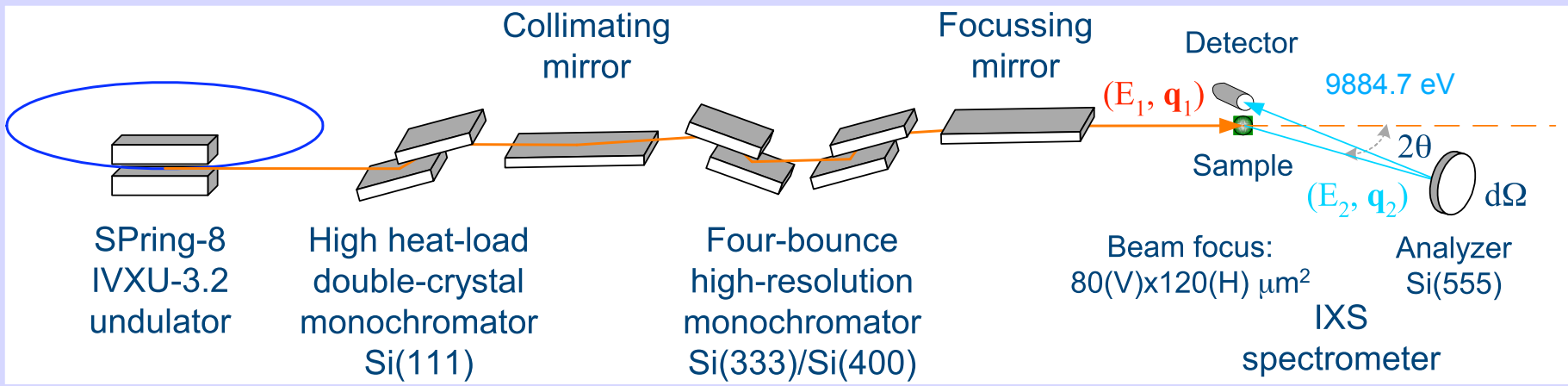

- **Performance at the near backscattering energy of Si(555) / Ge(555) reflection**

Beamline			IXS Spectrometer	
HRM Configuration	Flux ($\times 10^{11}$ photons/sec)	Bandwidth (meV)	Analyzer	Resolution (meV)
Si(333)	1.5	50	Si(555) 2-m diced	70
Si(440)	2.3	80	Si(555) 2-m DRIE diced	185
Si(400)	5.7	153	Si(555) 2-m bent	305
Si(220)	13.5	480	Si(555) 1-m bent	850
None (DCM)	120	1250	Ge(555) 1-m bent	1300

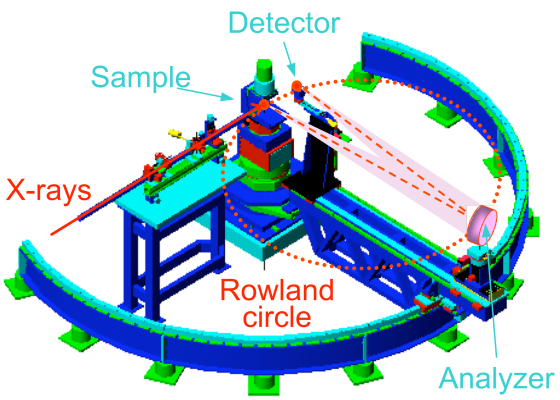

IXS Spectrometer

National Synchrotron Radiation Research Center

Courtesy: Yong Cai, NSRRC/Spring-8

Spectrometer Setups

✓ NRIXS Setup

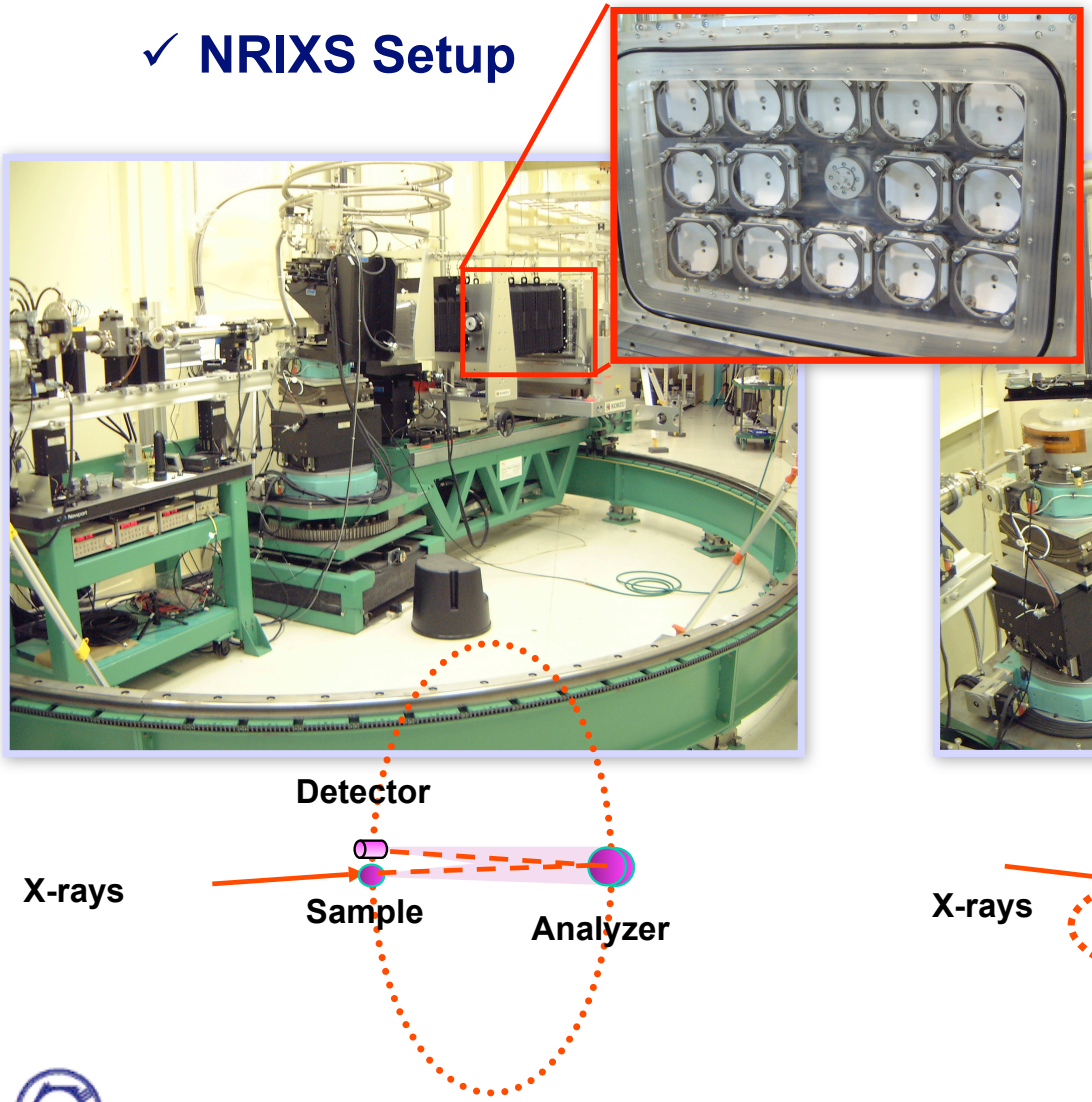

✓ RIXS Setup

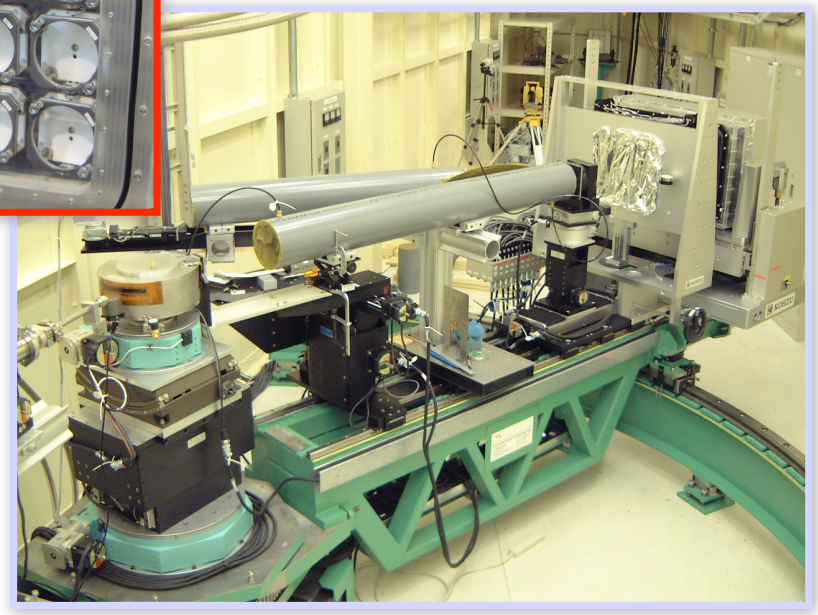

National Synchrotron Radiation Research Center

X-ray Raman Scattering (XRS)

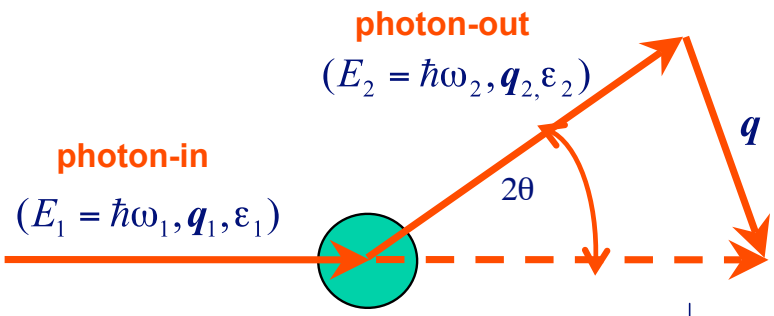

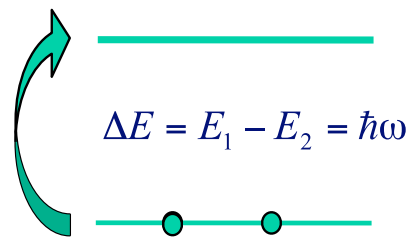

$$q = |\boldsymbol{q}_1 - \boldsymbol{q}_2| = 2q_1 \sin(2\theta / 2)$$

- **The double differential cross section:**

$$\frac{d^2\sigma}{d\Omega d\omega_2} \propto \sum_F \left| \langle F | \sum_j e^{i\mathbf{q}\mathbf{x}_j} | I \rangle \right|^2 \times \delta(E_F - E_I - \hbar\omega)$$

➔ **Dipolar regime:** $qr < 1 \Rightarrow e^{i\mathbf{q}\mathbf{x}} \approx 1 + iqr$

XRS identical to XAS
q equivalent to photon polarization vector

➔ **Multipolar regime:** $qr \geq 1$

Monopolar, dipolar and quadrupolar transitions possible

(Mizuno & Ohmura, J. Phys. Soc. Jpn. 22, 445)

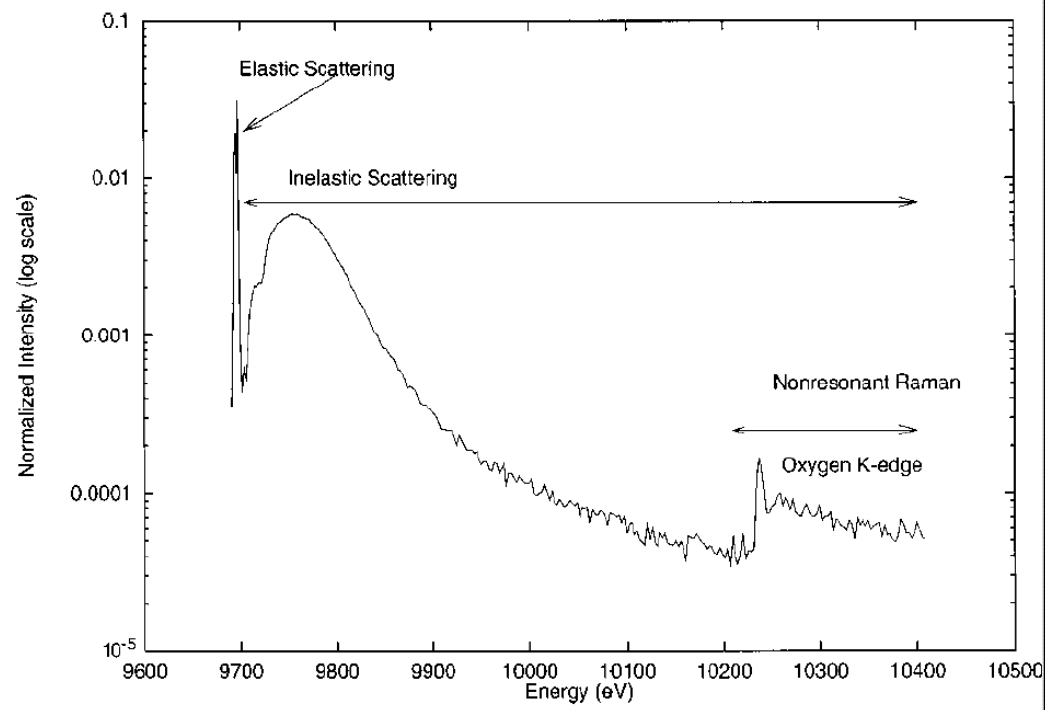

(D.T. Bowron et al, Phys. Rev. B 62 R9223)

National Synchrotron Radiation Research Center

Courtesy: Yong Cai, NSRRC/Spring-8

Fig. 1. High-pressure IXS spectra for graphite in horizontal and vertical directions plotted as normalized scattered intensity versus energy loss (incident energy − analyzer energy). The scattered intensity is normalized to the incoming intensity. The lower energy peak, labeled π, corresponds to 1s to π^* transitions and the higher energy portion, labeled σ, corresponds to 1s to σ^* transitions. The bottom spectra, taken in the horizontal direction, probes bonds in the *a* plane and does not show any π-bonding before and after the high-pressure transition. The top seven spectra, taken in the vertical direction, probe the *c* plane. After the transition, the σ bonds increase at the expense of the π bonds.

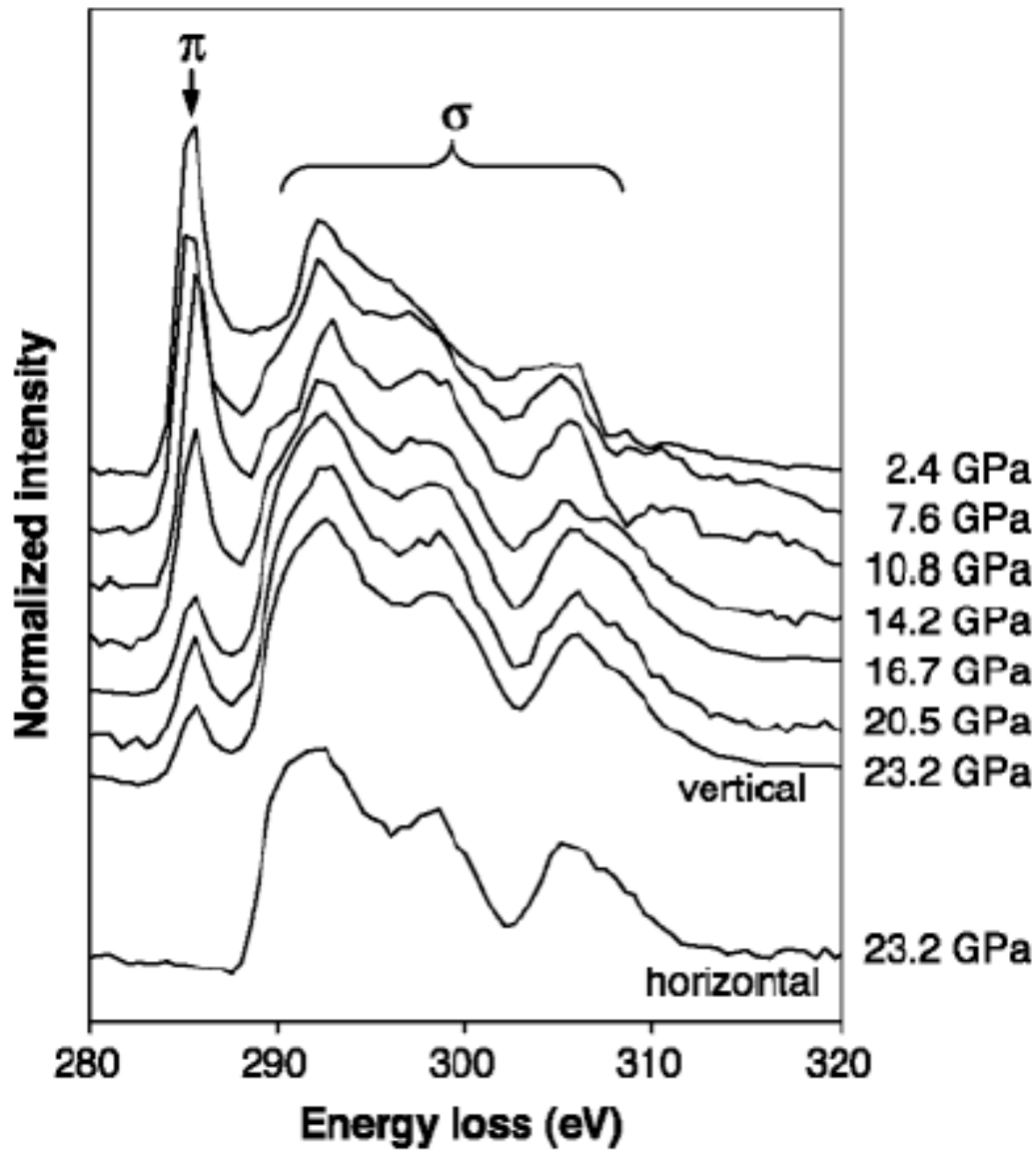

What is it ?

- **X-Ray Emission Spectroscopy (XES)**
  - Direct emission of a fluorescence line via absorption of the incident photon, whose energy is tuned to a particular point around the absorption edge, and scattered radiation is analyzed. Enables identification of features measured in a fluorescence measurement, sensitive to spin.
  - **Energy range: 1-20 keV,**
  - **Incident beam: monochromatic, tunable over 100 eV,**
  - **Scattered beam: Incoherent, polychromatic,**
  - **Analyzer: Bent, undiced Si or Ge crystal analyzer, for hard x-rays, gratings for soft x-rays**
  - **Energy Resolution : ~ 1 eV**
  - **Momentum transfer: Relevant to distinguish dipole transitions from higher order terms**
- **Main Features:**
  - **Allows better chemical (valence) state characterization compared to straight X-ray Absorption spectroscopy.**

Resonant X-Ray Emission Spectroscopy

- Variable incident energy tuned to a particular point near x-ray absorption edge, $\Delta E = 1$eV
- High resolution energy analysis of the scattered radiation (1 eV) by bent crystal analyzer (it can be flat)
- Tunable over large energy range

  $5 < E_{inc} < 12$ keV

Some definitions (still arbitrary)

- **X-Ray Absorption (XAS)**
  - Tuning the incident energy across an absorption edge with no analysis of the transmitted radiation
- **Partial Fluorescence Yield (PFY)**
  - Tuning the incident energy across an absorption edge with fixed energy filter
- **Resonant X-Ray Emission (RXES)**
  - Fixed incident energy with energy analysis of the scattered radiation
- **Resonant Inelastic X-Ray Spectroscopy (RIXS)**
  - Fixed incident energy with energy & momentum analysis of the scattered radiation

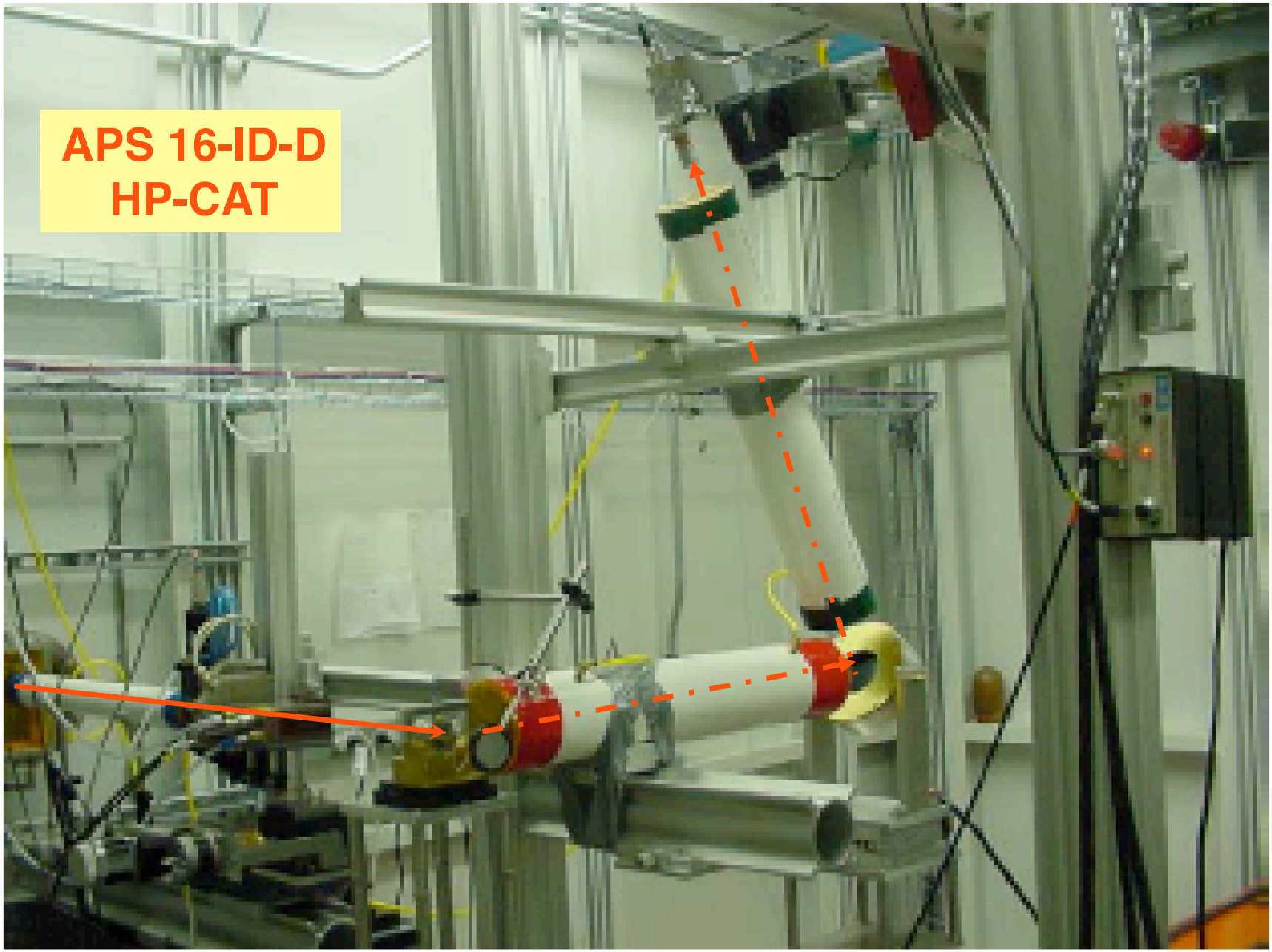
APS 16-ID-D
HP-CAT

Valence of YbS under pressure: A resonant inelastic x-ray emission study

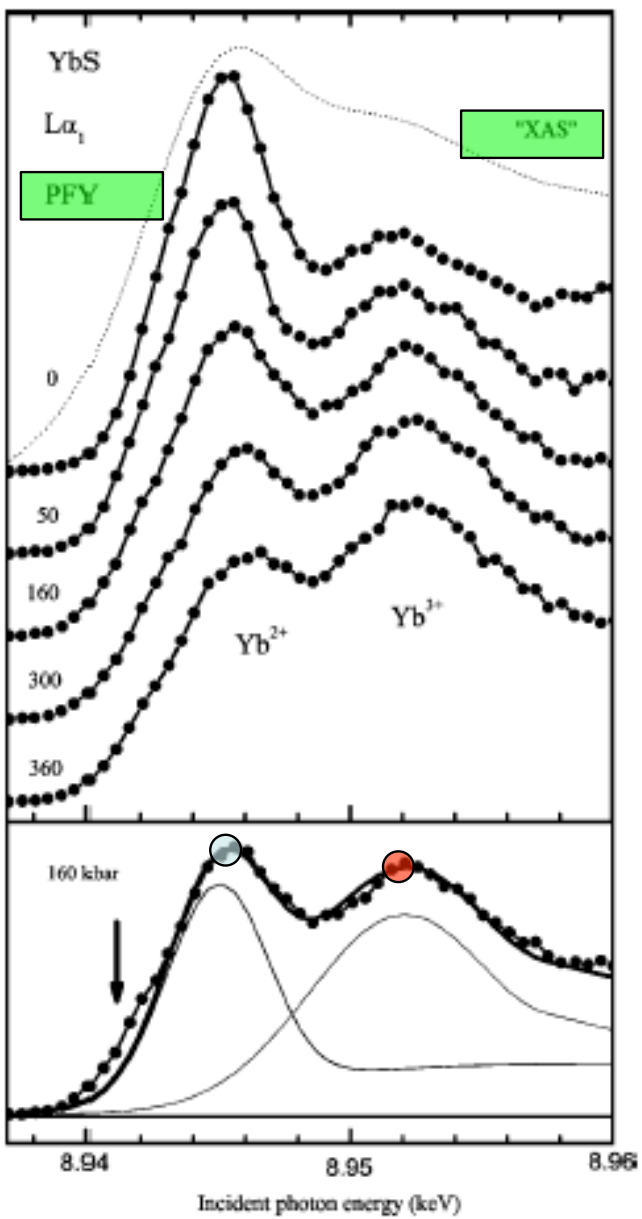

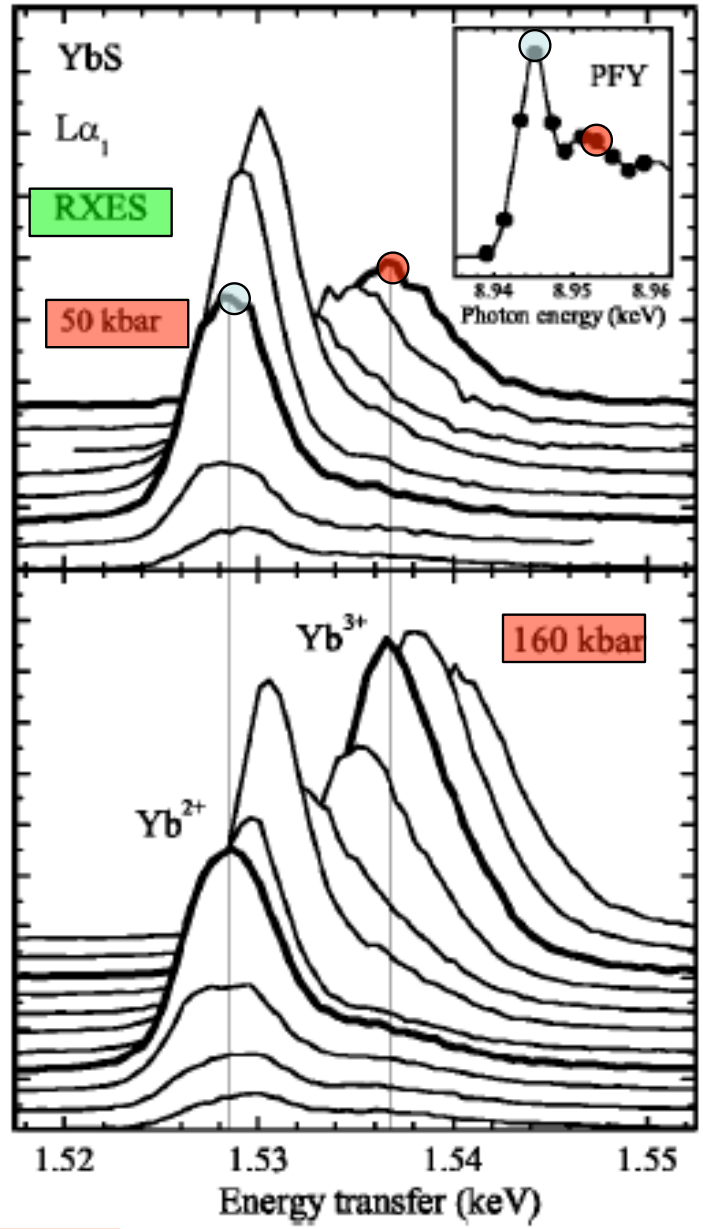

E. Annese, C. Dallera, et al, Phys. Rev. B 70 (2004) 075117

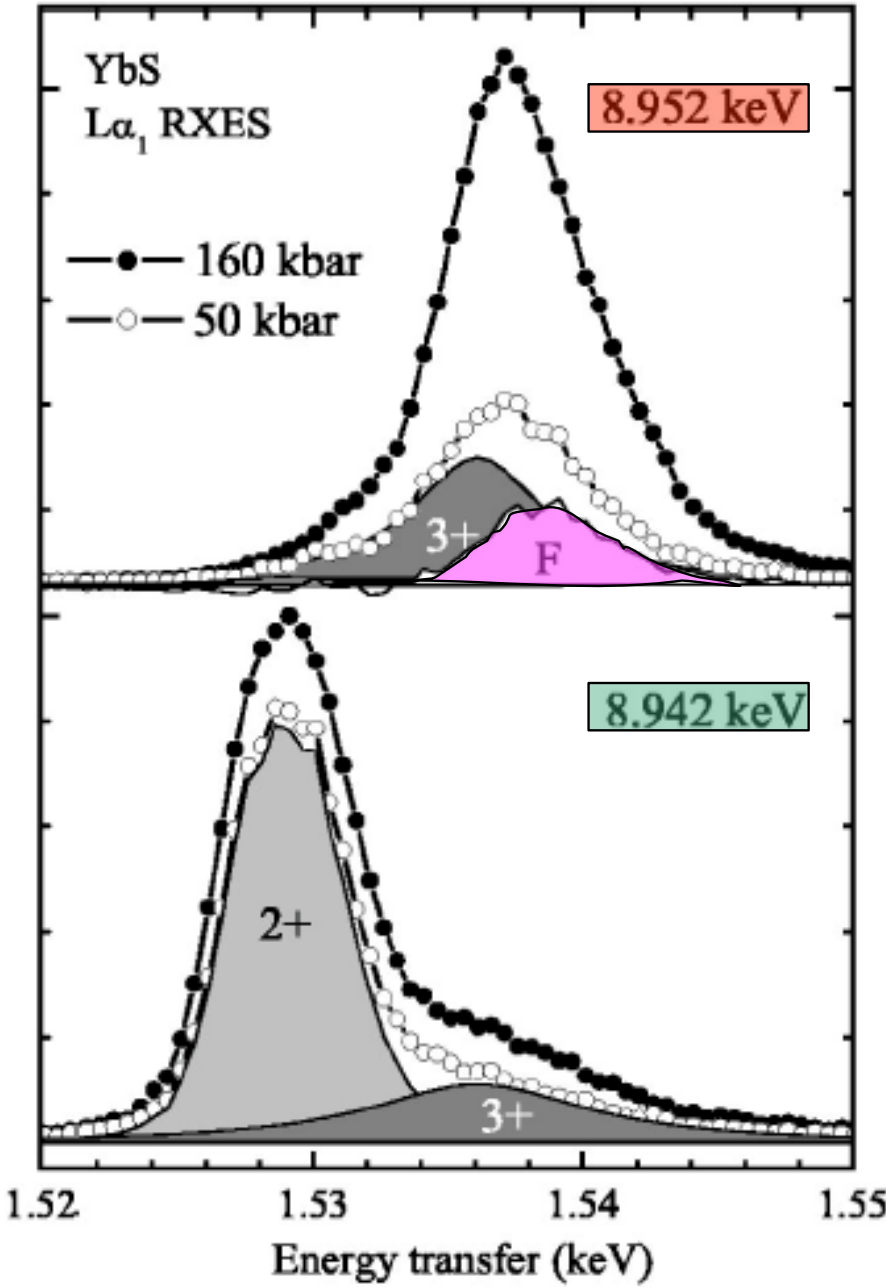

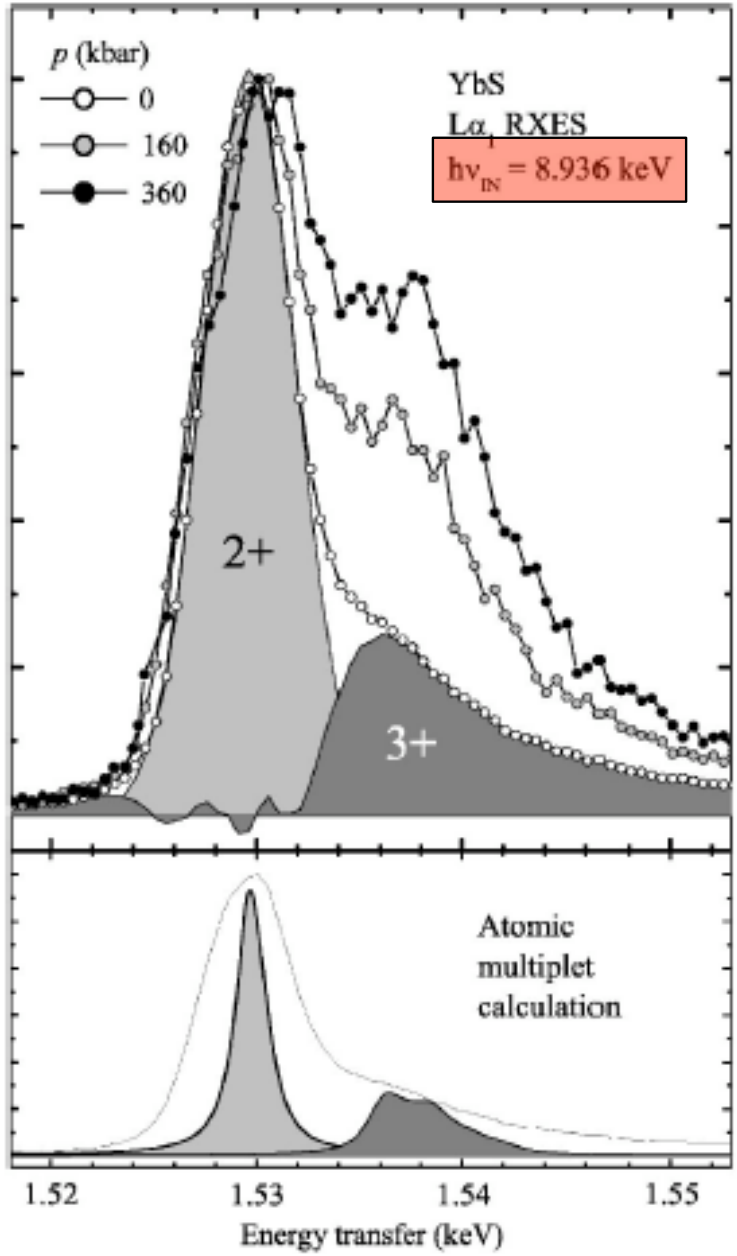

PHYSICAL REVIEW B **70**, 075117 (2004)

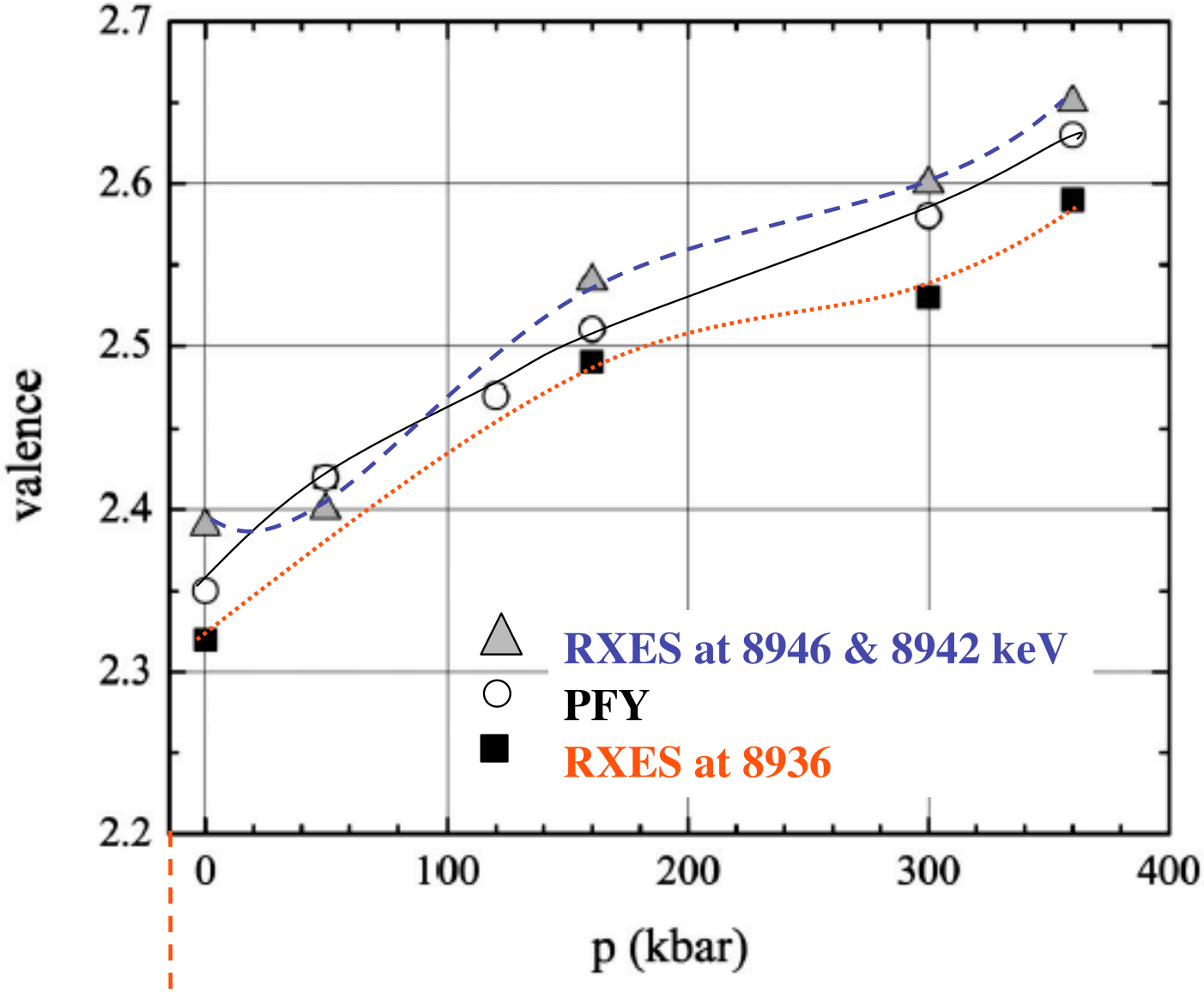

2.0 XAS

PHYSICAL REVIEW B **70**, 075117 (2004)

A high-spin to low-spin transition of Fe in magnesiowustite

Iron Partitioning in Earth's Mantle: Toward a Deep Lower Mantle Discontinuity

James Badro,[1] Guillaume Fiquet,[1] François Guyot,[1] Jean-Pascal Rueff,[2] Viktor V. Struzhkin,[3] György Vankó,[4] Giulio Monaco[4]

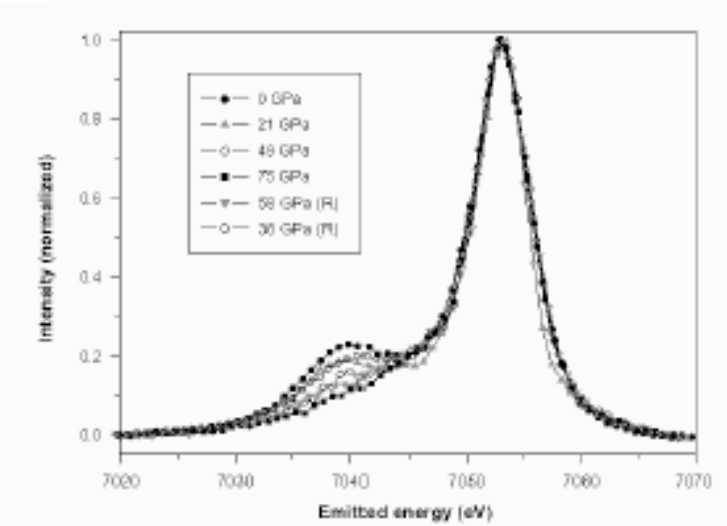

X-ray emission spectra of $(Mg_{0.83},Fe_{0.17})O$
Badro et al., Science, 2003

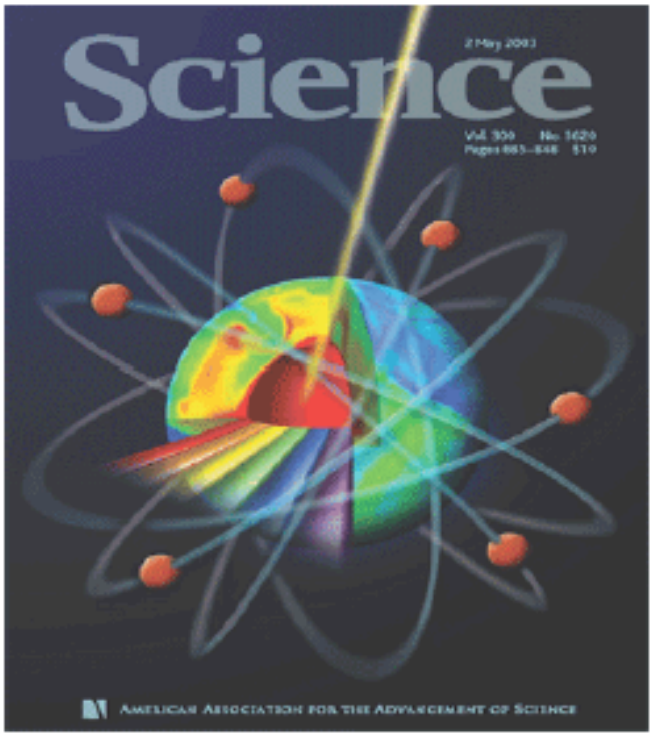

COVER An artist's interpretation of the deep Earth. Experiments on the electron spin state of iron at high pressures indicate unexpected processes occurring within Earth's lowermost mantle.

Based on simple thermodynamic calculations, it is predicted that all iron goes into magnesiowustite in the lower mantle. However, in situ study X-ray diffraction and quenched sample analyses on silicate perosvkite and magnesiowustite did not observe such strong effect.

X-ray emisson spectroscopy in a diamond anvil cell: Study spin states of Fe in Fe_3C and $(Mg_{0.4},Fe_{0.6})O$

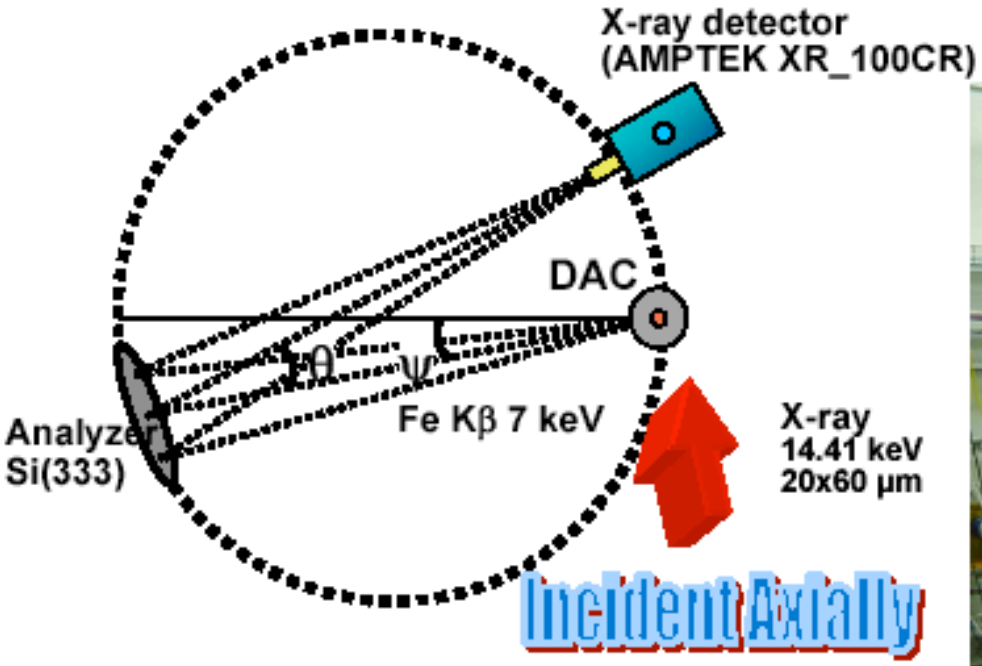

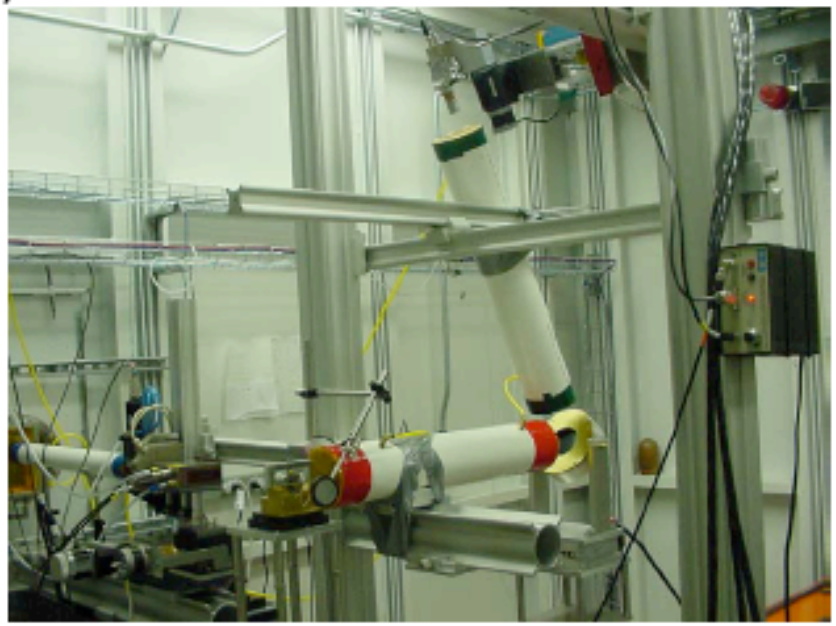

XES system setup at 16 ID-D, HPCAT

- XES of Fe Kβ at 16 ID-D, HPCAT, APS
- Focused X-ray beam (20x60 μm spot)
- High resolution Rowland-circle spectrometer (<1 eV)
- Beryllium+B gasket in a diamond cell

In cooperation with V. Struzhkin, M. Hu, P. Chow, H.K. Mao, and R.J. Hemley

What is it ?

- **Resonant Inelastic X-Ray Scattering (RIXS)**
  - Scattering from spatially localized or dispersed valence electron excitations near the Fermi level, enhanced due to resonance near the absorption edge.
  - **Energy range: 6-12 keV,**
  - **Incident beam: monochromatic, tunable over 100 eV,**
  - **Scattered beam: Incoherent, polychromatic,**
  - **Analyzer: Bent, diced or undiced Si, Ge, LiNbO3 crystal analyzer, for hard x-rays,**
  - **Energy Resolution : ~ 0.1 eV**
  - **Momentum transfer: Relevant to distinguish localized versus spatially dispersed excitations**
- **Main Features:**
  - **Allows determination of solid-state effects in electronic excitations with element selectivity in complex materials**

IXS-CDT Beamline: 30-ID

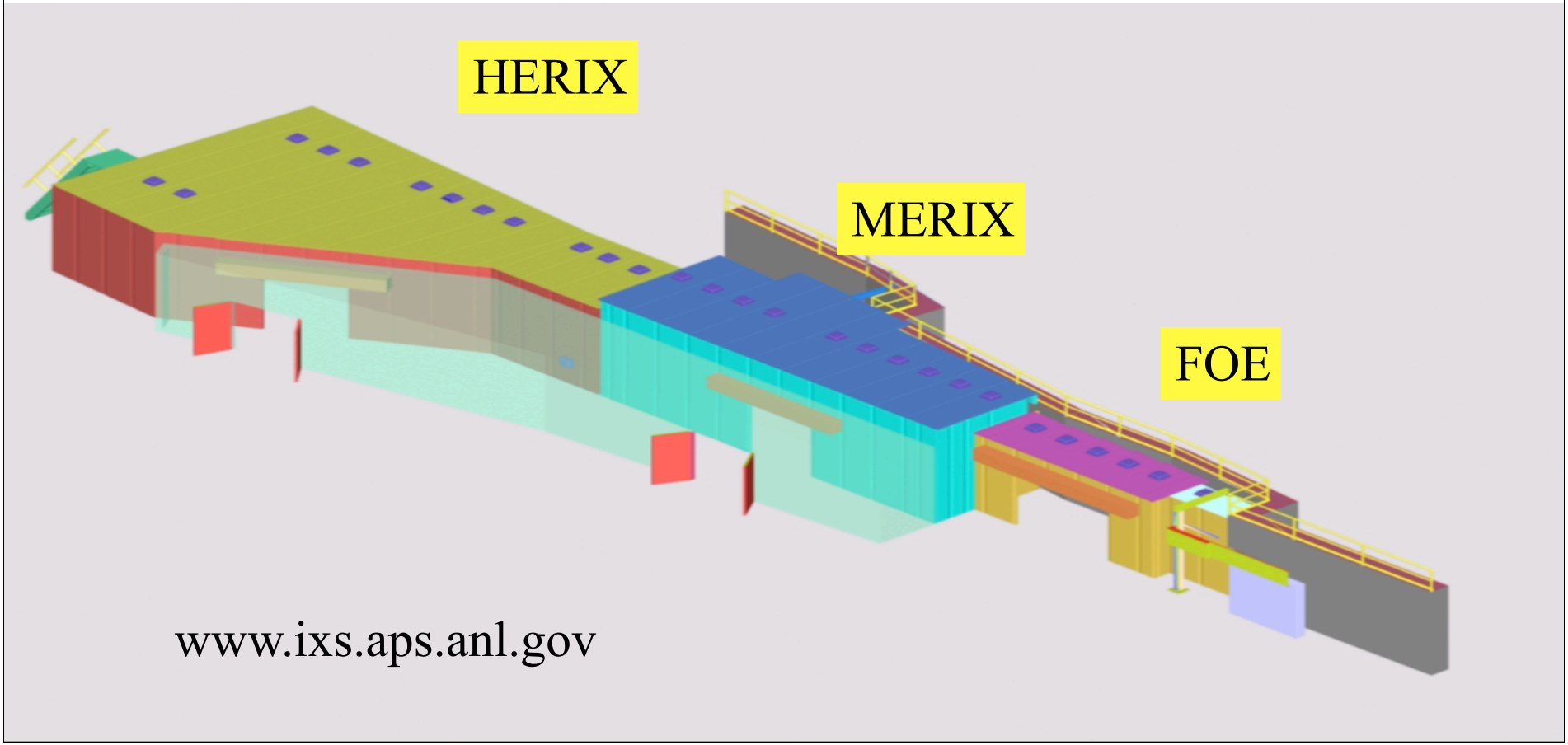

MERIX Monochromator

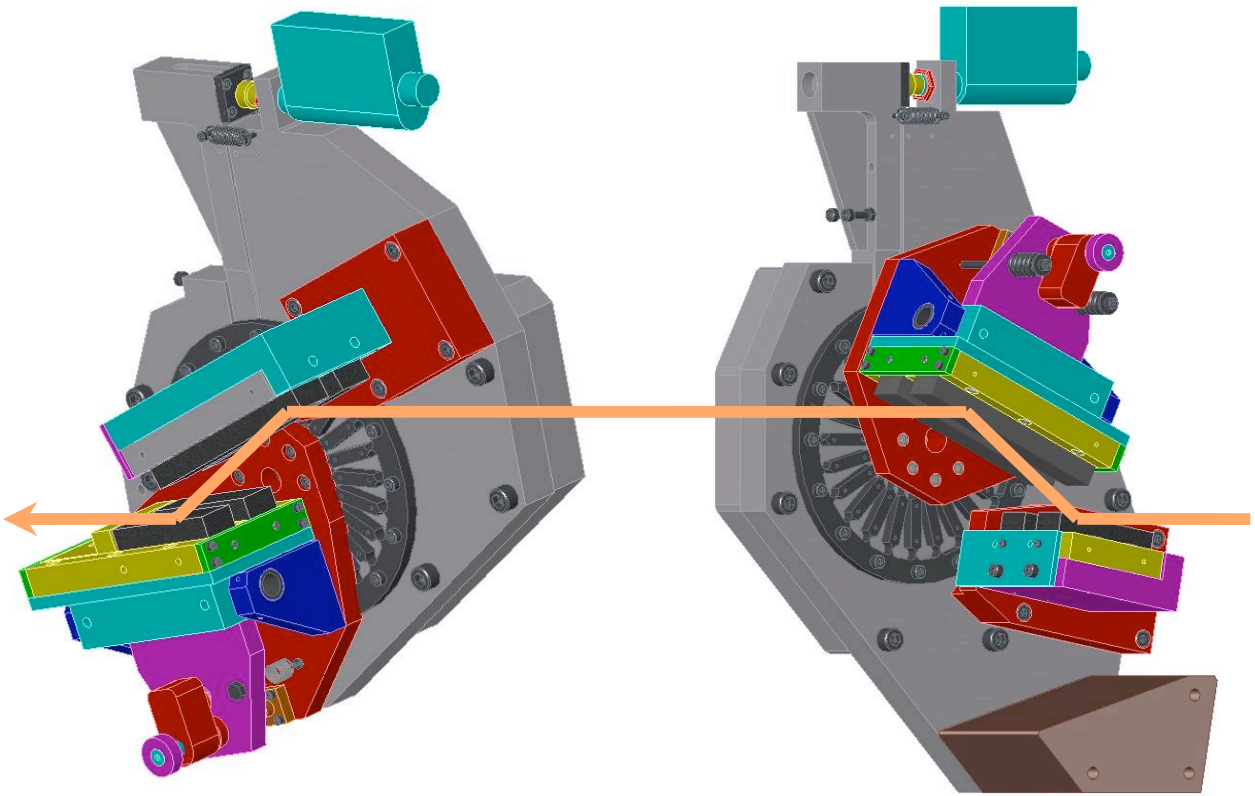

Two pairs of Si (220) and Si (400) crystals are aligned side by side to provide ~ 20, 50, 70, and 120 meV resolution over 5-15 keV range.

The Kohzu K15M stages capable of rotating 360 degrees with 35 μrad coarse resolution, and 0.025 microradian fine resolution over 2 degrees. This is a new design with a solenoid clutch mechanism to decouple coarse and fine motions.

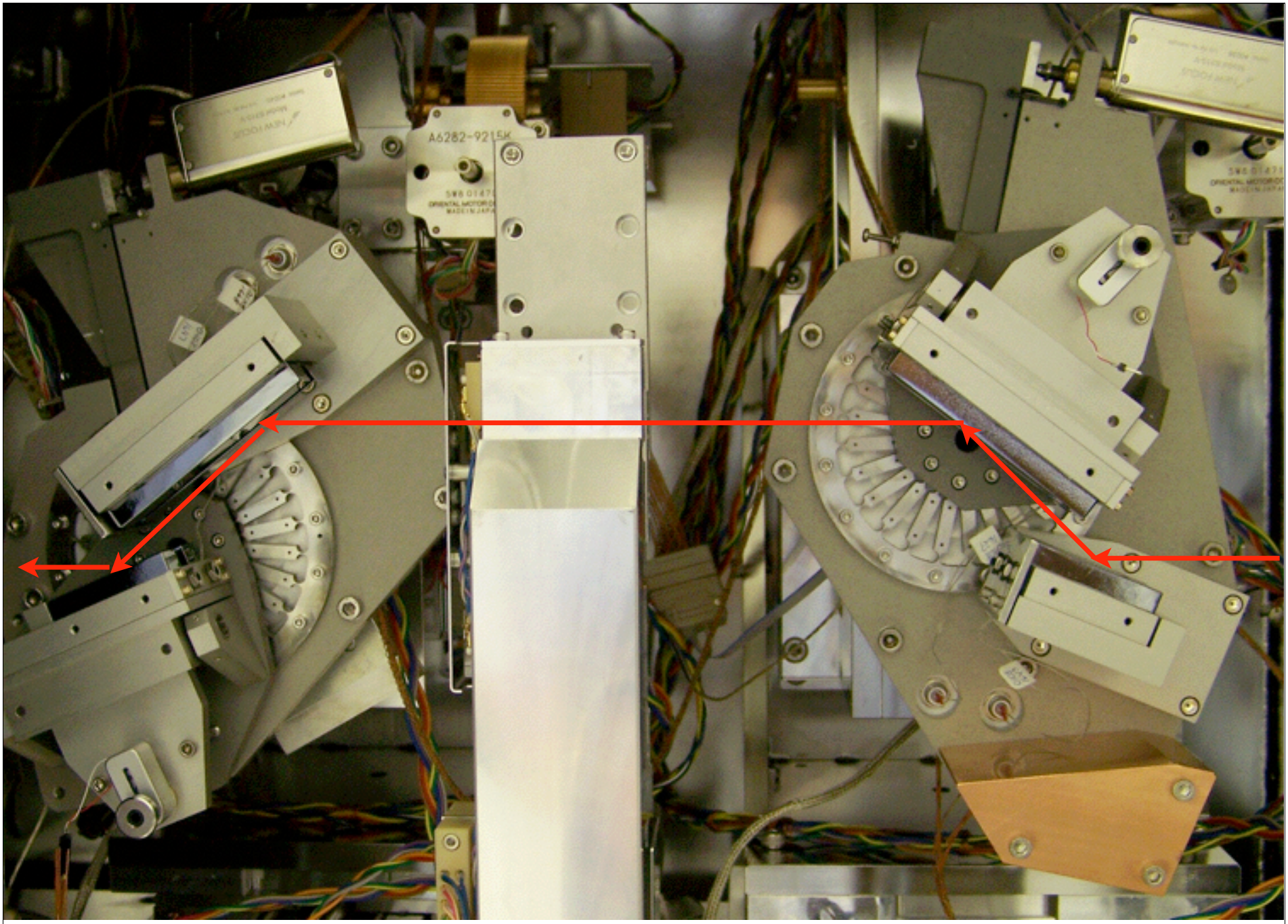
A6282-9215K

MERIX analyzers currently under development

Crystal analzyer	Energy	Status
Ge (7 3 3)	9 keV , Cu K-edge	2m, Ready to go (diced, and bent) 110 meV
Ge (6 2 4)	8.33 keV, Ni K-edge	1m analyzer diced 2m analyzer, diced and bent (260 meV) 1 unpolished wafer ready
LiNbO3 (0 6 0)	8.33 keV, Ni K-edge	1m diced 2 bonded and diced 2 polished wafers ready (1mm thick)
LiNbO3 (3 3 6)	7.71 keV, Co K-edge	15 wafers (1.5 mm) to be delivered10/10/06 5 wafers (0.5 mm) to be delivered 10/10/06
Ge (6 4 0)	7.11 keV, Fe K-edge	4 wafers (2mm thick) in production
Si (4 4 0)	6.54 keV, Mn K-edge	4 wafers polished (2 mm thick)
Si (5 1 1)	5.99 keV, Cr K-edge	4 wafers (2mm thick), in production
Si (8 0 0)	8.76 keV, non-resonant	1 m analyzer, diced 3 wafers, not-polished yet

Various analyzers under production
(Y. Shvydko, A. Said, N. Kodituwakku, H. Sinn)

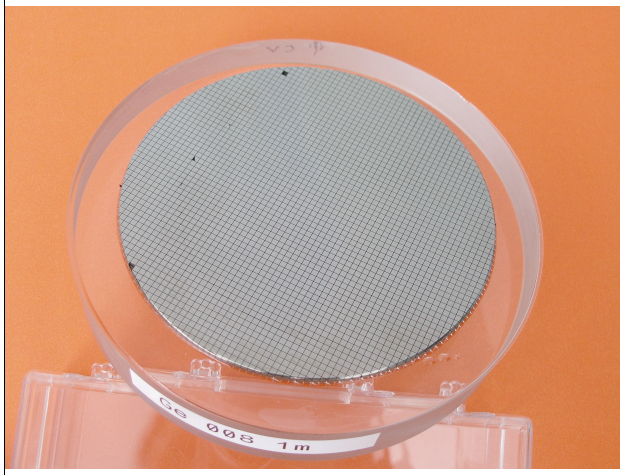

Ge (008) 1m

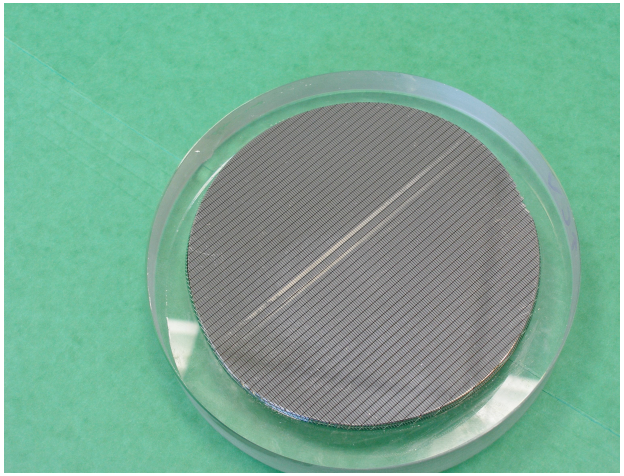

Ge (337) 2m

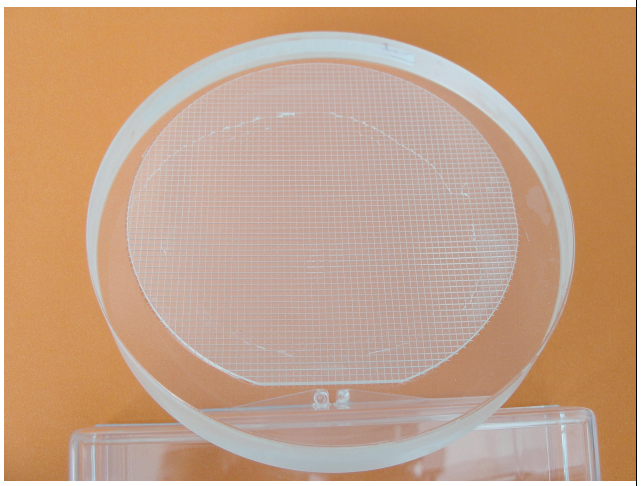

$LiNbO_3$ (0 6 0)

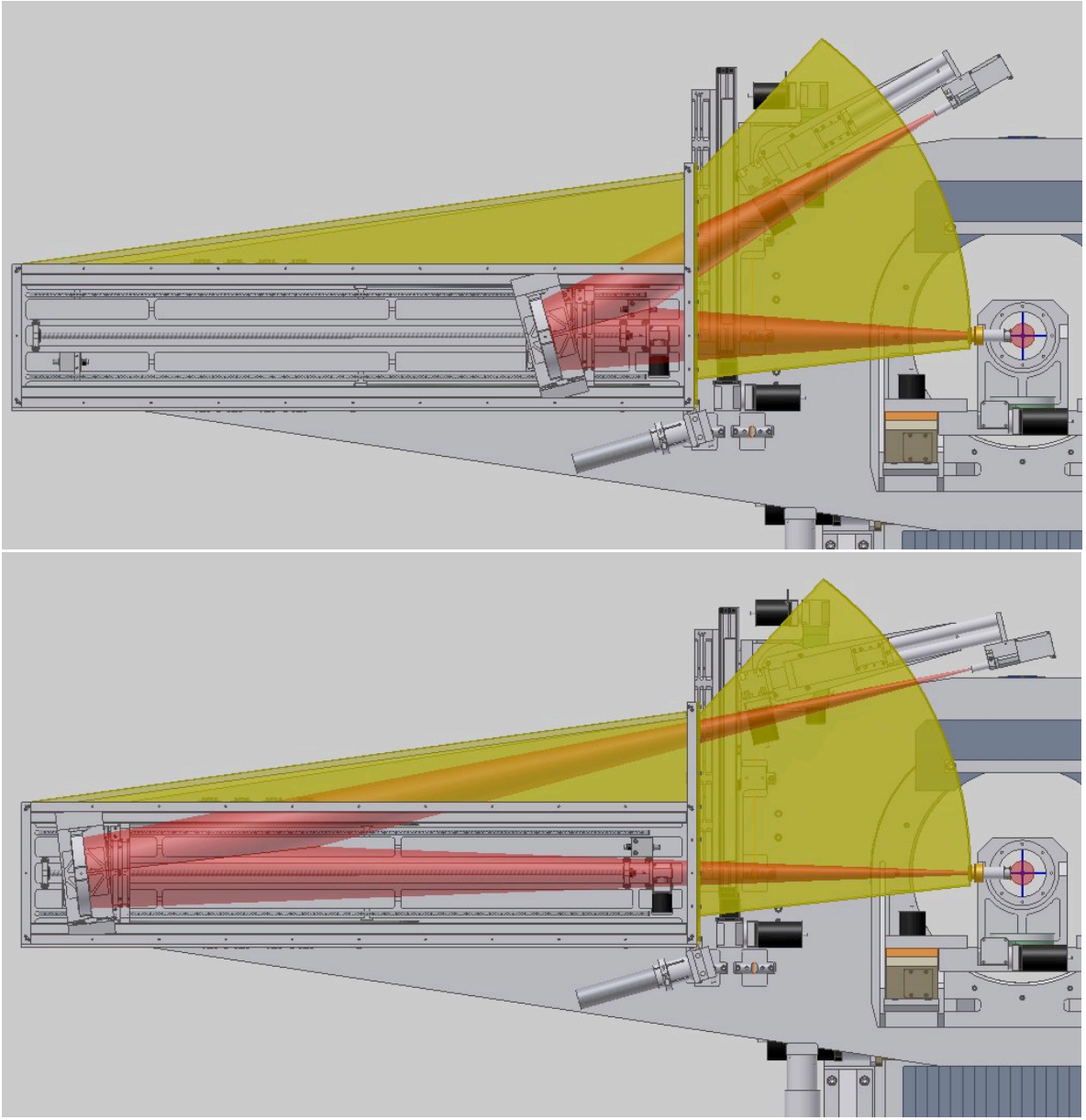

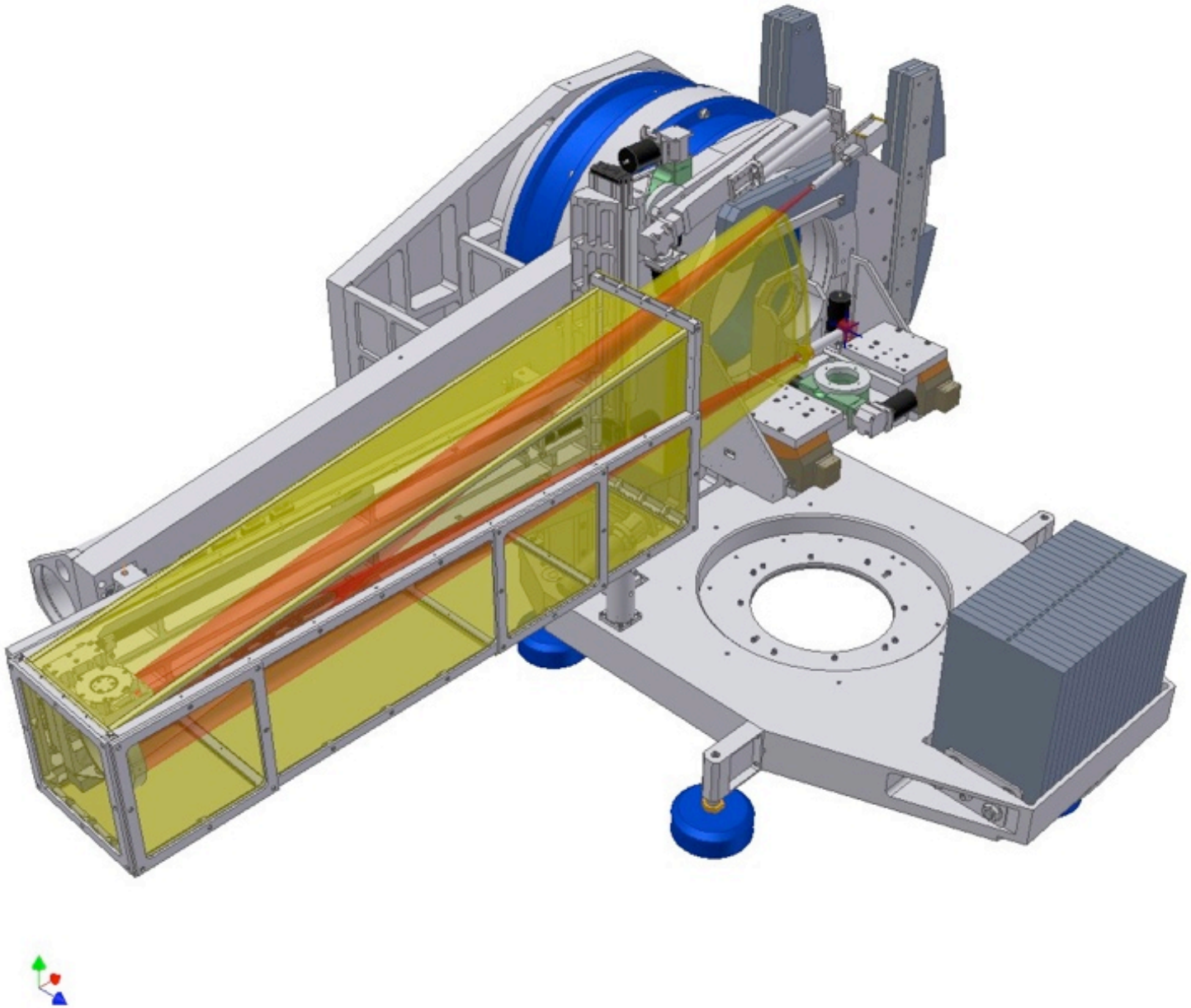

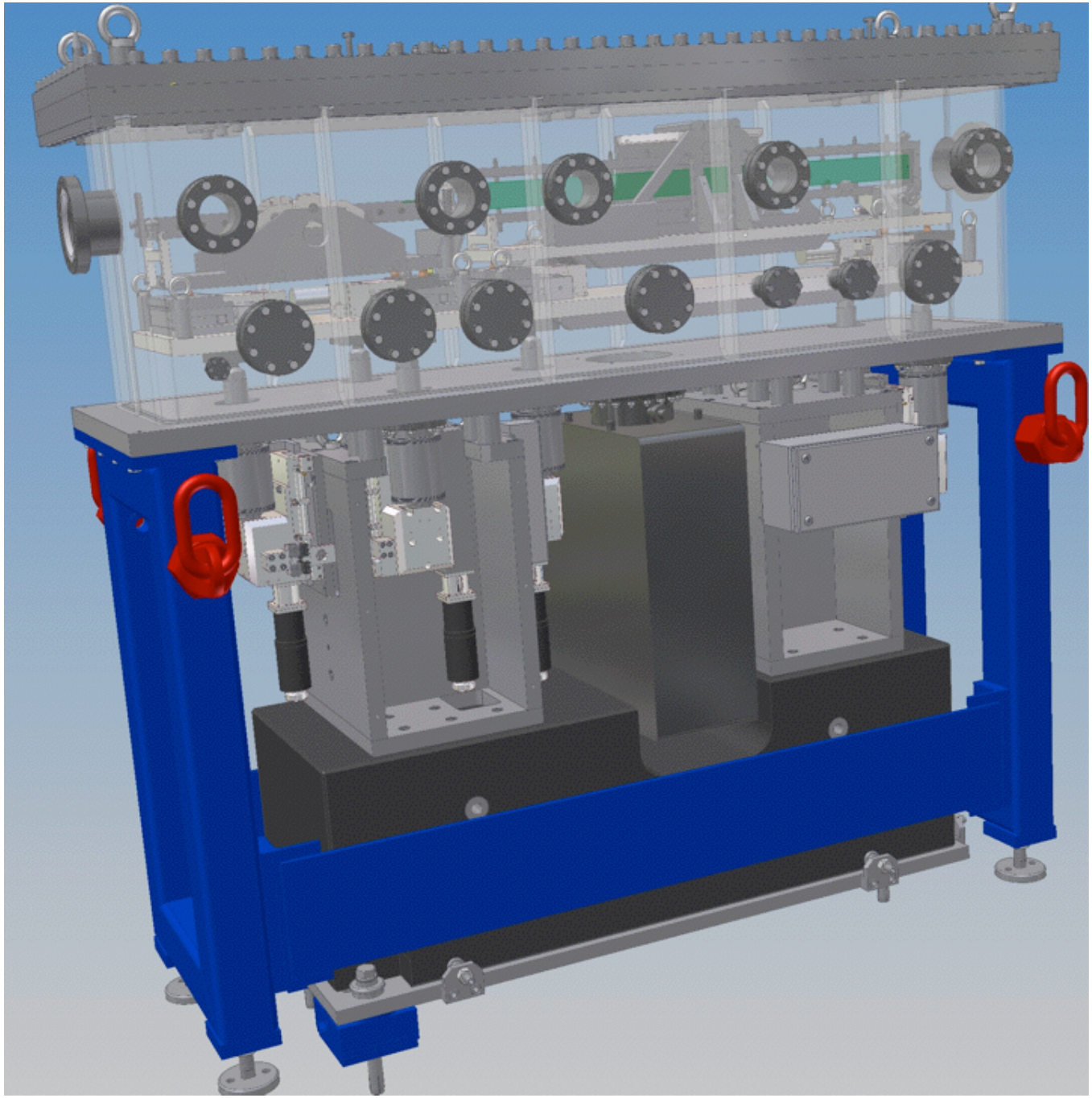


31-BM

Need for 100 meV

$La_{2-x}Sr_xCuO_4$

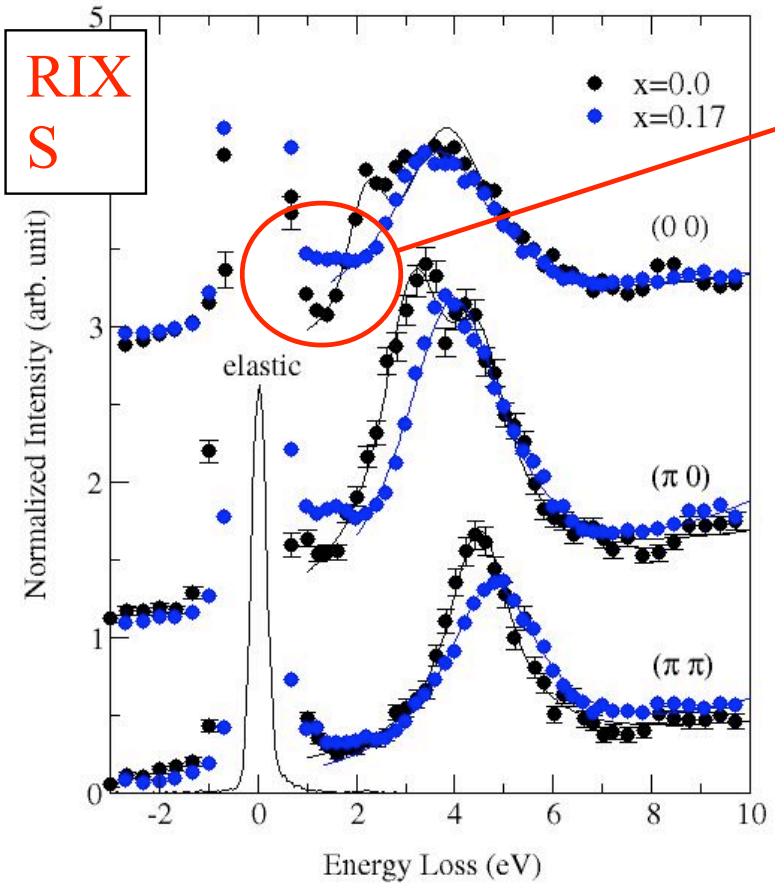

Gap filled as dope into metallic phase

Far-IR σ(ω)

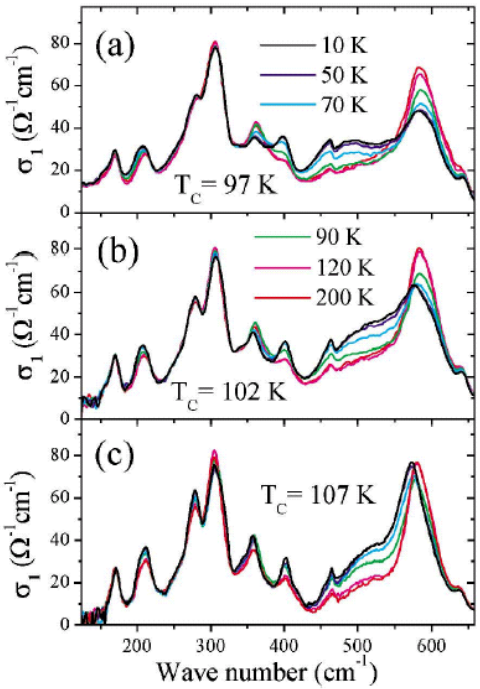

Boris *et al.*, PRL 89 277001 (2002)

Bi2223

Y.-J. Kim *et al.*, PRL **89** 177003 (2002).

Normalized RIXS spectra in CuO, Q=(300)

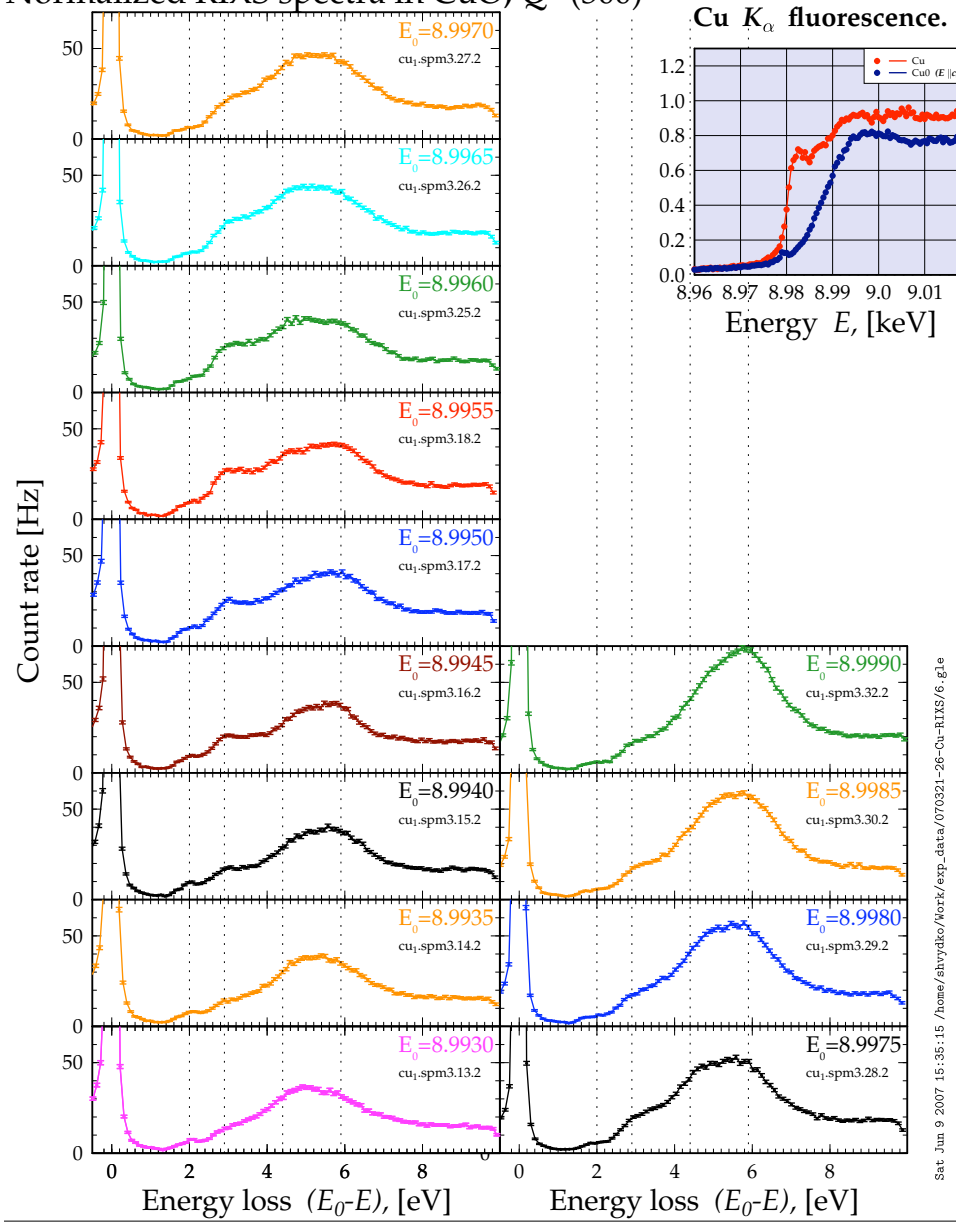

What is it ?

- **X-Ray Compton Scattering (CS, MCS):**
  - Deep inelastic scattering of photons from valence (and core) electrons, enabling the momentum-space depiction of the Fermi surface.
  - **Energy range: 6-200 keV,**
  - **Incident beam: monochromatic, linear or circularly polarized, fixed energy during the experiment**
  - **Scattered beam: Incoherent, polychromatic,**
  - **Analyzer: Germanium solid state detector for Magnetic Compton scattering, Bent Laue crystal analyzer combined with position sensitive detector for high resolution Compton Scattering**
  - **Energy Resolution : ~ 100-600 eV**
  - **Momentum transfer: Relevant to distinguish core electrons from valence electrons**
- **Main Features:**
  - **Allows determination of Fermi Surface in poor metals where deHass-vanAlphen method may nor work, Orbital occupancy breakdown in complex systems like in correlated electron systems, a true ground state spectroscopy**

Compton scattering by free electrons

The change in energy of photons as they are scattered by an electron is proportional to Compton scattering length given by

$$\lambda\!\!\!^{-}_c = \frac{\hbar}{mc}$$

$$\alpha = \frac{r_0}{\lambda\!\!\!^{-}_c} = \frac{1}{137}$$

$$\boxed{\frac{k}{k'} = \frac{\varepsilon}{\varepsilon'} = \frac{\lambda'}{\lambda} = 1 + \lambda_C k(1 - \cos\psi)}$$

It is interesting to note that the ratio between classical electron radius and Compton scattering length is a fundamental constant.

Furthermore, it should be noted that Compton scattering is an extreme example of inelastic x-ray scattering, and it can be used to differentiate between localized (core) electrons and valence (free) electrons.

Compton scattering by free electrons

- When the incident photon and electron in the solid collide, due to conservation of energy and momentum, the photon loses some of its energy and shifted downward. This shift is given by:

$$\lambda_{final} - \lambda_{initial} = \frac{h}{m_{el}c}(1 - \cos\theta)$$

- The key experimental elements are already in this equation:
  - The larger the scattering angle, the larger is the Compton shift.
- The larger the incident energy, the larger the penetration depth, and escape depth for the radiation

Fermi surface

Fermi surface defines the boundary between occupied and unoccupied states both in momentum and in energy space.

The 3-D topology of the Fermi surface in momentum space is one way to visualize the free electron distribution. This can be measured by finding the extremum in the first derivative of momentum density

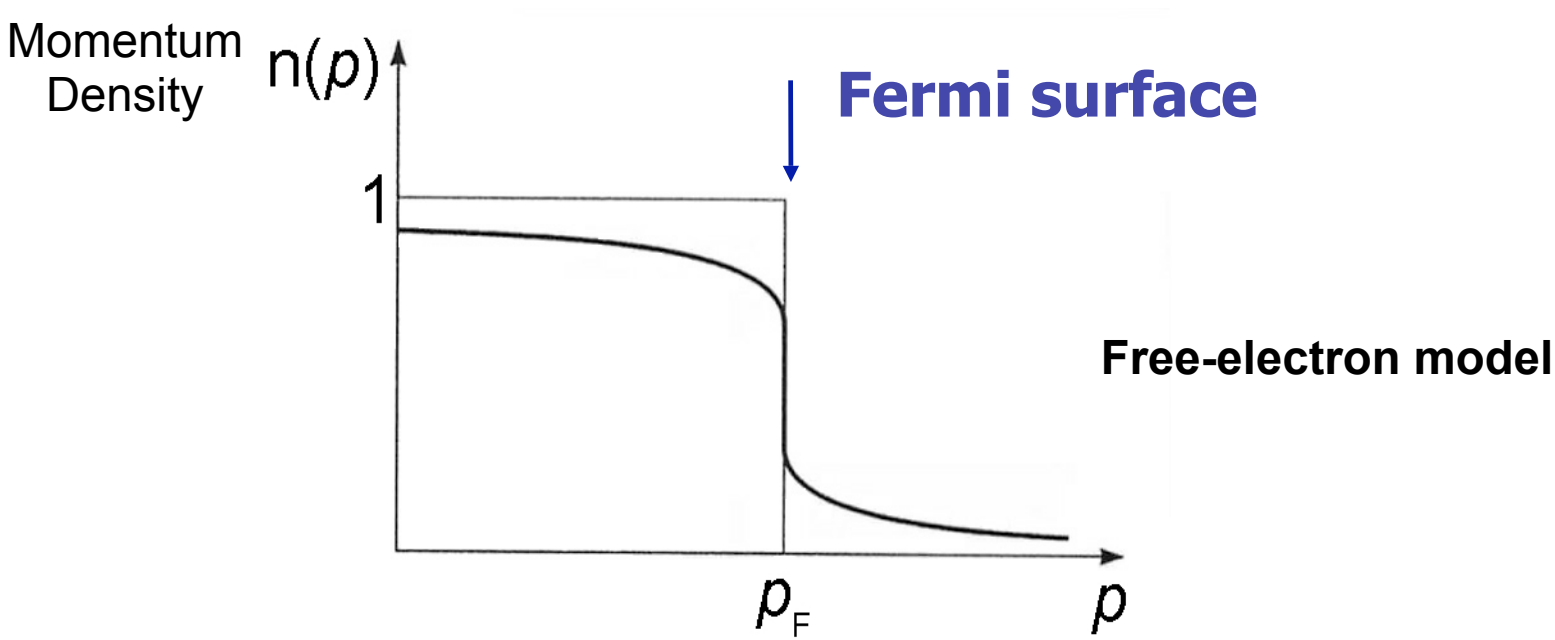

Compton Profile, CP

The measured Compton profile $J(p_z)$ is proportional to the twice integrated electron momentum density r (**p**):

$$J(p_z) = \iint \rho(\mathbf{p})\, dp_x dp_y$$

$$\rho(\mathbf{p}) = \frac{1}{2\pi^3} \sum_{\mathbf{k},\nu} \left| \psi_{\mathbf{k},\nu}(\mathbf{r}) e^{-i(\mathbf{p}\cdot\mathbf{r})} d\mathbf{r} \right|$$

$\psi_{\mathbf{k},\nu}(\mathbf{r})$ denotes the the electron wave function for state **k** and band v, and the summation is over all occupied states.

In a metallic system the CP will contain the clues for the positions and sizes of Fermi-surface-related discontinuities in the momentum density. However, the the double integral in above equation obscure this information. One approach is to measure CP's along a many directions, and to use the set of two-dimensional ~2D projections to "reconstruct" the 3D function r (**p**).

Three-dimensional Momentum Density Reconstruction

Three-dimensional momentum density, n(p), can be reconstructed from ~10 Compton profiles.

~10 Compton profiles:

$$J(p_z) = \iint n(\mathbf{p})\,dp_x\,dp_y$$

Reconstruction:

- Direct Fourier Method
- Fourier-Bessel Method
- Cormack Method
- Maximum Entropy Method

Momentum density, n(**p**)

Courtesy: Dr. Y. Sakurai, Spring-8

Compton Scattering

3-D reconstruction of electron momentum density in Li

Y. Tanaka, et al
Phys. Rev. B 63 (2001) 045120

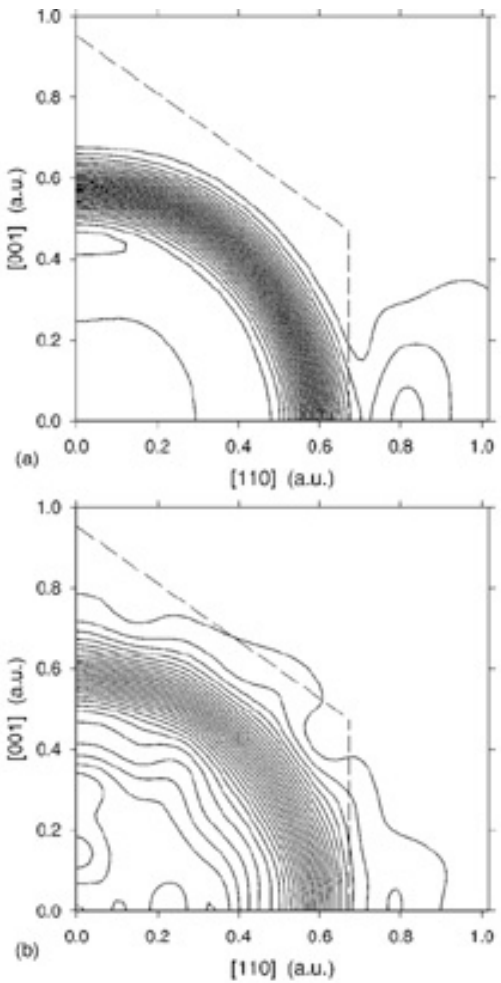

FIG. 4. Contour maps of the theoretical (a) and experimental (b) $\rho(\mathbf{p})$ on the (110) plane reconstructed using the filter function. Resolution broadening is included in the theory. The contour interval is 0.035 electrons/a.u.^{3} The dashed lines mark the first Brillouin-zone boundary.

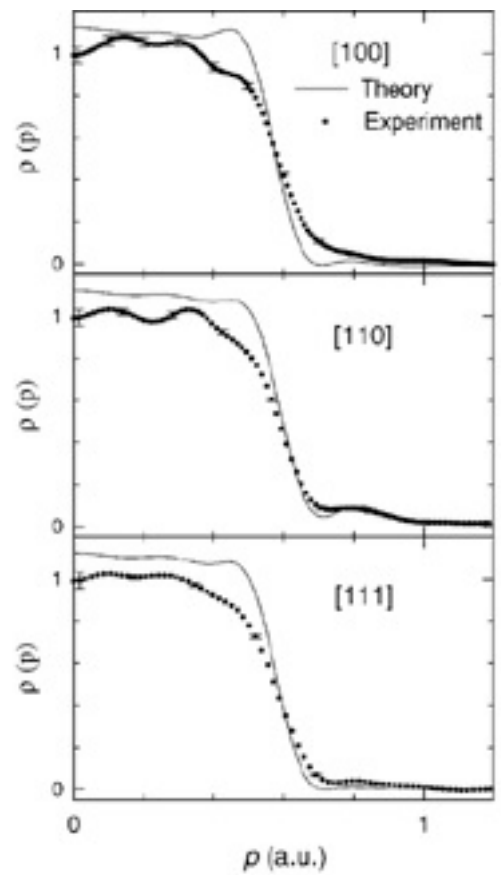

FIG. 6. [100], [110], and [111] sections through the reconstructed theoretical (solid lines) and experimental (dots) momentum densities shown in Fig. 4. Both sets of densities have been normalized such that $B(0)$ equals the number of valence electrons.

$$J(p_z) = \int\int \rho(\mathbf{p})\,dp_x\,dp_y,$$

$$\rho(\mathbf{p}) = (2\pi)^{-3}\sum_{\mathbf{k},\nu}^{\text{occ.}}\left|\int \psi_{\mathbf{k},\nu}(\mathbf{r})\exp(-i\mathbf{p}\cdot\mathbf{r})\,d\mathbf{r}\right|$$

BL08W: High Energy Inelastic Scattering

BL08W provides unique tools to study the electronic and magnetic properties of solids in terms of orbitals and Fermi surfaces.

Station A: 175-275 keV

Magnetic Compton Scattering

- CMR-related materials
- Magnetic multilayers
- Actinides, etc.

Station B: 115 keV

High-resolution Compton scattering

- Smart alloys
- Metal hydrides
- CMR materials
- High-Tc Cuprates
- Quasicrystals
- Water & Aqueous solution

Magnetic Compton

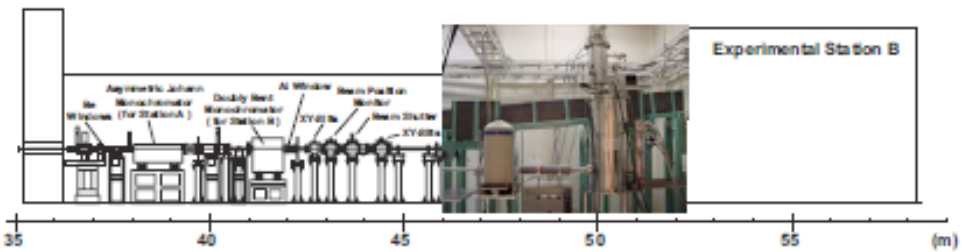

(a) Experimental Station-A Branch

High-resolution Compton

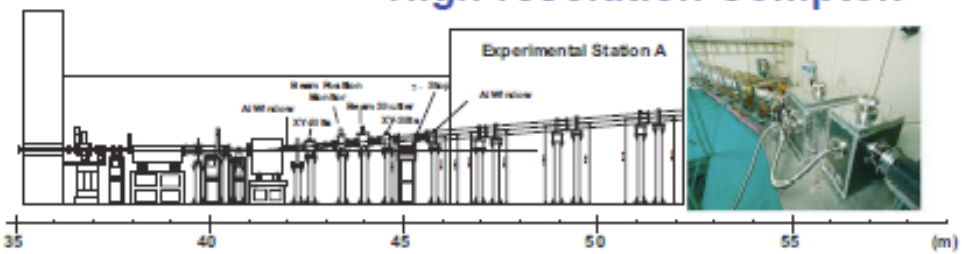

(b) Experimental Station-B Branch

Public Beamline: Open to Users Worldwide

Courtesy: Dr. Y. Sakurai, Spring-8

Magnetic Compton Scattering Spectrometer

BL08W, Station-A

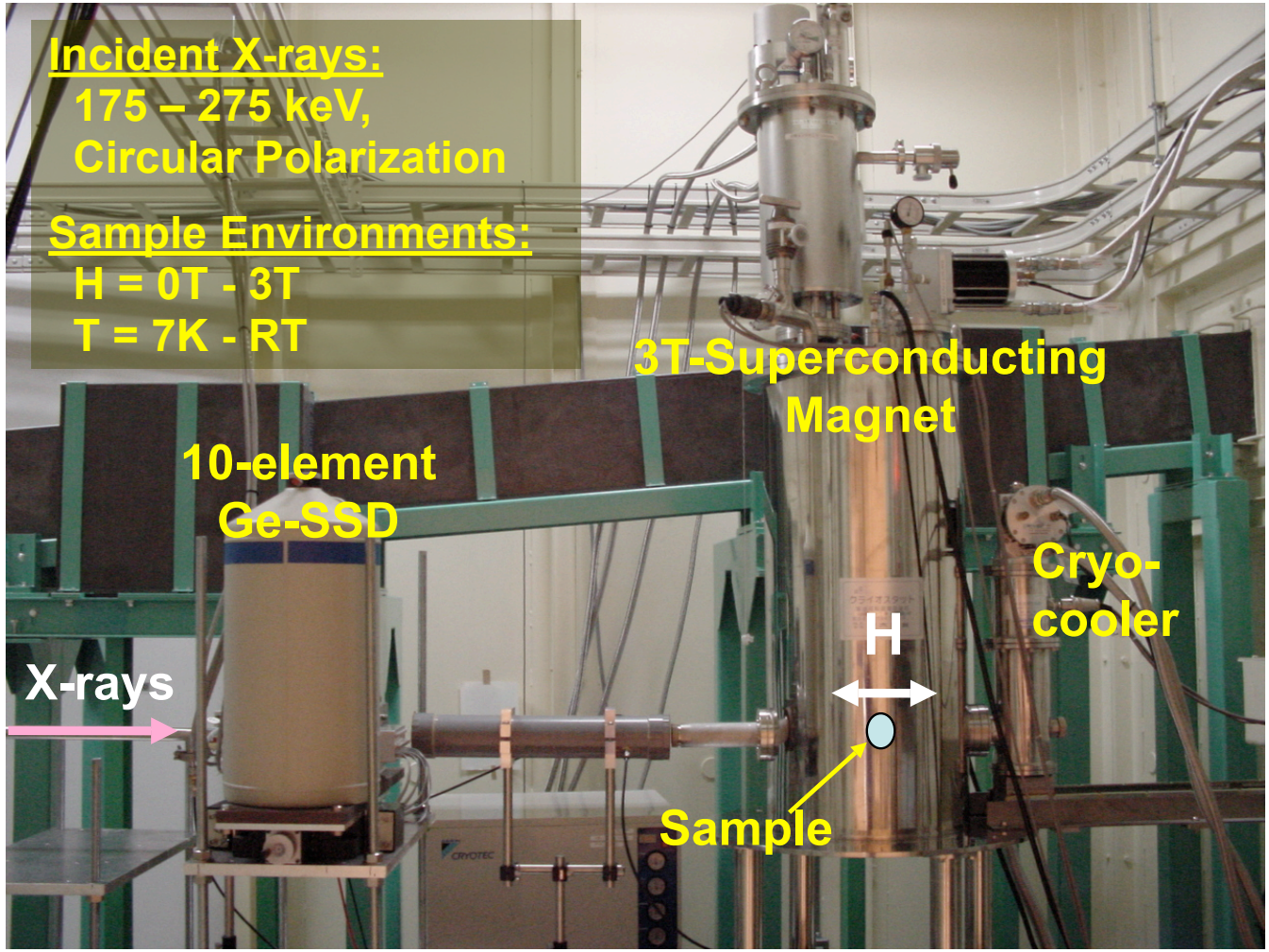

Cauchois-type Spectrometer:
High-resolution Compton Scattering Experiments

BL08W, Station-B

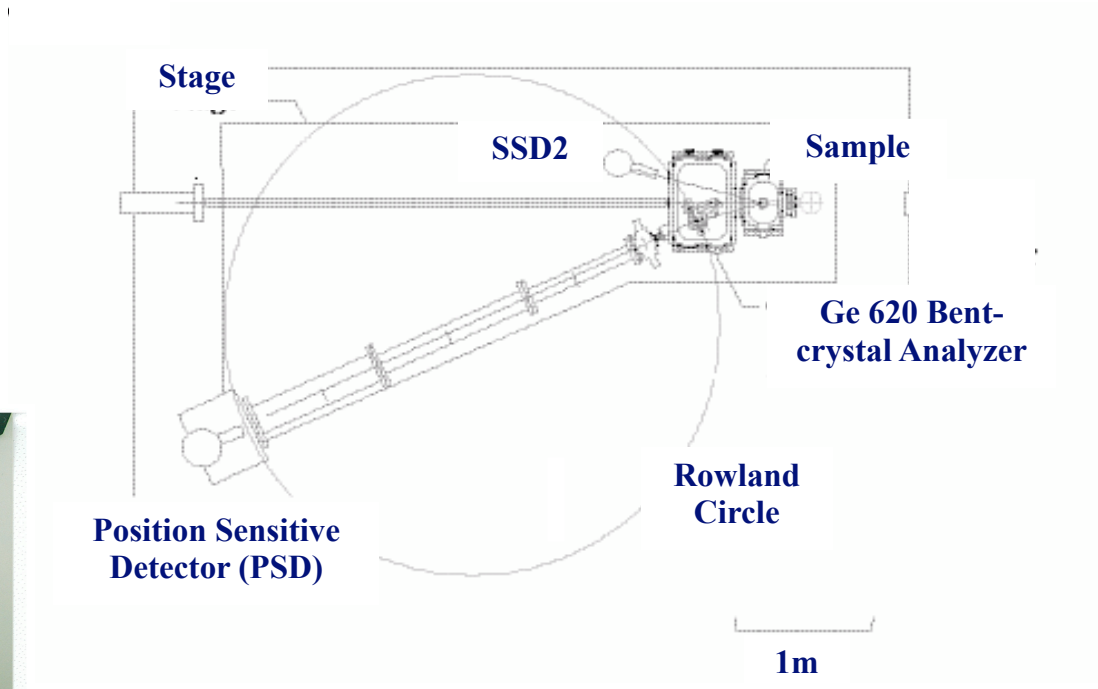

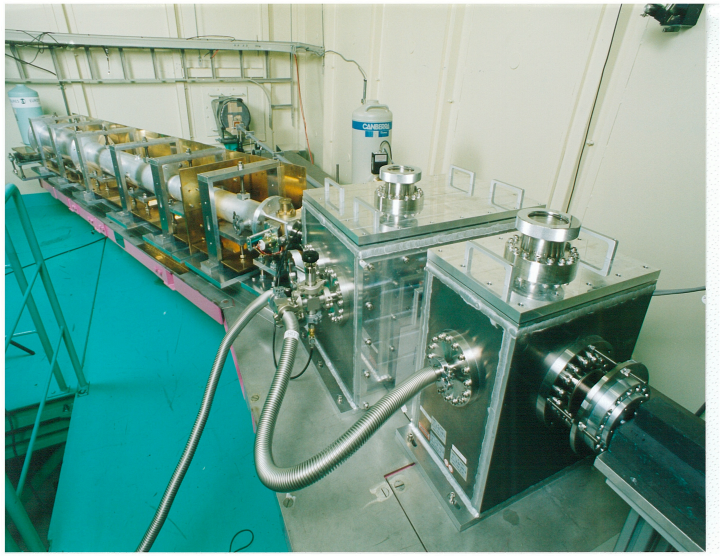

Incident X-rays : 115 keV
Scattering Angle :165 degrees
Resolution : 0.12 a.u. (~1/10 BZ)

Courtesy: Dr. Y. Sakurai, Spring-8

Formalism for obtaining electron density functions

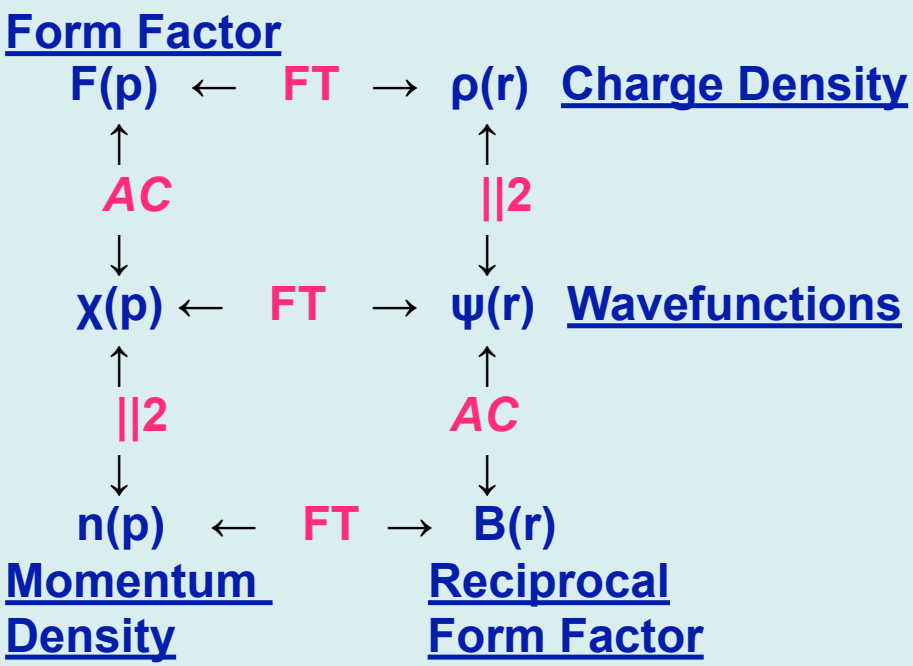

FT : Fourier Transform
AC : Autocorrelation
||2 : Squaring

Courtesy: Dr. Y. Sakurai, Spring-8

Population of e_g-orbitals in bilayer manganites

$La_{2-2x}Sr_{1+2x}Mn_2O_7$

Koizumi et al. Phys. Rev. Lett. 86 (2001) 5589
Kakutani et al. J.Phys. Soc. Japan 72 (2003) 599

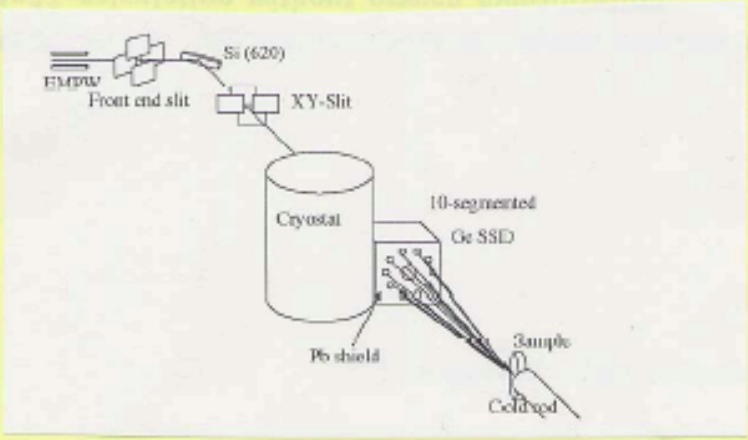

Experimental setup: beamline 08W, SPring-8

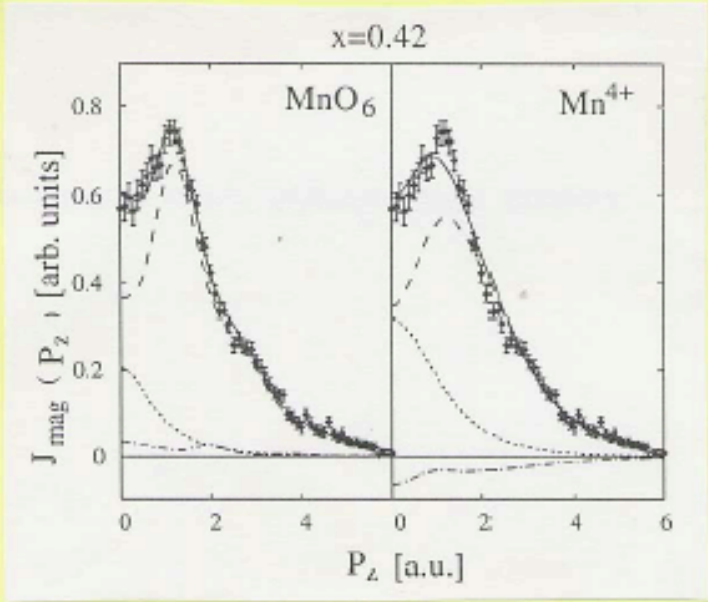

Magnetic Compton Scattering

Measurement of population of (x^2-y^2) and $(3z^2-r^2)$ of e_g orbitals in $La_{2-2x}Sr_{1+2x}Mn_2O_7$

(A. Koizumi, et al, Phys. Rev. Lett. 86 (2001) 5589.

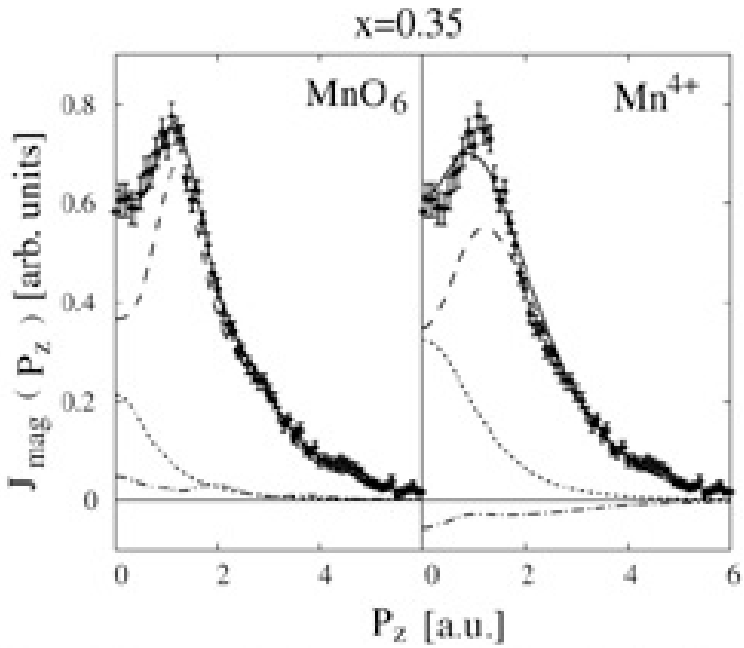

FIG. 1. The magnetic Compton profiles along the [001] direction at $x = 0.35$. Left: Experimental data (diamonds) are shown with fit (solid line) using the MnO_6 cluster orbitals. Error bars indicate experimental statistical errors. Also shown are the t_{2g} orbital contribution (dashed line), the $e_{x^2-y^2}$ orbital contribution (dotted line), and the $e_{3z^2-r^2}$ orbital contribution (dot-dashed line). The spin density per site is 3.65, of which the contribution from t_{2g} is fixed to 3.0. The $e_{x^2-y^2}$ and $e_{3z^2-r^2}$ contributions are 0.46 and 0.19, respectively. Right: The same as the left panel but using the Mn^{4+} orbitals. The $e_{x^2-y^2}$ and $e_{3z^2-r^2}$ contributions are 0.90 and −0.25, respectively.

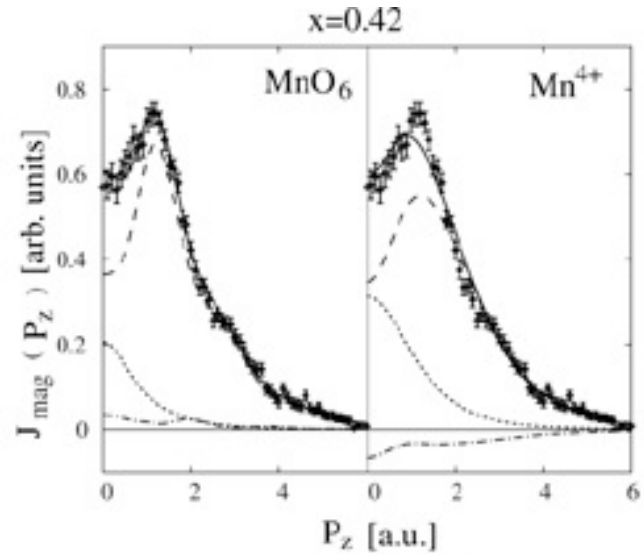

FIG. 2. The same as Fig. 1 but for $x = 0.42$. The spin density per site is 3.58, of which the contribution from t_{2g} is fixed to 3.0. The $e_{x^2-y^2}$ and $e_{3z^2-r^2}$ contributions are 0.44 and 0.14, respectively, for the MnO_6 fit (left), and 0.87 and −0.29, respectively, for the Mn^{4+} fit (right).

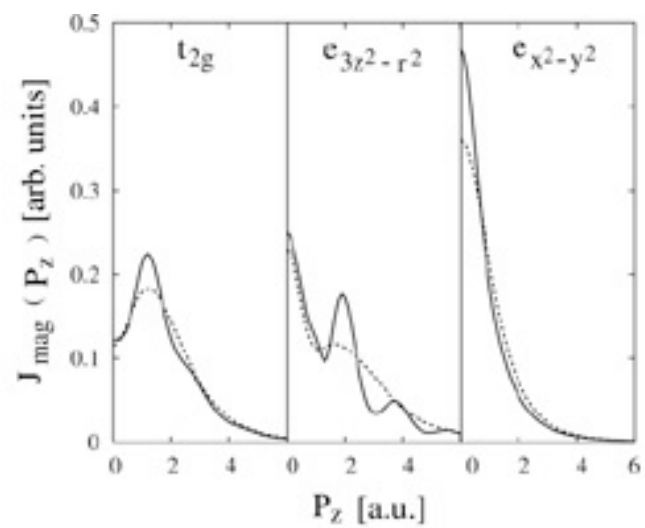

FIG. 3. Calculated magnetic Compton profiles of the t_{2g}, $e_{x^2-y^2}$, and $e_{3z^2-r^2}$ orbitals for the MnO_6 cluster (solid line) and by isolated Mn^{4+} (dashed line).

Fermi surface

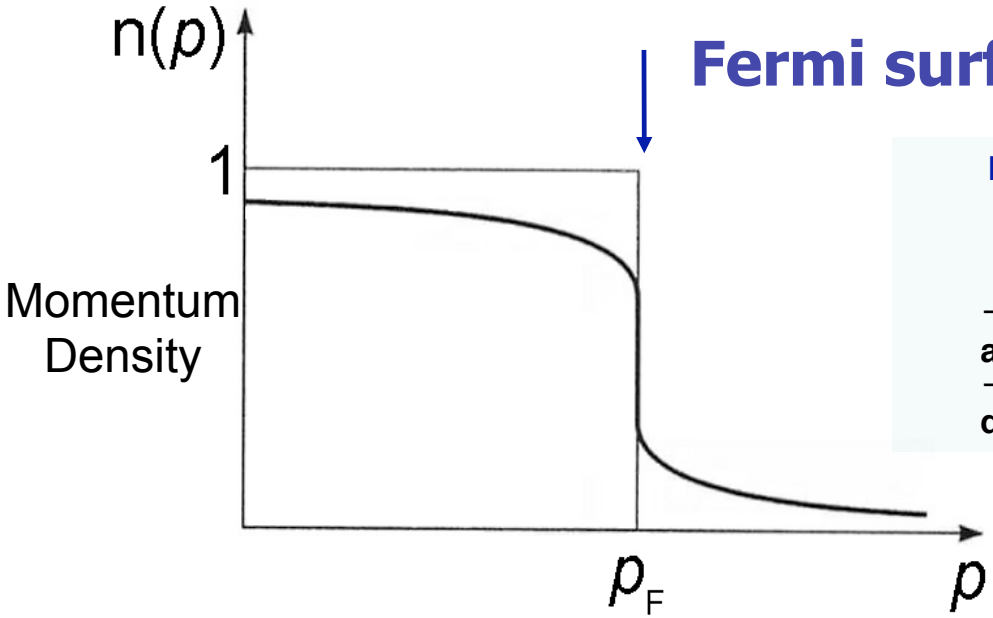

Fermi surface is defined by a boundary between occupied and unoccupied states in momentum space.

→ A map of momentum density provides a hint about the Fermi surface topology.
→ The extremum in the first derivative of momentum density can draw the Fermi surface.

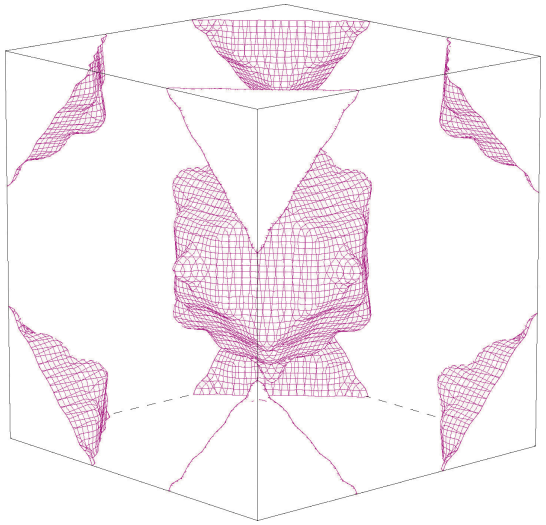

Pd

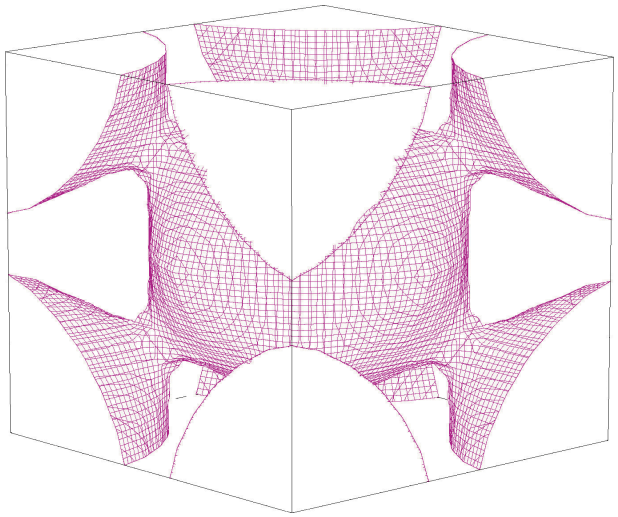

Ag

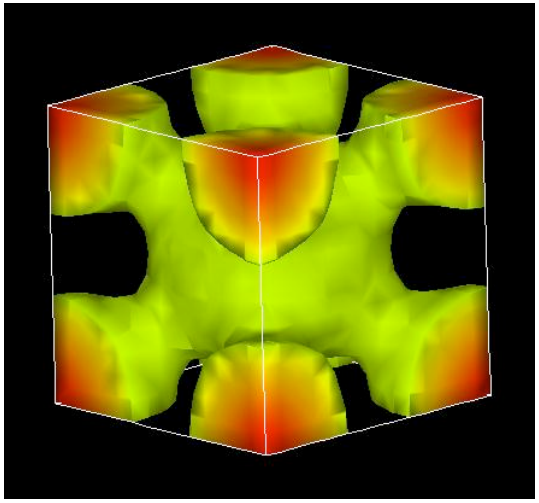

PdH

S. Mizusaki et al. Phys. Rev. B 73(2006)113101

Courtesy: Dr. Y. Sakurai, Spring-8

Near Future : 4GLS: the 4th Generation Light Sources

First generation:	Parasitic sources : SSRP-CHESS-HASYLAB-Daresbury LURE (1960-70's)
Second generation:	Dedicated sources, mostly from bending magnets NSLS, Photon Factory, SSRL,Super ACO, Aladdin
Third generation:	Dedicated, insertion device based, low emittance (nm-rad) ESRF, APS, Spring-8, SSRL-II, SLS, CLS, Diamond-SOLEIL
Fourth generation ?	Short pulse (fs), coherence, peak brightness ? Emittance ? All of the above ?

I believe the 4th generation sources will have to ***"multi-furcate"*** between time-resolved (fs) and imaging (coherent flux) vs. spectroscopy (flux) vs. size. The contenders:

a) Linear coherent light sources based on SASE Free Electron Principle
(SASE: Self-Amplified Spontaneous-Emission)
b) Energy recovery LINAC
c) Ultimate Storage Ring
d) Compact sources: Inverse Compton Sources.

Thank you